AD NUMBER: AD0876475

LIMITATION CHANGES

TO:

Approved for public release; distribution is unlimited.

FROM:

Distribution authorized to U.S. Gov't. agencies and their contractors; Administrative/Operational Use; 1 Oct 1970. Other requests shall be referred to Air Force Materials Lab., Wright-Patterson AFB, OH 45433

AUTHORITY

AFML ltr 21 May 1973 c/2 to a/1

AFML-TR-70-187

DEVELOPMENT OF COLUMBIUM ALLOY COMBINATIONS FOR GAS TURBINE BLADE APPLICATIONS

S. T. SCHEIRER
TRW Inc.

TECHNICAL REPORT AFML-TR-70-187

OCTOBER 1970

AIR FORCE MATERIALS LABORATORY
AIR FORCE SYSTEMS COMMAND
WRIGHT-PATTERSON AIR FORCE BASE, OHIO 45433

DEVELOPMENT OF COLUMBIUM ALLOY COMBINATIONS FOR GAS TURBINE BLADE APPLICATIONS

S.T. Scheirer

FOREWORD

This Final Technical Report covers all work performed under Contract F33615-67-C-1688 from 1 June 1967 to 31 May 1970, Project No. 7351, "Metallic Materials," Task No. 735101, "Refractory Metals". The manuscript was released on 1 July 1970 for publication as a technical report. TRW has assigned the report the internal number ER 7197-7.

This contract with TRW Inc., Cleveland, Ohio was initiated under Project Number 7351. The program was administered under the direction of the Air Force Materials Laboratory, Metals and Ceramics Division (MAMP). Mr. R.G. Ault was Project Engineer for the initial work while Mr. J.K. Elbaum served as Project Engineer for the remainder of the effort.

Dr. S.T. Scheirer of the Materials Technology Laboratory, TRW Inc., was the project engineer. Program management was provided by Mr. C.R. Cook, Section Manager, Materials Development Department. Mr. E. Thomas assisted with the execution of all phases of this program.

This technical report has been reviewed and is approved.

I. Perlmutter
Chief, Metals Branch
Metals and Ceramics Division
Air Force Materials Laboratory

ABSTRACT

A program designed to evaluate the feasibility of clad-core combination columbium alloy turbine blades has been completed. The concept was one in which a relatively oxidation resistant cladding alloy was used to prevent catastrophic oxidation of a high strength but easily oxidized core alloy. As envisioned, the entire system consisted of an oxidation resistant coating, the cladding alloy acting as an oxygen barrier, and the load bearing core. The program was divided into a screening of potential core and cladding alloys (with a diffusion bonding study) and an evaluation of the compatibility of the two components.

The high strength columbium alloys Cb132M, VAM-79, and SU-31 were evaluated as core alloys using 1200°F tensile and 2200°F creep-rupture testing. Several processing conditions and post-forging annealing treatments were studied. The highest tensile and creep strengths were obtained in Cb132M when in as-forged and forged plus 3600°F annealed conditions respectively. The best balance of tensile and creep properties was obtained in SU-31 when in a recrystallized and cold worked condition.

Nine columbium base alloys and one hafnium alloy were evaluated for possible use as a cladding alloy based on oxidation and ballistic impact resistance and fabricability to sheet. Generally, sheet fabricability and impact resistance were incompatible with oxidation resistance. Two alloys (Cb-15Ti-10Ta-10W-2Hf-3Al and Cb-5W-30Hf-5Ti-3Re) were selected for further study. A diffusion bonding technique was developed to join the core and cladding alloys. Bonding parameters were designed to minimize carbon diffusion from the high strength core alloy to the cladding.

A variety of studies were performed to evaluate the compatibility of the cladding alloys with a Cb132M core. During bonding and exposure at 2200°F carbon diffused from the core alloy to the cladding. This was accompanied by a loss of core hardness adjacent to the bond line and the formation of hafnium and/or titanium carbides in the cladding alloy. Tests of locally damaged bond samples, coated with CrTi-Si service coating showed that 0.020" of the cladding alloys (especially Cb-15Ti-10Ta-10W-2Hf-3Al) were capable of preventing catastrophic core alloy oxidation at 2200°F for times in excess of 64 hours. The bonded combinations exhibited good ballistic impact resistance at 2000°F although brittle behavior was encountered at room temperature. Compared with the unbonded condition, the 1200°F tensile properties of bonded Cb132M were slightly lowered whereas the 2200°F creep strength was significantly decreased. A 64 hour 2200°F exposure after bonding and coating had little effect on the mechanical properties tested.

The cladding concept for producing columbium alloy turbine blades is feasible in that diffusion bonding is an acceptable technique metallurgically and as a manufacturing technique. Also, a cladding can offer oxidation protection to the core alloy in the event of coating damage. However, the creep strength and microstructural stability of high temperature exposed clad Cb132M are marginal. It is felt that this aspect can be improved through the use of a core alloy having a superior balance of creep and tensile properties.

TABLE OF CONTENTS

Section		Page No.
I	INTRODUCTION	1
II	PHASE I - EVALUATION OF CANDIDATE MATERIALS	2
	A. High Strength Core Alloys	2
	B. Oxidation Resistant Alloys	19
	C. Bonding Study	29
	D. Conclusions and Selection for Phase II	34
III	PHASE II - COMPATIBILITY STUDY	99
	A. Microstructural Stability	99
	B. Oxidation Testing	102
	C. Ballistic Impact Testing	104
	D. Mechanical Property Testing	106
	E. Phase II Conclusions	112
IV	CONCLUSIONS AND RECOMMENDATIONS	149
	REFERENCES	151

LIST OF ILLUSTRATIONS

Figure No.	Title	Page No.
1	Columbium base alloys extruded 4:1 from 3". Molybdenum can intact.	36
2	Longitudinal microstructure of extruded Cb 132M (4:1 reduction at 3400°F), Heat No. indicated.	37
3	Longitudinal microstructure of extruded VAM-79 (4:1 reduction at 3200°F), Heat No. indicated.	38
4	Longitudinal microstructure of extruded SU 31 (4:1 reduction at 2642°F, stress relieved at 2372°F).	39
5	JT-3D first stage turbine rotor blade forging sequence as modified for Cb 132M Alloy. Note machining required (to broken line configuration) after operation 1.	40
6	Longitudinal microstructure of columbium-base alloys in the "extrude-forge" condition. 4:1 reduction at 2400°F.	41
7	Photomicrographs showing the recrystallization behavior of forged (2400°F) Cb 132M. Recrystallized for 1 hour at temperature indicated. Average microhardness (KHN) shown.	42
8	Photomicrographs showing the recrystallization behavior of forged (2400°F) VAM-79. Recrystallized for 1 hour at temperature indicated. Average microhardness (KHN) shown.	43
9	Photomicrographs showing the recrystallization behavior of forged (2400°F) SU-31. Recrystallized for 1 hour at temperature indicated. Average microhardness (KHN) shown.	44
10	Microstructure of columbium-base alloys in the recrystallized condition prior to cold working at 1600°F. Recrystallization temperature indicated.	45
11	Microstructure of Cb 132M forged at 2400°F. Heat No. M-493. Knoop hardness No. = 363.	46
12	Microstructure of forged and annealed Cb 132M. Annealing temperature and magnification indicated. Heat No. M-497.	47
13	Microstructure of forged, annealed, and aged (2200°F for 4 hours) Cb 132M. Annealing temperature and magnification indicated. Heat No. M-497.	48
14	Microstructure of cold worked Cb 132M in various stages of processing. Heat No. M-493.	49
15	Microstructure of VAM-79 forged at 2400°F. Heat No. VAM 96B Knoop hardness No. = 313.	50
16	Microstructure of forged and annealed VAM-79. Annealing temperature and magnification indicated. Heat No. VAM 96A.	51
17	Microstructure of forged, annealed, and aged (2200°F for 4 hours) VAM-79. Annealing temperature and magnification indicated. Heat No. VAM 96A.	52
18	Microstructure of cold worked VAM-79 in various stages of processing. Heat No. indicated.	53

LIST OF ILLUSTRATIONS (continued)

Figure No.	Title	Page No.
19	Microstructure of SU-31 forged at 2400°F. Heat No. 17A. Knoop hardness No. = 295.	54
20	Microstructure of forged and annealed SU-31. Annealing temperature and magnification indicated. Heat No. 17A.	55
21	Microstructure of forged, annealed, and aged (2200°F for 4 hours) SU-31. Annealing temperature and magnification indicated. Heat No. 17A.	56
22	Microstructure of cold worked SU-31 in various stages of processing. Heat No. 17A.	57
23	Configuration of tensile and creep rupture specimen utilized to test forged columbium alloy plate.	58
24	Comparison of 1200°F tensile properties for Cb 132M in various thermal-mechanical processing conditions as indicated. Heat number given when applicable. Tested in vacuum of 10^{-5} torr.; cross head speed of 0.020 in./min.	59
25	Comparison of 1200°F tensile properties for VAM-79 in various thermal-mechanical processing conditions as indicated. Tested in vacuum of 10^{-5} torr.; cross head speed of 0.020 in./min.	60
26	Comparison of 1200°F tensile properties for SU-31 in various thermal-mechanical processing conditions as indicated. Tested in vacuum of 10^{-5} torr.; cross head speed of 0.020 in./min.	61
27	Comparison of 2200°F 30,000 psi creep rupture properties for Cb 132M in various thermal-mechanical processing conditions as indicated. Heat number given when applicable. Tested in vacuum of 10^{-5} torr.	62
28	Comparison of 2200°F 30,000 psi creep rupture properties for VAM-79 in various thermal-mechanical processing conditions as indicated. Tested in vacuum of 10^{-5} torr.	63
29	Comparison of 2200°F 30,000 psi creep rupture properties for SU-31 in various thermal-mechanical processing conditions as indicated. Tested in vacuum of 10^{-5} torr.	64
30	Microstructures of oxidation resistant alloys in the as-cast condition.	65
31	Microstructures of oxidation resistant alloys in the as-cast condition.	66
32	Microstructures of oxidation resistant alloys in the as-cast condition.	67
33	Microstructures of oxidation resistant alloys in the as-cast condition.	68
34	Microstructures of oxidation resistant alloys in the as-cast condition.	69

LIST OF ILLUSTRATIONS (continued)

Figure No.	Title	Page No.
35	Oxidation test coupons following 1 hour exposure to air at 2200°F.	70
36	Oxidation test coupons following 4 hours exposure to air at 2200°F.	71
37	Oxidation test coupons following 20 hours exposure to air at 2200°F.	72
38	Oxidation test coupons following 64 hours exposure to air at 2200°F.	73
39	Photomicrographs of Alloy 1 (Cb-5Al-40Ti-10Mo) after exposure to air at 2200°F for times indicated.	74
40	Photomicrographs of Alloy 2 (Cb-10Al-50Ti) after exposure to air at 2200°F for times indicated.	75
41	Photomicrographs of Alloy 3 (Cb-5V-27Ti-3Al) after exposure to air at 2200°F for times indicated.	76
42	Photomicrographs of Alloy 4 (Cb-20W-10Ti-3V) after exposure to air at 2200°F for times indicated.	77
43	Photomicrographs of Alloy 5 (Cb-28W-7Ti) after exposure to air at 2200°F for times indicated.	78
44	Photomicrographs of Alloy 6 (Hf-25Ta-1.1Al-0.6Cr) after exposure to air at 2200°F for times indicated.	79
45	Photomicrographs of Alloy 7 (Cb-10Ti-10Ta-10W-1.8Hf) after exposure to air at 2200°F for times indicated.	80
46	Photomicrographs of Alloy 8 (Cb-10Ti-10Ta-10W-1.8Hf-3Mo-2Cr-2Re) after exposure to air at 2200°F for times indicated.	81
47	Photomicrographs of Alloy 9 (Cb-20Ti-3V-3Cr-3Al-3Co-2Fe-1Si-3Ni-3Ta-3W) after exposure to air at 2200°F for times indicated.	82
48	Photomicrographs of Alloy 10 (Cb-5W-30Hf-5Ti-3Re) after exposure to air at 2200°F for times indicated.	83
49	Oxidation resistant alloys in final state of fabrication.	84
50	Oxidation resistant alloys in final state of fabrication.	85
51	Oxidation resistant alloys in final state of fabrication.	86
52	Oxidation resistant alloys in final state of fabrication.	87
53	Oxidation resistant alloys in final state of fabrication.	88
54	Microstructures of fabricated oxidation resistant alloys.	89
55	Microstructures of fabricated oxidation resistant alloys.	90
56	Ballistic impact test apparatus.	91
57	Ballistic impact test specimens showing impact side of sample. Impact energy (ft-lbs) indicated.	92

LIST OF ILLUSTRATIONS (continued)

Figure No.	Title	Page No.
58	Experimental induction heated diffusion bonding apparatus.	93
59	Diagram showing specimen positioning in diffusion chamber.	94
60	Photomicrograph and microhardness traverse of Bond No. 5. Cb-10Ti-10W-1Zr diffusion bonded to annealed Cb 132M. Bonded at 2350°F for 1 hour.	95
61	Photomicrograph and microhardness traverse of Bond No. 6. Cb-10Ti-10W-1Zr diffusion bonded to annealed Cb 132M using a Ta foil interlayer. Bonded at 2350°F for 1 hour.	96
62	Photomicrograph and microhardness traverse of Bond No. 14. Cb-10Ti-10W-1Zr diffusion bonded to annealed Cb 132M using a V foil interlayer. Bonded at 2200°F for 30 minutes at 5000 psi.	97
63	Photomicrograph and microhardness traverse of Bond No. 17. Cb-10Ti-10W-1Zr diffusion bonded to annealed Cb 132M. Bonded at 2000°F for 30 minutes.	98
64	Photomicrograph and microhardness traverse of Cb 132M diffusion bonded to Alloy 7 Modified shown as-bonded at 2000°F for 30 minutes.	115
65	Photomicrograph and microhardness traverse of Cb 132M diffusion bonded to Alloy 7 Modified. Exposed 1 hour at 2200°F after bonding.	116
66	Photomicrograph and microhardness traverse of Cb 132M diffusion bonded to Alloy 7 Modified. Exposed 4 hours at 2200°F after bonding.	117
67	Photomicrograph and microhardness traverse of Cb 132M diffusion bonded to Alloy 7 Modified. Exposed 20 hours at 2200°F after bonding.	118
68	Photomicrograph and microhardness traverse of Cb 132M diffusion bonded to Alloy Modified. Exposed 64 hours at 2200°F after bonding.	119
69	Photomicrograph and microhardness traverse of Cb 132M diffusion bonded to Alloy 10. Shown as-bonded at 2000°F for 30 minutes.	120
70	Photomicrograph and microhardness traverse of Cb 132M diffusion bonded to Alloy 10. Exposed 1 hour at 2200°F after bonding.	121
71	Photomicrograph and microhardness traverse of Cb 132M diffusion bonded to Alloy 10. Exposed 4 hours at 2200°F after bonding.	122
72	Photomicrograph and microhardness traverse of Cb 132M diffusion bonded to Alloy 10. Exposed 20 hours at 2200°F after bonding.	123

LIST OF ILLUSTRATIONS (continued)

Figure No.	Title	Page No.
73	Photomicrographs and microhardness traverse of Cb 132M diffusion bonded to Alloy 10. Exposed 64 hours at 2200°F after bonding.	124
74	Photographs showing oxidation test samples. Cb 132M bonded to cladding alloy indicated, Cr-Ti-Si coating, damaged, and exposed at 2200°F in air for times indicated. (Arrow shows damaged region.)	125
75	Photomicrographs of bonded oxidation test samples. Alloy 7 Modified diffusion bonded to Cb 132M. Exposed for times shown at 2200°F after coating and intentional damage.	126
76	Photomicrographs of bonded oxidation test samples. Alloy 7 Modified diffusion bonded to Cb 132M. Exposed for times shown at 2200°F after coating and intentional damage.	127
77	Photomicrographs of bonded oxidation test samples. Alloy 10 diffusion bonded to Cb 132M. Exposed for times shown at 2200°F after coating and intentional damage.	128
78	Photomicrographs of bonded oxidation test samples. Alloy 10 diffusion bonded to Cb 132M. Exposed for times shown at 2200°F after coating and intentional damage.	129
79	Microhardness traverse for bonded oxidation test sample. Alloy 7 Modified diffusion bonded to Cb 132M. Coated, damaged, and exposed 1 hour at 2200°F.	130
80	Microhardness traverse for bonded oxidation test sample. Alloy 7 Modified diffusion bonded to Cb 132M. Coated, damaged, and exposed 4 hours at 2200°F.	131
81	Microhardness traverse for bonded oxidation test sample. Alloy 7 Modified diffusion bonded to Cb 132M. Coated, damaged, and exposed 20 hours at 2200°F.	132
82	Microhardness traverse for bonded oxidation test sample. Alloy 7 Modified diffusion bonded to Cb 132M. Coated, damaged, and exposed 64 hours at 2200°F.	133
83	Microhardness traverses for bonded oxidation test samples. Alloy 10 diffusion bonded to Cb 132M. Coated, damaged, and exposed for 1 and 4 hours respectively at 2200°F.	134
84	Microhardness traverse for bonded oxidation test sample. Alloy 10 diffusion bonded to Cb 132M. Coated, damaged, and exposed for 20 hours at 2200°F.	135
85	Microhardness traverse for bonded oxidation test sample. Alloy 10 diffusion bonded to Cb 132M. Coated, damaged, and exposed for 64 hours at 2200°F.	136
86	Ballistic impact test specimens for Alloy 7 Modified. Impact energy (ft-lbs) and test temperature indicated.	137

LIST OF ILLUSTRATIONS (continued)

Figure No.	Title	Page No.
87	Ballistic impact test specimens for diffusion bonded and coated columbium alloy combinations. Cladding alloy shown, substrate: Cb 132M. Impact energy (ft-lbs) and test temperature indicated.	138
88	Resistance heated experimental diffusion bonding apparatus.	139
89	Schematic representation of pre-bonding specimen configuration.	140
90	Diffusion bonded columbium alloy tensile specimen blank (A), and stainless steel plate used for alignment (B).	141
91	Fractured columbium alloy combination tensile specimens tested at 1200°F. Condition of Cb 132M core indicated.	142
92	Fractured surfaces of 1200°F tensile tested columbium alloy combinations produced by diffusion bonding.	143
93	Fractured columbium alloy combination creep rupture specimens tested at 2200°F. Condition of Cb 132M core indicated.	144
94	Unetched photomicrographs of columbium alloy combinations showing fracture area of 1200°F tensile specimens. Condition of Cb 132M core as indicated.	145
95	Photomicrographs of columbium alloy combinations showing fracture area and microstructure of 1200°F tensile specimens. Condition of Cb 132M core as indicated.	146
96	Unetched photomicrographs of columbium alloy combinations showing area near fracture in 2200°F; 30,000 psi creep specimens. Condition of Cb 132M core as indicated.	147
97	Photomicrographs of columbium alloy combinations showing microstructure after 2200°F; 30,000 psi creep testing. Condition of Cb 132M core as indicated.	148

LIST OF TABLES

Table No.	Title	Page No.
I	Chemical Analysis of Columbium Base Alloys	4
II	Extrusion Data for Columbium Base Alloys	6
III	Forging Data for High Strength Columbium Core Alloys	8
IV	Thermal-Mechanical Treatments for High Strength Columbium Alloys	11
V	1200°F Tensile Properties of Thermal-Mechanically Treated Columbium Alloys	14
VI	Room Temperature Tensile Properties of Thermal-Mechanically Treated Columbium Alloys	15
VII	2200°F, 30,000 psi Creep-Rupture Properties of Thermal-Mechanically Treated Columbium-Base Alloys	17
VIII	Chemical Analysis of Arc Cast Alloys Selected for Cladding Alloy	21
IX	Oxidation Test Data (2200°F) for Potential Cladding Alloys	24
X	Fabrication Data for Oxidation Resistant Alloys	25
XI	Chemical Analysis of Oxidation Resistant Alloys after Fabrication	27
XII	Ballistic Impact Data for Oxidation Resistant Columbium-Base Alloys	28
XIII	Summary of Phase I Bonding Studies (Cb 132M to Cb-10Ti-10W-1Zr)	32
XIV	Processing Summary for Alloy 7 Modified (Cb-15Ti-10W-10Ta-2Hf-2.2Al)	101
XV	Ballistic Impact Data for Alloy 7 Modified and Columbium Alloy Combinations	105
XVI	1200°F Tensile Properties of Coated Columbium Alloy Combinations and Cb 132M	109
XVII	2200°F, 30,000 psi Creep Rupture Properties of Coated Columbium Alloy Combinations and Cb 132M	110

SECTION I

INTRODUCTION

The development of high temperature alloys has been closely linked with the evolution of more powerful gas turbine engines. Concepts for future engines require materials for rotating parts capable of operating at metal temperatures well above 2000°F. For operation between 2000°F and 2500°F the strength to density ratio of high strength columbium alloys is particularly attractive. The ability of these alloys to be precision forged into turbine blade configurations has been demonstrated[1]. However, the very limited oxidation resistance at operating temperatures has prevented the use of columbium-base alloys in gas turbine power plants. To combat oxidation various protective coatings have been developed (for example see refs. 2 and 3), which have been successfully employed in numerous aerospace applications. Unfortunately these coatings are generally brittle and if impacted can fracture, thus exposing the substrate to rapid and often catastrophic oxidation.

The subject program was initiated to investigate the feasibility of introducing a columbium alloy barrier layer as a second-line of oxidation protection in the event of coating damage. Primary protection would, of course, be provided by the coating. However, a localized coating failure would expose the cladding layer rather than the easily attacked core. It is assumed that the cladding alloy would be oxidized slowly enough to insure that the high-strength core properties would be unaffected for at least 50 hours from the time of damage. The experimental effort was conducted in two phases: a selection of materials and methods, and an evaluation of the concept feasibility.

In Phase I, potential core and barrier alloys were evaluated, first by literature survey and then by testing and comparison. Carbide and solid solution strengthened columbium-base alloys were forged in a sequence designed to simulate the fabrication of a turbine blade. Various in-process and post forging heat treatments, all compatible with blade forging, were employed in an effort to obtain a balance of 2200°F creep strength and 1200°F tensile properties. Oxidation resistant alloys were prepared and exposed to determine their ability to prevent oxygen penetration. Fabricability to sheet and ballistic impact testing were used as measures of an alloy's applicability as a barrier alloy in a combination blade. Preliminary diffusion bonding trials were also conducted to determine processing parameters.

Phase II of the program was designed to evaluate: 1) the compatibility of the bonded core and barrier alloys during exposure; 2) the degree of oxidation protection provided by the barrier; and 3) the effect of the barrier on mechanical properties. The interactions of the two columbium alloys during bonding and exposure were studied in terms of microstructure and mechanical properties such as tensile, creep, and ballistic impact. The ability of the barrier to prevent loss of core properties through oxidation or oxygen contamination was also evaluated. In this way the feasibility of the concept was determined.

This final report describes the experimental procedures and results obtained in each phase.

SECTION II

PHASE I - EVALUATION OF CANDIDATE MATERIALS

An investigation of columbium alloy combination turbine blade feasibility requires the selection of three components (high strength core, oxidation retarding barrier alloy, and oxidation resistant coating) as well as a consideration of processing methods. In view of the numerous recent and current coating development programs this aspect of the problem has not been investigated here. Instead a standard coating procedure characteristic of the best type available was used where required. However, the continuing development of high strength columbium alloys and the rather specialized requirements of forged blades necessitated a close look at potential core alloys. Likewise, the requirements of fabricability and impact resistance as well as oxidation resistance suggested a re-evaluation of oxidation resistant compositions. Processing parameters for diffusion bonding also required study, since this is a potential means of part manufacture and is a convenient means of laboratory study. Considerations of combination blade manufacture will be discussed in a later section.

A. High Strength Core Alloys

1. Background and Selection

Columbium base alloys intended for creep resistance up to 2500°F have been developed to advanced generation status over a period of time. It is generally held that their high strength is dependent on solid solution alloying and the precipitation of second phase particles. Combinations of high melting point elements, usually other refractory metals, strengthen by solid solution interactions. The controlled addition of carbon and occasionally nitrogen in conjunction with certain reactive metals, often zirconium or hafnium, results in the precipitation of certain carbides and carbonitrides. When a finely dispersed precipitation of these compounds can be produced through suitable thermal-mechanical treatments, a significant contribution to creep resistance can be realized.

Among the properties considered essential in a columbium core material are creep and tensile strength and tensile ductility. The airfoil section is considered to operate near 2200°F while the root or attachment section of the blade would operate at a lower temperature (1000°F to 1500°F). Therefore, a suitable alloy must possess adequate high temperature creep rupture strength as well as intermediate temperature tensile yield strength. Adequate ductility at all temperatures and, of course, adequate forgeability would also be required.

Several alloy compositions, available at the start of this program showed potential for use as a core material. Among these were B-88 and its companion Cb-W-Hf-C alloys[4], Cb-1 a similar alloy containing zirconium and nitrogen[5], and Cb 132M a Cb-Ta-W-Mo-Zr-C alloy utilized in a previous forging study[1]. However, test conditions for reported data varied and, more importantly, the thermal-mechanical histories often were incompatible with forged blades. Thus it was felt that a study of thermal-mechanical processing techniques applicable to blade processing should be incorporated into an early phase of the program in conjunction with the core alloy selection.

Aside from the need to screen potential alloys after blade type forging (rather than swaging, rolling, etc.) it was necessary to explore heat treatments capable of developing maximum properties in a forging. It has been demonstrated that the excellent balance of high and low temperature properties characteristic of columbium alloy extrusions is destroyed by the precision forging operation[1]. While creep rupture strength can be restored by a recrystallization-solution-precipitation treatment, ductility and lower temperature tensile properties are adversely affected.

The thermal mechanical processing study included in this program was limited to combinations of metal working and thermal treatment completely compatible with turbine blade forging practice. Forging temperatures, recrystallization (solution) annealing temperatures and aging temperatures were varied. Cold working of a recrystallized structure was also investigated.

Three high-strength columbium base alloys were selected for evaluation: Cb 132M (Cb-20Ta-15W-5Mo-1.5Zr-0.12C), VAM-79 (Cb-22W-2Hf-0.067C), and SU-31 (Cb-17W-3.5Hf-0.12C). Cb 132M is an alloy which has been successfully forged into turbine blades and has exhibited high creep strength in annealed conditions[1]. The alloy VAM-79 is similar to B-88, a composition also capable of being forged and possessing high strength[6]. Experimental data[4] indicated that VAM-79, containing 22% W instead of 28%, would maintain nearly the same 2200°F strength as B-88 while providing a density advantage. SU-31 was chosen as the third alloy on the basis of information showing that British researchers have developed high creep strength with satisfactory intermediate temperature strength and ductility in this alloy[7].

2. Materials

The vendor supplied chemical analyses of the three columbium alloy core materials used in this program are shown in Table I. Nominal compositions are also given. Note that while the carbon level in both heats of Cb 132M is similar (and slightly lower than specified) the zirconium content varies considerably from 1.1 wt. % to 1.9 wt. %. The resulting variation in zirconium to carbon ratio should be considered when evaluating the mechanical properties discussed in a later section of this report.

The initial condition of each extrusion billet varied as supplied by the vendor. The Cb 132M was purchased from Du Pont as nominal 3" diameter x 5" long cylinders. They had previously been extruded from 6" diameter ingots through approximately a 3.5 to 1 reduction ratio. Westinghouse Astronuclear Laboratory supplied the VAM-79 as nominal 3" diameter x 5" long consumable electrode vacuum arc melted ingots. All cast and extruded billets were zyglo checked for surface cracks and ultrasonically inspected for internal defects. They were found to be satisfactory. The IMI developed alloy, SU-31, was furnished by Kawecki-Berylco Industries as a 1 1/2" diameter x 12" long machined bar. It had been previously extruded 4:1 at 2642°F from a 4" diameter billet. After machining the bar was stress relieved for 1 hour at 2372°F.

3. Conversion to Forging Stock

Extrusion was utilized to convert Cb 132M and VAM-79 ingot and large diameter bar to forging stock for simulated turbine blade fabrication. The columbium alloy extrusion billets were machined to approximately 2.8" diameter and nosed to match the included angle of the extrusion die. They were then canned in a sintered, unalloyed molybdenum sleeve incorporating

TABLE I

CHEMICAL ANALYSIS OF COLUMBIUM BASE ALLOYS

Chemical Analysis wt. %

Material	Vendor	Heat No.	Cb	Ta	W	Mo	Zr	Hf	C	O	N	H
Cb 132M	du Pont	M-493-3*	Bal.	18.8	15.1	5.2	1.1	-	0.10	0.002	0.003	0.0005
		M-493-1*	Bal.	18.8	15.1	5.2	1.1	-	0.10	0.002	0.003	0.0005
		M-497-1	Bal.	18.8	15.1	5.0	1.9	-	0.094	0.006	0.005	0.0001
		Nominal	Bal.	20	15	5	1.5	-	0.12/0.20			
VAM-79	Westinghouse	Vam-96A	Bal.	-	21.4	-	-	1.95	0.065	0.005	0.004	0.001
		Vam-96B	Bal.	-	21.0	-	-	1.85	0.071	0.003	0.001	0.0007
		Nominal	Bal.	-	22	-	-	2	0.067			
SU-31	Kawecki	17-A	Bal.		17.3			3.75	0.14			
		Nominal	Bal.	-	17	-	-	3.5	0.12			

* Both billets cut from same primary extrusion.

an integral nose which matched the die entrance angle and the shaped billet. The sleeves were tack welded to the rear of the billet. One billet of Cb 132M (Heat No. M-493-3) was extruded on the TRW 700 ton Loewy press while the remaining Cb 132M and all of the VAM-79 was processed on the AFML 700 ton Lombard press as shown in Table II. Small differences in the size and shape of press tooling were compensated for by using a 0.100" wall thickness molybdenum can for the billet extruded at TRW and a 0.040" thick sleeve for those extruded at AFML. The die angle was also changed from 120° to 90°. A high frequency induction unit was used to heat the billet to the extrusion temperature in an argon atmosphere. Temperature was monitored by a W-W/Re thermocouple in contact with the base of the billet. The tool steel dies were faced with a thin layer of zirconia. A commercial graphite and grease lubricant was swabbed on the interior of the liner while a Cr_2O_3-graphite preparation was applied to the die. The nominal extrusion ratio was 4:1. Pertinent data are given, Table II. Of particular note is that Cb 132M was extruded at a higher temperature (3400°F vs 3200°F) and speed 14 to 16 ips vs 4.5 ips) than was VAM-79. These variations were based on prior TRW experience with Cb 132M and the recommendations of Westinghouse in the case of VAM-79. Considering the extrusion conditions and recorded pressures it would appear that VAM-79 has a significantly lower flow stress than Cb 132M.

Photographs of four extrusions are shown in Figure 1 prior to sectioning, stripping, and machining for further processing. These products were of good quality, enabling a large percentage to be utilized. Microstructures of all 1 1/2" diameter extruded bar used in this program are shown, Figures 2, 3, and 4. (An etchant consisting of 64% H_2O, 15% HF, 15% H_2SO_4, and 8% HNO_3 was used for all metallography.) The higher degree of recrystallization evident in the TRW extruded Cb 132M, Figure 2a, is probably caused by a greater degree of heat retention due to the thicker molybdenum can. The other alloys, VAM-79 and SU-31, extruded at 3200°F and 2642°F respectively, exhibit very little or no recrystallization reflecting the lower working temperatures.

4. Simulated Blade Forging

The fabrication of turbine blades involves a series of complex forging operations[1]. Typically, this may involve extrusion, upsetting, roll forging, and press forging. These operations are shown schematically for the forging of a JT3D first stage blade, Figure 5. Considering the high strength of columbium alloys and their oxygen affinity, effective lubrication and workpiece protective coatings are vital. Following each separate forging step all traces of oxidation must be removed and the protective coating re-applied. (It should be noted that the coating referred to here is for protection during forging only and should not be confused with the high temperature in-service coating applied to columbium alloys.)

A simplified forging sequence consisting of extrusion and side forging between flat dies was chosen to simulate the forging procedure depicted in Figure 5. The heading and roll-forging steps were omitted. The objective was to produce material of the approximate thickness of a JT3D airfoil at the maximum pitch thickness while approaching the thermal-mechanical working associated with blade manufacture.

TABLE II

EXTRUSION DATA FOR COLUMBIUM BASE ALLOYS

Alloy	Heat No.	Location of Extrusion	Extrusion Ratio	Included Die Angle	Temp. (°F)	Breakthrough Pressure (psi)	Running Pressure (psi)	Avg. Speed (ips)	Useful Extruded Length (inches)
Cb 132M	M-493-3	TRW	4:1	120°	3400	82,800	92,000	16.0	15
	M-493-1	AFML	4:1	90°	3400	100,000	100,000	14.5	15
	M-497-1	AFML	4:1	90°	3400	93,000	88,000	14.5	10
VAM-79	Vam 96A	AFML	4:1	90°	3200	92,000	95,000	4.5	13
	Vam 96B	AFML	4:1	90°	3200	101,000	101,000	4.5	19

The extruded bar was prepared for the first forging operation, "extrude-forging", by first stripping the protective molybdenum cladding and then machining off surface irregularities and oxides. The forging billets ranged from approximately 1.3" diameter for Cb 132M and VAM-79 to nearly 1.5" for the previously machined SU-31. The average lengths were 2.75". Prior to extrusion the billets were dipped in a Corning 7740 coating modified with a low fusion point component. Extrusion was performed with a 2000-ton capacity mechanical crank press of the type used for turbine blade precision forging. Billets were heated for five minutes to the appropriate forging temperature (2300°F to 2450°F for heat M-493-3 of Cb 132M and 2400°F for all other material) using a globar box furnace and an argon enriched atmosphere. A water-based graphite lubricant was sprayed onto all tooling followed by a swab application of a commercial graphite-grease lubricant to the inside of the container and bottom surface of the punch. The die utilized consisted of a zirconia (Zircoa 1027) insert supported by tool steel. Allowing for billet upsetting in the container, the extrusion ratio was approximately 4:1, finishing at 0.750" diameter.

The extrusions were all processed in a manner to provide the maximum amount of extruded material. They were generally of excellent quality with the exception of the first group of five, all from Cb 132M heat M-493-3. The surfaces of these five extrusions were marred by small circumferential cracks. This condition was caused by the omission of the low melting component from the protective coating, thereby permitting significant oxidation during heat-up. These defects were readily removed by machining while preparing the extrusions for flat forgings. Microhardness measurements indicated that oxygen contamination did not penetrate beyond the base of the cracks and was entirely removed.

The microstructures of typical extrusions of the three alloys are shown at 100X, Figure 6. Upon comparison of this figure with Figures 2, 3 and 4, showing the microstructure of the 1 1/2" diameter extrusions, the additional amount of working is obvious. Hardnesses were correspondingly increased. The Cb 132M, which had the highest percentage of recrystallization in the starting material, is seen to have the least heavily worked structure.

The closed die portion of an airfoil forging sequence was approximated by three flat forging steps. The nominal 3/4" diameter "extrude-forged" material was sectioned into 2" to 3" lengths and machined to remove oxide and damaged metal. Three separate reductions were employed in forging from an initial diameter of between .630" and .700" to a final thickness of approximately .175". Specimens were heated to the forging temperature in five minutes using an argon enriched atmosphere. The pieces were conditioned and then given a protective coating of TRW modified Corning 7740[1] prior to each forging operation. A commercial graphitic lubricant, Delta 45, was sprayed on the die surfaces. Forging was conducted on a 1600 ton mechanical crank press of the type used for blade forging. The use of a mechanical press is considered important in this study because of the influence of thermal-mechanical processing on final microstructure and properties of columbium alloys.

The forging conditions, average thicknesses and approximate reductions are shown in Table III. Note that the thicknesses and reductions differed slightly for the initial group of Cb 132M (Heat M-493-3). The smaller starting diameter (0.630" vs 0.705") was due to the necessity of

TABLE III

FORGING DATA FOR HIGH STRENGTH COLUMBIUM CORE ALLOYS

A. Cb 132M Heat Number M-493-3

Step	Forging Temp.	Pre-Forging Thickness	Finish Thickness	Thickness % Reduction
1	2400°F	0.630"	0.345"	45
2	2400°F	0.310"	0.240"	25
3	2200°F & 2400°F	0.220"	0.170"	25

B. Cb 132M Heat Numbers M-493-1, M-497-1
VAM-79 Heat Numbers VAM 96A, VAM 96B
SU-31 Heat Number 17A

Step	Forging Temp.	Pre-Forging Thickness	Finish Thickness	Thickness % Reduction
1	2400°F	0.705"	0.415"	40
2	2400°F	0.390"	0.270"	30
3	1600°F or 2400°F	0.230"	0.185	20

removing the surface cracks in these extrusions. Later extrusions were free of this surface defect and could be "cleaned up" at a larger diameter. The initial reduction to 45% resulted in shear-type end cracking in the forged Cb 132M specimens. The defective metal was easily removed and the cracking did not reappear during subsequent passes. A lighter pass of 40% in subsequent runs helped to alleviate this problem, although slight cracking was still noted after the initial reduction in the Cb 132M samples. VAM-79 and SU-31 samples were not cracked during any of the forging operations.

Forging of all three alloys was accomplished without difficulty at 1600°F as well as 2400°F. There was no noticeable difference in the flow of metal at these two temperatures. However, this observation should not be used to infer an equal response for closed die blade forgings where pressure requirements may be higher and die wear must be considered. In spite of the protective coating a small amount of surface oxidation was observed after forging, particularly at the higher forging temperatures. This was easily removed by grinding and pickling in acid.

As shown in Table III, three different temperatures were utilized for the final forging step. Cb 132M from Heat M-493-3 was finished at both 2200°F and 2400°F in order to study the effects of slight processing temperature changes on forgeability, microstructure, and mechanical properties. The third step forging at 1600°F, which was performed on all compositions, is a result of the suggestion that the problem of low ductility and strength in the intermediate temperature range can be resolved by lightly cold working a recrystallized structure[7]. Samples which were processed in this manner were given a recrystallization anneal after the second flat forging step and then forged a third time at 1600°F rather than 2400°F. The recrystallization treatment and the varied thermal-mechanical treatments are described in the next two sections of this report.

5. Recrystallization Study

In conjunction with the thermal-mechanical processing study it was necessary to determine the recrystallization behavior of the three columbium alloys prior to cold working. It was felt that the most desirable microstructure for cold working at 1600°F was 100% recrystallized but without appreciable grain growth or Widmanstatten carbide precipitation. In order to determine the appropriate recrystallization temperature for each alloy, metallographic samples were treated in vacuum for one hour at temperatures ranging from 2850°F to 3150°F. The resulting microstructures are shown for each alloy, Figures 7, 8, and 9. The starting "as-forged" microstructure is also shown (two blows at 2400°F resulting in 40% and 30% reductions). Recrystallization is nearly complete in the Cb 132M and VAM-79 alloys at 2950°F. Higher temperatures had only a slight grain coarsening effect on Cb 132M but treatments above 3000°F resulted in greatly enlarged grains in VAM-79. Appreciable recrystallization was not observed below 3100°F in SU-31 and was not totally complete at 3150°F. However, it was expected (and subsequently verified in later treatments) that temperatures in excess of 3150°F would result in enlarged grains and Widmanstatten and grain boundary carbide precipitation.

On the basis of these studies 2950°F was selected as the recrystallization temperature for Cb 132M and VAM-79. The SU-31 was treated at 3150°F.

Two hour treatments were utilized in an effort to obtain complete recrystallization while avoiding the excessive grain growth likely to occur at higher temperatures. The microstructures of specimens treated in this manner are shown, Figure 10. The two hour treatment apparently succeeded in producing a greater degree of recrystallization without grain growth in the Cb 132M and VAM-79 alloys. In the case of SU-31 some additional recrystallization occurred although it is not yet complete. Some grain coarsening has also occurred.

The reason(s) for the varied response of the alloys during recrystallization is not entirely clear. The carbon levels of Cb 132M and SU-31 are nearly twice that of VAM-79 but it is Cb 132M and VAM-79 which exhibit similar recrystallization behavior. Aside from composition the major difference between the three alloys prior to the simulated blade forging concerns the history of the 1 1/2" diameter extruded bar. Cb 132M and VAM-79 had been extruded at 3400°F and 3200°F respectively, temperatures high enough to cause some recrystallization, Figures 2 and 3. The SU-31 had been extruded at a lower temperature and already was heavily worked, Figure 4. It is likely that the degree of recrystallization can also be affected by the prior forging temperature, a variable not examined. Forging at a temperature below 2400°F could promote more complete recrystallization at lower temperatures.

6. Thermal Mechanical Processing

The necessity for thermal treatments during and/or after forging to restore favorable high temperature properties has been discussed previously in this report and elsewhere. The various treatments investigated here included: cold (1600°F) working after recrystallization and combinations of solution-annealing and aging treatments. These are summarized for each alloy in Table IV. Material supply limitations prevented all treatments from being applied to each alloy.

Microstructures for the three alloys in the various conditions are shown, Figures 11 to 22, beginning with Cb 132M. The as-forged (2400°F) microstructures, Figures 11, 15 and 19, are similar for each alloy, being heavily and uniformly worked. The slightly more striated nature of the forged SU-31 and VAM-79 probably is a result of the smaller percentage of recrystallized grains in the starting 1 1/2" diameter bar. Forging at 2200°F rather than 2400°F, in the case of Cb 132M only (not shown), did not appreciably alter the microstructure.

Solution annealing treatments were performed on material forged at 2400°F. These were conducted in a tantalum element resistance heated vacuum furnace. Cooling was by radiation, without the use of an inert gas quenching medium. The intent of these treatments was to provide a small grained recrystallized structure, a larger grained recrystallized structure, and with the 3600°F treatment a large recrystallized grain size with a Widmanstatten carbide structure precipitated on cooling. Unfortunately these objectives were not fully realized for all alloys. Little difference in grain size exists between the Cb 132M treated at 3000°F and that annealed at 3200°F, Figure 12. In the case of VAM-79, Figure 16, there is an increase in grain size at the 3200°F annealing temperature, but this is accompanied by Widmanstatten carbide precipitation. The structure produced in SU-31 at 3000°F, Figure 20, shows

TABLE IV

THERMAL-MECHANICAL TREATMENTS FOR HIGH STRENGTH COLUMBIUM ALLOYS

Treatment	Alloy		
	Cb 132M	VAM-79	SU-31
forged (2400°F)	X*	X	X
forged (2400°F) + 3600°F/1 hr	X	X	
forged (2400°F) + 3600°F/1 hr + 2900°F/1 hr	X		
forged (2400°F) + 3600°F/1 hr + 2200°F/4 hrs	X	X	
forged (2400°F) + 3200°F/1 hr	X	X	X
forged (2400°F) + 3200°F/1 hr + 2200°F/4 hrs	X	X	X
forged (2400°F) + 3000°F/1 hr	X	X	X
forged (2400°F) + 3000°F/1 hr + 2200°F/4 hrs	X	X	X
2950°F/2 hrs + forged (1600°F)	X	X	
2950°F/2 hrs + forged (1600°F) + 2000°F/4 hrs	X	X	
3150°F/2 hrs + forged (1600°F)			X
3150°F/2 hrs + forged (1600°F) + 2000°F/4 hrs			X
forged (2200°F)	X		
forged (2200°F) + 3600°F/1 hr	X		
forged (2200°F) + 3600°F/1 hr + 2900°F/1 hr	X		

* "X" indicates treatment performed.

very little recrystallization whereas that formed at 3200°F resembles Cb 132M and VAM-79 treated at 3000°F. The ease of recrystallization can most likely be attributed to the carbide level, which is visually lowest in VAM-79 and greatest in SU-31, and its solutioning behavior in the alloys. In addition to these conditions, other samples were aged at 2200°F for four hours after the high temperature treatment, Figures 13, 17, and 21. Aside from slightly more carbide precipitation, especially in SU-31, there does not appear to be a significant microstructural change brought about by aging 4 hours at 2200°F.

The various stages of the recrystallizing-cold working-aging treatment are shown in Figures 14, 18, and 22. There are slight differences in recrystallized grain size between Cb 132M and VAM-79. Furthermore, SU-31 has a lower degree of recrystallization despite the higher temperature of treatment (3150°F vs 2950°F). The cold working procedure appears to have a similar effect in each case, that of slightly elongating the grains. Aging at 2000°F slightly increased the population of carbide precipitate. However, it is difficult to determine the nature of these particles at optical magnifications.

The temperatures for cold working (1600°F) and subsequently aging (2000°F) were based on recommendations of Imperial Metal Industries (IMI) personnel through Kawecki-Berylco[7] and TRW experience in forging columbium base alloys. However, they should not be considered as ideal for all alloys studied. In view of the excellent forgeability of all alloys at 1600°F, it is possible that a lower temperature should be considered for cold working, and for all forging. Provided that metal flow is adequate and die wear tolerable, lower forging temperatures would have the advantage of causing less workpiece oxidation.

The various columbium alloy microstructures studied here are significant as they relate to properties, especially strength and creep resistance. These mechanical properties and their relation to microstructures are presented and discussed in the following sections. Frequent reference is made to the photomicrographs.

7. Mechanical Properties

The mechanical property tests performed in this portion of the study included tensile testing at 1200°F and creep-rupture testing at 2200°F. Room temperature tensile tests were also performed for certain promising thermal-mechanical treatments. The 1200°F test was intended to evaluate each alloy under temperature conditions similar to those experienced by the root or attachment portion of a turbine blade. The elevated temperature creep testing should be representative of airfoil operating conditions. A plate type tensile specimen, shown in Figure 23, was used for both tensile and creep testing. This configuration permitted the testing of material flat forged to airfoil thickness.

a. Tensile Testing

All 1200°F tensile testing was performed in a resistance heated vacuum chamber fitted to an Instron testing machine. A vacuum of 10^{-5} torr or less was maintained during the 1200°F tests. Crosshead speed was 0.020 inches per minute. Test conditions were the same for room temperature tensile tests except for the omission of the vacuum chamber. The 1200°F tensile

properties are given, Table V, and summarized in graph form for each alloy, Figure 24, 25, and 26. (The recorded ultimate strength and 0.2% offset yield strength of VAM-79 in the as-forged condition are identical. It is thought that this is due to an accidental pre-straining of the specimen while heating to 1200°F. It is expected that the yield strength should be at approximately this level while the true ultimate strength is somewhat higher.)

For all alloys the best strength and ductility combinations were obtained for the following two conditions: as forged (2400°F); and recrystallized and cold worked (1600°F). Brittle fracture behavior was exhibited by these alloys when annealed at 3600°F, as indicated in Table V. The considerable elongations reported for certain of these specimens is uniform throughout the gage length, the necking phenomenon not being observed. Although all fractures observed in SU-31 were of a ductile nature, it is possible that annealing at 3600°F would have resulted in embrittlement as was the case with Cb 132M and VAM-79.

In addition to the brittle behavior exhibited by certain conditions, the relatively low yield strength of all alloys after an annealing treatment represents a serious deficiency. Discontinuous yielding was observed in all alloys when in annealed conditions (3000°F, 3200°F, or 3600°F). Similar behavior was observed in those samples which had been recrystallized and cold worked. Aging at 2200°F or 2000°F had the effect of removing or diminishing this condition. This yielding phenomena is probably due to the dislocation pinning action of carbon atoms, taken into interstitial solution during annealing. VAM-79, containing the lowest carbon content of the three alloys, displayed the smallest effect.

Low temperature aging had the effect of generally reducing the tensile yield and ultimate strengths while slightly improving ductility. The low carbon alloy, VAM-79 showed the smallest change in properties upon aging. SU-31 annealed at 3200°F was an exception, exhibiting an improvement in strength upon aging at 2200°F.

Considering all conditions tested the alloy Cb 132M exhibited the best 1200°F tensile properties. The as-forged and the recrystallized and cold worked samples had the highest strength with adequate ductility. Strength levels for the various annealed conditions were also superior to the other alloys given identical treatments.

Room temperature tensile tests were conducted on samples treated for high 1200°F yield strength (cold working at 1600°F) and highest 2200°F creep rupture strength (3600°F annealed, see the following section). These data presented in Table VI, clearly show the brittle behavior of columbium base alloys at room temperature. Both Cb 132M and VAM-79, annealed at 3600°F prior to testing, fractured at a very low stress before a yield point was reached. Only the Cb-W-Hf-C alloys, VAM-79 and SU-31 in the cold worked condition displayed strength levels comparable with their 1200°F properties. However, the low ductility and brittle fracture behavior of these specimens is undesirable.

TABLE V

1200°F TENSILE PROPERTIES OF THERMAL-MECHANICALLY TREATED COLUMBIUM ALLOYS+

Heat No.	Forging Temp. (°F)	Annealing Temp. & Time (°F/Hrs.)	Aging Temp. & Time (°F/Hrs.)	U.T.S. (KSI)	0.2% Y.S. (KSI)	Elong. (%)
A. Cb 132M						
M-493	2400	-	-	131.3	115.6	14.9
M-493	2400	-	-	127.2	107.2	15.1
M-497	2400	3000/1	-	102.4	66.4	29.2
M-497	2400	3000/1	2200/4	85.6	55.2	25.8
M-497	2400	3200/1	-	103.9	66.9	26.5
M-497	2400	3200/1	2200/4	87.6	54.2	29.0
M-493	2400	3600/1	-	83.0	57.8	11.8 [b]
M-497	2400	3600/1	-	100.5	65.5	7.9 [b]
M-493	2400	3600/1	2900/1	84.5	54.9	7.7 [b]
M-497	2400	3600/1	2200/4	93.7	65.4	18.7 [b]
M-493	2200	-	-	131.6	117.1	15.2
M-493	2200	3600/1	-	73.8	56.9	3.9 [b]
M-493	2200	3600/1	2900/1	85.1	55.3	11.1 [b]
M-493	1600*	-	-	116.3	98.3	16.1
M-493	1600*	-	2000/4	100.4	87.9	22.5
B. VAM 79						
96B	2400	-	-	86.7**	86.7**	22.9
96A	2400	3000/1	-	82.0	49.4	24.7
96A	2400	3000/1	2200/4	76.0	46.5	25.6
96A	2400	3200/1	-	73.0	43.7	5.9 [b]
96A	2400	3200/1	2200/4	74.4	45.7	22.7
96A	2400	3600/1	-	76.7	47.2	20.5 [b]
96A	2400	3600/1	2200/4	75.0	44.8	25.9 [b]
96B	1600*	-	-	99.0	87.8	15.6
96A	1600*	-	2000/4	94.5	84.7	24.2
C. SU 31						
	2400	-	-	96.5	82.5	21.6
	2400	3000/1	-	81.3	52.6	26.9
	2400	3000/1	2200/4	64.9	43.9	24.7
	2400	3200/1	-	66.5	41.0	26.6
	2400	3200/1	2200/4	76.3	44.3	23.1
	1600*	-	-	100.7	90.7	10.2
	1600*	-	2000/4	92.0	81.0	23.7

[b] Brittle behavior

* Cold worked 20% at 1600°F after partial forging at 2400°F and recrystallization at 2950°F for 2 hours (Cb 132M and VAM 79) or 3150°F for 2 hours (SU 31).

** Specimen accidentally pre-strained, ultimate strength and yield strength identical.

+ Tested in vacuum of 10^{-5} torr.; cross-head speed of 0.020 in./min.

TABLE VI

ROOM TEMPERATURE TENSILE PROPERTIES
OF THERMAL-MECHANICALLY TREATED COLUMBIUM ALLOYS[+]

Alloy	Heat No.	Forging Temp. (°F)	Annealing Temp. & Time (°F/Hrs.)	U.T.S. (KSI)	0.2% Y.S. (KSI)	Elong. (%)
Cb 132M	493-1	2400	3600/1	28.3	**	0 [b]
Cb 132M	493-1	1600*	-	82.1	**	1.5 [b]
VAM-79	VAM 96A	2400	3600/1	24.9	**	0 [b]
VAM-79	VAM 96A	1600*	-	135.3	123.7	0.9 [b]
SU-31	17A	1600*	-	134.1	127.2	3.9 [b]

[b] Brittle Behavior

* Cold worked 20% at 1600°F after partial forging at 2400°F and recrystallization at 2950°F for 2 hours (Cb 132M and VAM-79 or 3150°F for 2 hours (SU-31).

** 0.2% offset yield strength not reached.

[+] Tested in air; cross-head speed of 0.020 in./min.

b. Creep Testing

Creep testing was performed at 2200°F in a vacuum environment of 10^{-5} torr or less using a tantalum element cold wall furnace. The results of this testing are shown, Table VII. The creep-rupture data are summarized in Figures 27, 28, and 29. As in the case of tensile properties, Cb 132M was superior in creep properties under the testing conditions. Annealing treatments generally improved creep rupture lives of all alloys over the as-forged (2400°F) condition while aging after the anneal tended to shorten life. Contrary to the behavior of the other alloys, the recrystallization and cold working treatment provided the best creep properties in SU-31.

The minimum second stage creep rates are also shown in Table VII. Rates of less than 0.1%/hour were obtainable only in Cb 132M and VAM-79 when annealed at 3200°F or 3600°F. A 2200°F aging treatment after the anneal tended to increase creep rates. The lowest creep rate for SU-31 was obtained for material in the recrystallized and cold worked condition.

8. Discussion

Superior tensile properties were obtained for all alloys when in worked conditions, either the cold working treatment or forged at 2400°F which appears to be a warm working temperature. Loss of what is presumed to be a favorable dislocation network through recovery or recrystallization at annealing temperatures above 3000°F resulted in a pronounced decrease in yield strength. Aging at 2200°F generally resulted in a slight additional strength reduction. This is probably due to the precipitation during aging of carbon previously taken into solution during annealing. The discontinuous yielding behavior observed in annealed material is further evidence for this view. Micrographs comparing the annealed with the annealed and aged conditions, Figures 12, 13, 16, 17, 20, and 21, show only slight differences primarily in Cb 132M annealed at 3600°F where additional carbide precipitation is detected. Room temperature microhardness data generally correlate with the observed lower strengths after aging.

In contrast to the intermediate temperature tensile properties, acceptable creep behavior in Cb 132M and VAM-79 required an annealing treatment, the longest rupture lives being obtained after a 3600°F exposure. This treatment produced a fully recrystallized structure with significant grain growth compared to lower temperature anneals. The Widmanstatten type carbides were probably precipitated upon cooling from the recrystallization temperature. In most instances a 2200°F aging treatment reduced the rupture life. Since the aging temperature is the same as the test temperature, it appears that a stress influenced precipitation of residual carbon during testing is responsible for the improved properties in unaged samples. This carbon is not available for precipitation during the test in pre-aged material.

The alloy SU-31 exhibited somewhat lower properties in the annealed condition than the other compositions under investigation. Examination of the appropriate microstructures, Figures 20 and 21, indicate that full recrystallization was not obtained. (The recrystallization behavior of these alloys was reported in a previous section.) However, the difference in creep behavior of aged material from that which was only annealed indicates that some carbon

TABLE VII

2200°F, 30,000 PSI CREEP-RUPTURE PROPERTIES OF THERMAL-MECHANICALLY TREATED COLUMBIUM-BASE ALLOYS++

Heat No.	Forging Temp. (°F)	Annealing Temp. & Time (°F/Hrs.)	Aging Temp. & Time (°F/Hrs.)	Min. Creep Rate (%/Hr.)	Approx. Time to Third Stage Creep(Hrs.)	Rupture Life (Hrs.)	Total Elong. (%)
A. Cb 132M							
M-493	2400	-	-	.71	5	10.2	30.8
M-497	2400	3000/1	-	.18	15	27.8	20.2
M-497	2400	3000/1	2200/4	.20	15	25.3	20.2
M-497	2400	3200/1	-	.094	40	61.3	19.1
M-497	2400	3200/1	2200/4	.18	15	28.4	21.1
M-493	2400	3600/1	-	.0337	>135.8	135.8**	14.0
M-497	2400	3600/1	-	.043	53	62.6	6.5
M-497	2400	3600/1	2200/4	.037	75	88.3	5.7
M-493	2200	-	-	.83	4	8.9	40.1
M-493	2200	3600/1	-	.0226	>124.9	124.9**	3.1
M-493	1600*	-	-	.67	6	7.6	9.6
M-493	1600*	-	2000/4	.48	15	19.7	14.1
B. VAM-79							
96B	2400	-	-	.26	15	23.0	25.2
96A	2400	3000/1	-	.28	13	17.9	26.3
96A	2400	3000/1	2200/4	.27	8	13.8	25.3
96A	2400	3200/1	-	.08	30	40.0	21.7
96A	2400	3200/1	2200/4	.18	14	20.1+	22.5
96A	2400	3600/1	-	.05	35	48.7	13.8
96A	2400	3600/1	2200/4	.19	11	16.8	14.8
96B	1600*	-	-	.46	12	16.4	25.7
96A	1600*	-	2000/4	.32	21	24.3	23.3
C. SU-31							
	2400	-	-	3.06	2	3.3	29.2
	2400	3000/1	-	.30	15	20.4	26.4
	2400	3000/1	2200/4	.53	4	10.7	28.5
	2400	3200/1	-	.26	15	22.4	29.5
	2400	3200/1	2200/4	.43	5	11.0	27.3
	1600*	-	-	.13	40	54.1	17.9
	1600*	-	2000/4	.12	27	46.0	19.7

*Cold worked 20% at 1600°F after partial forging at 2400°F and recrystallization at 2950°F for 2 hours (Cb 132M and VAM-79) or 3150°F for 2 hours (SU-31).

**Specimen unloaded

+Power Failure - specimen under load at room temperature for 18 hours prior to reloading.

++Tested in vacuum of 10^{-5} torr.

was taken into solution at all annealing temperatures, a situation analogous to that discussed above. The best creep properties in this alloy were obtained in recrystallized and cold worked material. The fact that these properties were significantly better than those obtained for Cb 132M and VAM-79 in a similar condition is possibly a reflection of the higher temperature required to produce recrystallization. Additional carbon would then be available for precipitation to stabilize the cold worked structure at the creep testing temperature.

Property data obtained on forged and annealed (3600°F) Cb 132M indicate a significant effect resulting from small variations in chemistry. While carbon levels in the two heats are similar an increase in the zirconium content from 1.1% in heat M-493 to 1.9% in heat M-497 has resulted in an improvement in 1200°F tensile strength and a significant decrease in 2200°F creep rupture life. While it is likely that changes in the carbide phase stability at annealing and testing temperatures are caused by this compositional variation, it is not apparent how the resulting changes in carbide type affect properties.

The data obtained on VAM-79 may be compared with that obtained by other investigators. Begley, et al,[4] have published 2200°F creep-rupture data for VAM-79 annealed at 3632°F for two hours after swaging which indicate life considerably greater than obtained in this study for a similar condition. A rupture life of 46.4 hours was obtained at 37,000 psi compared to 48.7 hours at 30,000 psi in the present investigation. Since compositional differences do not appear to be significant it must be assumed that either cooling rate variations or the different working history are responsible. Furnace radiation cooling was employed in this study while the previous investigators used a hellum quench after the 3600°F annealing treatment.

Cold working studies have also been performed by swaging on recrystallized VAM-79[8]. Unfortunately, the experimental conditions (deformation at 1472°F, and tensile testing at 1400°F) do not permit a direct comparison with this study. A 20% deformation after recrystallization at 3092°F was found to increase the tensile yield strength from 49,400 psi to 117,200 psi, an improvement of 75,000 psi. In this study, 20% deformation by forging at 1600°F after a 2950°F recrystallization resulted in a smaller increase in yield strength over samples recrystallized at 3000°F for 1 hour. Presumably, the lower cold working temperature and possibly the higher (by 150°F) recrystallization temperature used in the referenced work accounted for the higher strength of the swaged material.

In consideration of its superior tensile properties in worked conditions and greater creep resistance when annealed, Cb 132 was selected for further study as a core alloy. The various thermal-mechanically treated conditions tested are thought to be representative of that which could be applied to turbine blade processing. Other working methods such as rolling or swaging and rapid quenching of parts would be difficult to apply in practice. Although the relative workability of Cb 132M is slightly poorer than the other two alloys, it has been demonstrated to be sufficient for blade fabrication[1].

It is hoped that future studies of thermal-mechanical processing will result in greater improvement in properties. Obviously, cold working and recrystallization temperatures have not been optimized. However, the results presented here offer encouragement for this method of balancing creep and tensile properties in forged parts.

B. Oxidation Resistant Alloys

1. Background and Selection

A great deal of experimental work has been devoted to an understanding of the nature of the oxidation of columbium and columbium-base alloys. In addition to the formation of a complex non-protective scale, the rapid inward diffusion of oxygen embrittles the substrate columbium alloy. Basic studies of this problem and of the effect of alloying on oxidation resistance have been summarized[9]. Consideration of the problem suggests certain potential remedies including: 1) the addition of elements having a higher valence than columbium to retard oxygen transport through the scale, 2) introduction of elements of smaller ionic size which may reduce the oxide volume, 3) the addition of elements promoting the formation of protective spinel type oxides, and 4) addition of elements which retard the inward movement of oxygen to the substrate. Judicious additions of alloying elements have resulted in a several-fold improvement in the oxidation resistance of columbium-base alloys. However, most of the data available on these alloys are of limited usefulness for the purposes of this program because of varying test temperatures and because results are often quoted as a weight gain due to oxidation, a measurement which does not relate directly to the remaining metal.

To be useful as a barrier alloy in the type application envisioned in this program, an alloy must of course possess significant oxidation resistance. Considering the application of a 0.020" layer of the barrier alloy, the limit of tolerable oxidation within reasonable time is obviously small. In order to provide total protection to the core alloy, oxidation resistance must relate both to a low rate of metal loss through scaling as well as imperviousness to oxygen. For most practical applications, non-brittle behavior is nearly as important as is oxidation resistance. Resistance to damage by foreign object impingement is necessary from low temperatures to 2200°F. Furthermore, in view of the probable method of attachment of the oxidation resistant alloy to the core alloy (discussed in a later section), the former must possess significant fabricability. Finally, the oxidation resistant alloy must be amenable to protective coatings and not fail catastrophically should the coating be damaged.

In order to evaluate these requirements, certain tests were selected for use. Oxidation tests in moving air at 2200°F allow measurement of weight changes, depth of oxygen penetration by microhardness survey, and the amount of metal lost. Room and elevated temperature ballistic impact tests using weighted BB's fired from a calibrated air pistol permitted an evaluation of resistance to brittle behavior. The ductility during fabrication was gaged by the ease of working to sheet material for impact testing.

In addition to the requirements discussed above, it is mandatory that the cladding or barrier alloy be compatible with the core alloy. When bonded to the core, it must not degrade the properties of the core by means of mechanical incompatibility nor must it deprive the core of strength over a period of time at high temperatures. Diffusion of undesirable elements into the core or the migration of elements such as carbon outward to the case (the "interstitial sink" effect)[10] must be avoided. This final requirement was not directly evaluated in Phase I of the program. However, it did receive considerable attention during Phase II.

Numerous alloy compositions have been developed with the intent of improving the oxidation resistance of pure columbium. From this group, ten significantly varied alloys were chosen which had the potential of fulfilling the requirements of a cladding or barrier alloy in columbium alloy turbine blade combinations. The nominal compositions of these alloys are given in Table VIII.

Alloys 1, 2, and 3 were chosen from a large number of experimental columbium base alloys which were expected to combine fabricability with oxidation resistance[11]. Alloys 4 and 5 were early commercially available alloys designed for improved strength[12]. For the purposes of this study, their improved oxidation resistance and fabricability compared to most structural columbium-base alloys were of special interest. A hafnium-base alloy (composition 6) which was reported to combine excellent resistance to oxidation and sufficient formability to produce sheet[13] has also been included although it may not be compatible with the selected columbium-base core alloy. Alloy No. 7 is the initial base alloy of a recent study conducted to develop a new oxidation resistant alloy[14]. This base was modified slightly to form composition 8 by the addition of small amounts of several elements including rhenium, the beneficial effect of which has been noted previously[15]. Composition 9 was similar to a cast alloy which exhibited excellent oxidation resistance at 2200°F during an AFML "in-house" study. An alloy similar to those studied under another Air Force program was included as alloy 10[16]. The Cb-5W-30Hf base was selected as one combining low oxygen penetration and acceptable fabricability. It was then modified for this study, hopefully to provide improved oxidation resistance.

2. Materials

The oxidation resistant alloy compositions were supplied by Battelle Memorial Institute in the form of cast rectangles measuring 1/2" x 1" x approximately 3". Castings were prepared by arc melting and re-melting each composition by the nonconsumable tungsten electrode method using reactor grade starting materials. After the final homogenization melt, metal was drop-cast into a chilled copper mold. All melting and casting operations were performed in an atmosphere of helium. A 1-1/2" length of each casting was utilized for oxidation testing while the remaining portion was rolled to sheet form by the vendor. (In the case of alloys 4 through 10, it was necessary to prepare two castings in order to provide sufficient material for both the oxidation tests and the ballistic impact tests of sheet specimens.)

TABLE VIII

CHEMICAL ANALYSIS OF ARC CAST ALLOYS SELECTED FOR CLADDING ALLOY*

Chemical Analysis (wt %)

Alloy No.	Density+	Cb	Ti	W	Al	Ta	Hf	Mo	V	Cr	Re	NI	Si	Co	Fe	O_2 (ppm)
1.**	0.216	Bal.	40	-	5	-	-	10	-	-	-	-	-	-	-	-
	5.97	Bal.	39.2	-	4.75	-	-	10.1	-	-	-	-	-	-	0.020	1020
2.	0.189	Bal.	50	-	10	-	-	-	-	-	-	-	-	-	-	-
	5.24	Bal.	51.4	<0.3	10.4	-	-	-	-	-	-	-	-	-	0.020	630
3.	0.236	Bal.	27	-	3	-	-	-	5	-	-	-	-	-	-	-
	6.53	Bal.	29.0	<0.3	2.90	-	-	-	4.6	-	-	-	-	-	0.030	525
4. (Cb 16)	0.318	Bal.	10	20	-	-	-	-	3	-	-	-	-	-	-	-
	8.81	Bal.	9.6	21.3	-	-	-	-	2.8	-	-	-	-	-	0.021	330
5. (Cb 7)	0.350	Bal.	7	28	-	-	-	-	-	-	-	-	-	-	-	-
	9.69	Bal.	6.8	28.8	-	-	-	-	-	-	-	-	-	-	<0.001	250
6.	0.476	-	-	-	1.1	25	Bal.	-	-	0.6	-	-	-	-	-	-
	13.16	-	-	0.3	1.6	25.5	Bal.	-	-	0.15	-	-	-	-	0.013	470
7.	0.320	Bal.	10	10	-	10	1.8	-	-	-	-	-	-	-	-	-
	8.85	Bal.	9.8	10.5	-	12.0	1.9	-	-	-	-	-	-	-	0.004	325
8.	0.323	Bal.	10	10	-	10	1.8	3	-	2	2	-	-	-	-	-
	8.93	Bal.	10.4	10.1	-	10.3	2.0	2.9	-	2.3	1.85	-	-	-	0.005	300
9.	0.253	Bal.	20	3	3	3	-	-	3	3	-	3	1	3	2	-
	7.01	Bal.	21.2	3.1	3.2	4.0	-	-	3.0	3.5	-	3.0	0.48	3.1	2.0	260
10.	0.347	Bal.	5	5	-	-	30	-	-	-	3	-	-	-	-	-
	9.61	Bal.	5.3	5.1	-	-	29.2	-	-	-	2.2	-	-	-	0.053	240

* Analysis supplied by Battelle Memorial Institute.

** Nominal compositions shown in first line.

+ First figur .n lbs/in^3
Second figure in gms/cm^3

The chemical analyses, shown in Table VIII, were taken from riser material by the vendor. They include an analysis for major element content; possible pickup of copper, tungsten, and iron; and a check of oxygen, hydrogen, and nitrogen levels. Hydrogen was under 50 ppm in all alloys and nitrogen less than 30 ppm. Copper pickup was insignificant. The other impurity levels are shown in Table VIII. Oxygen levels were generally low except in alloys 1 and 2, each of which contain a large percentage of titanium. The density of each alloy is also shown in Table VIII. Although an application of only 0.020" of an oxidation resistant alloy to the core would minimize density effects, there are considerable variations of from 0.189 lbs/in^3 for alloy 2 to 0.476 lbs/in^3 for alloy 6.

Photomicrographs, supplied by Battelle Memorial Institute, of each alloy in the "as-cast" condition are shown in Figures 30 through 34. (The etchant used consisted of 45% H_2O, 30% HCl, 20% HNO_3, and 5% HF). A typical dendritic microstructure is noted for all alloys. Although not readily apparent in the micrograph, there was considerable microporosity in alloy 9. All castings were radiographed prior to further processing and determined to be internally sound.

3. Oxidation Testing

Oxidation tests were performed on samples cut from the cast portions of each alloy. The specimens used were 1/2 inch square coupons surface ground on both faces to a thickness of approximately 0.100". After degreasing, these samples were exposed in a Marshall tube type furnace at 2200°F. The temperature was maintained in the 3-1/2" long hot zone to within ±7°F as measured by a sealed Chromel-Alumel thermocouple. A filtered air flow of 2 cu. ft./hr. was maintained during testing. Grooved zirconia fixtures were used to position the coupons vertically such that both faces were exposed to the air flow. The sample and holder were covered upon removal from the furnace to prevent loss of spalled oxide while cooling in air. Exposure times of 1, 4, 20, and 64 hours were used for all alloys.

Photographs of the specimens after 2200°F exposure for 1, 4, 20 and 64 hours are shown in Figures 35 through 38. On the basis of these photographs, it would appear that alloys 1, 6 and 9 are the least heavily oxidized. However, it is necessary to consider microstructures in order to correctly ascertain oxidation resistance in terms of oxygen penetration and the amount of metal converted to oxide. Representative photomicrographs of each alloy after various oxidation exposures are shown in Figures 39 through 48. In most cases, the formation of intragranular oxide particles and an accentuation of grain boundaries indicates the increasing depth of oxygen penetration with longer exposure times. In alloy 6 (hafnium base) the entire thickness became internally oxidized after 1 hour. Longer exposures increased the size of these particles and the thickness of the oxidized surface layer. The oxide did not spall off of this alloy to the extent common with the other nine columbium base alloys.

Data recorded from the test coupons included: weight change as a result of oxidation, amount of metal lost due to surface oxide formation, and the depth of oxygen penetration into the substrate alloy. Table IX gives these results and summarizes the photomicrographs. Because of the loss of small particles due to spalling, the weight gain measurements are considered to be of lesser value than the other measurements presented. Surface recession data are averages of several readings across the thickness of each specimen. Depth of oxygen contamination was measured metallographically and by microhardness traverse (100 gram Knoop indentor).

Several of the alloys tested resisted metal loss to a tolerable degree (less than 0.020" in 64 hours). However, all permitted oxygen contamination to a much greater depth. Using the twenty hour exposure data, only alloys 5, 7, 8, 9 and 10 appear to have potential. However, after 64 hours, alloy 8 was totally consumed and alloys 5 and 7 had considerable penetration.

Other government sponsored research, current with this phase of the program, has resulted in an improvement to alloy 7[14]. According to Westinghouse data, the addition of 3% aluminum to the base composition of alloy 7 (Cb-10Ti-10W-10Ta-1.8HF) reduces surface recession after 64 hours from 13.0 mils to 9.3 mils with a corresponding reduction in oxygen penetration. (A later modification was introduced into Phase II studies of this program.)

4. Fabrication

Portions of the cast material representing each alloy investigated were used by the supplier for attempted production of 20 mil sheet to be used for testing of impact resistance. Aside from the sheet production, this procedure provided information relative to the fabricability of each alloy. In the case of alloys 4 through 10, it was necessary to prepare two castings in order to provide sufficient material for rolling. The chemical analyses of the castings used for fabrication were substantially the same as those reported for the oxidation tested material, Table VIII.

The castings were prepared for rolling by surface conditioning, annealing, and in most cases, enclosing in an electron beam welded molybdenum jacket. The annealing temperatures were determined individually and are shown in a compilation of pertinent fabrication data, Table X. It was possible to process alloys 1 and 3 at room temperature. Attempts to roll alloy 2 under similar conditions were unsuccessful. The billet was then reconditioned, jacketed in molybdenum and processed hot. Special comment relating to the processing of certain alloys and the final status of each is indicated in Table X. Photographs of the material in the terminal condition are included, Figures 49 to 53. It was possible to produce sheet of reasonable quality from only four alloys; 1, 3, 7, and 10. Alloys 5 (Cb 7) and 9 were essentially unworkable, while varying degrees of success were experienced with the remaining compositions.

TABLE IX

OXIDATION TEST DATA (2200°F) FOR POTENTIAL CLADDING ALLOYS[a]

Alloy No.	Weight Gain (mg/cm^2)				Surface Recession (mils)				Oxygen Substrate Penetration (mils)++			
	1 hr	4 hrs	20 hrs	64 hrs	1 hr	4 hrs	20 hrs	64 hrs	1 hr	4 hrs	20 hrs	64 hrs
1	5.5	14.3	36.4	246.7*	1.0	1.0	28.5	47.5*	3/22	5/36	19+/19+	*
2**	1.6	1.9	6.2	19.9	0.5	0.5	2.0	4.5	15/38	45/41	46+/46+	43.5+/43.5
3	10.6	21.9	69.7	162.2	1.0	2.5	8.0	18.5	5/40	9/47+	41.5+/41.5+	31.5+/31.5
4	11.9	34.5	52.3	133.5	1.0	3.5	10.5	15.0	6/12	10/20	26/45	45.5+/45.5
5**	0.5	24.5	29.9	59.1	3.5	1.0	4.0	8.0	9/13	14/15	30/25	46/43
6	12.9	12.5	23.5	171.3	2.5	4.0	6.5	11.0	45.5+/45.5+	44+/44+	41.5+/41.5+	37+/37+
7**	2.3	3.6	54.5	99.6	1.5	1.5	4.5	13.0	9/15	9/30	26/32	40/40
8	7.2	30.6	43.9	212.6*	1.5	3.0	8.5	44.0*	6/7	10/14	21/30	*
9	4.8	9.1	21.9	137.3	1.0	1.5	3.0	9.0	5/8	10/-	18/-	30/-
10	20.6	35.5	64.6	144.1	1.5	1.5	2.5	6.5	7/8	13/13	19/20	35/34

* Substrate totally consumed

** Weight gain data probably affected by oxide loss.

\+ Total oxygen penetration.

++ Penetration determined optically/penetration determined by Knoop microhardness traverse (100 gm load).

[a] Air flow of 2 cu. ft./in. maintained during tests.

TABLE X

FABRICATION DATA FOR OXIDATION RESISTANT ALLOYS

Alloy	Initial Annealing Temp. (°F)	Rolling Temp. (°F)	Intermediate Annealing Temp. (°F)	Final Rolling Temp. (°F)	Final Thickness (in.)	Final Condition
1	2400	Room Temp.	2200	Room Temp.	0.020	Annealed 2200°F
2	2400	2200	2600	900	0.041	*
3	2400	Room Temp.	2200	Room Temp.	0.0195	Annealed 2200°F
4	3100	2200	2600	900	0.039	*
5	3100	2200	-	-	-	*
6	2400	2200	2600	-	0.043	*
7	3100	2200	2400	800	0.020	Annealed 2400°F
8	3100	2200	2600	900	0.043	*
9	2200	1900	-	-	-	*
10	3100	2200	2600	900	0.020	Annealed 2400°F

* Notes on Present Condition

Alloy 2. Annealed 2600°F, reduced from 0.043" to 0.041" at 900°F, rolling discontinued.
Alloy 4. Annealed 2600°F, reduced from 0.042" to 0.039" at 900°F, rolling discontinued.
Alloy 5. Failed in early stages of rolling at 2200°F.
Alloy 6. Specimen split lengthwise upon removal of molybdenum can, rolling discontinued, annealed 2400°F.
Alloy 8. Annealed 2600°F, reduced 0.052" to 0.043" at 900°F, rolling discontinued.
Alloy 9. Alloy found to be disintegrated upon removal of molybdenum jacket, see Figure 53.

Typical microstructures of each alloy except 5 and 9 are shown in the terminal condition, Figures 54 and 55. Alloy 5 exhibited an essentially cast structure, as would be expected, similar to Figure 34. It was not possible to obtain a metallographic sample for alloy 9. The microstructures shown are typical of the alloy condition, showing varying degrees of deformation in the alloys which failed during processing and a recrystallized structure in the annealed alloys. A chemical analysis for interstitial content and iron pickup was performed on each alloy after fabrication, Table XI. The high oxygen levels in alloys 1, 2, and 6 are reflected in the microstructures of these alloys. It should be noted that the initial oxygen levels for these alloys were 960 ppm, 915 ppm, and 860 ppm respectively. The iron content in alloy 10 is also the result of a high concentration (0.104%) in the starting material. Apparently, contamination of these alloys from the atmosphere or from processing equipment during carefully controlled processing will not be a severe problem.

The inability of many of these alloys to be fabricated successfully is certainly a matter of concern when selecting compositions for Phase II studies. However, it is encouraging to note that two of the alloys successfully reduced to sheet, 7 and 10, were two which also showed superior oxidation and oxygen penetration resistance. Furthermore, improved versions of alloy 7 appear to possess adequate fabricability[14].

5. Ballistic Impact Testing

Ballistic impact testing was utilized to assess the resistance of the alloy sheet to the damage which might occur in an engine if struck by ingested particles. Stainless steel BB's weighted with lead pellets were used as the impacting particle, the average pellet weight being 1.178 grams. The helium powered air pistol apparatus utilized is shown in Figure 56. The gun was instrumented to read helium fire pressure which was converted to projectile velocity using a previously derived calibration curve. Rectangles approximately 1" x 1-1/4" were cut from 0.020" sheet for test samples. Testing was conducted at room temperature and 2100°F on material in the as-received (annealed) condition and also after a 20-hour exposure in air at 2200°F. Sufficiently high quality sheet for testing was available only for alloys 1, 3, 7, and 10.

Because of the small amount of material available, it was necessary to use the same specimen for all testing at successively higher impacting energies. This procedure presented no special problem at room temperature but did necessitate cooling and reheating the specimen after each test at 2100°F. This was required to examine and re-position the sample. Each reheating was accomplished in approximately 12 minutes.

Impact test data are given in Table XII. The tested samples and appropriate impact energies are shown in Figure 57. Attempts were also made to test material after 2200°F exposure. However, only alloy 1 was not fully oxidized after the exposure, and it was totally demolished after a single impact at the lowest energy. The extremely brittle nature of this specimen indicates that while it was not fully oxidized, oxygen penetration was complete. Testing of as-annealed sheet indicated little difference in impact resistance for all alloys between room temperature and 2100°F.

TABLE XI

CHEMICAL ANALYSIS OF OXIDATION RESISTANT ALLOYS AFTER FABRICATION

Alloy No.	ppm by weight			
	Iron	Oxygen	Hydrogen	Nitrogen
1	280	1240	<2	130
2	330	1010	5	125
3	290	655	8	85
4	30	510	<2	100
5	-	-	-	-
6	120	1080	<2	90
7	50	430	4	95
8	160	390	<2	120
9	-	-	-	-
10	1010	460	5	90

TABLE XII

BALLISTIC IMPACT DATA FOR OXIDATION RESISTANT COLUMBIUM-BASE ALLOYS

Alloy No.	Test Temp. (°F)	Pellet Velocity cm/sec. (x 10^4)	Pellet Velocity ft/sec.	Impact Energy ergs (x 10^8)	Impact Energy ft/lbs.	Remarks
1*	R.T.	1.29	425	0.987	7.25	
	"	1.78	585	1.875	13.8	
	"	2.23	730	2.92	21.5	slight cracking
	"	2.59	850	3.96	29.1	cracking
3*	"	1.29	425	0.987	7.25	
	"	1.78	585	1.875	13.8	
	"	2.23	730	2.92	21.5	slight cracking
	"	2.59	850	3.96	29.1	ruptured
7*	"	1.29	425	0.987	7.25	
	"	1.78	585	1.875	13.8	cracking
10*	"	1.29	425	0.987	7.25	cracking
	"	1.78	585	1.875	13.8	shattered
1*	2100	1.29	425	0.987	7.25	
	"	1.78	585	1.875	13.8	perforated
3*	"	1.29	425	0.987	7.25	
	"	1.78	585	1.875	13.8	
	"	2.23	730	2.92	21.5	
	"	2.59	850	3.96	29.1	perforated
7*	"	1.29	425	0.987	7.25	
	"	1.78	585	1.875	13.8	cracking
	"	2.23	730	2.92	21.5	perforated
10*	"	1.29	425	0.987	7.25	
	"	1.78	585	1.875	13.8	perforated
1+	R.T.	1.29	425	0.987	7.25	shattered
1+	2100	1.29	425	0.987	7.25	shattered

* Sheet tested in the as-annealed condition.

\+ Sheet tested after a 20-hour exposure in air at 2200°F.

It is difficult to compare these impact tests with data for other materials. There is no firm indication of what level of resistance is required for the application in question other than to protect the core material. None of the alloys can be considered as being completely brittle although alloys 1 and 3 are more resistant to impact damage than 7 and 10. (Unfortunately, the oxidation resistance of alloys 1 and 3 is unacceptable.) It is likely that the impact resistance of any cladding alloy sheet will be changed when it is bonded to the relatively thick core alloy. This aspect will be discussed in the Phase II section of this report.

6. Discussion

Consideration of the performance of the ten oxidation resistant alloys in the areas of oxidation resistance, sheet fabricability, and ballistic impact resistance indicates that only alloys 7 (Cb-10Ti-10Ta-10W-1.8 Hf) and 10 (Cb-5W-30Hf-5Ti-3Re) can be considered for further study in combination blades. While these compositions are really inadequate for the intended use, it was felt that they would be of sufficient use to adequately evaluate the feasibility of the combination blade concept. Meanwhile, these compositions have been upgraded and other new oxidation resistant alloys will probably be developed. These should be applicable to the barrier layer concept evaluated in this program.

C. Bonding Study

1. Selection of Attachment Method

The fabrication of gas turbine blades is generally accomplished by precision casting or precision forging. Since methods for casting columbium base alloys to the tolerances and integrity required have not yet been developed, multi-step forging sequences must be used for blade fabrication. Considering the production of the composite blade contemplated in this program by forging, two basic approaches may be utilized:

1. Forge the desired part from a suitable high strength core alloy and apply the oxidation resistant alloy during the final forging operation, or after the completion of forging, by some suitable method; or

2. Encase the high-strength alloy forging blank in a sleeve of the oxidation-resistant alloy and forge the composite to the desired configuration.

A number of reasons dictate against the second approach:

1. Variability in thickness of the outer material can result from unequal flow properties at the forging temperature.

2. During forging, separation of the two components can occur resulting in voids and forging laps.

3. It may prove to be impossible to prevent oxidation of the inner core alloy during forging, especially at voids (item 2 above).

4. Both the forging operations and post-forging heat treatments will probably result in diffusion to an intolerable degree between the high strength core and the oxidation resistant alloy.

Thus, the method of application chosen for this program is that of attaching the two components after final forging.

Various techniques could be used to attach the oxidation resistant layer to the core alloy. Deposition processes are often used to produce protective coatings on refractory alloys. However, it does not seem feasible to deposit multi-component columbium alloys onto the core in this manner. Particle methods such as plasma spraying, spray-sintering, or slurry-sintering would not be expected to yield a sufficiently dense layer. The method chosen for this program is diffusion bonding, a technique which has frequently been used to join dissimilar metals. This technique has the additional advantage of permitting small experimental samples to be easily produced. In Phase I, basic parameters for diffusion bonding of dissimilar columbium alloys were examined.

2. Requirements for Diffusion Bonding

In general, diffusion bonding requires two processes: localized plastic flow resulting in intimate contact between the surfaces to be bonded, and the formation of a continuous bond through solid state diffusion across the interface. Important process variables include pressure, temperature, time, atmosphere, and interface preparation. Included in the latter category are such items as surface condition and the use of intermediate foils which promote bonding, probably by the establishment of intimate contact between the two components at lower bonding pressures. The intermediate foil can also be chosen to retard or promote diffusion between the two materials being bonded. Also, the foil must not form brittle intermetallic compounds with either the core or cladding alloys.

For the system under consideration in which two different alloys, each having unique properties, are to be joined in intimate contact, it is important to retard excessive interdiffusion during bonding. Specific effects which could be experienced in a composite part because of diffusion are:

1. The core mechanical properties, especially ductility, may be reduced to undesirable levels.

2. The oxidation resistant barrier alloy may become embrittled and thus prone to cracking resulting in a loss of protection for the core.

3. The barrier alloy may suffer a progressive loss of oxidation resistance.

Minimization of diffusional effects demands that any high temperature thermal mechanical processing of the core alloy be completed prior to bonding and also that careful attention be given to the choice of bonding parameters.

Such bonding variables as temperature, pressure, and time should be minimized in order to reduce structural changes during processing. Pressure can be applied either by direct mechanical coupling or transmitted by a fluid. However, it is necessary that force be applied normal to the bonded surface to prevent cocking of the specimen and partial bonding. This requirement becomes more important as temperatures and pressures are lowered since if the workpiece yield strength is not exceeded, it will not flow to accommodate non-uniform loading.

3. Materials and Equipment

For the preliminary bonding studies conducted in Phase I, 1/2" square coupons of a representative core alloy (Cb 132M) and an oxidation resistant type alloy (Cb-10Ti-10W-1Zr) were employed. The thicknesses were approximately 0.125" and 0.050" respectively. The Cb-10Ti-10W-1Zr sheet had been produced by room temperature rolling and was bonded in the as-rolled condition. The Cb 132M was processed at 2400°F in a manner described previously in this report to simulate blade forging. Some bond coupons were in the as-forged condition. However, since Cb 132M will probably require a high temperature recrystallization-anneal prior to bonding for optimum creep rupture properties, most bonding was performed using samples previously heat treated at 3600°F for 1 hour. Prior to bonding, the mating surfaces of both components were polished through 3/0 paper, degreased, and chemically etched in a solution consisting of 65% HNO_3 and 35% HF[17].

The apparatus used for these studies is shown, Figure 58. The sample, positioned in a quartz tube, as shown in Figure 59, was heated by induction coils acting upon molybdenum susceptors. Temperature was monitored by a Pt/Pt-10% Rh thermocouple in contact with the columbium alloy specimens and controlled manually by adjusting the induction phase controller. A vacuum of approximately 5×10^{-5} Torr was maintained throughout the processing. Bonding pressure was applied by means of a compressed air pressure multiplier acting through steel and alumina rods to the specimen. Samples were brought to bonding temperature within 20 minutes under vacuum and pressure. These conditions were maintained until the specimen had cooled to room temperature following a run.

4. Bonding Parameter Studies

The study of diffusion bonding parameters for dissimilar columbium base alloys was undertaken for two reasons: to determine if diffusion bonding was a feasible means of attaching the cladding layer to the core; and, secondly to establish suitable times, temperatures, and pressures for Phase II studies. Temperatures between 2000°F and 2400°F, times of 30 minutes and 1 hour, and pressures of 1000 psi and 5000 psi were investigated. The use of tantalum (0.5 mil) and vanadium (1 mil) foil as an intermediate layer was also studied.

The results of these bonding trials are summarized, Table XIII. The approximate depth of carbon depletion in the Cb 132M due to bonding was determined by microhardness traverses (100 gram Knoop indentor) perpendicular to the bonded interface. Bond quality was considered to be good if both components were joined across the entire width of the sample with very few voids present due to initial surface irregularities.

TABLE XIII

SUMMARY OF PHASE I BONDING STUDIES (Cb 132M to Cb-10Ti-10W-1Zr)

TRW Bond No.	Cb 132M Condition	Temp. (°F)	Time (hr)	Pressure (psi)	Intermediate Foil	Approx. Depth of Carbon Depletion in Cb 132M (mils)*	Bond Quality	Remarks
1	As Forged (2400°F)	2050	1	5000	-	<5	Poor	Only one side bonded, voids.
2	As Forged (2400°F)	2350	1	5000	-	~30	Fair	2/3 bonded, carbide precipitation in sheet.
3	As Forged (2400°F)	2400	1	5000	-	~30	Good	Occasional voids carbide precipitation.
5	3600°F/1 hr.	2350	1	5000	-	30	Good	Carbide precipitation.
6	3600°F/1 hr.	2350	1	5000	Ta	>30	Good	Carbide precipitation.
7	3600°F/1 hr.	2400	0.5	5000	-	30	Good	Carbide precipitation in sheet.
8	3600°F/1 hr.	2200	1	5000	-	5	Fair	Partially bonded.
9	3600°F/1 hr.	2200	1	5000	Ta	5	Fair	Partially bonded.
10	3600°F/1 hr.	2200	1	5000	V	5	Good	
14	3600°F/1 hr.	2200	0.5	5000	V	8	Fair	Partially bonded.
13	3600°F/1 hr.	2200	0.5	1000	V	8	Fair	Partially bonded.
15	3600°F/1 hr.	2000	0.5	1000	V	-	Poor	Bonded on one edge only.
17	3600°F/1 hr.	2000	0.5	1000	V	5	Good	Adapter plates used.

* Determined by measuring depth of significant hardness decrease by 100 gram Knoop indentor.

Initial trials were conducted in order to determine whether diffusion bonding could be utilized to join the two components. The results, using as-forged Cb 132M, indicated that bonds were possible at 2400°F but that exposure to this temperature resulted in severe carbon depletion in the core (probably due to the 10% titanium in the sheet alloy). Bonds produced at lower temperatures (Numbers 1 and 2) were not joined across the entire sample. However, it was felt that this was at least partially due to an eccentricity of load application in the bonder. Steps were subsequently taken to more carefully align the bonding apparatus.

As noted previously, a heat treated structure will probably be necessary in order to obtain sufficient creep strength. Therefore, all additional bonding was conducted with annealed (3600°F for 1 hour) Cb 132M. A typical bond, Number 5 produced at 2350°F, is shown in Figure 60. Carbide precipitation is evident in the Cb-10Ti-10W-1Zr adjacent to the bond line. The loss of carbon in the Cb 132M is verified by the microhardness traverse also shown, Figure 60. The use of a 0.005" tantalum foil interlayer, Number 6, Figure 61, resulted in a slightly superior bond for the same bonding conditions but did not alleviate the carbon depletion problem, In this case, carbide particles were formed at the Ta-Cb 132M bond line rather than in the Cb-10Ti-10W-1Zr. While good quality bonds could be produced at 2350°F and above, it was evident that serious carbon depletion of the core alloy during processing could not be prevented.

Samples prepared at 2200°F and 2000°F resulted in significantly less carbon depletion, Table XIII. By insuring careful alignment of the bonding fixtures and using intermediate foils, it was generally possible to produce good bonds. Bond Number 14, in which a vanadium foil was used to promote contact and reduce carbon transfer, is illustrated in Figure 62. The portion of this sample which was bonded (about 3/4) was of good quality and the level of carbon depletion was reduced considerably. An alloy consisting of 95%V-5%Ti has been previously shown to have no effect at 2200°F on the carbon content of the columbium alloy D-43 when bonded to it(10).

The use of small adapter plates of 304 stainless steel to accommodate non-uniform loading was investigated. These plates of 0.090" thick stainless were placed between the alumina dies and the columbium sandwich. At the bonding temperature and pressure, they were able to flow plastically to conform to the space between the rigid dies and columbium sandwich, thus acting as a fluid medium to transmit pressure. Bond Number 17, produced at 2000°F using adapter plates is shown in Figure 63. Bond quality was excellent across the entire sample width and carbon depletion is relatively minor.

5. Discussion

The diffusion bonding trials conducted in Phase I of this program have aided in establishing bonding parameters for further study. While satisfactory bonds could most easily be obtained at temperatures of 2350°F and above, the level of carbon depletion in the core alloy is probably intolerable. Therefore, lower bonding temperatures are mandatory. Tantalum and vanadium foil interlayers seemed to aid in bonding by promoting surface contact and in the case of vanadium perhaps by reducing carbon migration.

Samples prepared at 2400°F and found to be bonded over the entire specimen width were generally deformed slightly, the sample thickness gradually decreasing across the sample from one edge to the other. This observation indicates that the ability of the sample to flow in order to accommodate eccentric loading is most responsible for the high quality of these bonds. The lack of complete bonding at lower temperatures is probably due to this slightly non-uniform loading and the inability of the bond sample to deform plastically. The use of adapter plates is a preferred solution to this problem, since increased pressures and temperatures will cause sample deformation and in the case of temperature, excessive carbon migration. For the temperatures investigated, the bonding times and pressures used appeared to have little effect on overall bond quality.

D. Conclusions and Selection for Phase II

In consideration of the results presented and discussed previously in this section of the report, the following conclusions are warranted. Selections of materials and methods for Phase II studies are also stated.

1. Core Alloy

a. The forgeability of all columbium-base alloys studied studied (Cb 132M, VAM-79, and SU-31) appears to be adequate for turbine blade fabrication.

b. The recrystallization behavior of Cb 132M, VAM-79, and SU-31 forged at 2400°F to a 70% thickness reduction was found to vary significantly. SU-31 was more resistant to recrystallization than the other two alloys.

c. The specific thermal-mechanical processing sequence used to fabricate high strength columbium alloys greatly affects mechanical properties.

d. Annealing at 3600°F for 1 hour resulted in the highest 2200°F creep strength for Cb 132M and VAM-79. However, this condition was brittle and low in strength at 1200°F.

e. The highest 1200°F tensile strength for Cb 132M and VAM-79 was observed in as-forged material (2400°F). However, creep rate at 2200°F was high for this material.

f. Recrystallization after partial forging followed by 20% deformation at 1600°F resulted in a particularly good balance of 1200°F tensile and 2200°F creep strength in SU-31. Similar treatment gave good 1200°F tensile properties in Cb 132M and VAM-79.

g. These data showed that the highest 2200°F creep strength and 1200°F tensile strengths were obtained in Cb 132M. Therefore, this alloy was selected for studies in Phase II of this program.

2. Oxidation Resistant Alloy

a. Measuring oxidation resistance by metal-loss and oxygen penetration, it appears that experimental alloys 5,7,9, and 10 can provide protection to a core alloy for times of at least 20 hours.

b. The oxidation resistant alloys are characterized by poor fabricability; two of the more oxidation resistant alloys (specifically 5 and 9) could not be fabricated to sheet.

c. Ballistic impact tests at room temperature and 2100°F showed that Alloys 7 and 10 could withstand particle impact without shattering. Performance was similar at both test temperatures.

d. Based on oxidation resistance, fabricability and impact resistance, Alloys 7 and 10 were selected for Phase II studies. Alloy 7 was later replaced with a modification containing 3% Al and 5% additional Ti.

3. Diffusion Bonding

a. Solid state diffusion (particularly of carbon) and specimen deformation occur to an intolerable degree when bonding is conducted above 2300°F.

b. A vanadium foil interlayer aids bonding by promoting interfacial contact between the two major components and probably by restricting carbon diffusion from the high strength core alloy to the cladding layer.

c. Diffusion bonds were successfully produced at 2000°F when using relatively ductile adapter plates to accommodate eccentricity in loading.

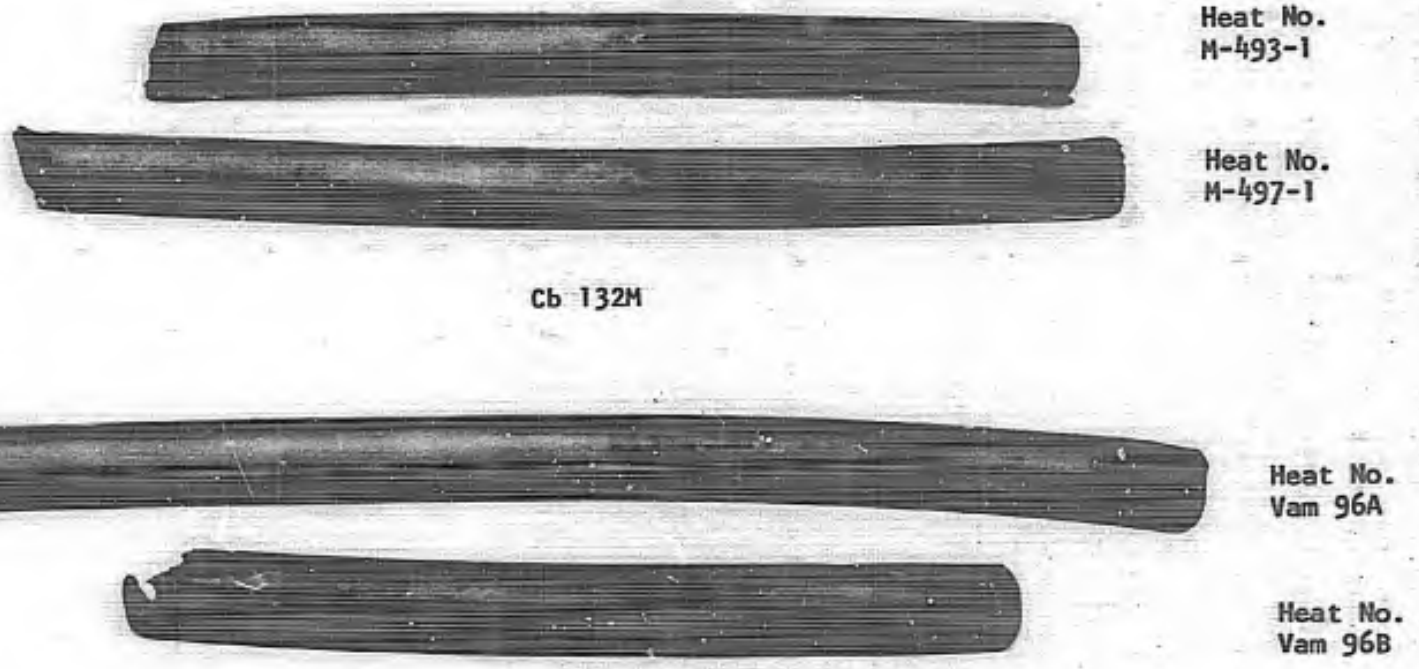

Figure 1. Columbium base alloys extruded 4:1 from 3". Molybdenum can intact.

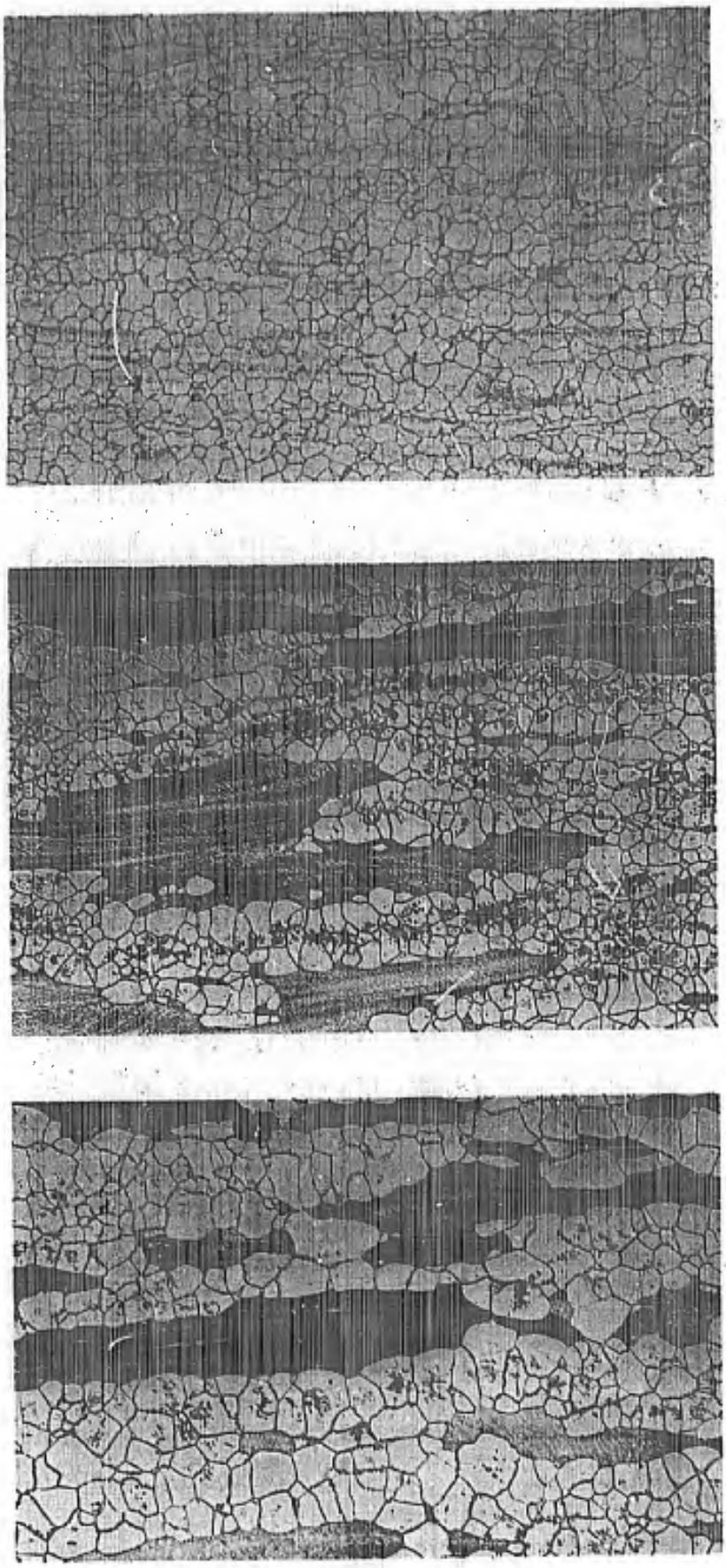

A. Heat No. M-493-3
Knoop HN=325
(100 gm load)

B. Heat No. M-493-1
Knoop HN=327
(100 gm load)

C. Heat No. M-497-1
Knoop HN=327
(100 gm load)

Figure 2. Longitudinal microstructure of extruded Cb 132M (4:1 reduction at 3400°F), Heat No. indicated. Magnification: 100X.

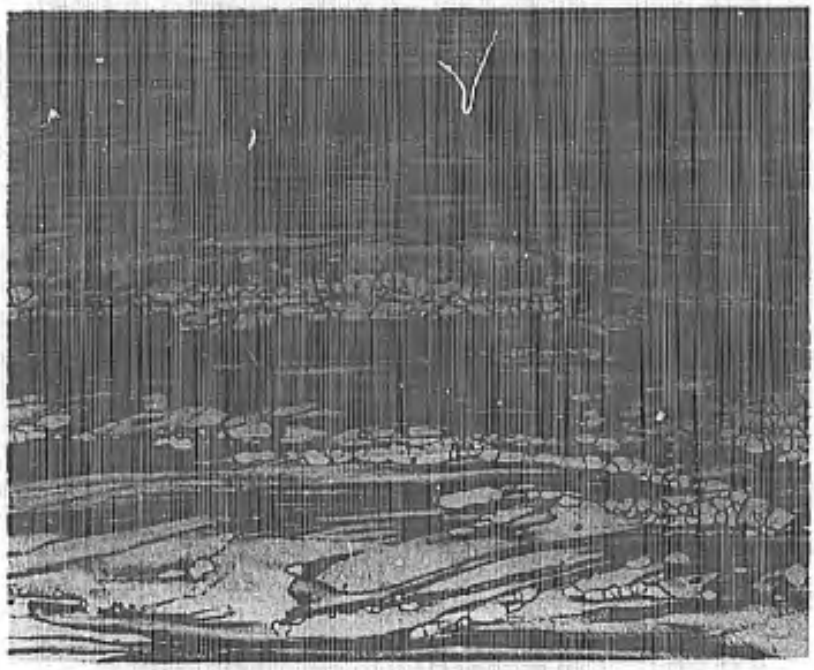

A. Heat No. Vam 96A — Knoop HN=296 (100 gm load)

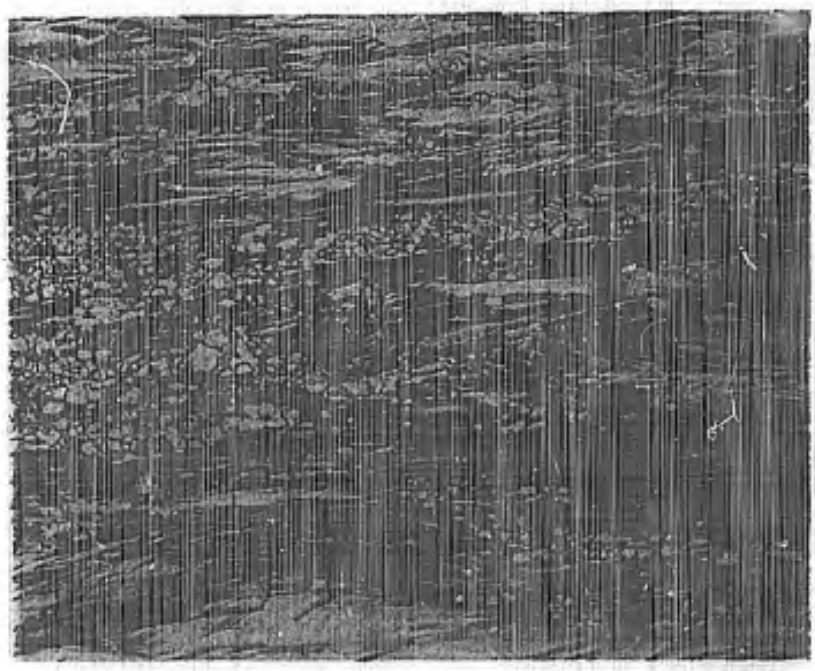

B. Heat No. Vam 96B — Knoop HN=309 (100 gm load)

Figure 3. Longitudinal microstructure of extruded VAM-79 (4:1 reduction at 3200°F), Heat No. indicated. Magnification: 100X.

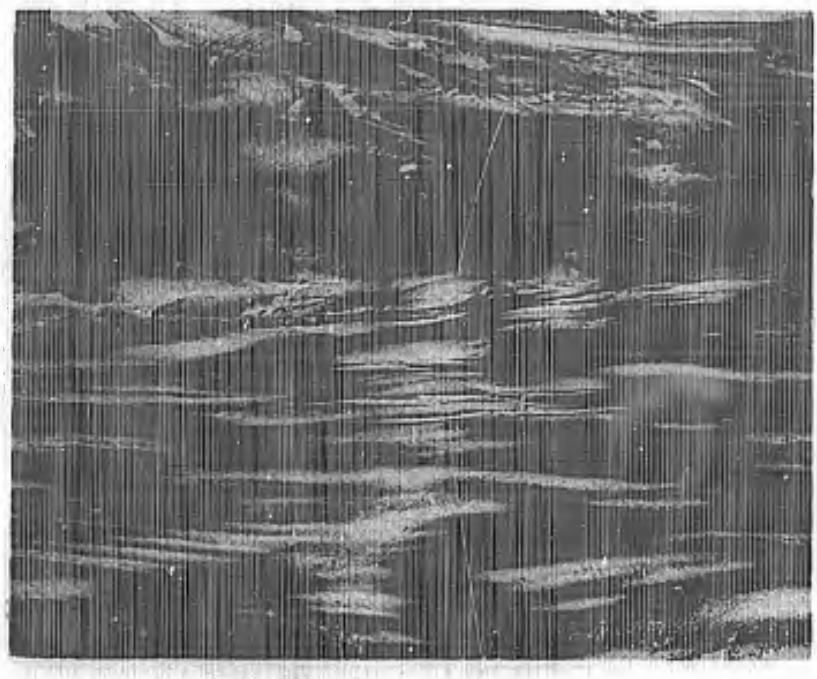

Knoop HN=269
(100 gm load)

Figure 4. Longitudinal microstructure of extruded SU 31 (4:1 reduction at 2642°F, stress relieved at 2372°F). Heat No. 17A. Magnification: 100X.

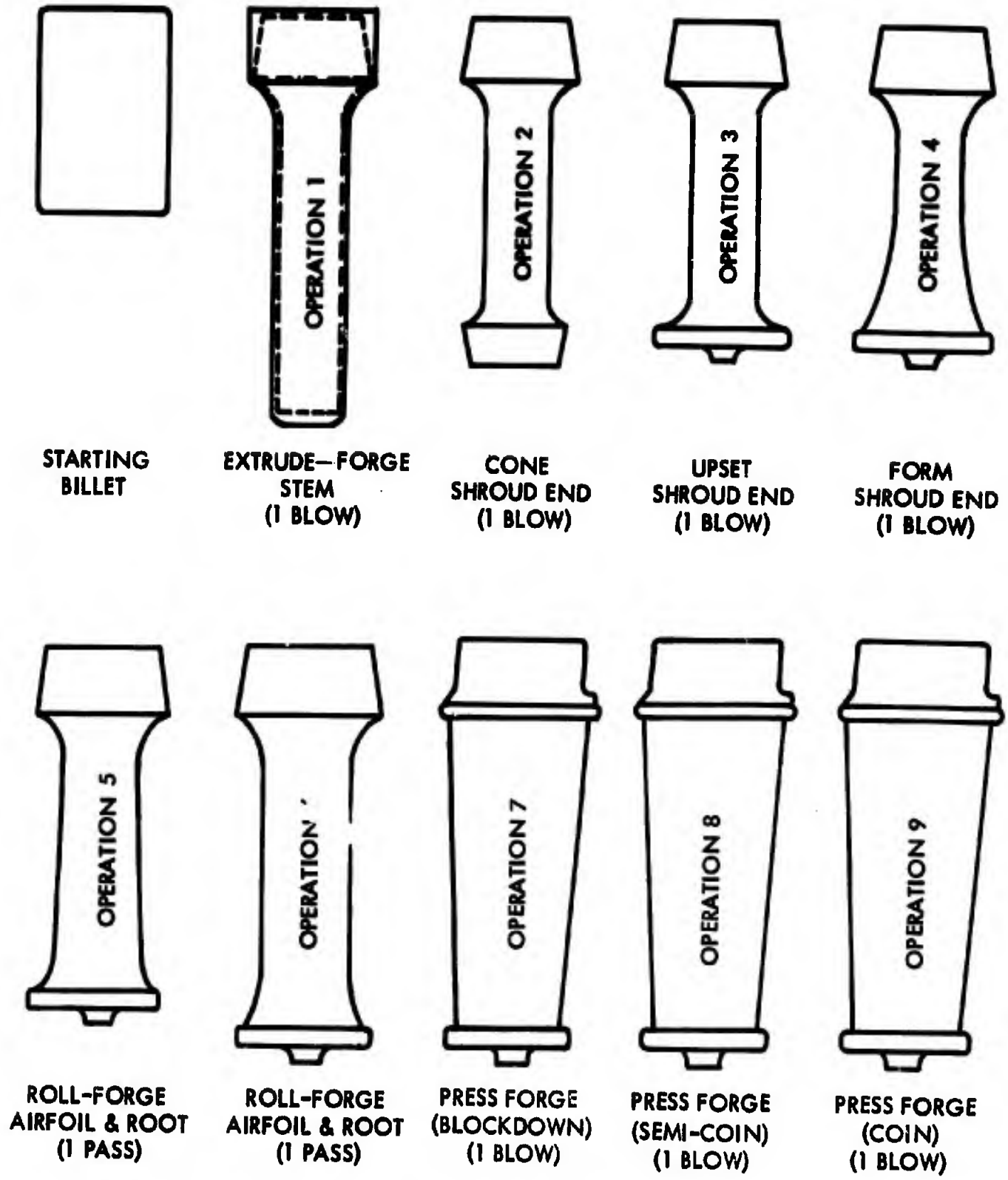

Figure 5. JT-3D first stage turbine rotor blade forging sequence as modified for Cb 132M Alloy. Note machining required (to broken line configuration) after operation 1.

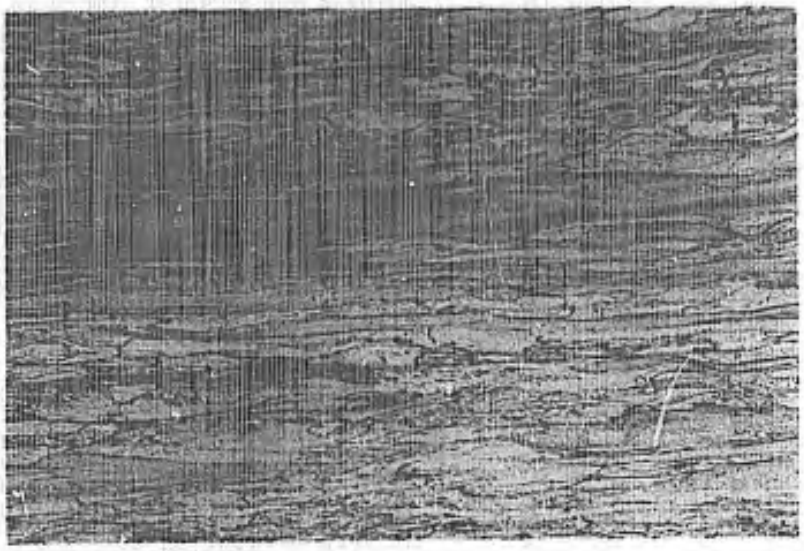

A. Cb 132M
Heat No. M-497-1

Knoop HN=379
(100 gm load)

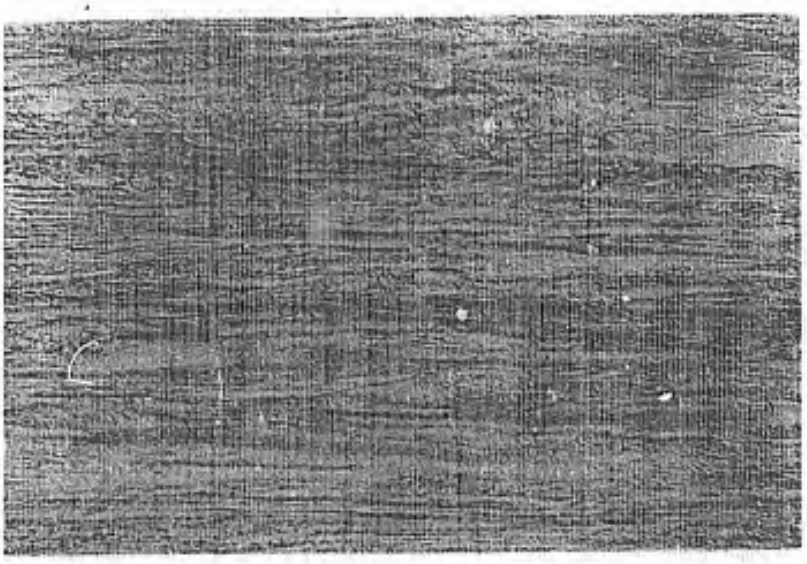

B. VAM-79
Heat No. Vam 96A

Knoop HN=342
(100 gm load)

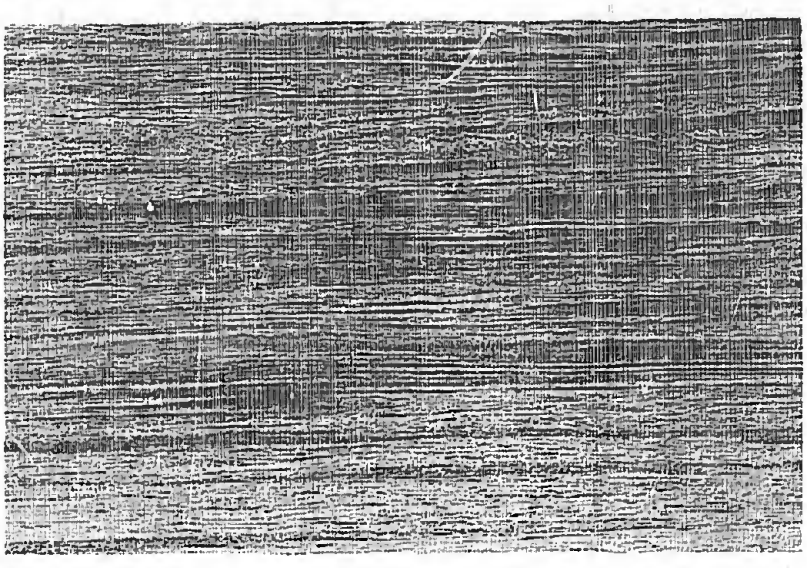

C. SU-31
Heat No. 17A

Knoop HN=298
(100 gm load)

Figure 6. Longitudinal microstructure of columbium-base alloys in the "extrude-forge" condition. 4:1 reduction at 2400°F. Magnification: 100X.

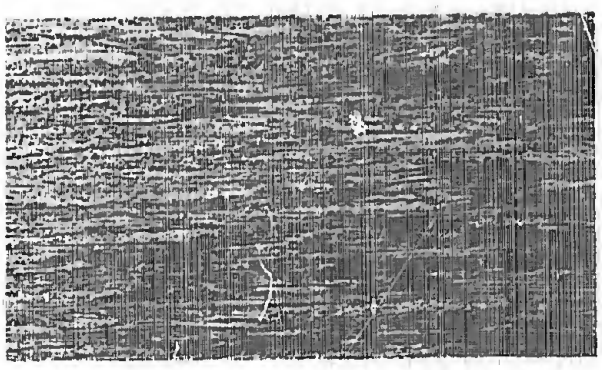

A. As-forged at 2400°F
KHN = 363

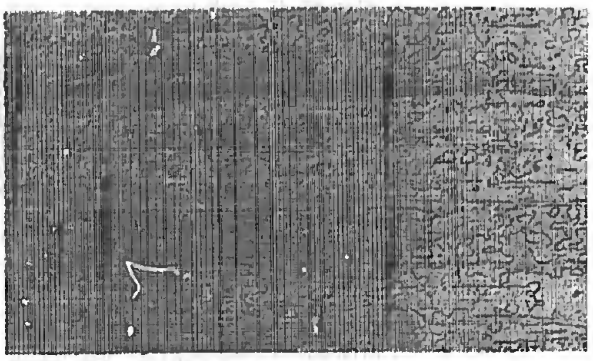

B. 2850°F
KHN = 293

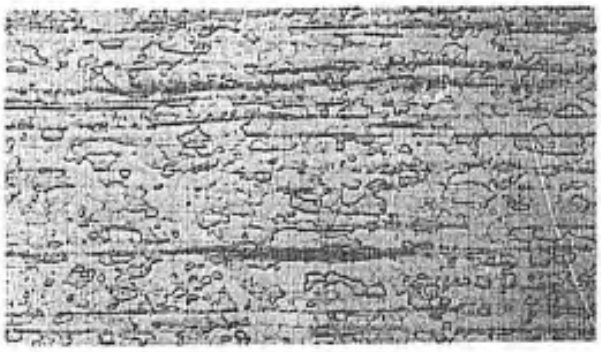

C. 2900°F
KHN = 301

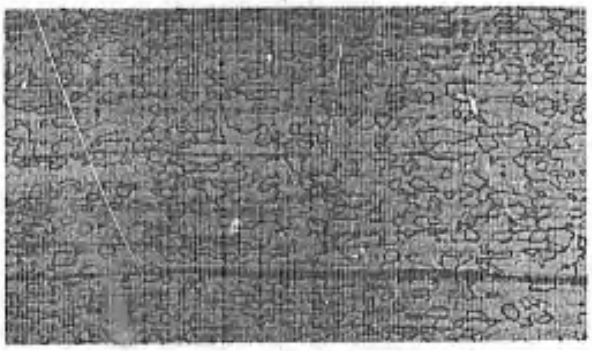

D. 2950°F
KHN = 324

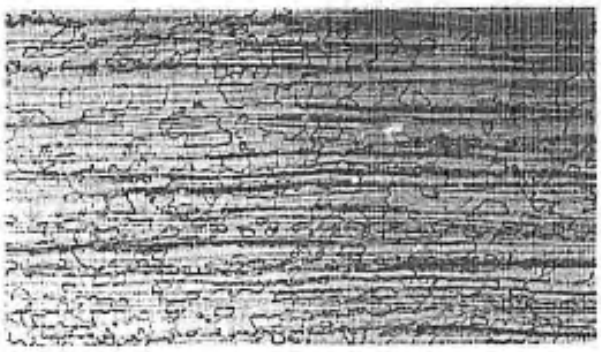

E. 3000°F
KHN = 301

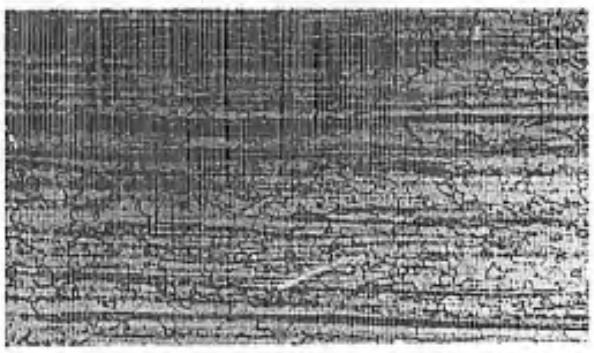

F. 3050°F
KHN = 319

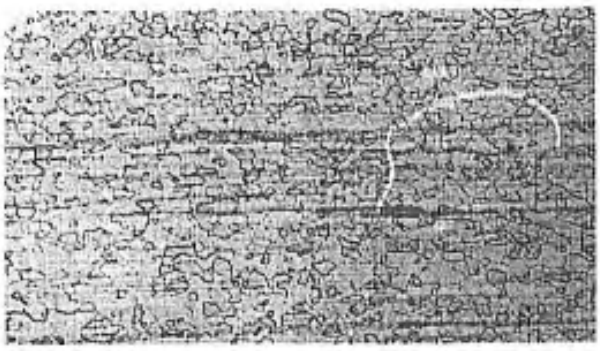

G. 3100°F
KHN = 318

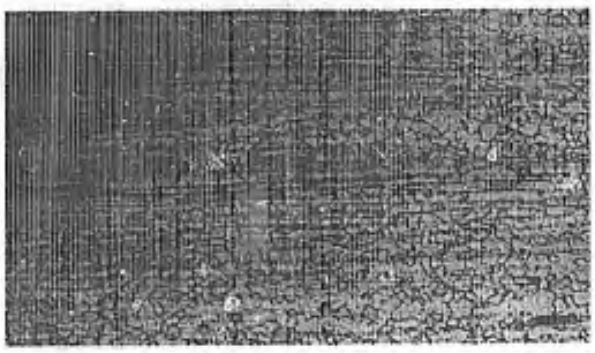

H. 3150°F
KHN = 308

Figure 7. Photomicrographs showing the recrystallization behavior of forged (2400°F) Cb 132M. Recrystallized for 1 hour at temperature indicated. Average microhardness (KHN) shown. Magnification: 100X.

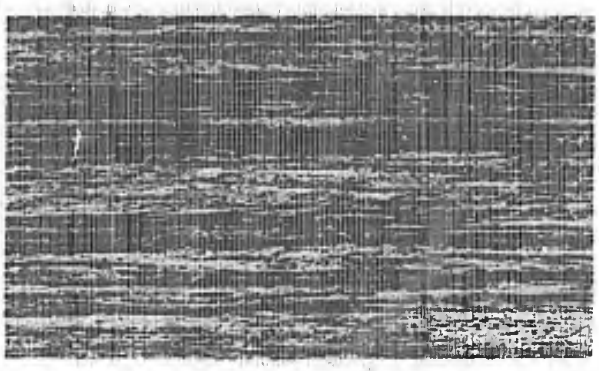

A. As-forged at 2400°F
KHN = 310

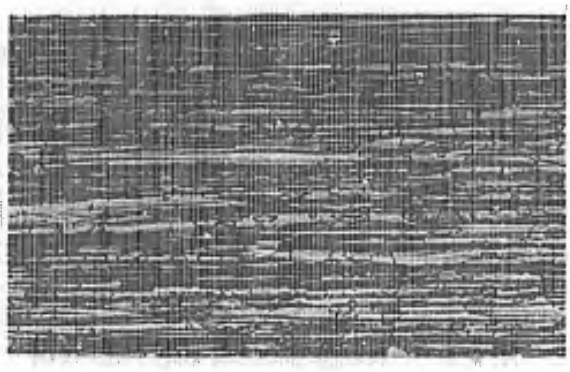

B. 2850°F
KHN = 271

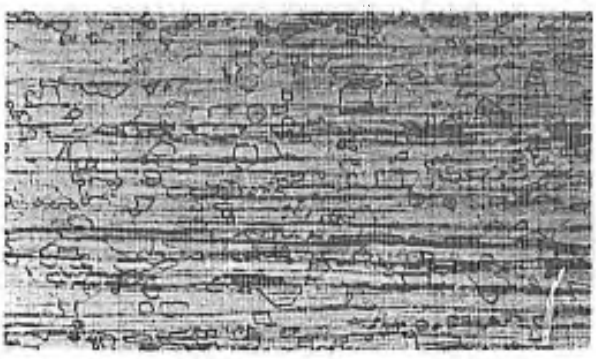

C. 2900°F
KHN = 272

D. 2950°F
KHN = 262

E. 3000°F
KHN = 259

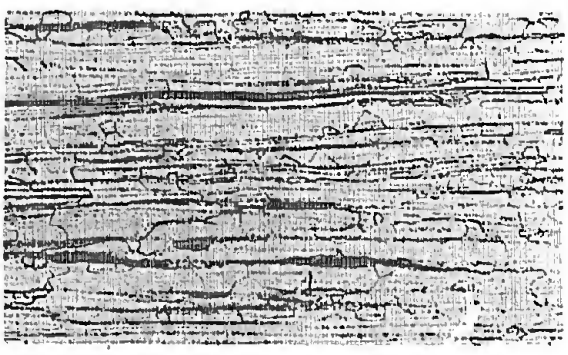

F. 3050°F
KHN = 279

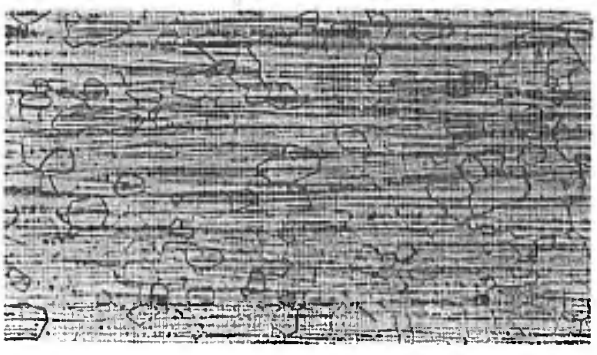

G. 3100°F
KHN = 282

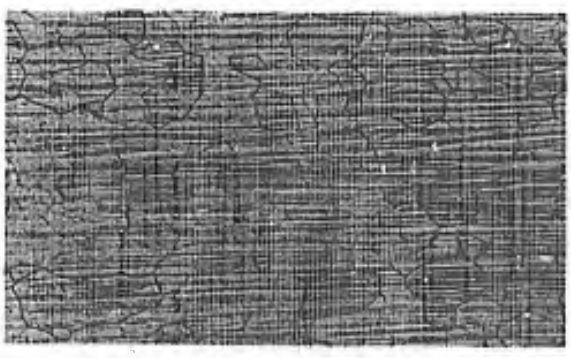

H. 3150°F
KHN = 298

Figure 8. Photomicrographs showing the recrystallization behavior of forged (2400°F) VAM-79. Recrystallized for 1 hour at temperature indicated. Average microhardness (KHN) shown. Magnification: 100X.

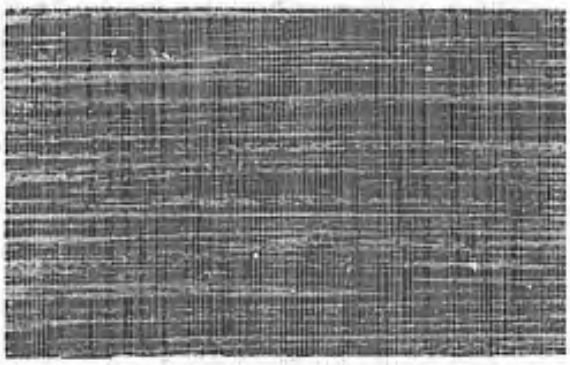

A. As-forged at 2400°F
KHN = 293

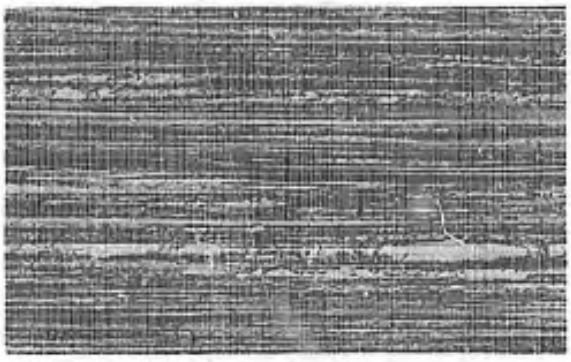

B. 2850°F
KHN = 265

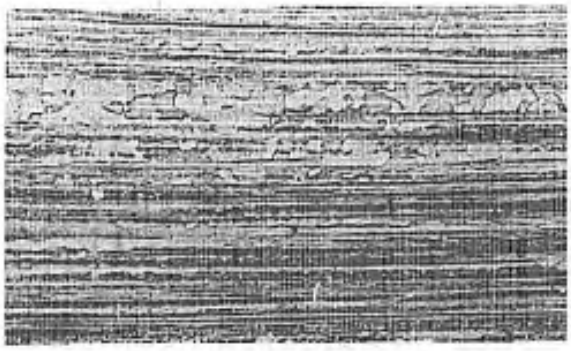

C. 2900°F
KHN = 247

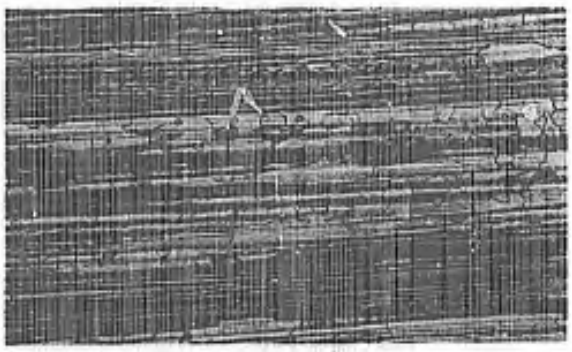

D. 2950°F
KHN = 233

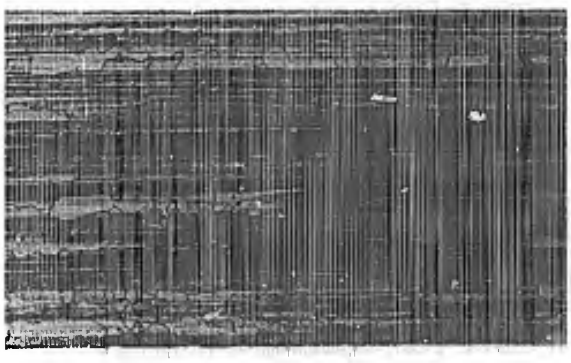

E. 3000°F
KHN = 266

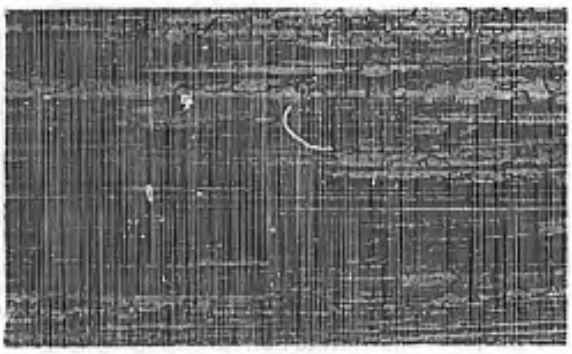

F. 3050°F
KHN = 296

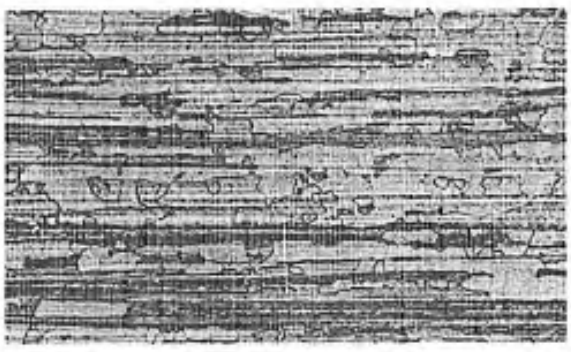

G. 3100°F
KHN = 260

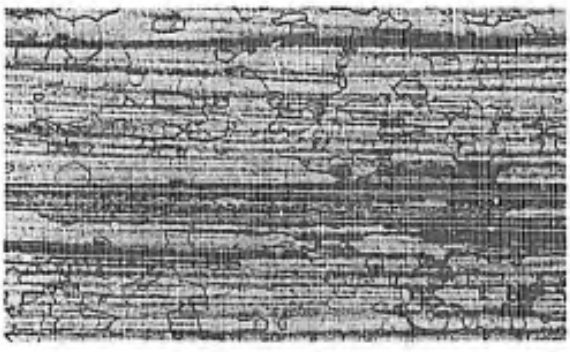

H. 3150°F
KHN = 249

Figure 9. Photomicrographs showing the recrystallization behavior of forged (2400°F) SU-31. Recrystallized for 1 hour at temperature indicated. Average microhardness (KHN) shown. Magnification: 100X.

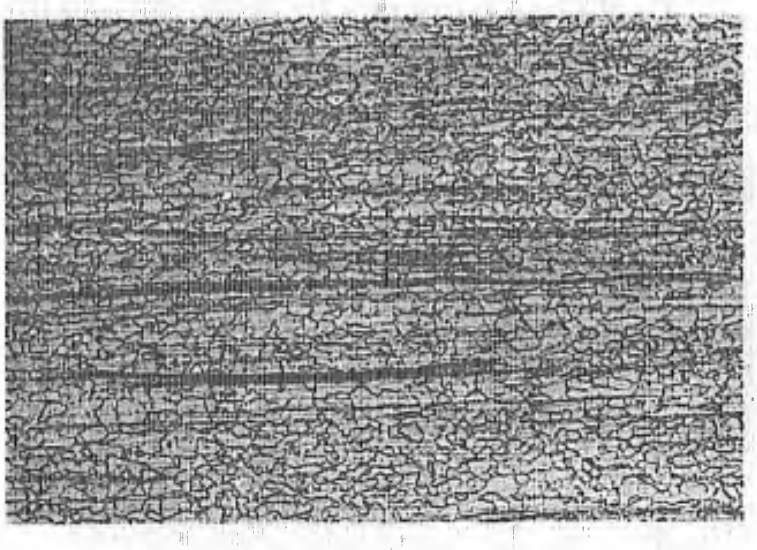

A.

Cb 132M
Heat No. M-493
2950°F; 2 hours
Knoop hardness No. = 302

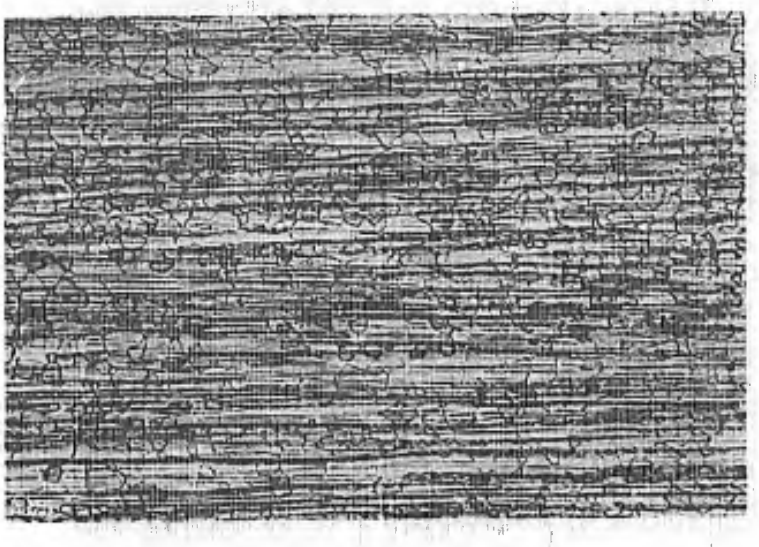

B.

VAM-79
Heat No. Vam 96A
2950°F; 2 hours
Knoop hardness No. = 263

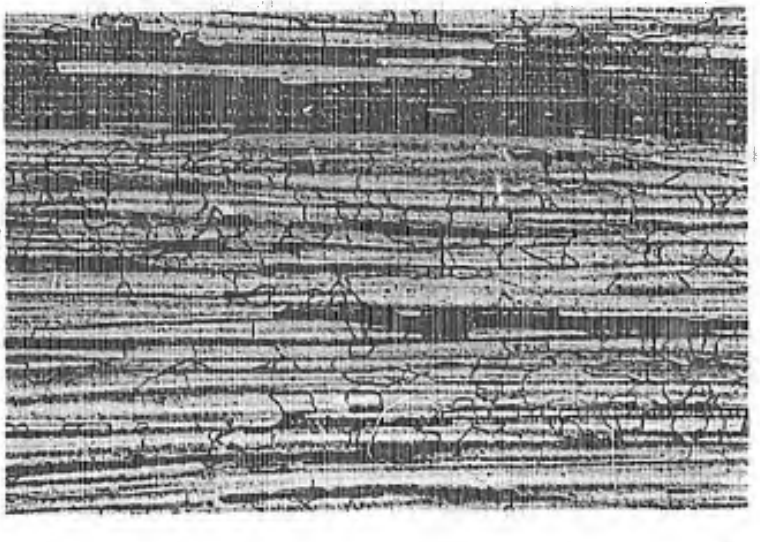

C.

SU-31
Heat No. 17A
3150°F; 2 hours
Knoop hardness No. = 268

Figure 10. Microstructure of columbium-base alloys in the recrystallized condition prior to cold working at 1600°F. Recrystallization temperature indicated. Magnification: 100X.

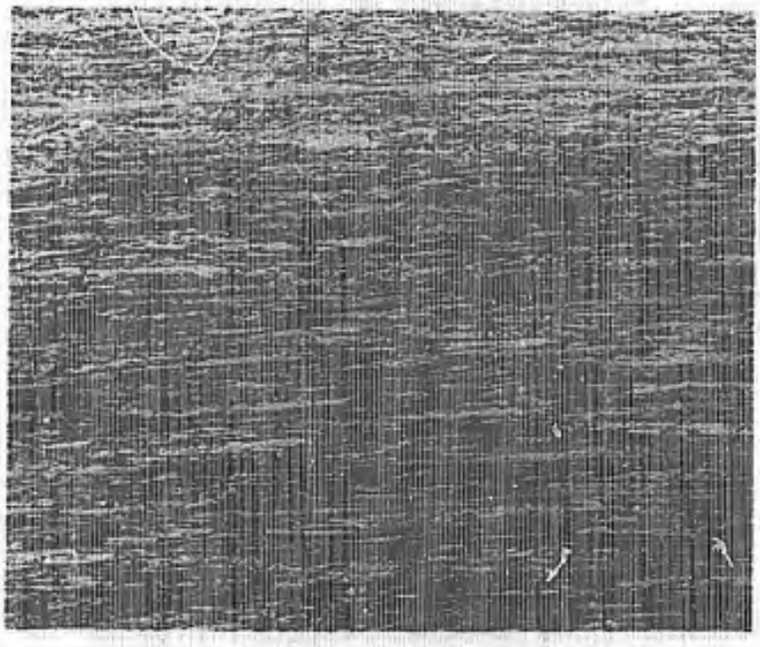

A. 100X

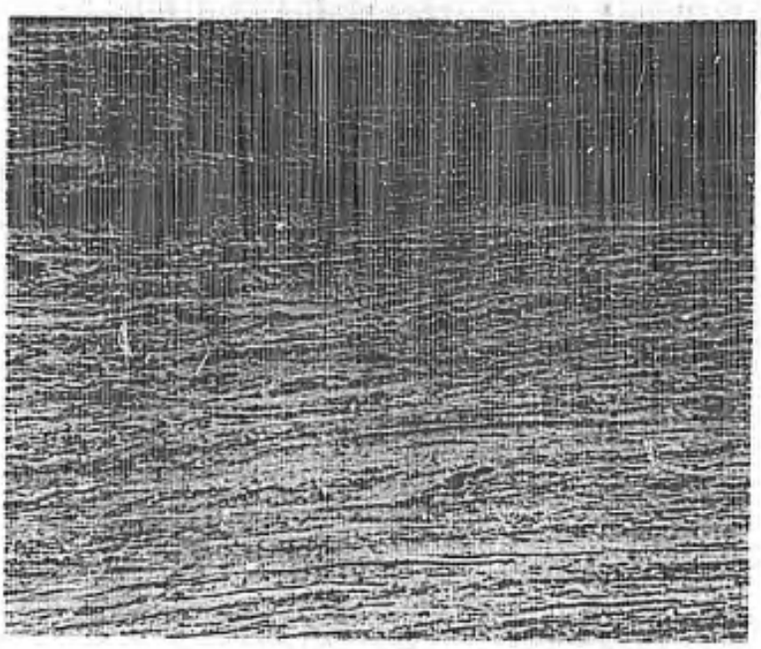

B. 500X

Figure 11. Microstructure of Cb 132M forged at 2400°F. Heat No. M-493. Knoop hardness No. = 363.

100X 500X

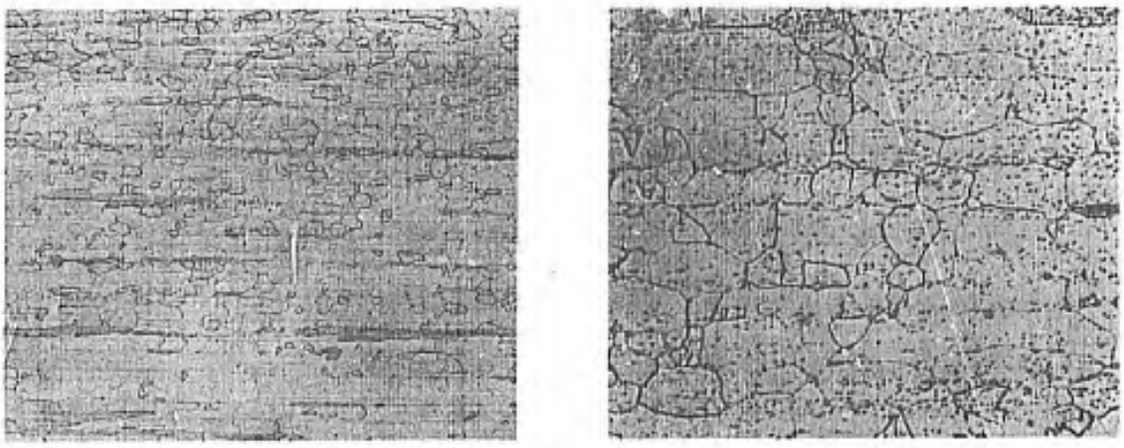

3000°F, 1 hour: Knoop hardness No. = 343

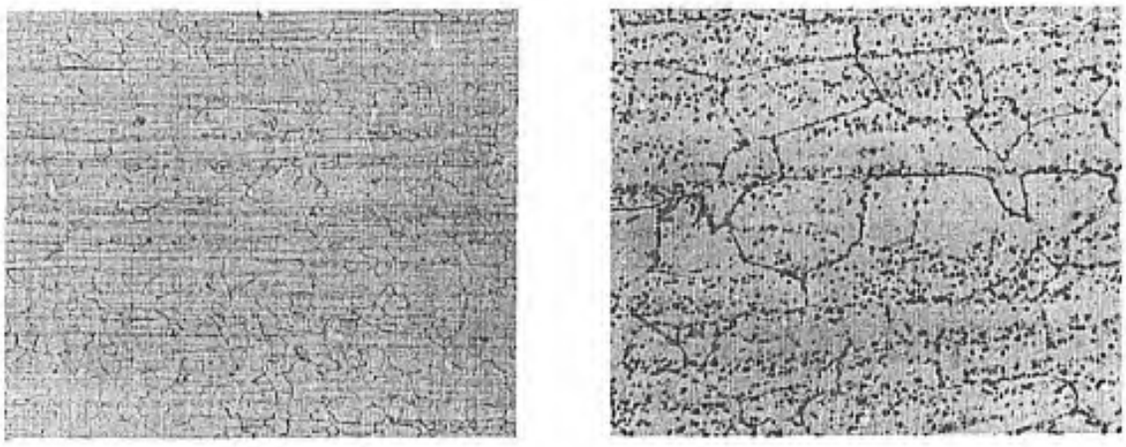

3200°F, 1 hour: Knoop hardness No. = 313

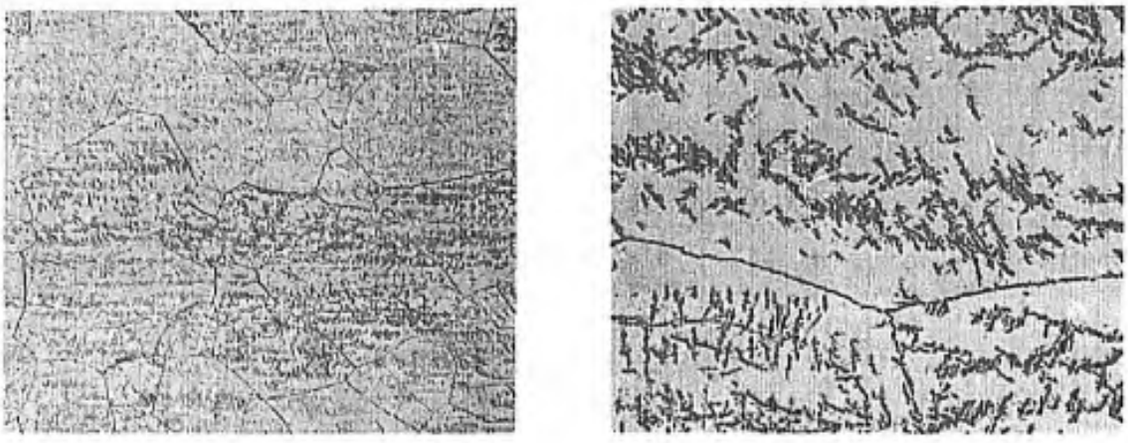

3600°F, 1 hour: Knoop hardness No. = 338

Figure 12. Microstructure of forged and annealed Cb 132M. Annealing temperature and magnification indicated. Heat No. M-497.

100X

500X

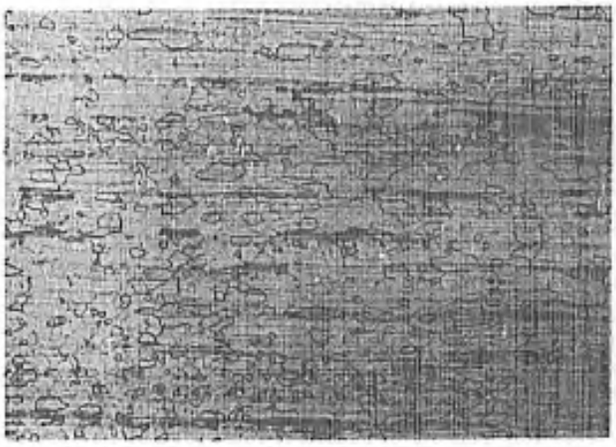

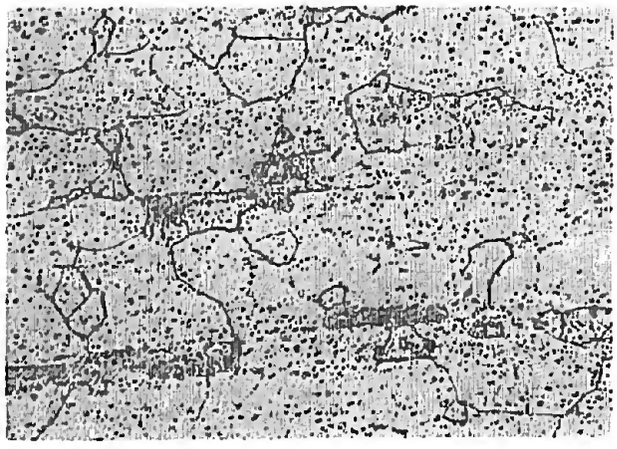

3000°F, 1 hour: Knoop hardness No. = 315

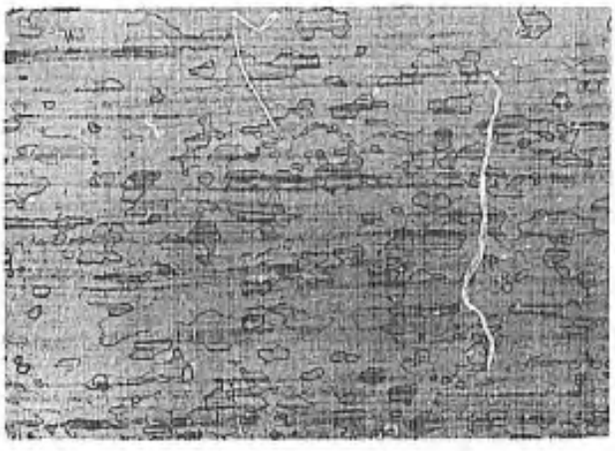

3200°F, 1 hour: Knoop hardness No. = 308

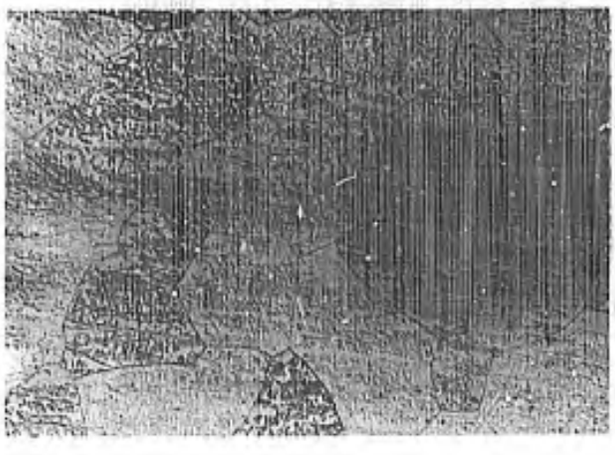

3600°F, 1 hour: Knoop hardness No. = 318

Figure 13. Microstructure of forged, annealed, and aged (2200°F for 4 hours) Cb 132M. Annealing temperature and magnification indicated. Heat No. M-497.

100X

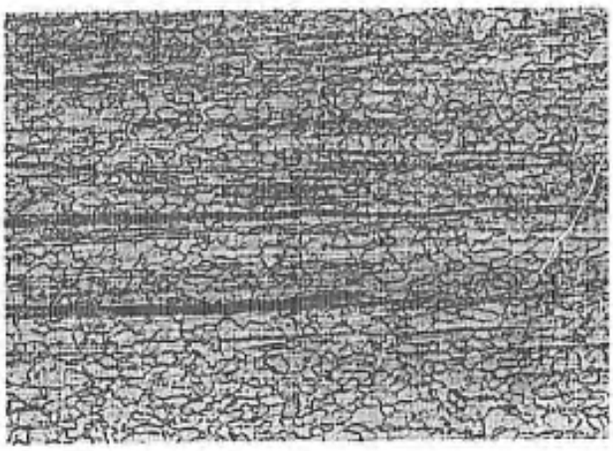

500X

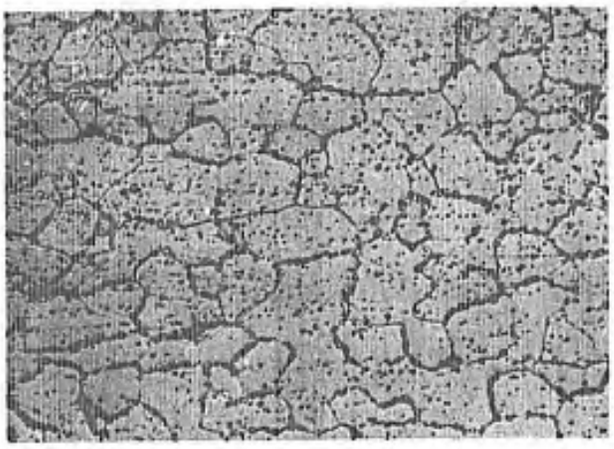

A. Recrystallized 2950°F, 2 hours: Knoop hardness No. = 302

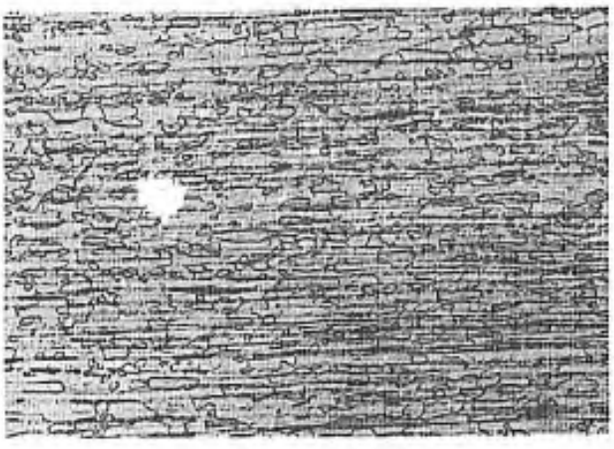

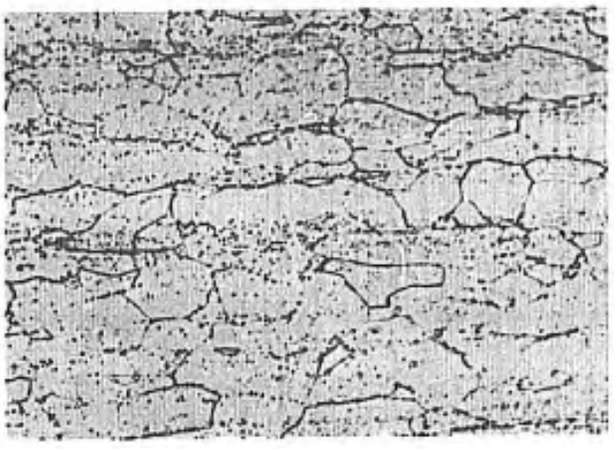

B. A + cold worked 20% at 1600°F: Knoop hardness No. = 365

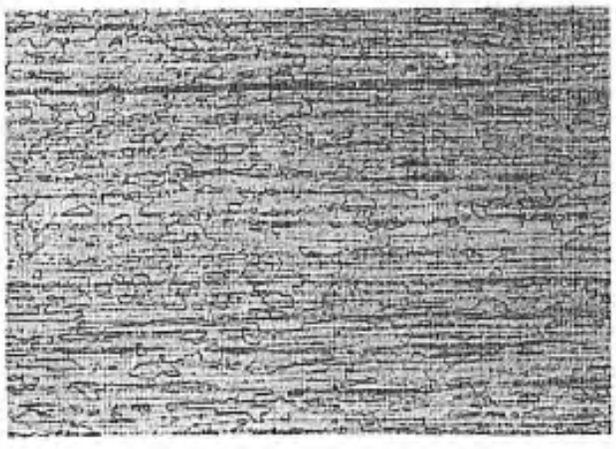

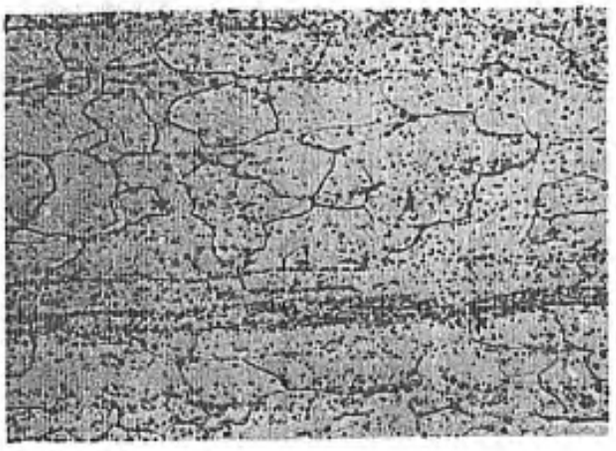

C. B + aged at 2000°F, 4 hours: Knoop hardness No. = 307

Figure 14. Microstructure of cold worked Cb 132M in various stages of processing. Heat No. M-493.

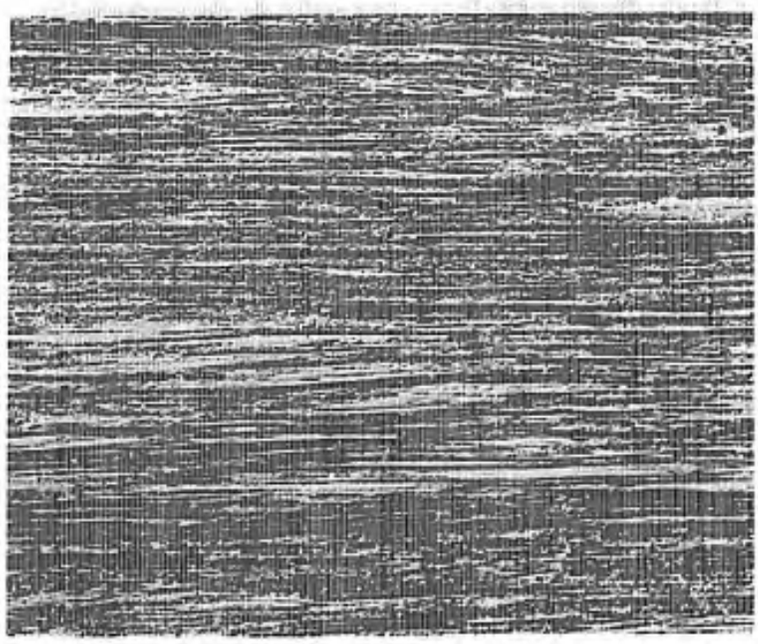

A. 100X

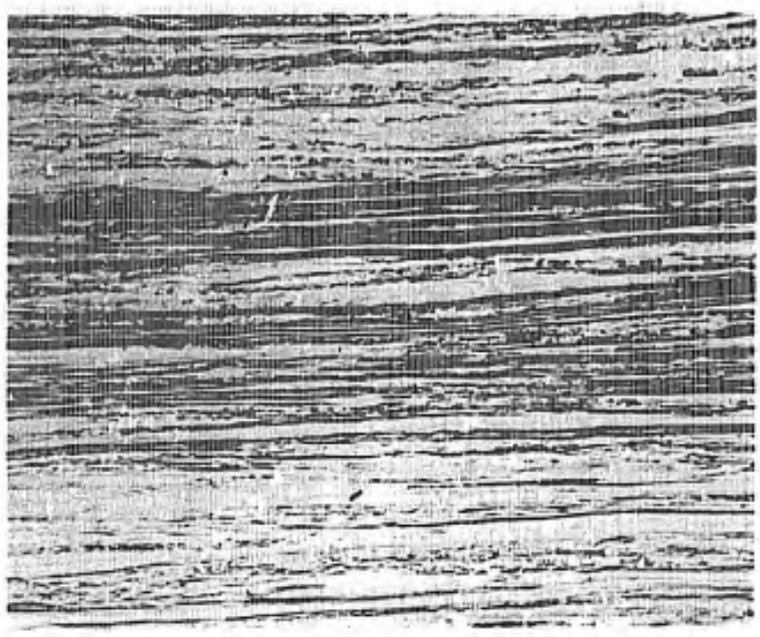

B. 500X

Figure 15. Microstructure of VAM-79 forged at 2400°F. Heat No. VAM 96B. Knoop hardness No. = 313.

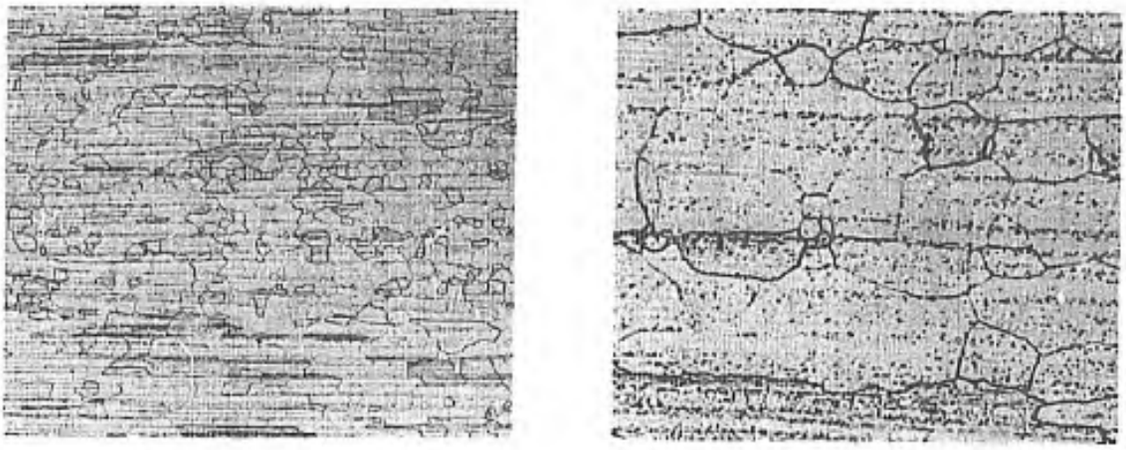

3000°F, 1 hour: Knoop hardness No. = 299

3200°F, 1 hour: Knoop hardness No. = 293

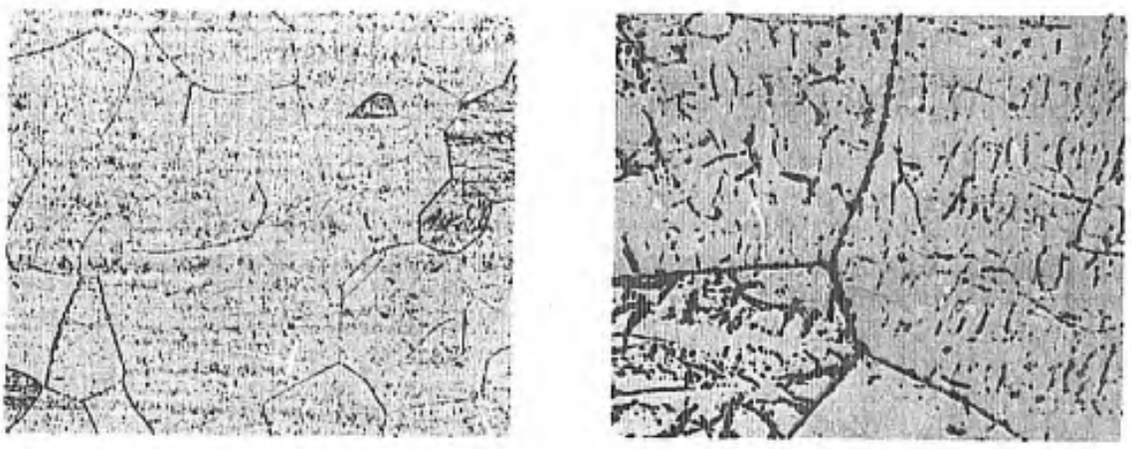

3600°F, 1 hour: Knoop hardness No. = 303

Figure 16. Microstructure of forged and annealed VAM-79. Annealing temperature and magnification indicated. Heat No. VAM 96A.

100X

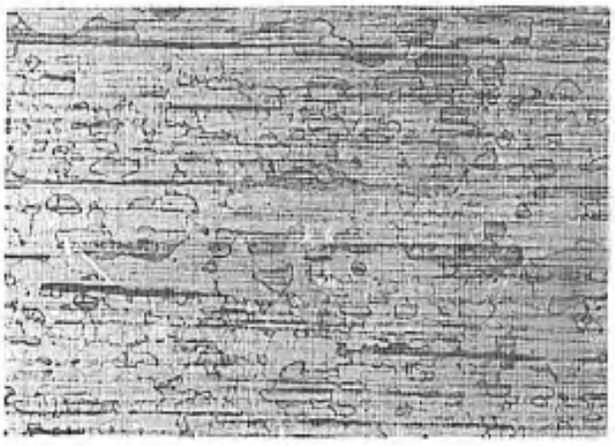

500X

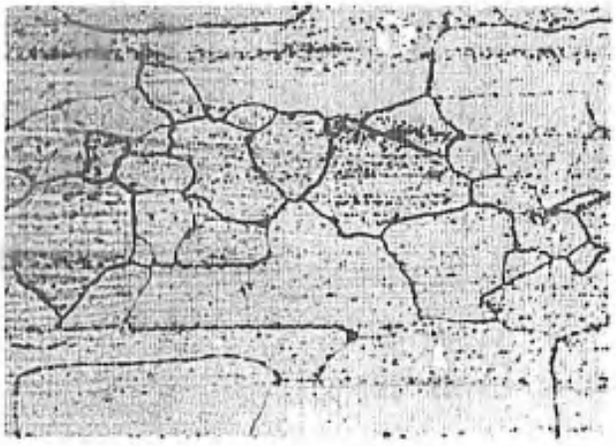

3000°F, 1 hour: Knoop hardness No. = 287

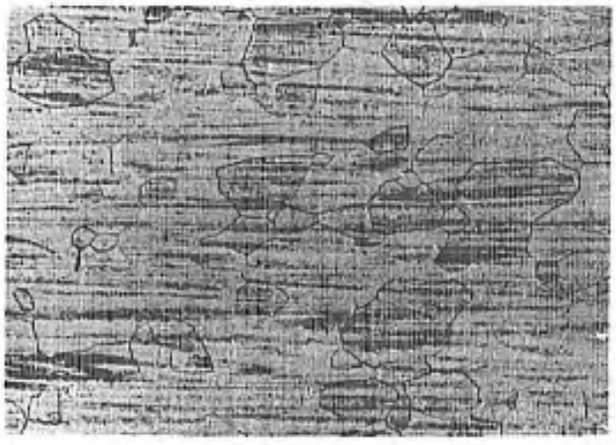

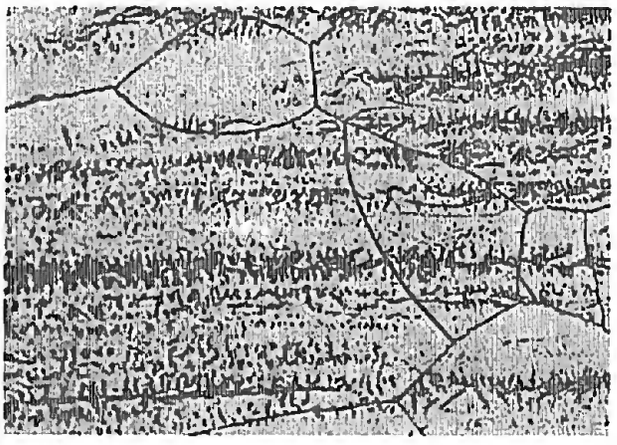

3200°F, 1 hour: Knoop hardness No. = 308

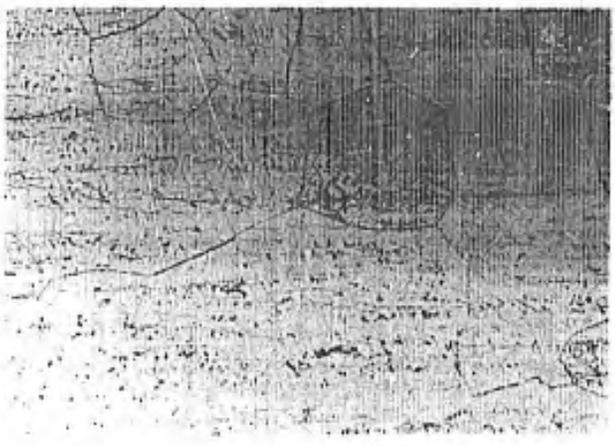

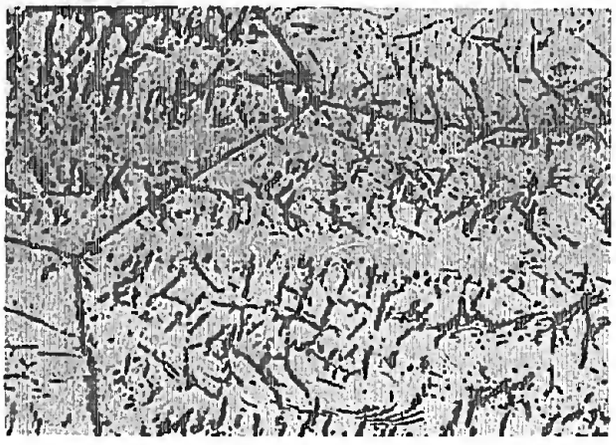

3600°F, 1 hour: Knoop hardness No. = 283

Figure 17. Microstructure of forged, annealed, and aged (2200°F for 4 hours) VAM-79. Annealing temperature and magnification indicated. Heat No. VAM 96A.

100X

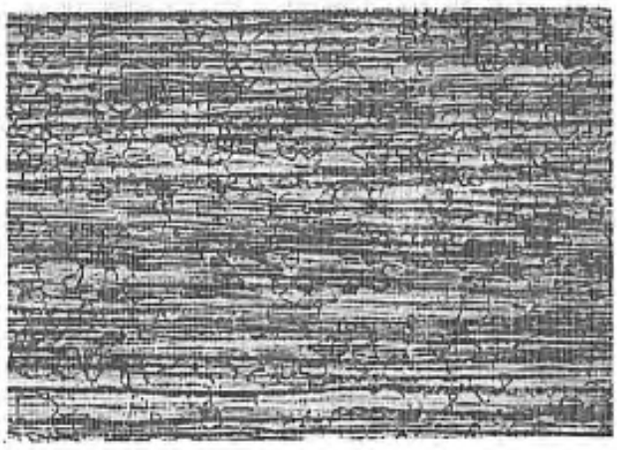

500X

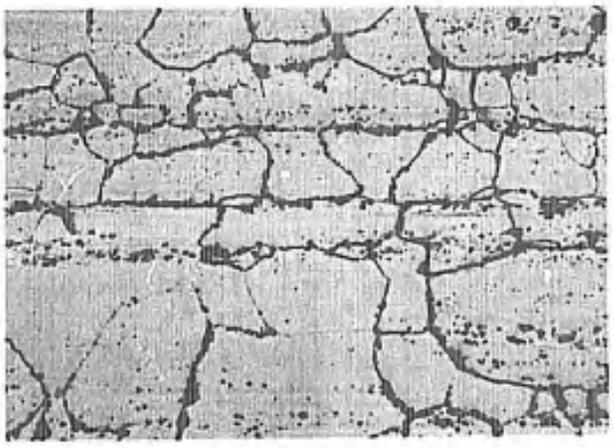

A. Recrystallized 2950°F, 2 hours: Knoop hardness No. = 263
Heat No. VAM 96A

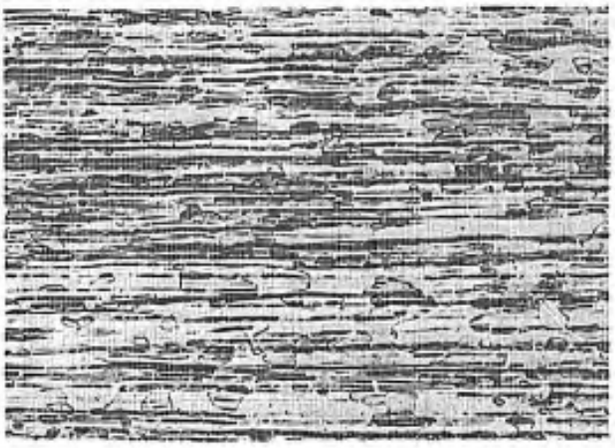

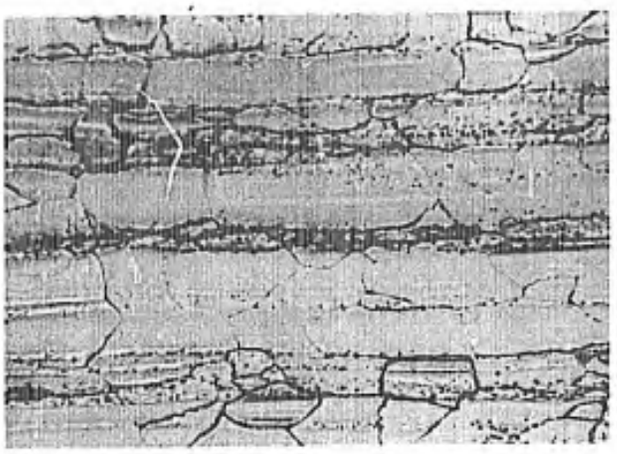

B. A + cold worked 20% at 1600°F: Knoop hardness No. = 349
Heat No. VAM 96B

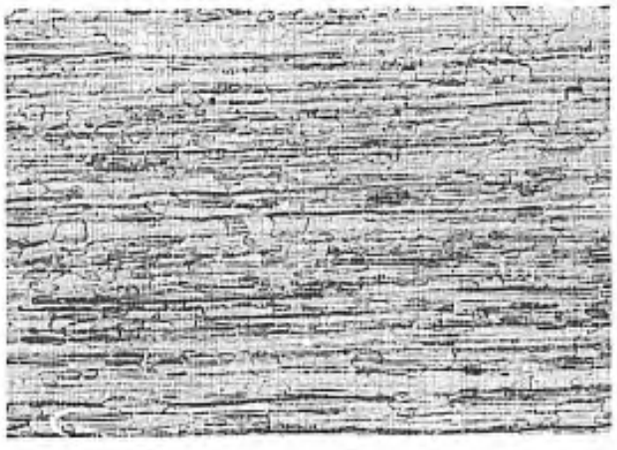

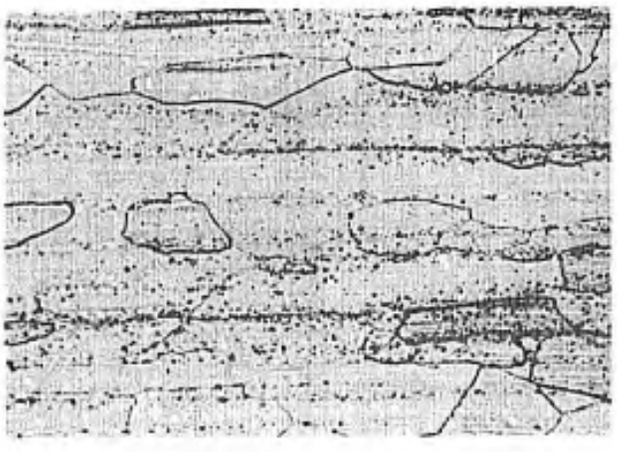

C. B + aged at 2000°F, 4 hours: Knoop hardness No. = 297
Heat No. VAM 96B

Figure 18. Microstructure of cold worked VAM-79 in various stages of processing. Heat No. indicated.

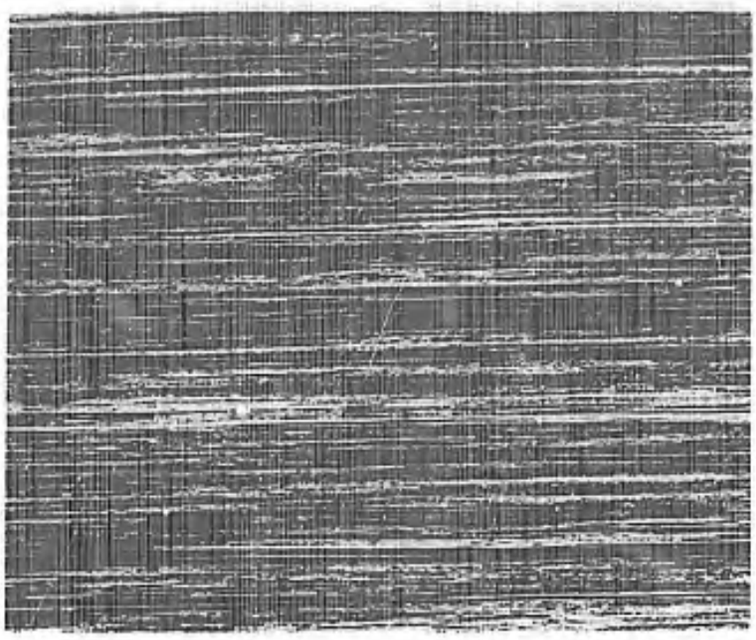

A. 100X

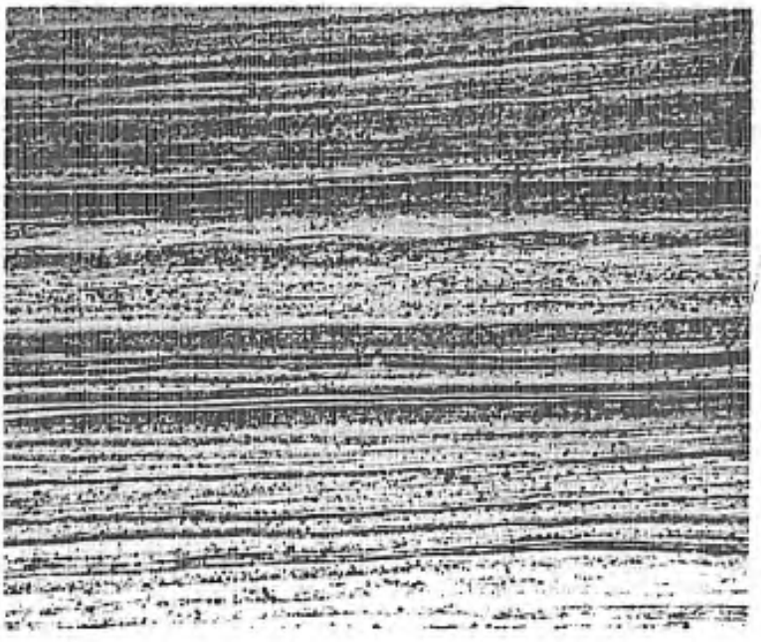

B. 500X

Figure 19. Microstructure of SU-31 forged at 2400°F. Heat No. 17A. Knoop hardness No. = 295

100X

500X

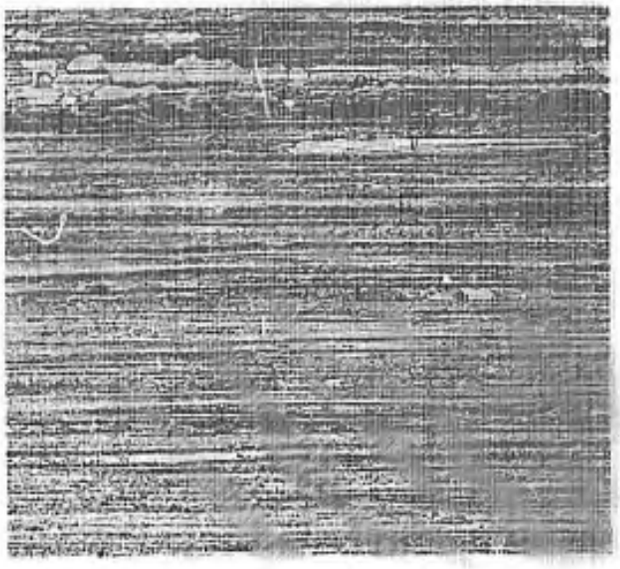

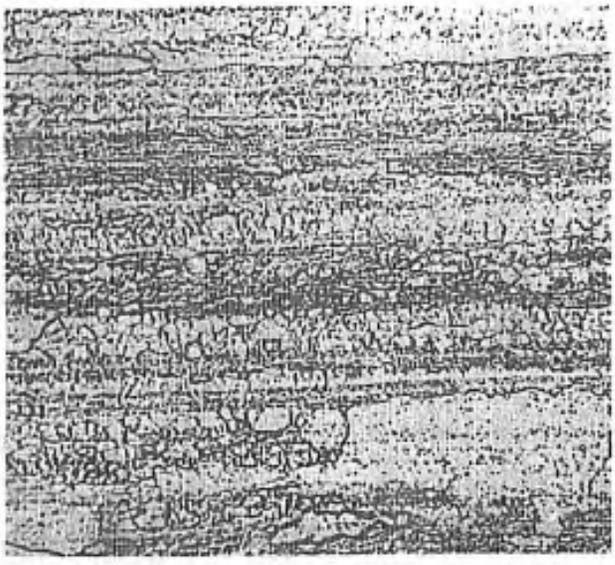

3000°F, 1 hour: Knoop hardness No. 281

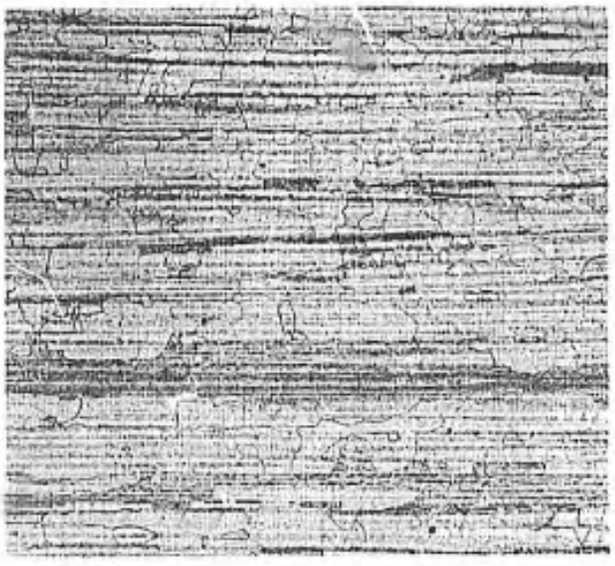

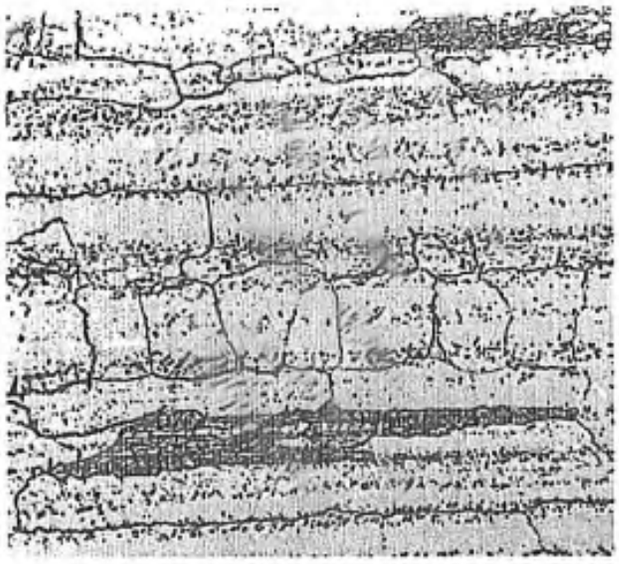

3200°F, 1 hour: Knoop hardness No. = 271

Figure 20. Microstructure of forged and annealed SU-31. Annealing temperature and magnification indicated. Heat No. 17A.

100X

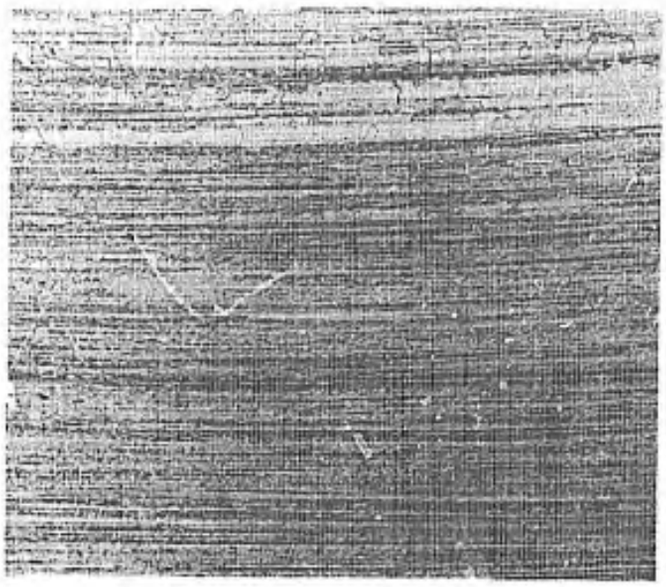

500X

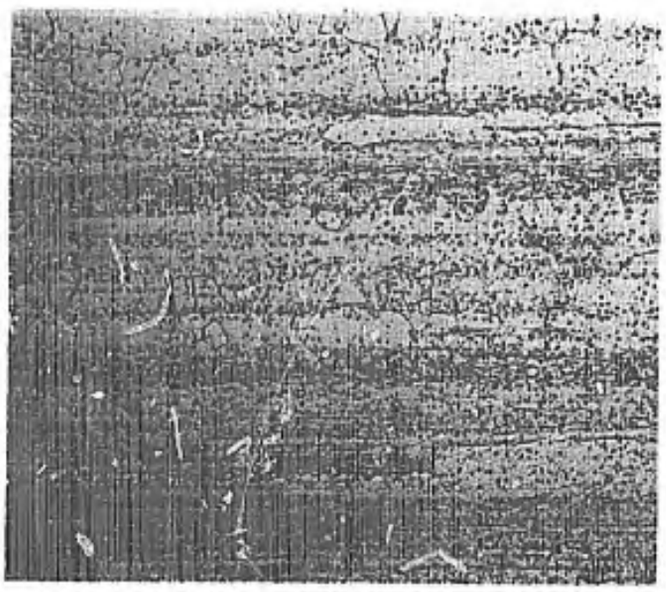

3000°F, 1 hour: Knoop hardness No. = 254

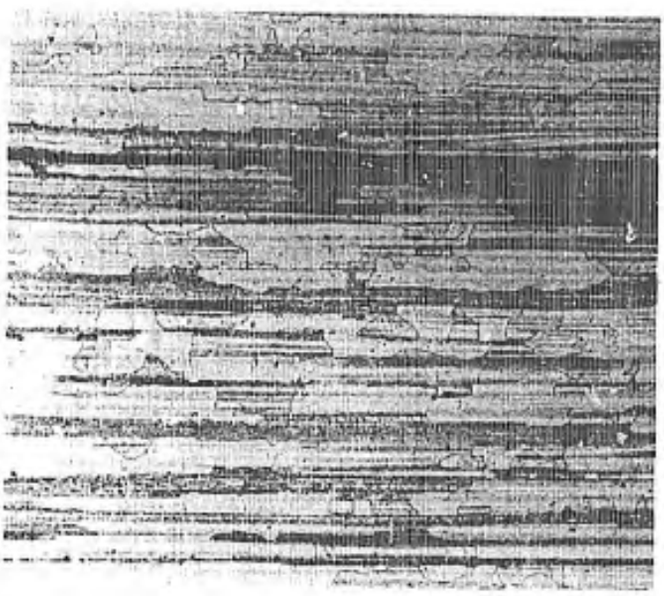

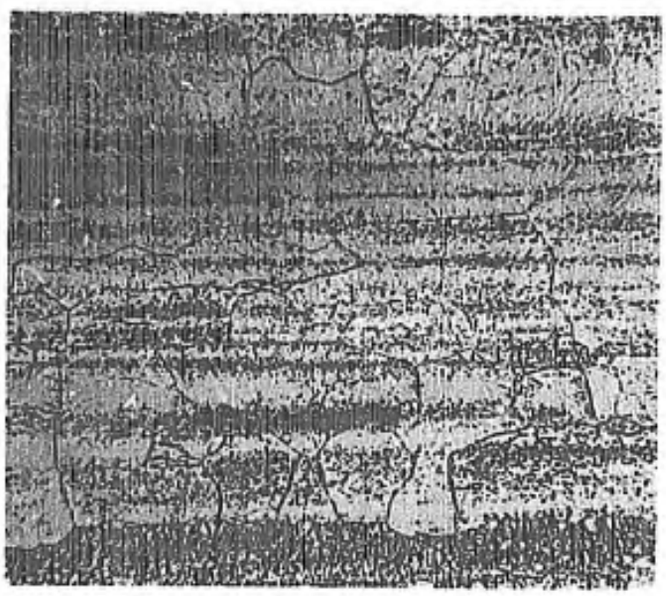

3200°F, 1 hour: Knoop hardness No. = 290

Figure 21. Microstructure of forged, annealed, and aged (2200°F for 4 hours) SU-31. Annealing temperature and magnification indicated. Heat No. 17A.

100X 500X

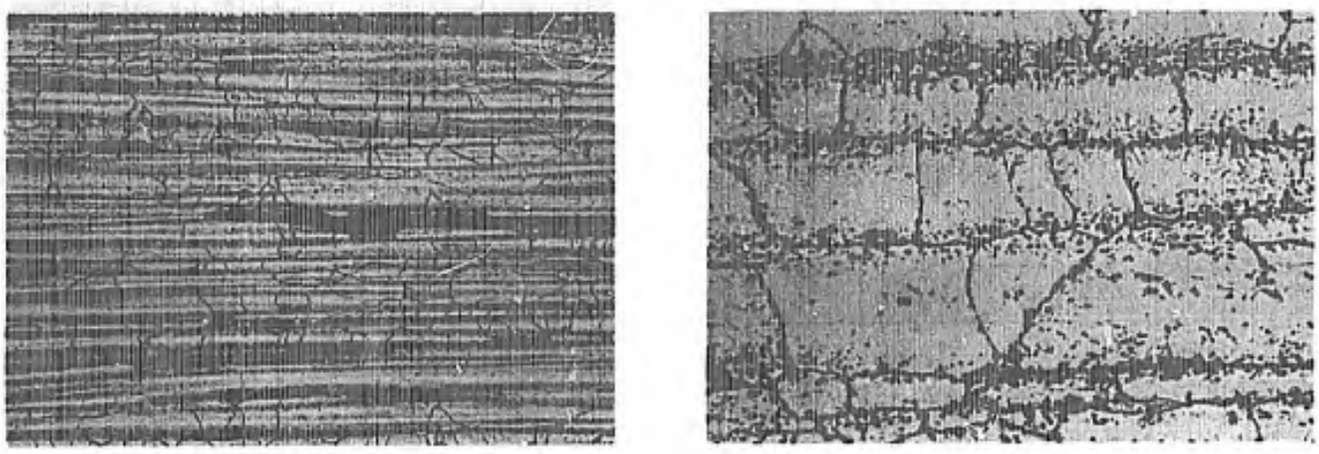

A. Recrystallized 3150°F, 2 hours: Knoop hardness No. = 268

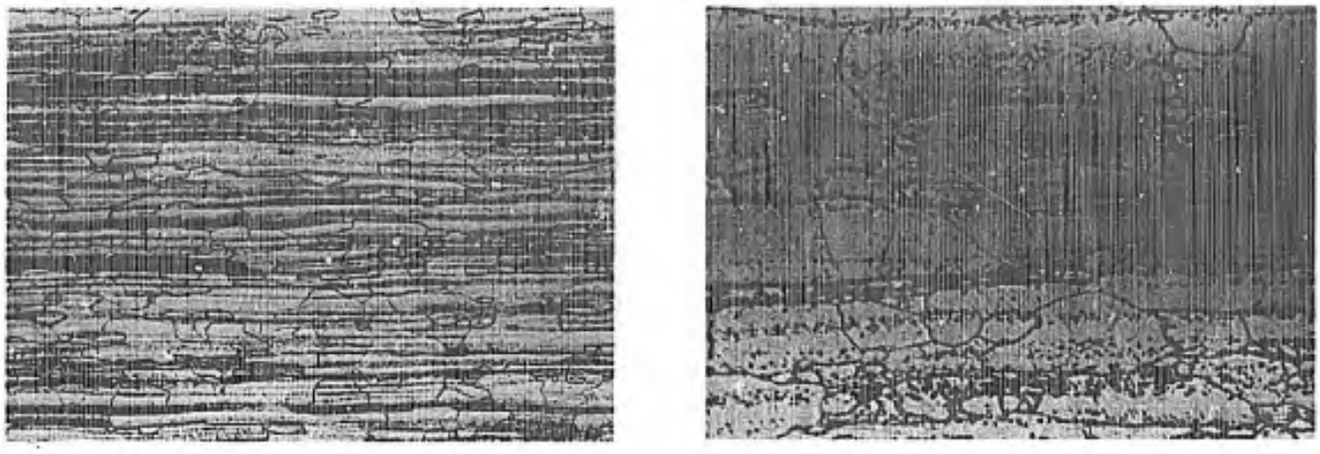

B. A + cold worked 20% at 1600°F: Knoop hardness No. = 336

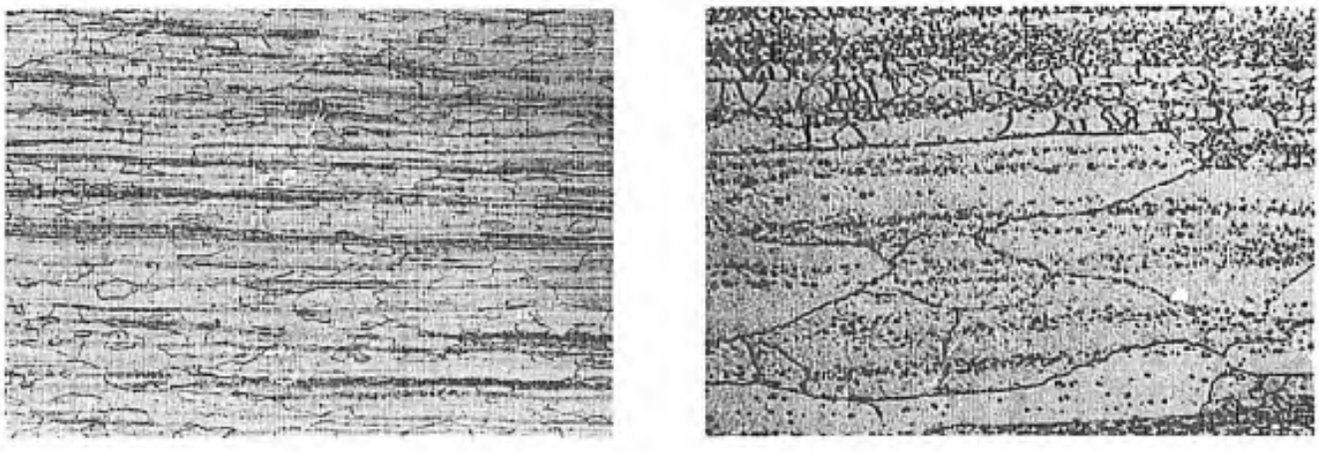

C. B + aged at 2000°F, 4 hours: Knoop hardness No. = 325

Figure 22. Microstructure of cold worked SU-31 in various stages of processing. Heat No. 17A.

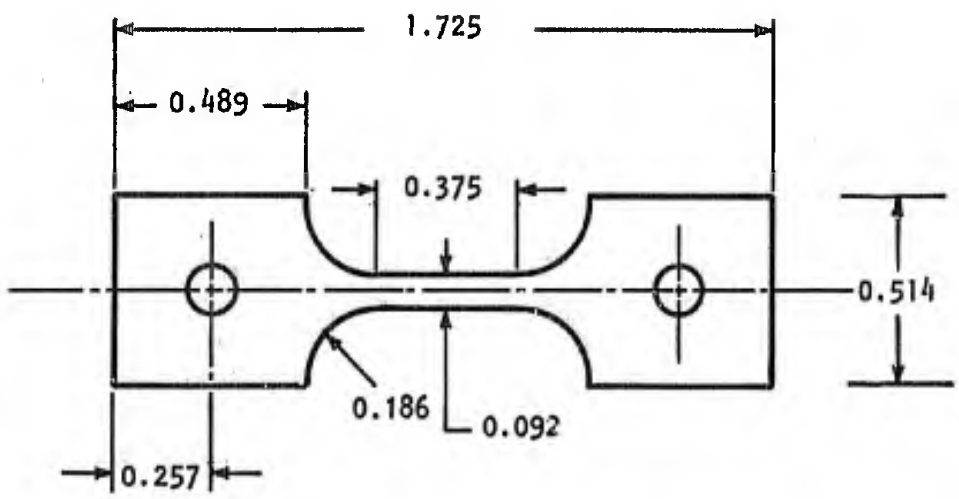

Thickness = 0.092

All dimensions in inches

Figure 23. Configuration of tensile and creep rupture specimen utilized to test forged columbium alloy plate.

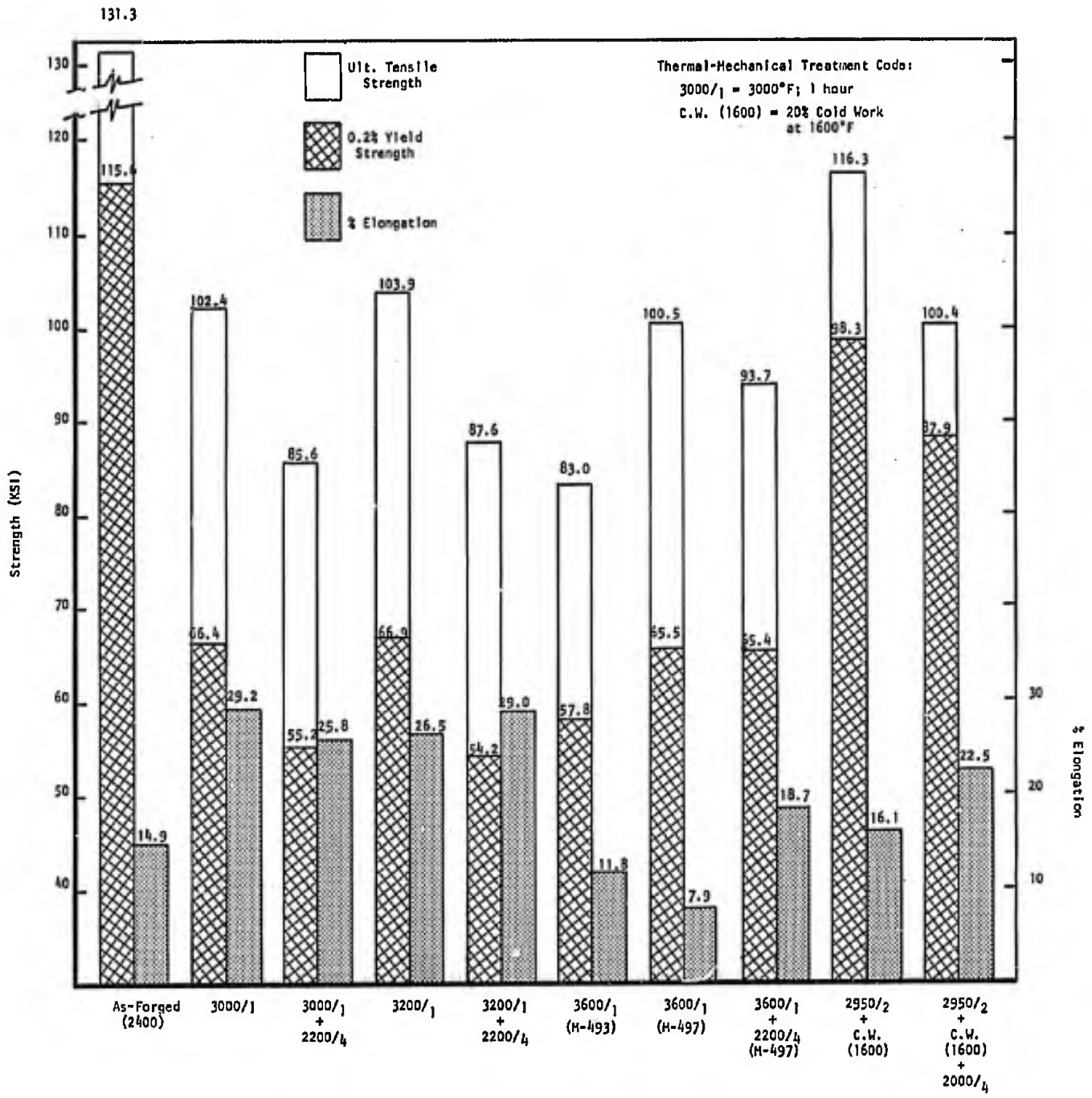

Figure 24. Comparison of 1200°F tensile properties for Cb 132M in various thermal-mechanical processing conditions as indicated. Heat number given when applicable. Tested in vacuum of 10^{-5}torr.; cross head speed of 0.020 in./min.

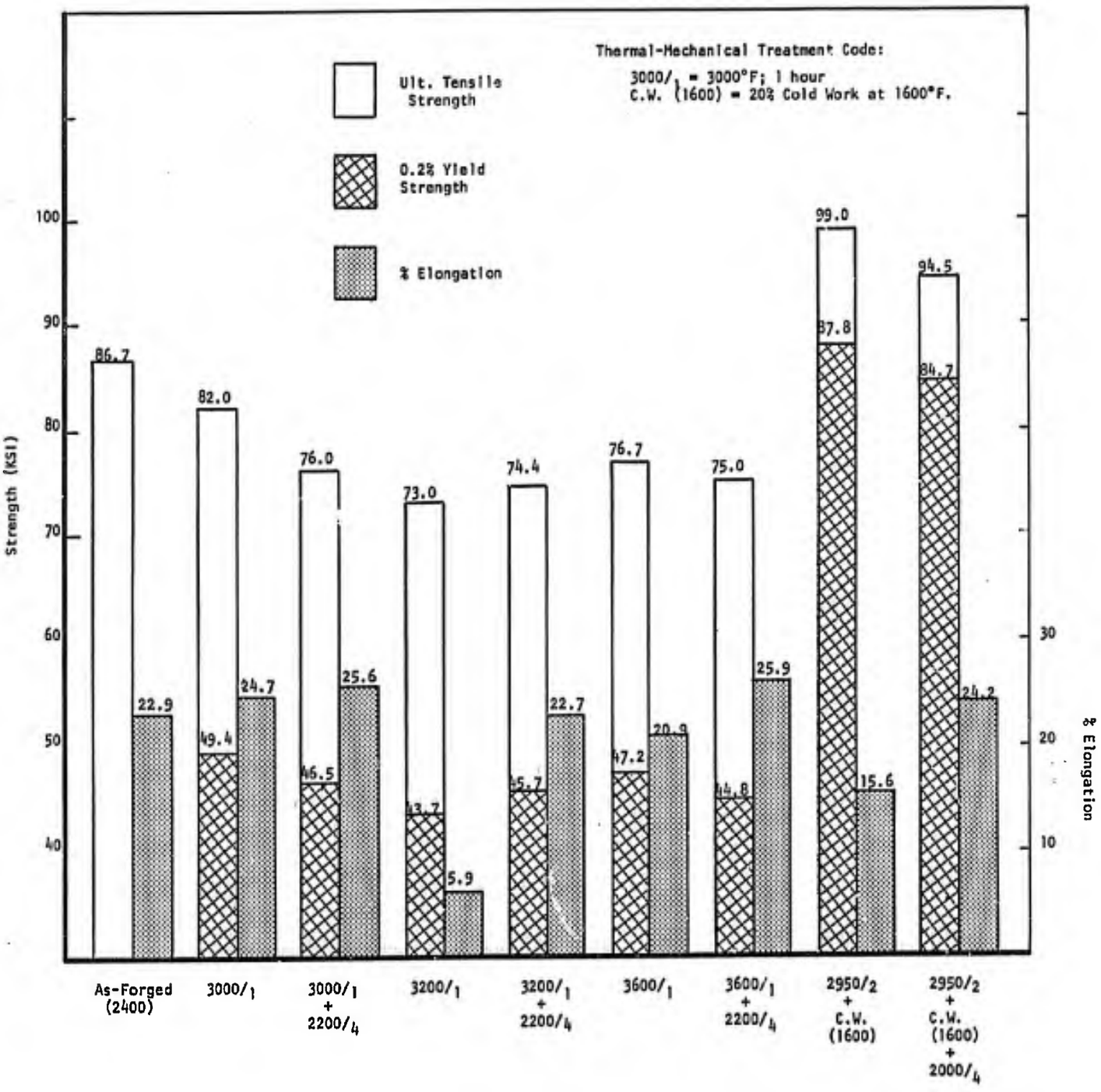

Figure 25. Comparison of 1200°F tensile properties for VAM-79 in various thermal-mechanical processing conditions as indicated. Tested in vacuum of 10^{-5} torr.; cross-head speed of 0.020 in/min.

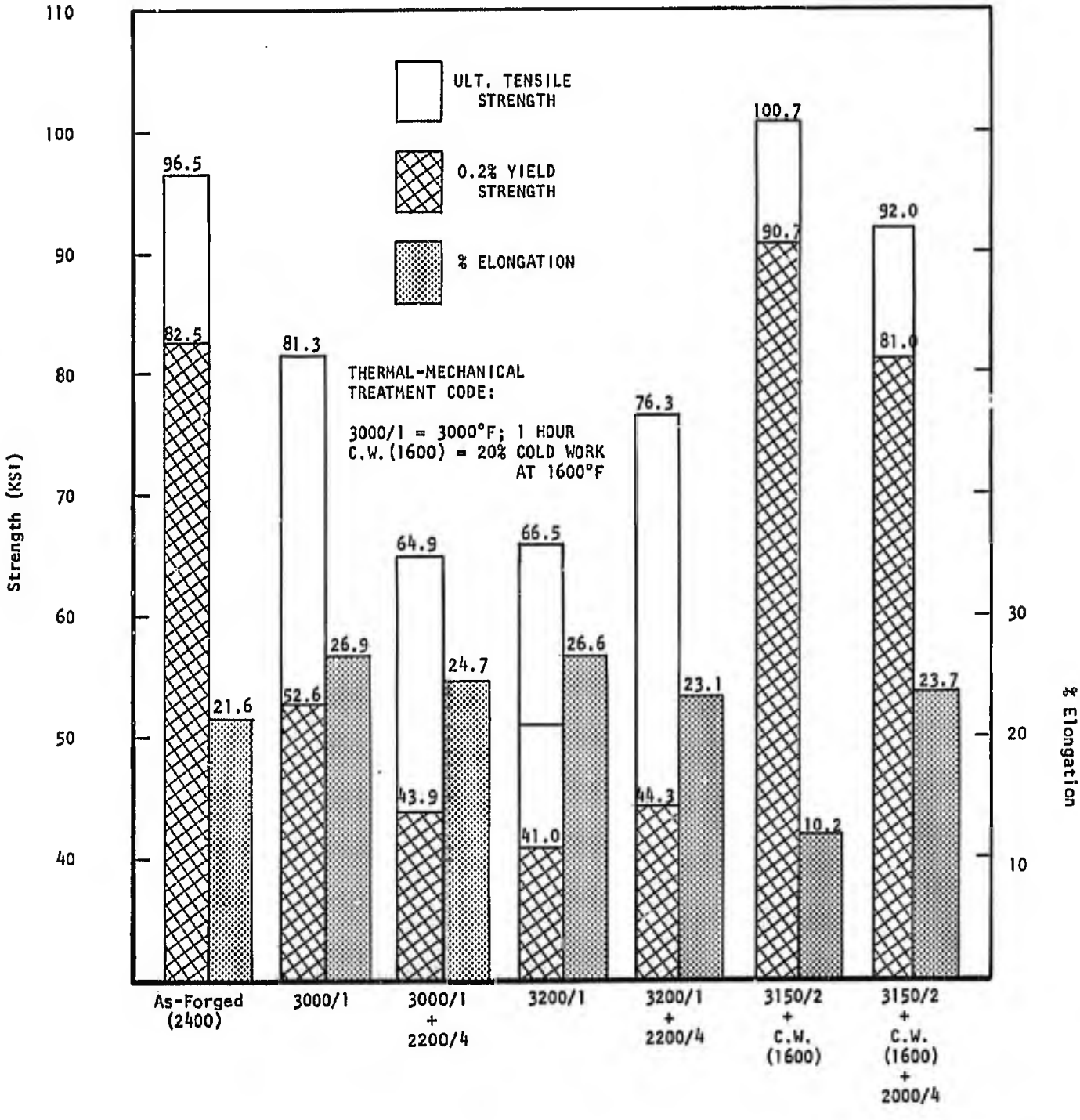

Figure 26. Comparison of 1200°F tensile properties for SU-31 in various thermal-mechanical processing conditions as indicated. Tested in vacuum of 10^{-5} torr.; cross head speed of 0.020 in./min.

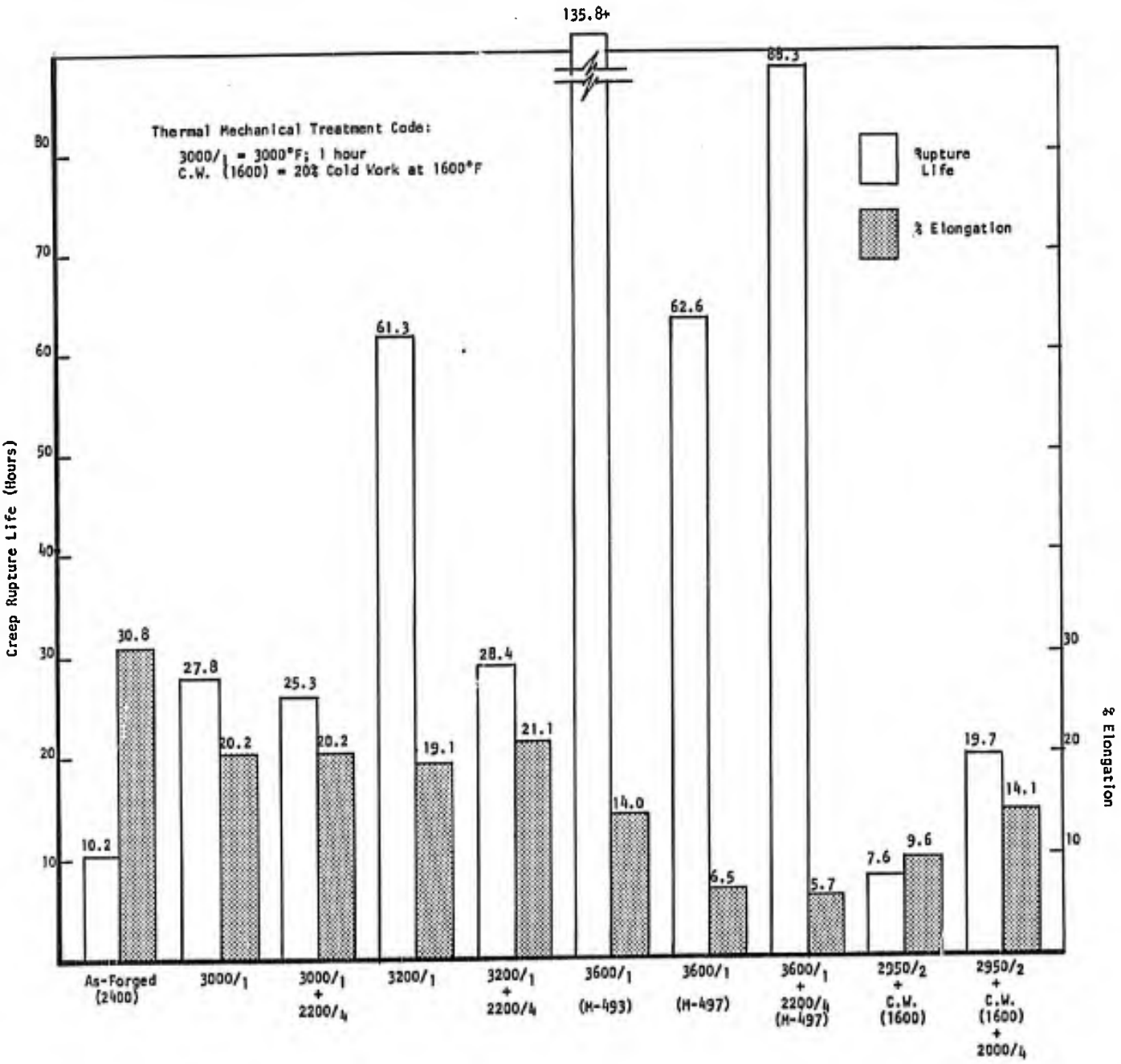

Figure 27. Comparison of 2200°F 30,000 psi creep rupture properties for Cb 132M in various thermal-mechanical processing conditions as indicated. Heat number given when applicable. Tested in vacuum of 10^{-5} torr.

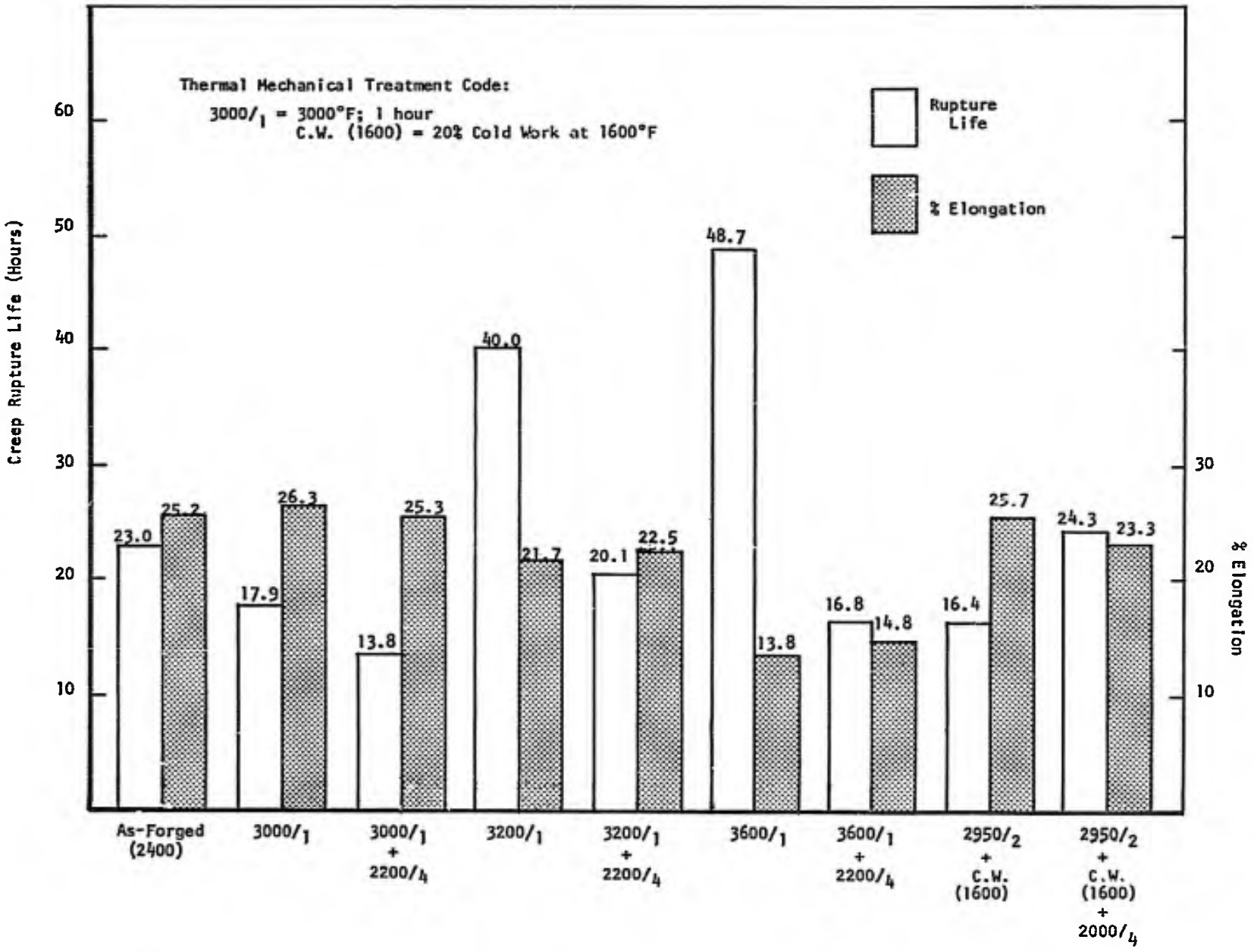

Figure 28. Comparison of 2200°F 30,000 psi creep rupture properties for VAM-79 in various thermal-mechanical processing conditions as indicated. Tested in vacuum of 10^{-5} torr.

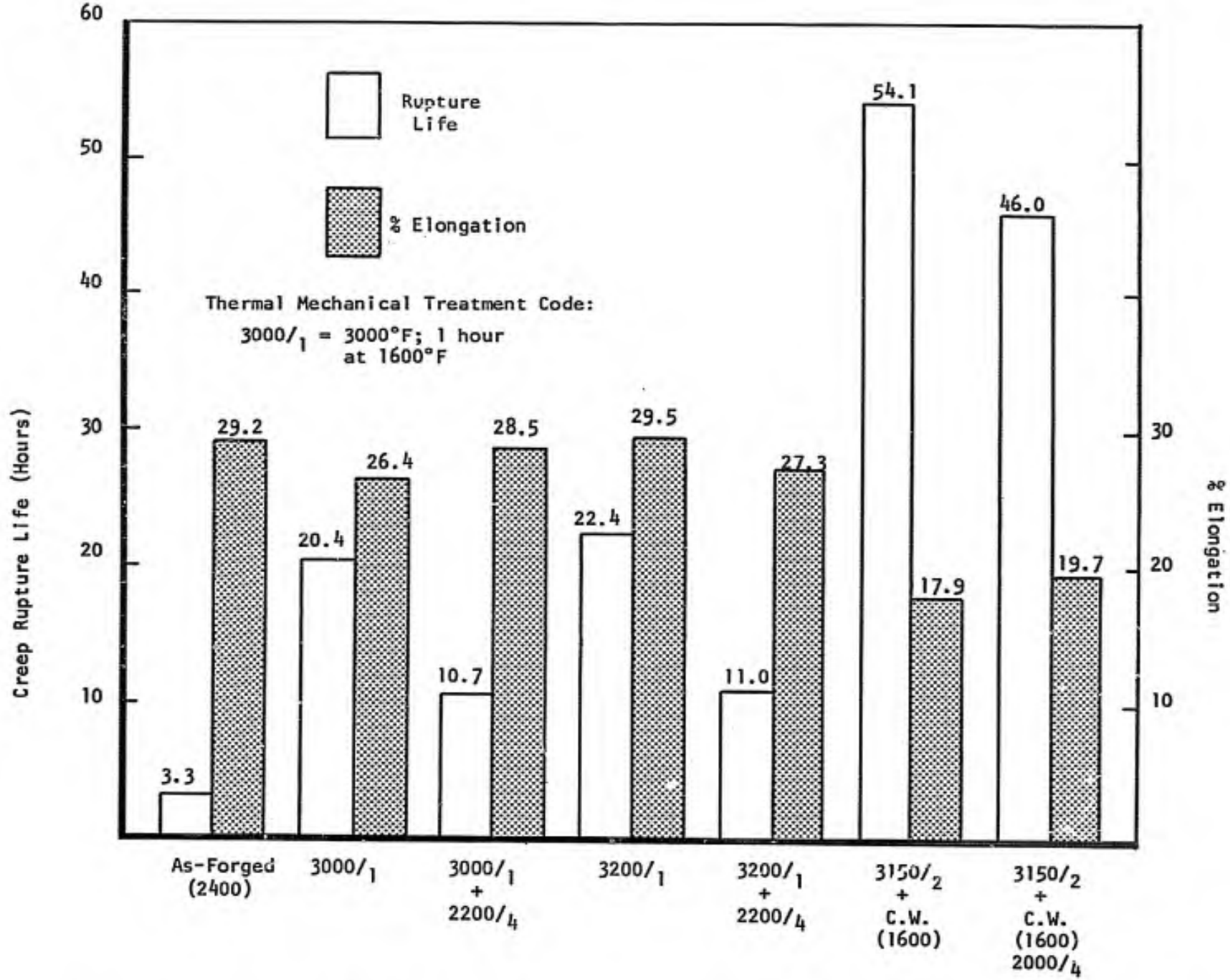

Figure 29. Comparison of 2200°F 30,000 psi creep rupture properties for SU-31 in various thermal-mechanical processing conditions as indicated. Tested in vacuum of 10^{-5} torr.

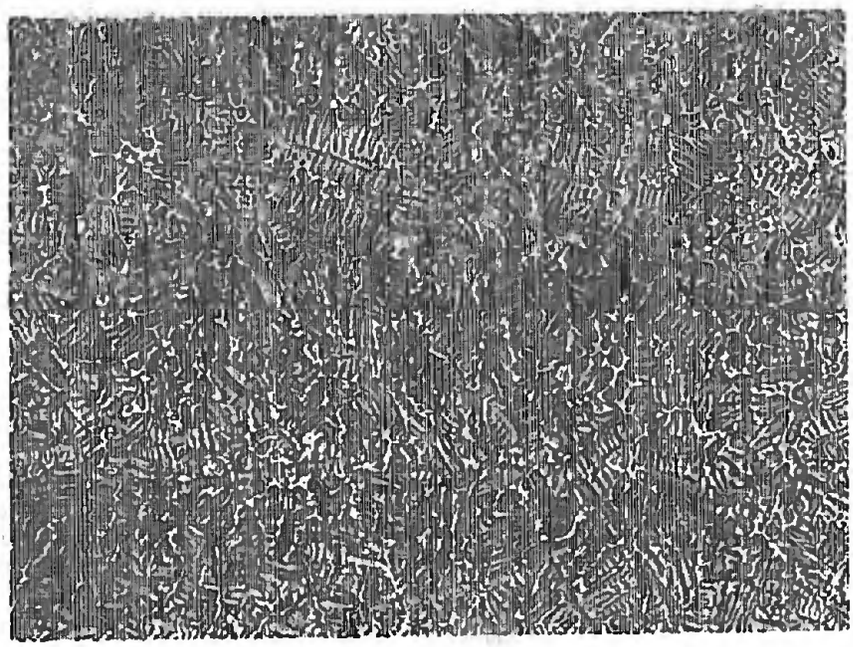

A. Alloy 1

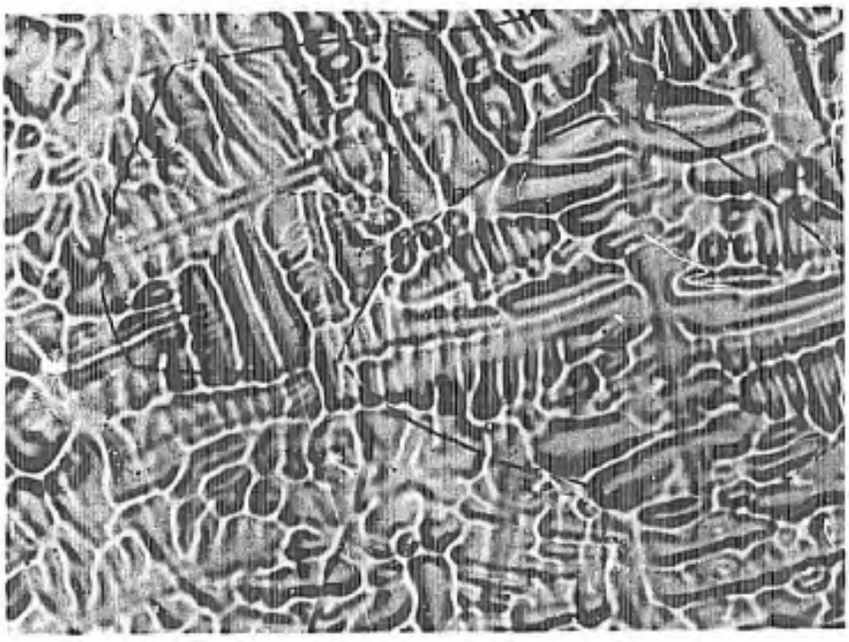

B. Alloy 2

Figure 30. Microstructures of oxidation resistant alloys in the as-cast condition. Magnification: 150X.

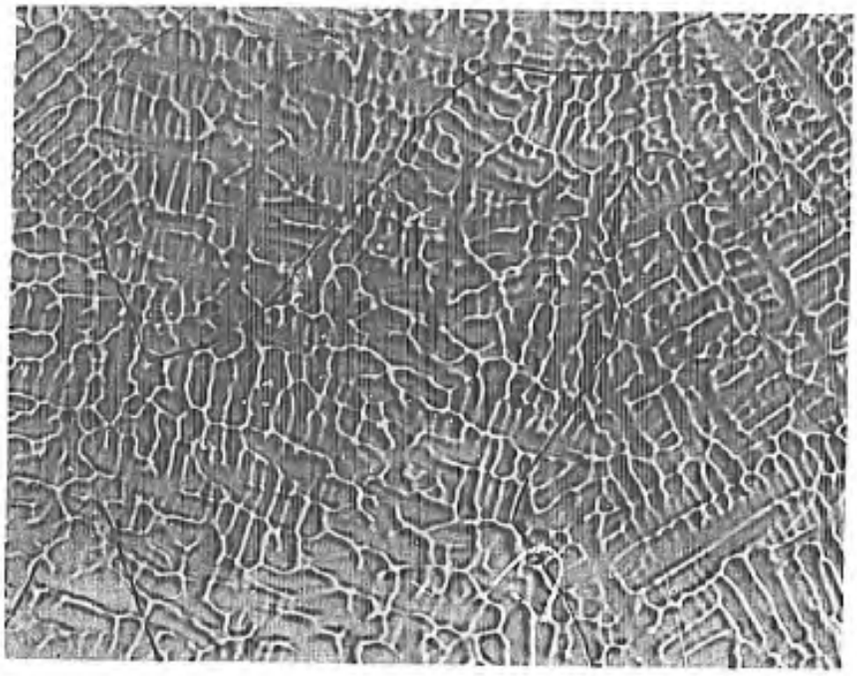

A. Alloy 3

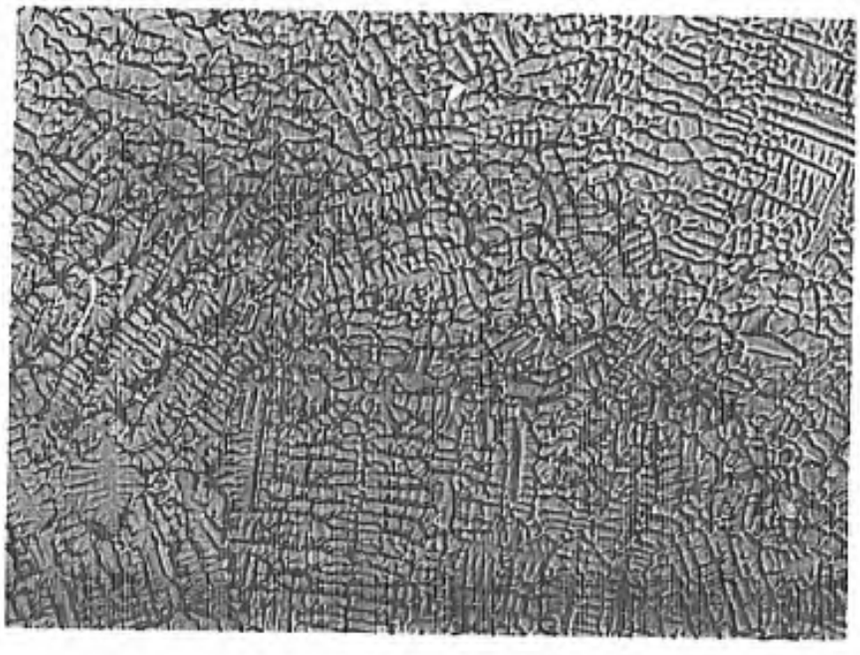

B. Alloy 4

Figure 31. Microstructures of oxidation resistant alloys in the as-cast condition. Magnification: 150X.

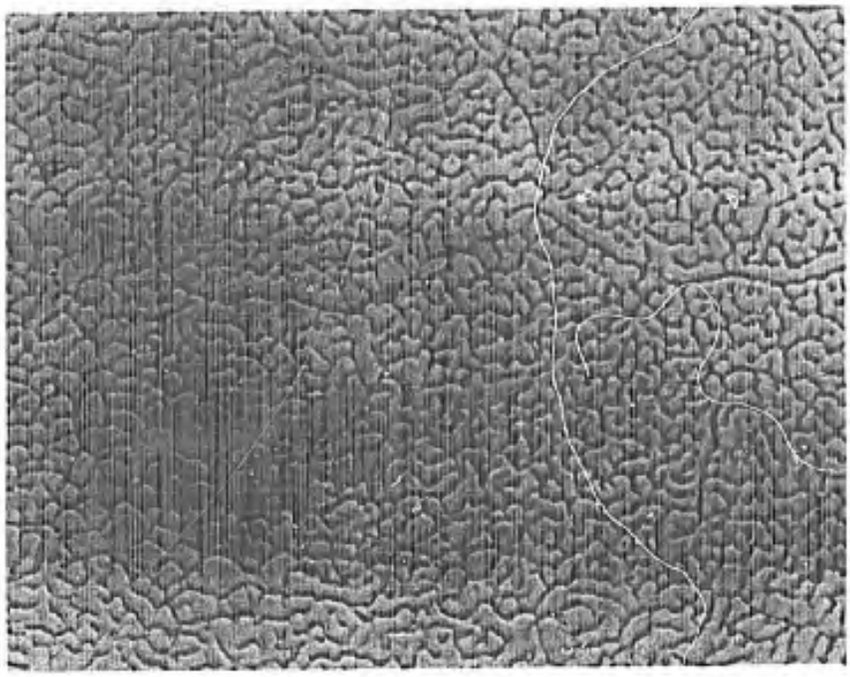

A. Alloy 5

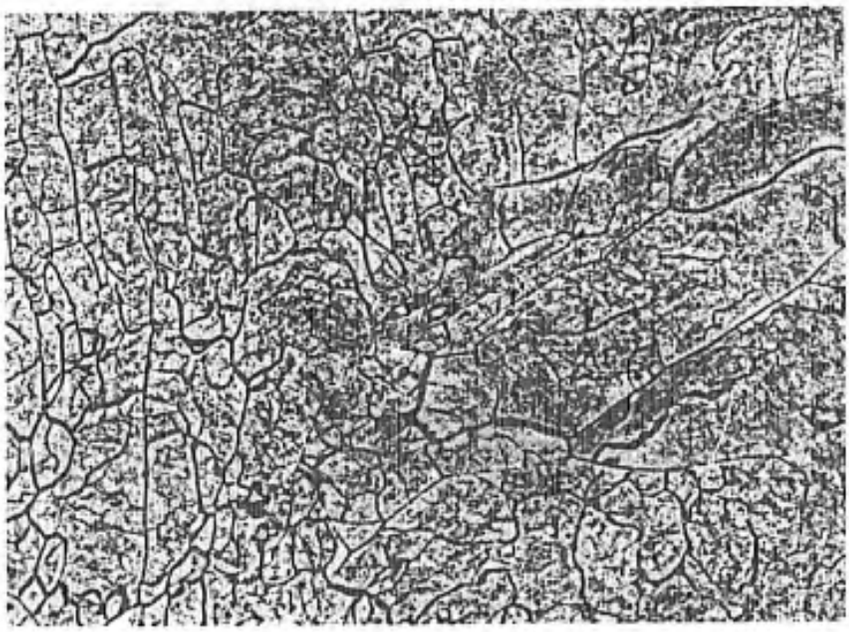

B. Alloy 6 (Hafnium Base)

Figure 32. Microstructures of oxidation resistant alloys in the as-cast condition. Magnification: 150X.

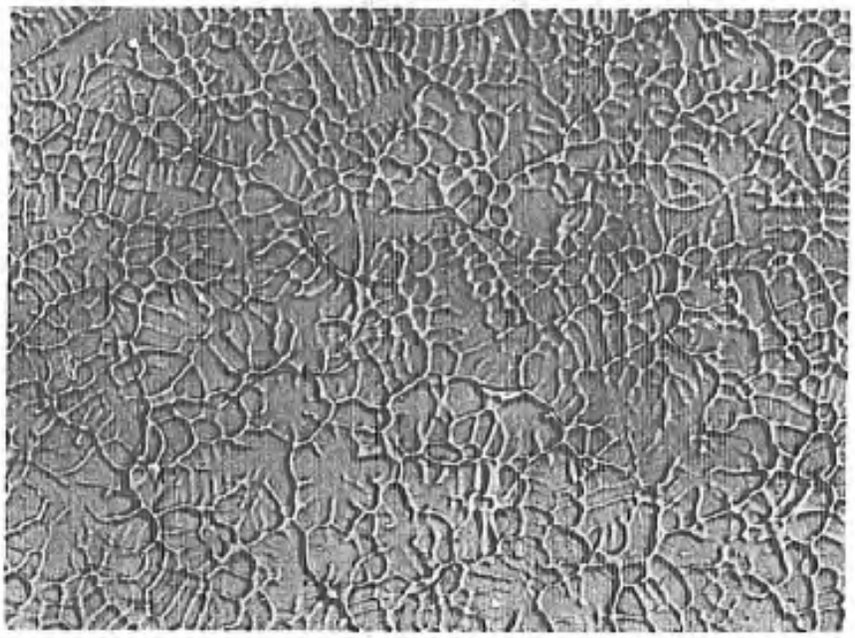

A. Alloy 7

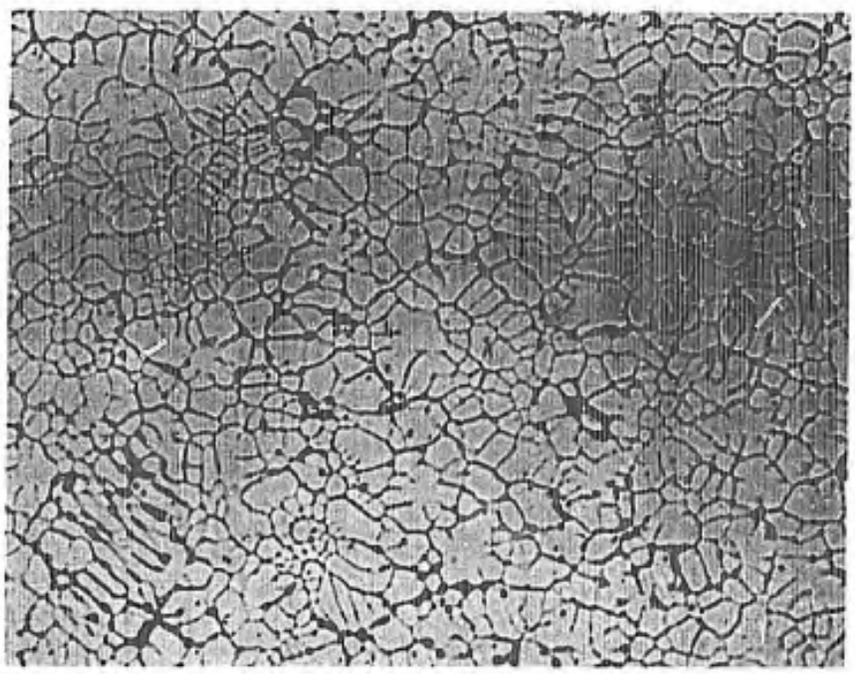

B. Alloy 8

Figure 33. Microstructures of oxidation resistant alloys in the as-cast condition. Magnification: 150X

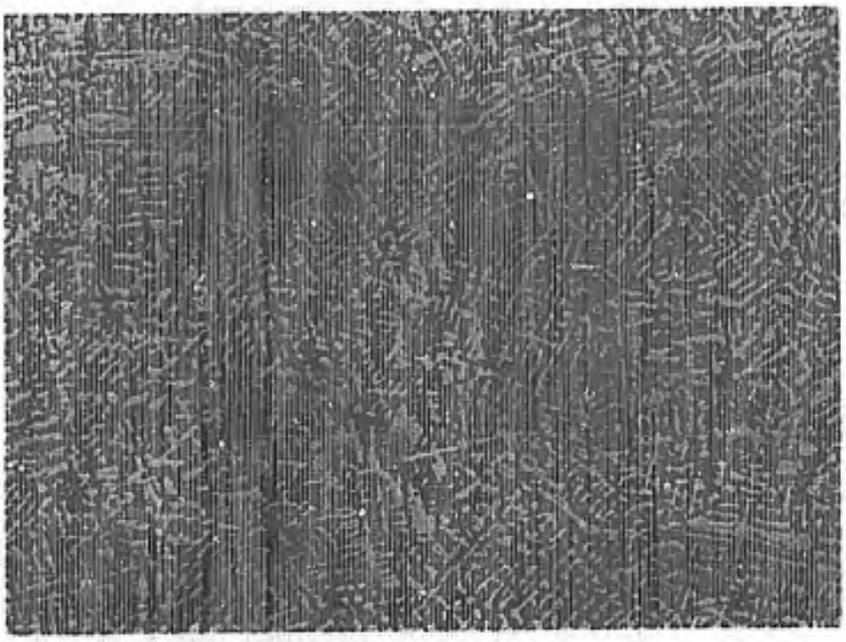

A. Alloy 9

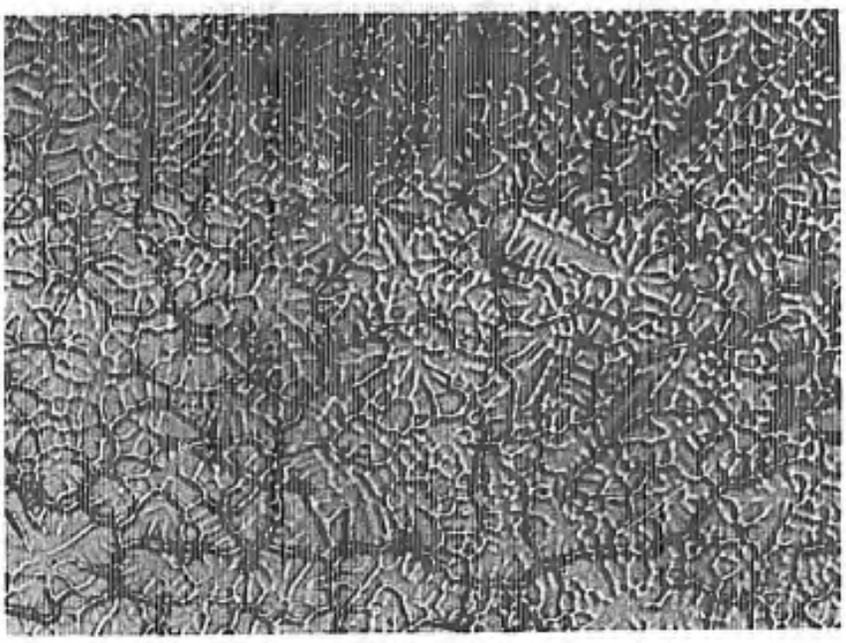

B. Alloy 10

Figure 34. Microstructures of oxidation resistant alloys in the as-cast condition. Magnification: 150X.

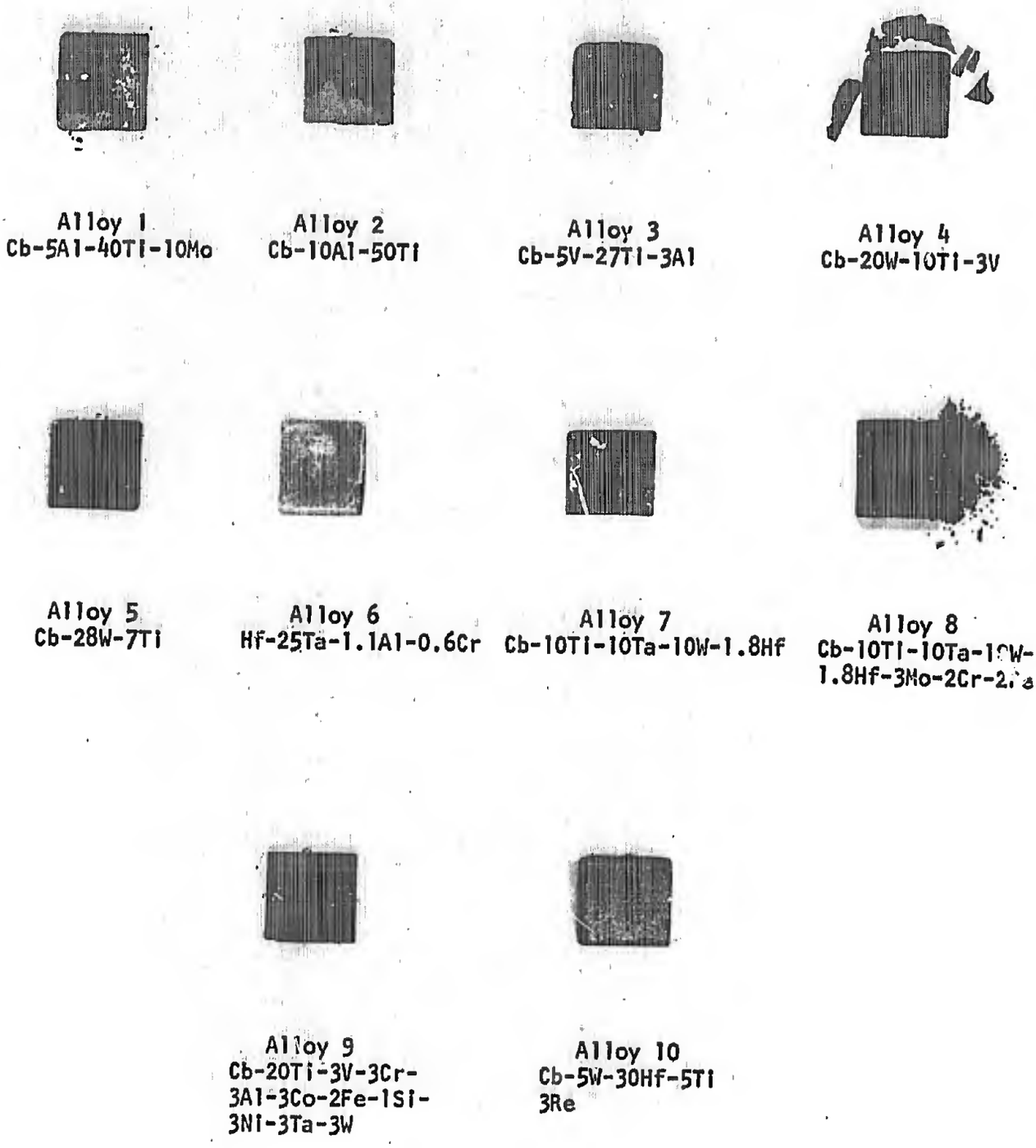

Figure 35. Oxidation test coupons following 1 hour exposure to air at 2200°F.

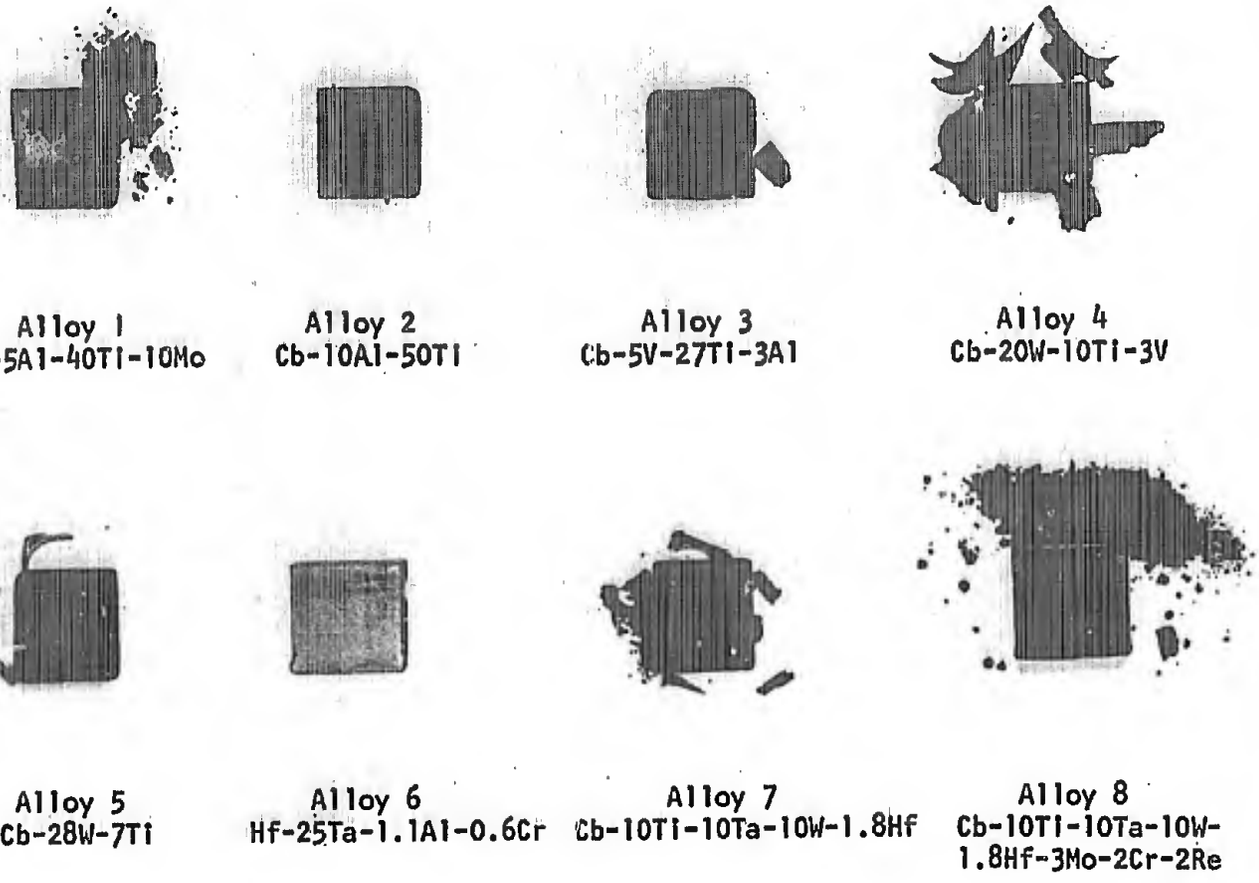

Alloy 1
Cb-5Al-40Ti-10Mo

Alloy 2
Cb-10Al-50Ti

Alloy 3
Cb-5V-27Ti-3Al

Alloy 4
Cb-20W-10Ti-3V

Alloy 5
Cb-28W-7Ti

Alloy 6
Hf-25Ta-1.1Al-0.6Cr

Alloy 7
Cb-10Ti-10Ta-10W-1.8Hf

Alloy 8
Cb-10Ti-10Ta-10W-
1.8Hf-3Mo-2Cr-2Re

Alloy 9
Cb-20Ti-3V-3Cr-
3Al-3Co-2Fe-1Si-
3Ni-3Ta-3W

Alloy 10
Cb-5W-30Hf-5Ti
3Re

Figure 36. Oxidation test coupons following 4 hours exposure to air at 2200°F.

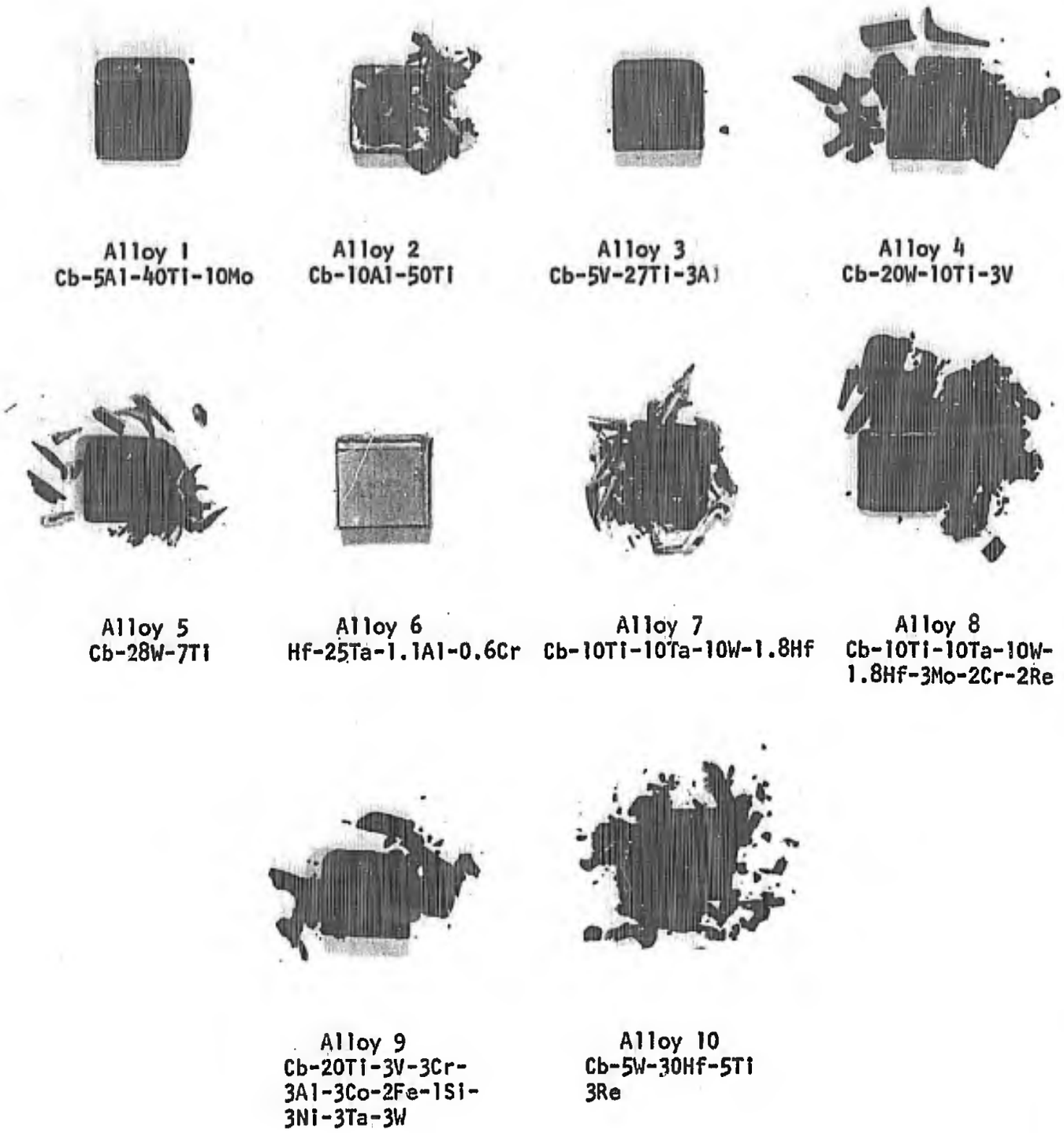

Figure 37. Oxidation test coupons following 20 hours exposure to air at 2200°F.

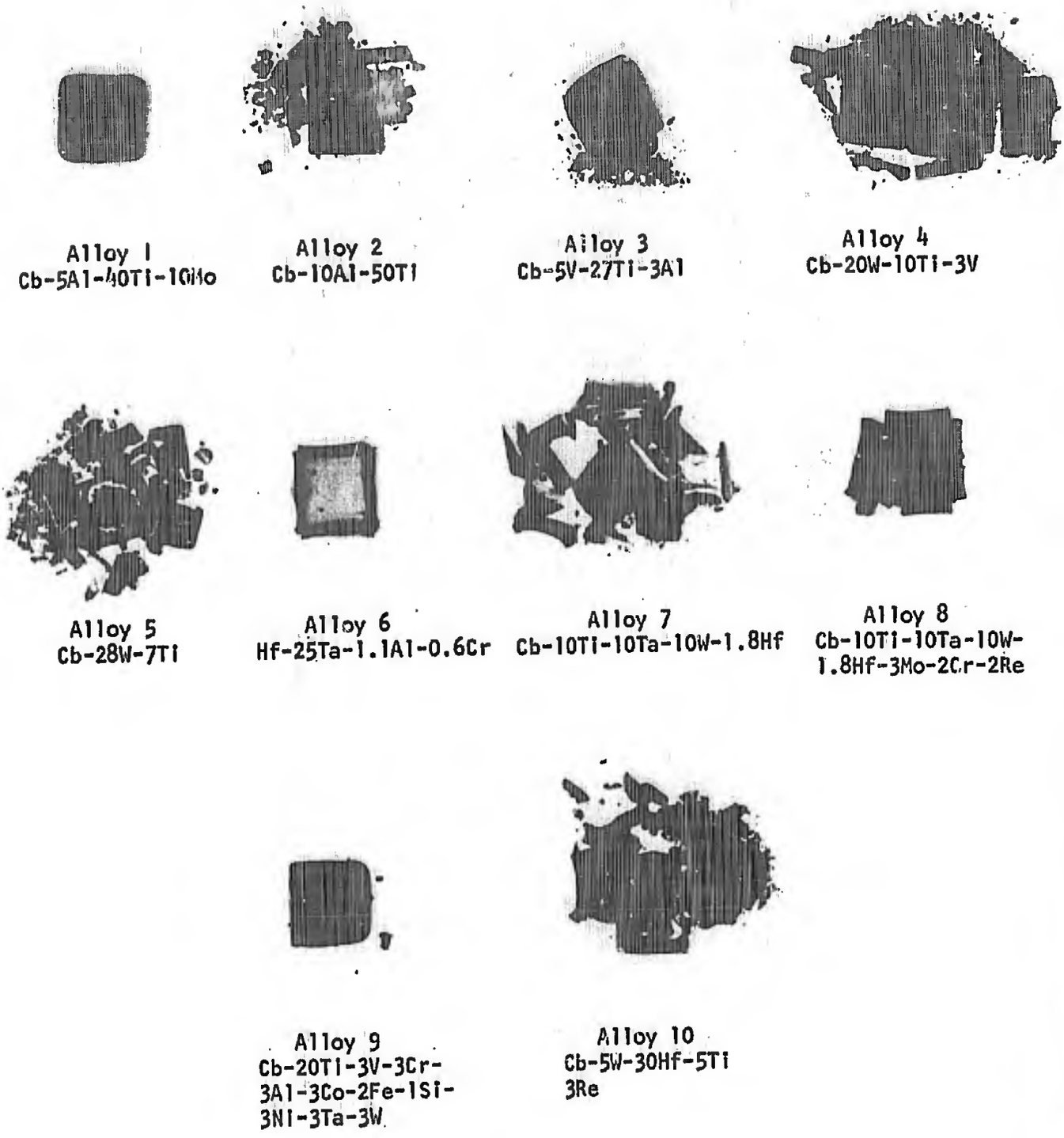

Figure 38. Oxidation test coupons following 64 hours exposure to air at 2200°F.

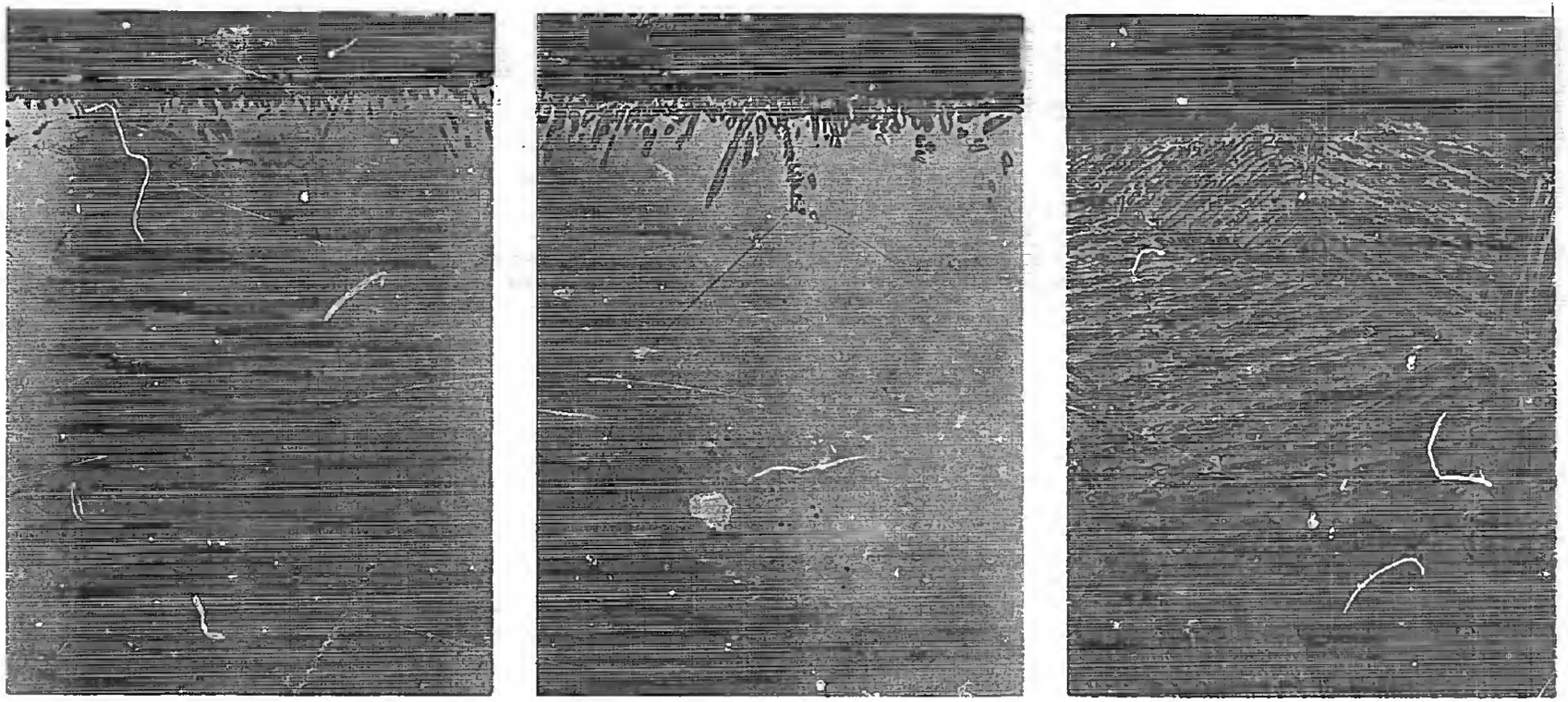

A. 1 hour B. 4 hours C. 20 hours

Figure 39. Photomicrographs of Alloy I (Cb-5Al-40Ti-10Mo) after exposure to air at 2200°F for times indicated. Magnification: 250X.

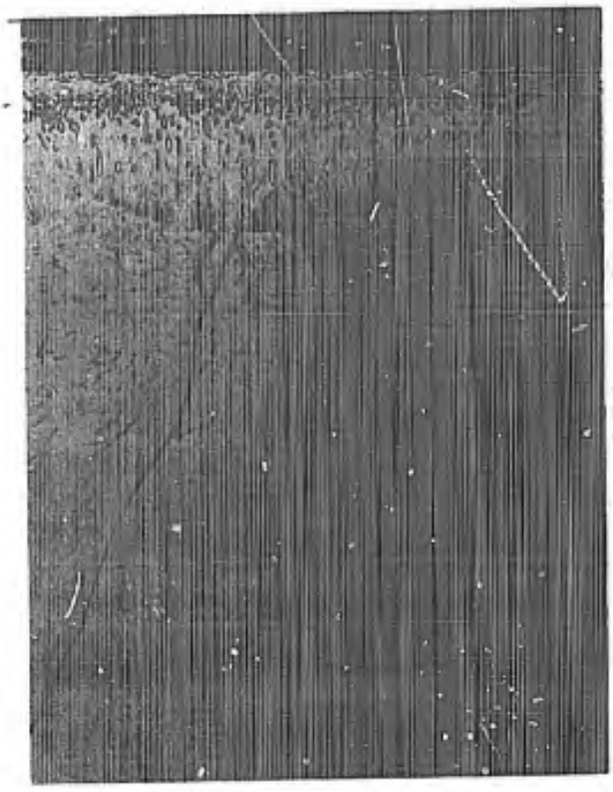

B. 4 hours

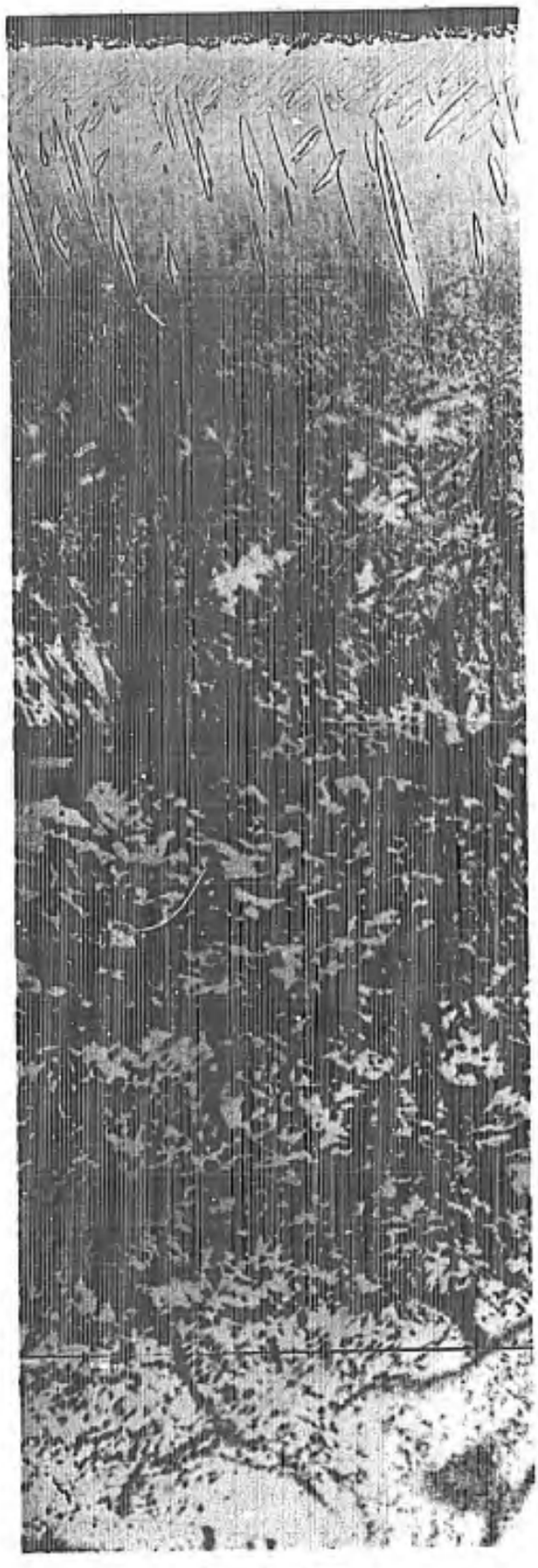

A. 1 hour

Figure 40. Photomicrographs of Alloy 2 (Cb-10Al-50Ti) after exposure to air at 2200°F for times indicated. Magnification: 250X.

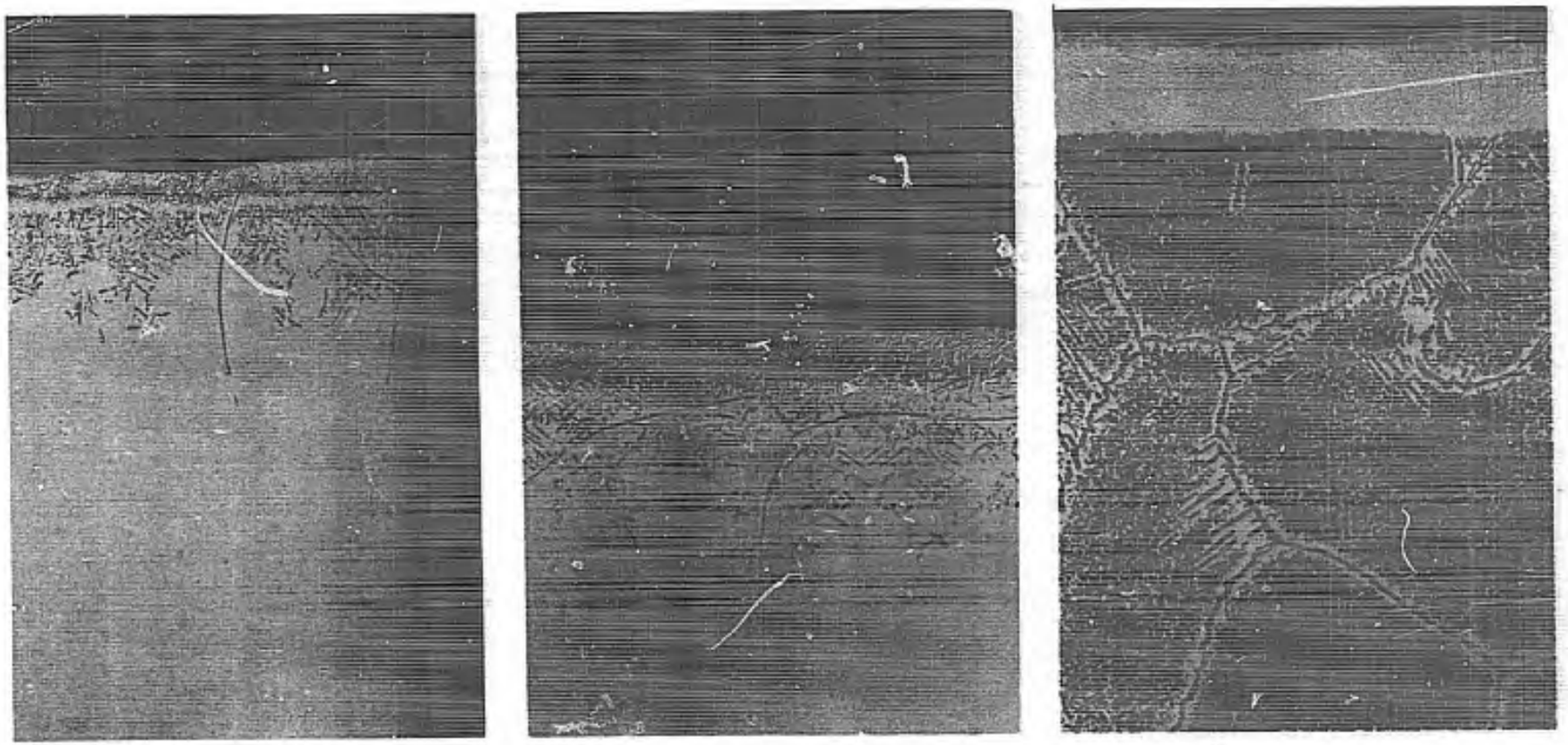

A. 1 hour

B. 4 hours

C. 64 hours

Figure 41. Photomicrographs of Alloy 3 (Cb-5V-27Ti-3Al) after exposure to air at 2200°F for times indicated. Magnification: 250X.

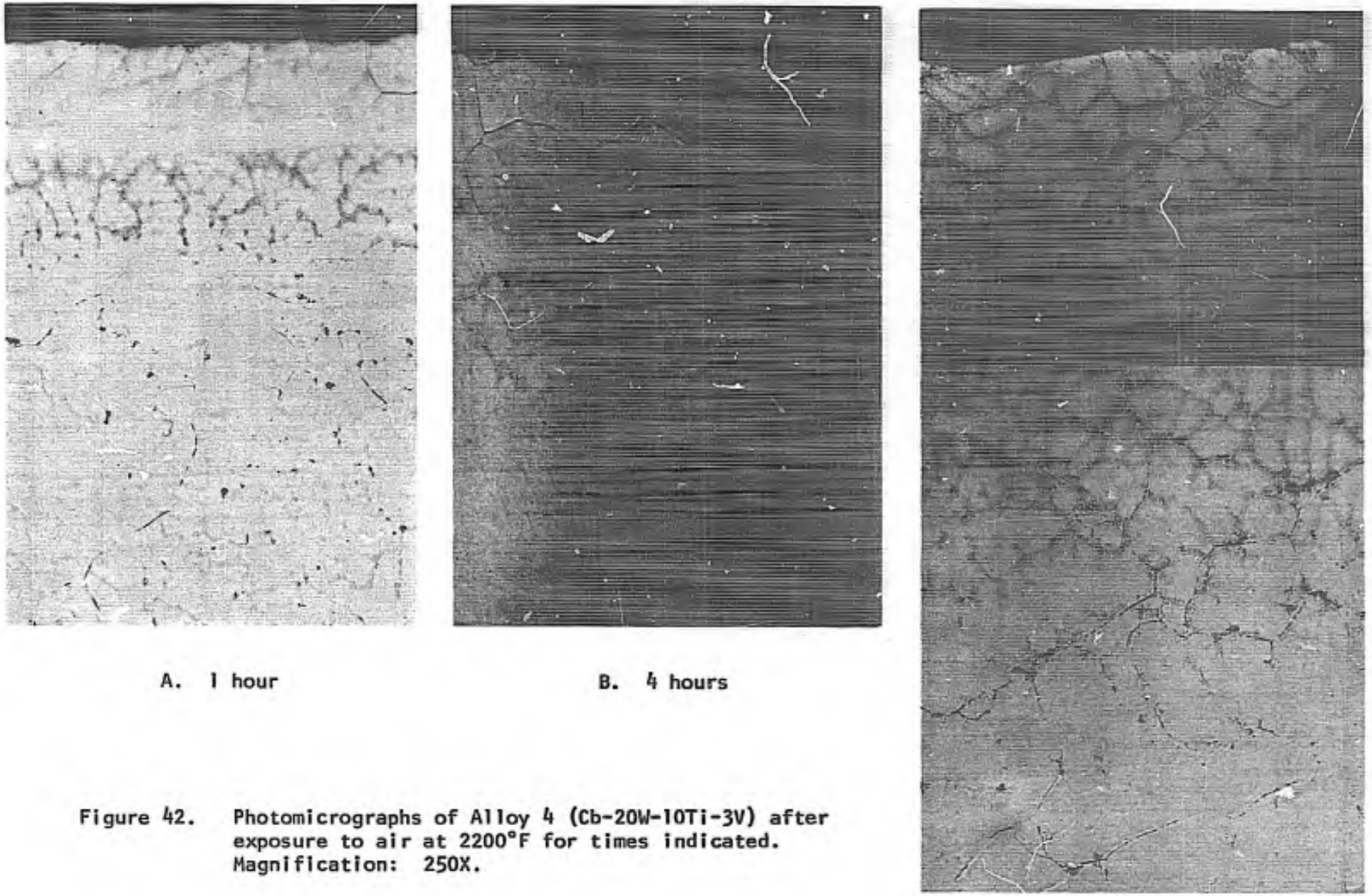

A. 1 hour

B. 4 hours

C. 20 hours

Figure 42. Photomicrographs of Alloy 4 (Cb-20W-10Ti-3V) after exposure to air at 2200°F for times indicated. Magnification: 250X.

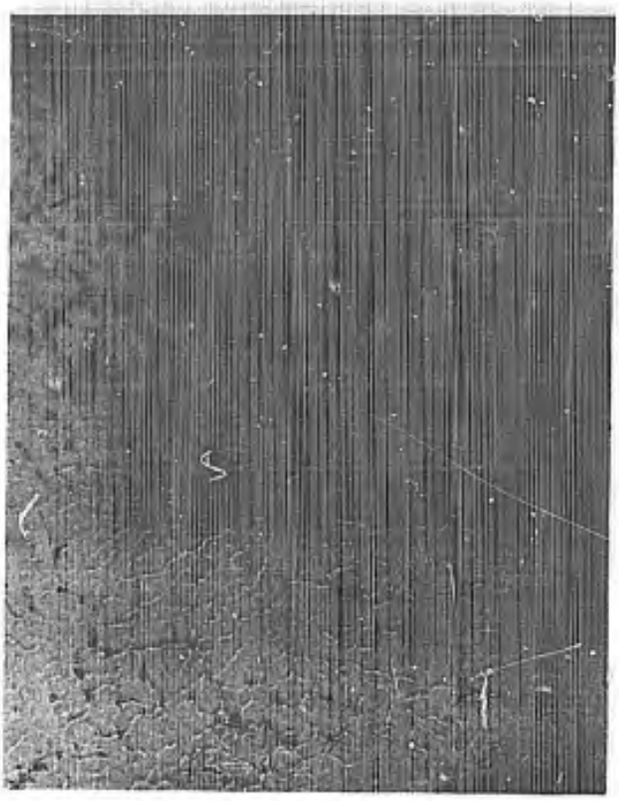

A. 1 hour

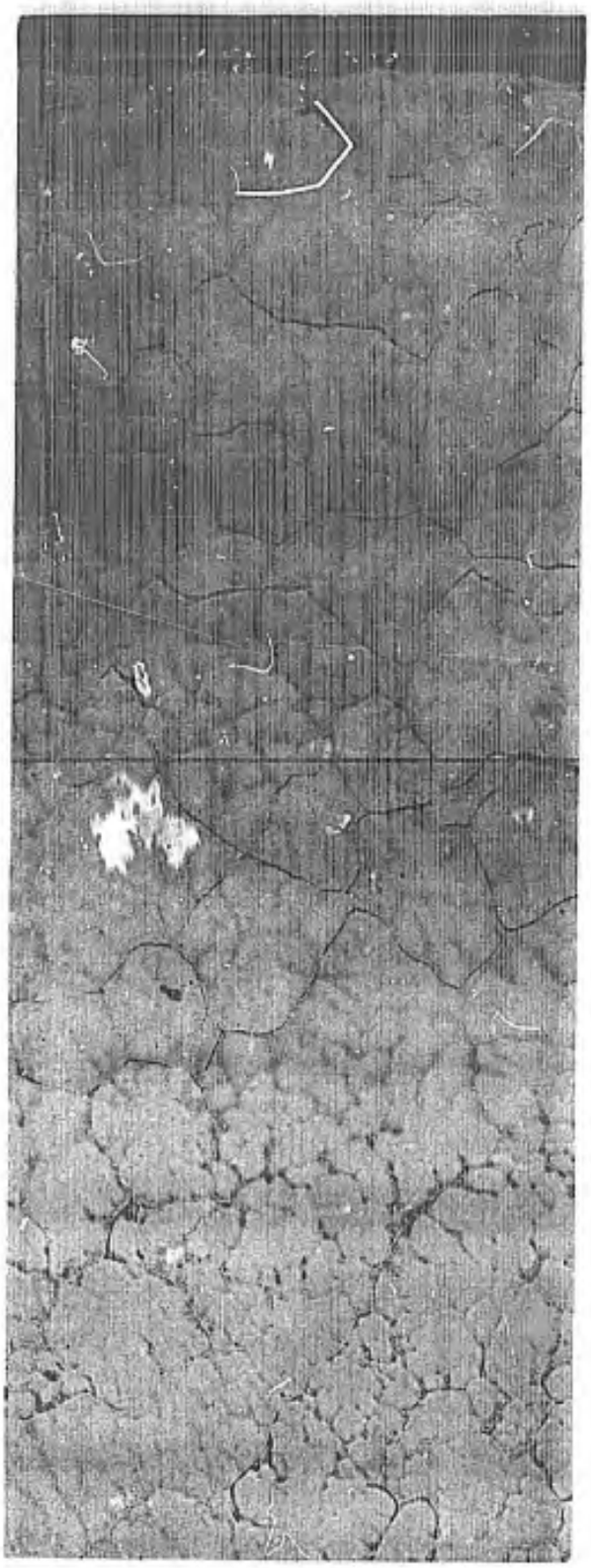

B. 20 hours

Figure 43. Photomicrographs of Alloy 5 (Cb-28W-7Ti) after exposure to air at 2200°F for times indicated. Magnification: 250X.

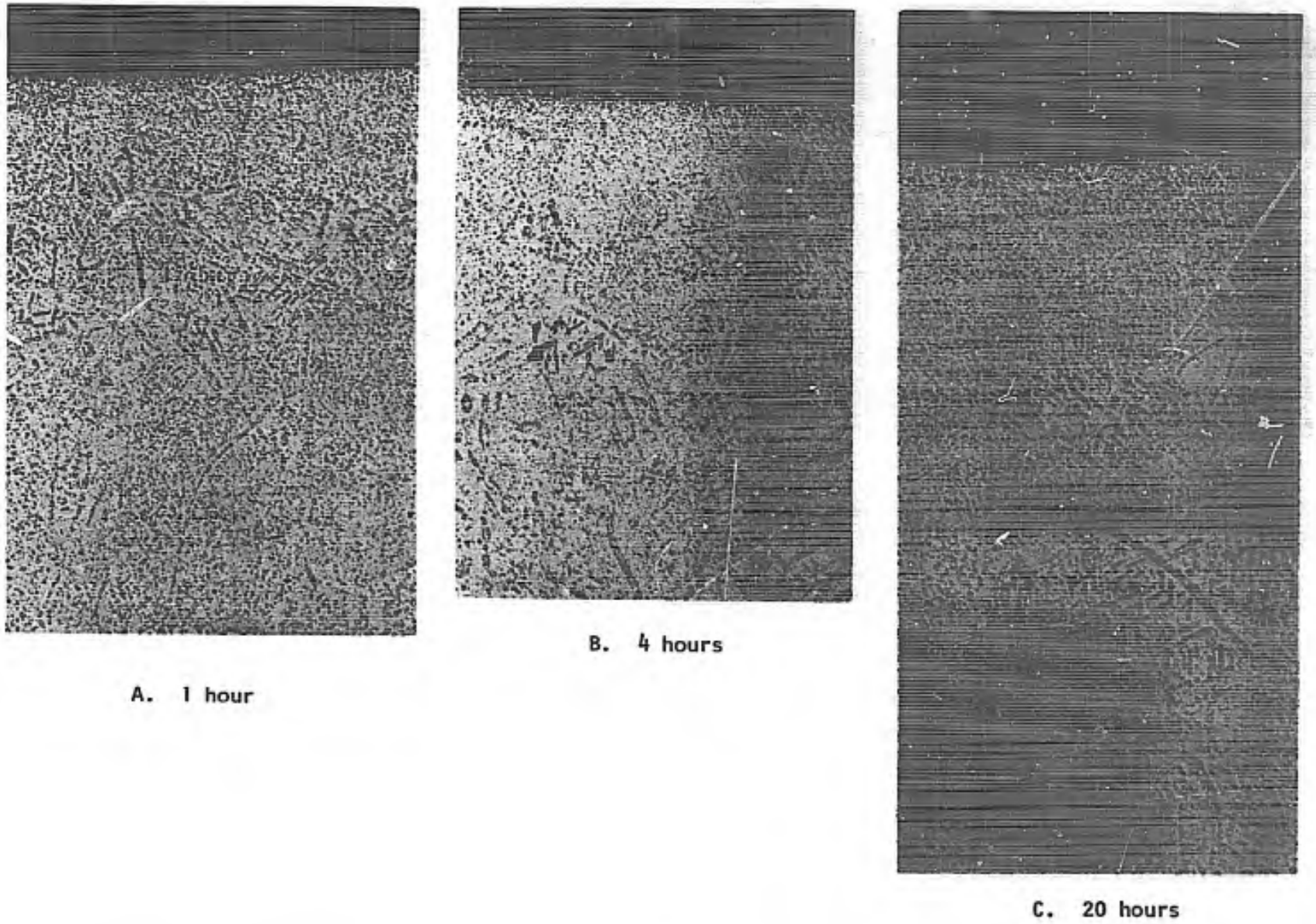

A. 1 hour

B. 4 hours

C. 20 hours

Figure 44. Photomicrographs of Alloy 6 (Hf-25Ta-1.1Al-0.6Cr) after exposure to air at 2200°F for times indicated. Magnification: 250X.

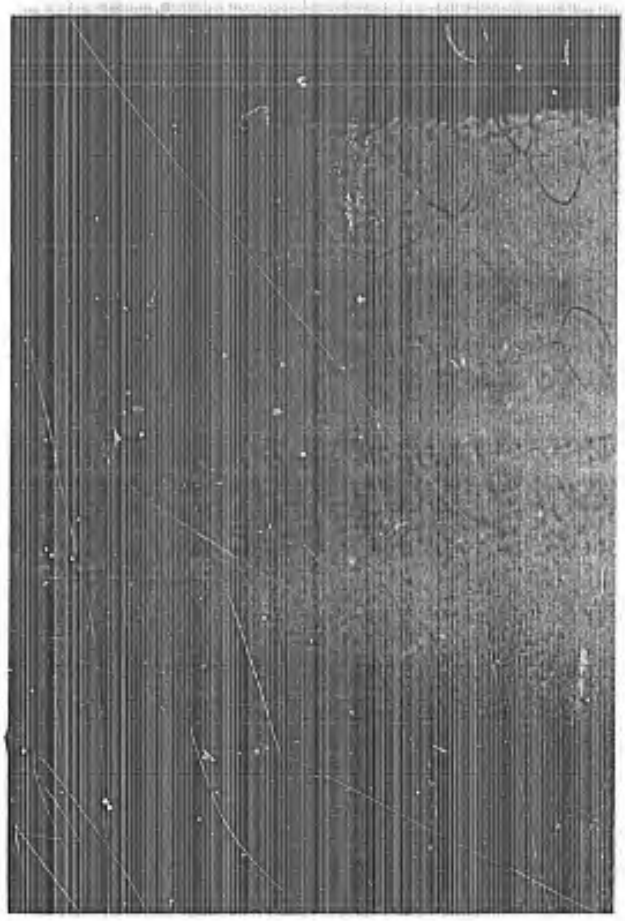

A. 1 hour

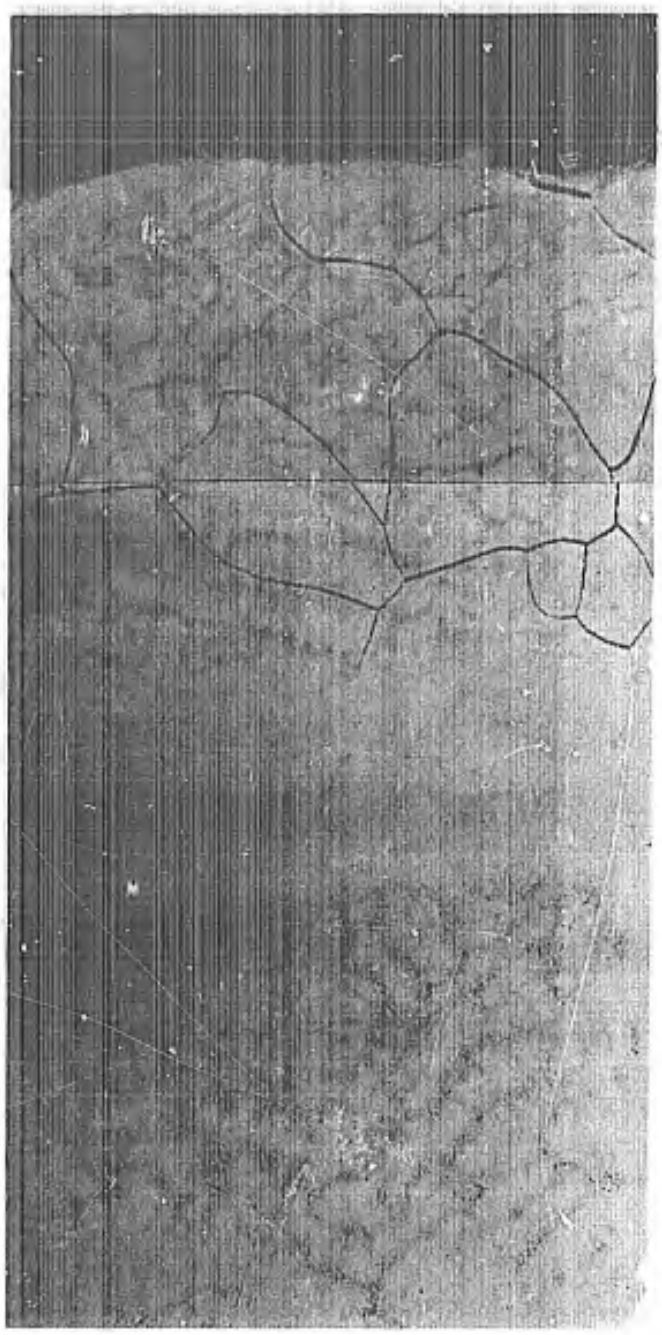

B. 20 hours

Figure 45. Photomicrographs of Alloy 7 (Cb-10Ti-10Ta-10W-1.8Hf) after exposure to air at 2200°F for times indicated. Magnification: 250X.

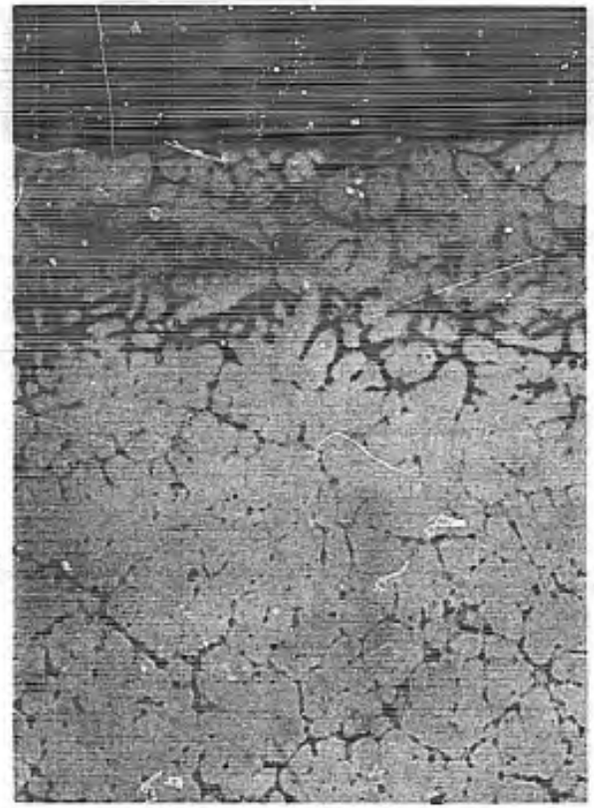

A. 1 hour

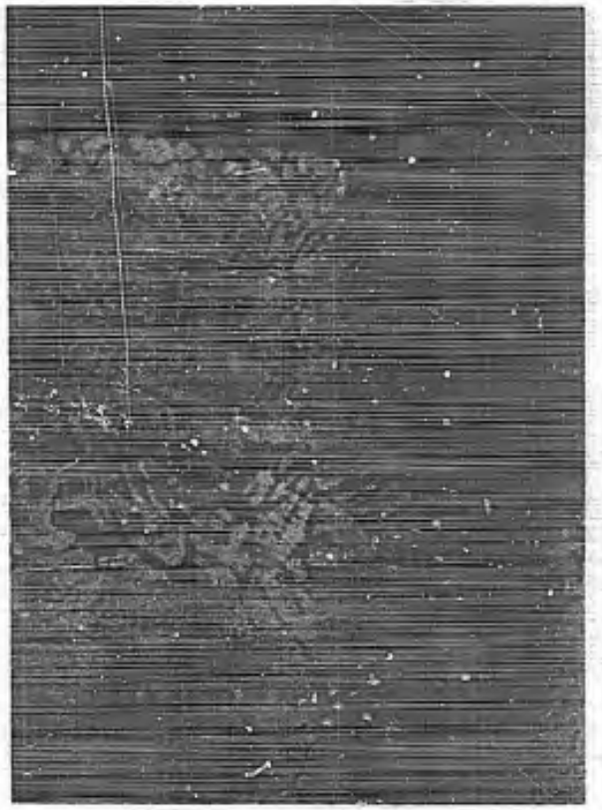

B. 4 hours

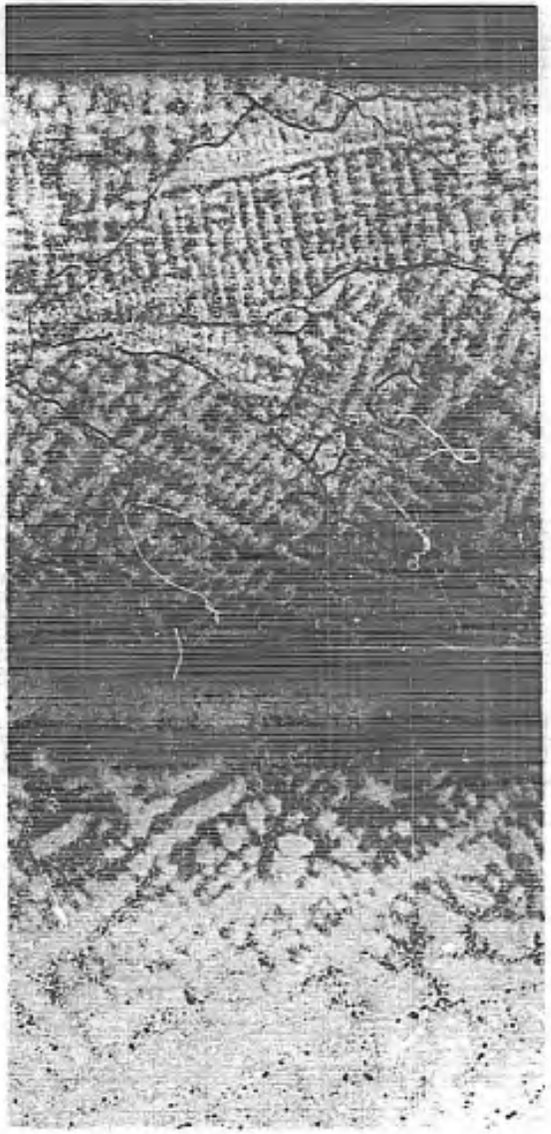

C. 20 hours

Figure 46. Photomicrographs of Alloy 8 (Cb-10Ti-10Ta-10W-1.8Hf-3Mo-2Cr-2Re) after exposure to air at 2200°F for times indicated. Magnification: 250X.

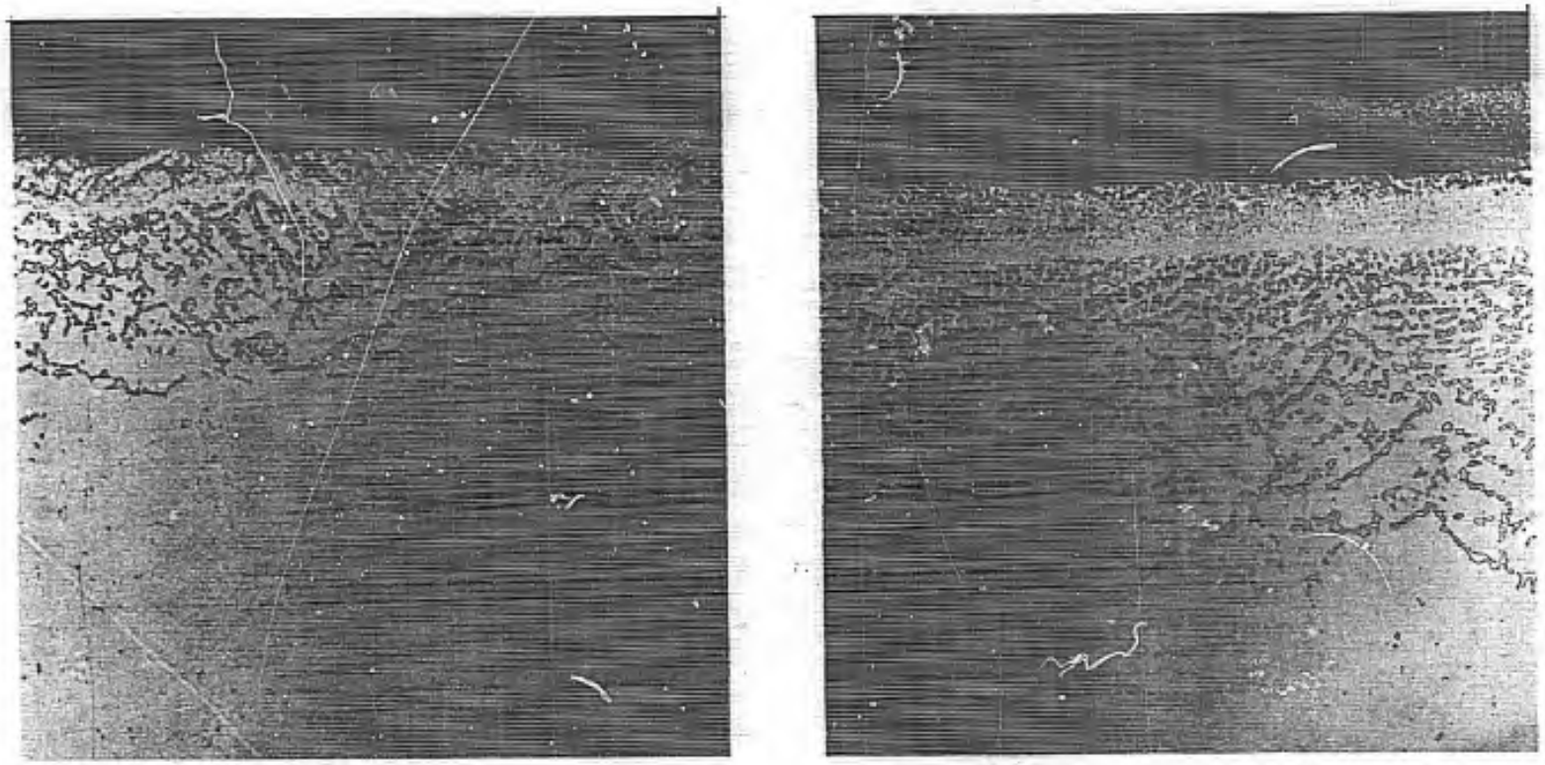

A. 1 hour

B. 4 hours

Figure 47. Photomicrographs of Alloy 9 (Cb-20Ti-3V-3Cr-3Al-3Co-2Fe-1Si-3Ni-3Ta-3W) after exposure to air at 2200°F for times indicated. Magnification: 250X.

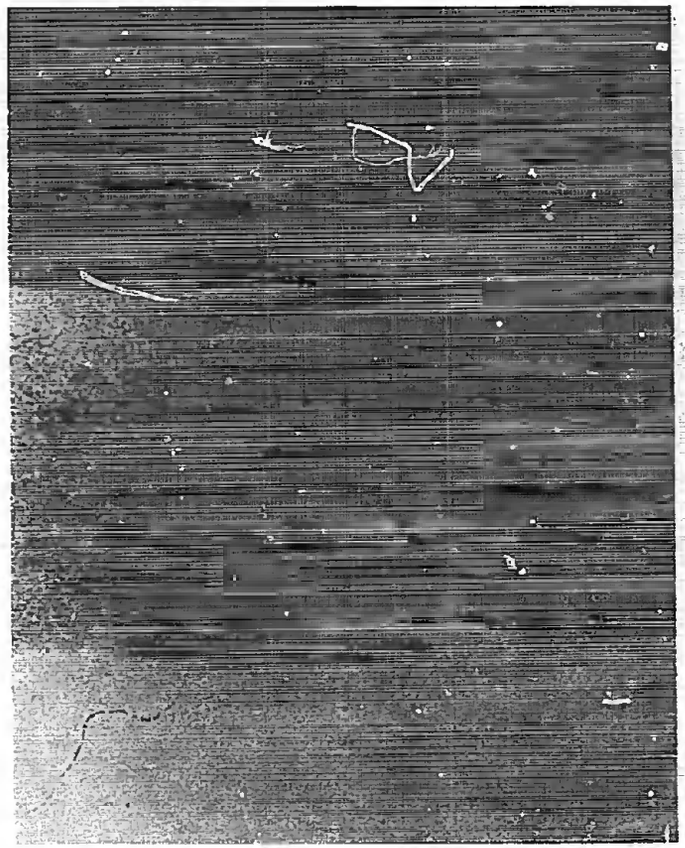

A. 1 hour

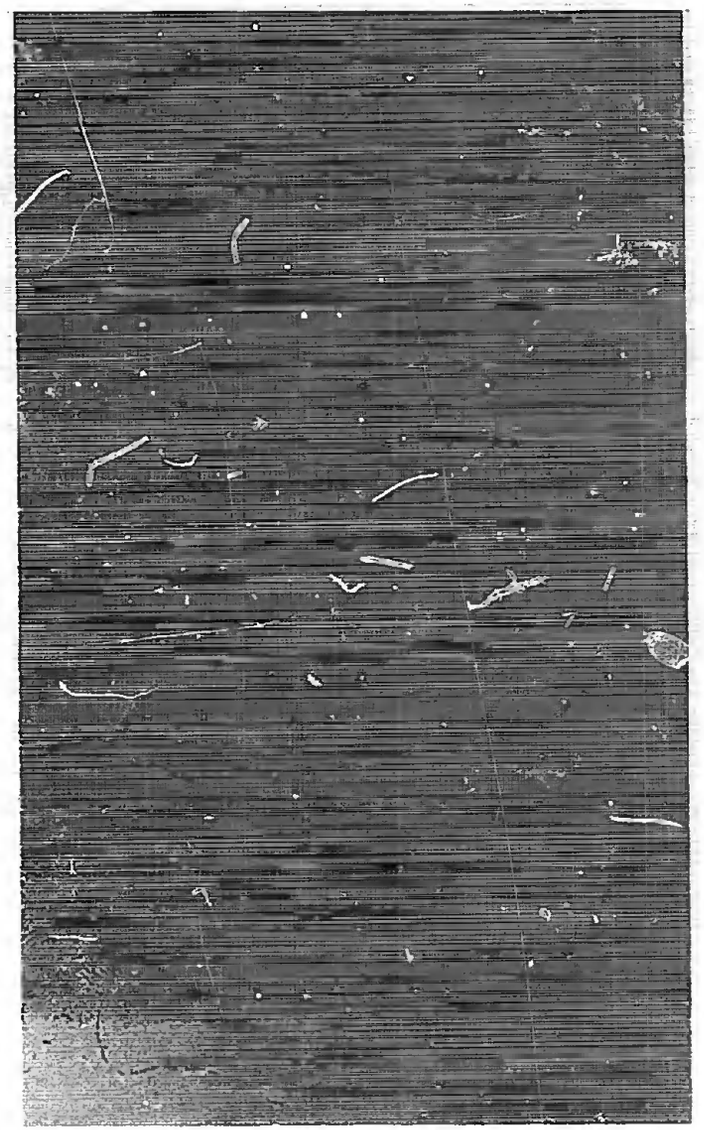

B. 4 hours

Figure 48. Photomicrographs of Alloy 10 (Cb-5W-30Hf-5Ti-3Re) after exposure to air at 2200°F for times indicated. Magnification: 250X.

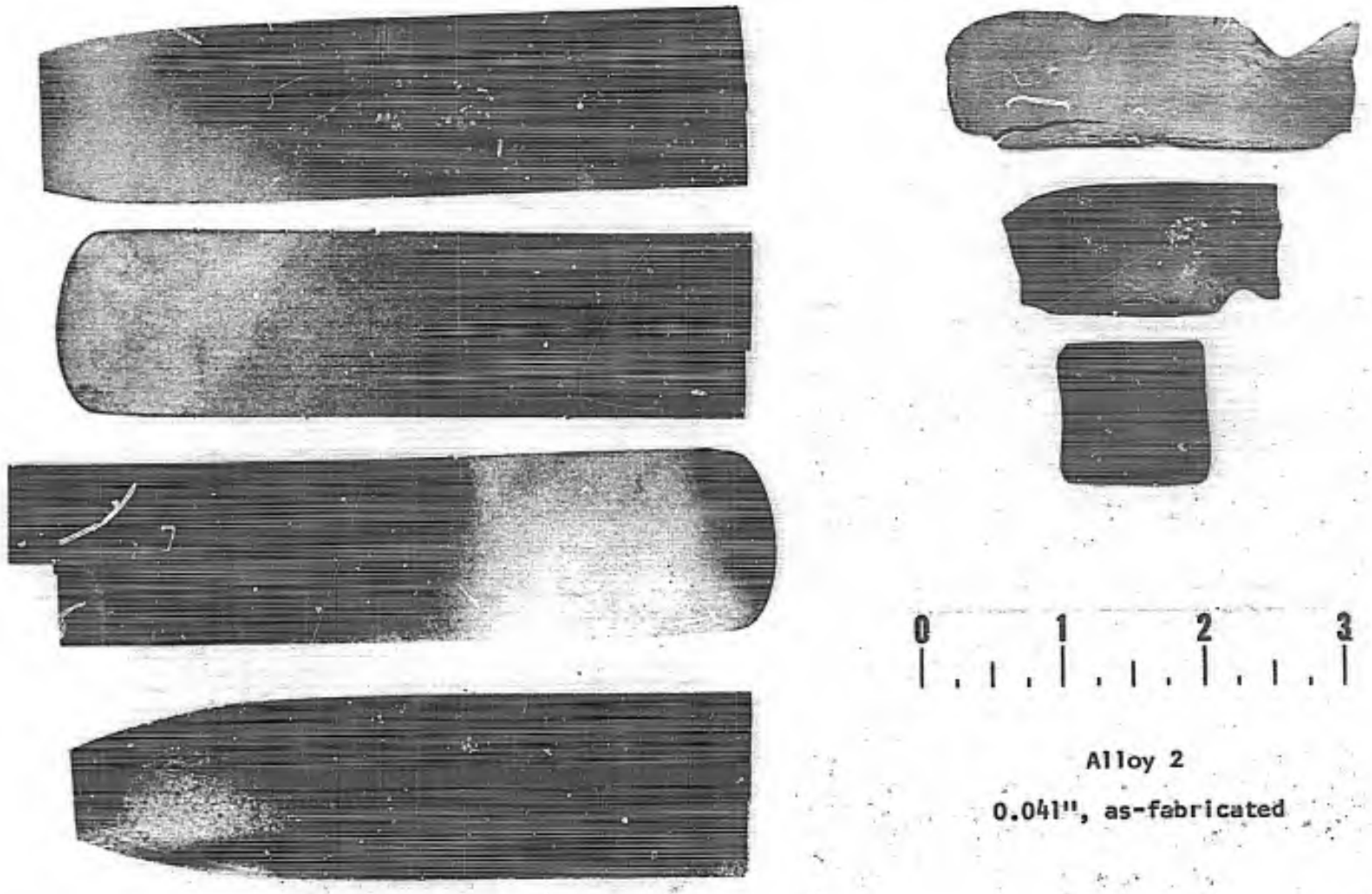

Alloy 1

0.020", annealed 2200°F

Alloy 2

0.041", as-fabricated

Figure 49. Oxidation resistant alloys in final state of fabrication.

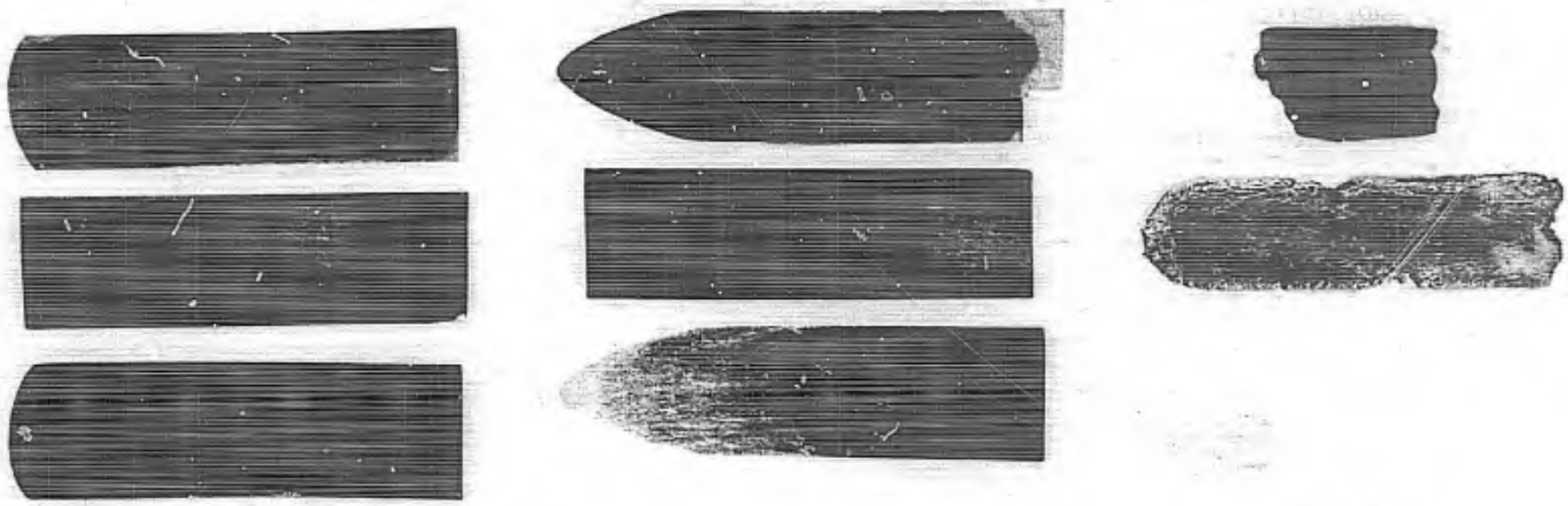

Alloy 3

0.0195", annealed 2200°F

Alloy 4

0.039" as-fabricated

0 1 2 3

Figure 50. Oxidation resistant alloys in final state of fabrication.

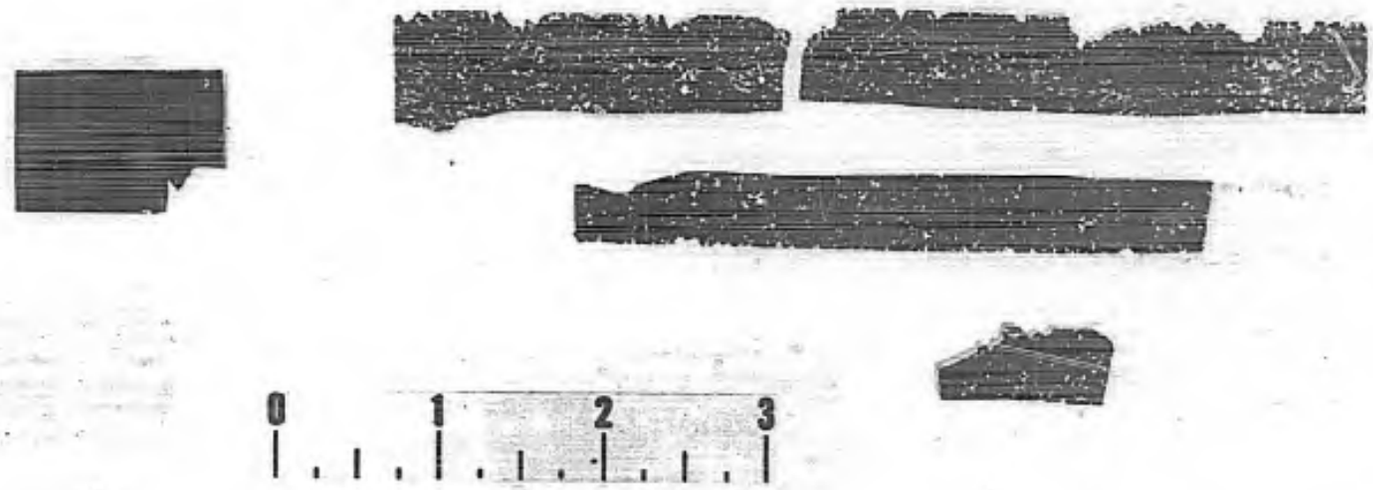

Alloy 5

failed billet

Alloy 6

0.043", annealed 2400°F

Figure 51. Oxidation resistant alloys in final state of fabrication.

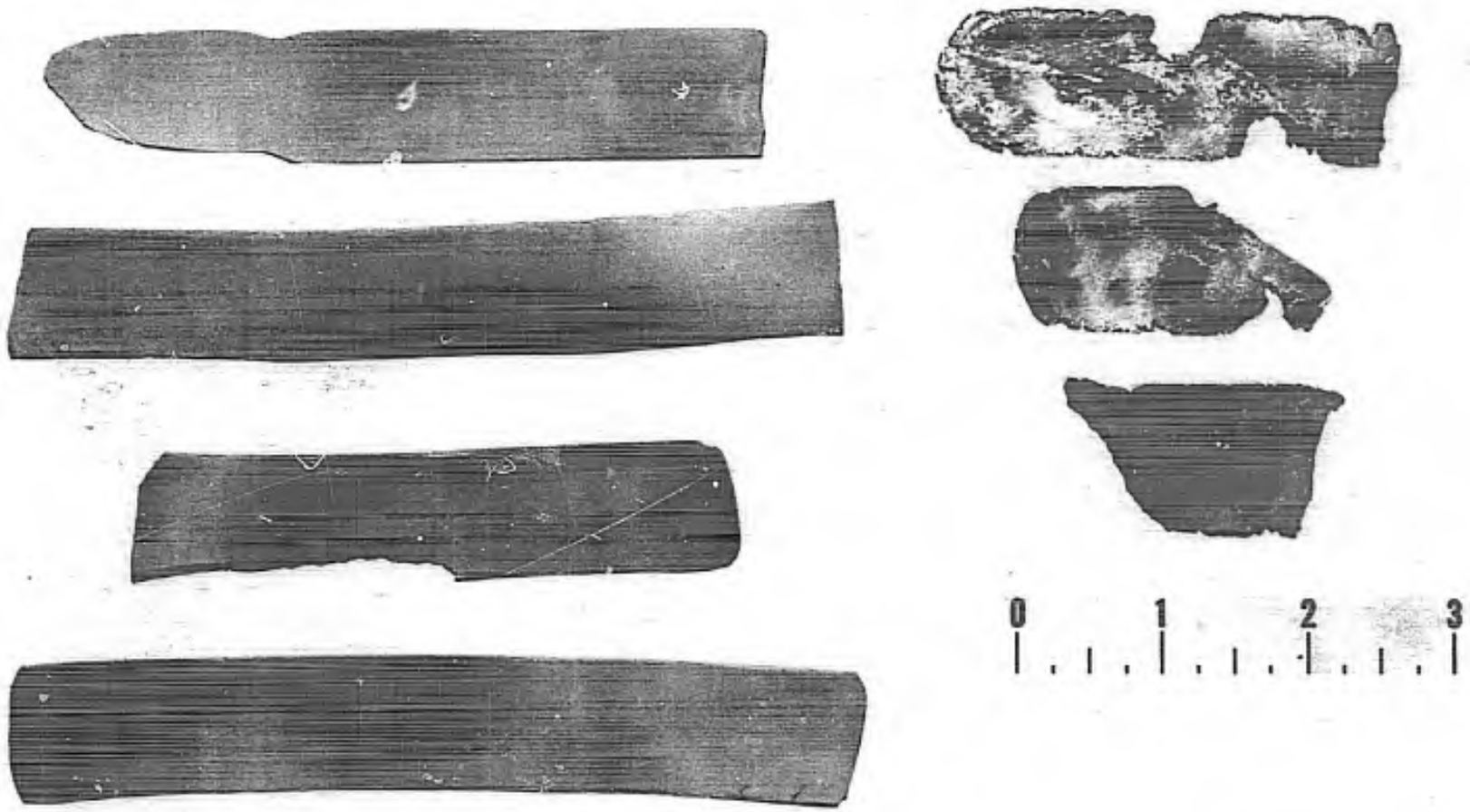

Alloy 7

0.020", annealed 2400°F

Alloy 8

0.043", as-fabricated

Figure 52. Oxidation resistant alloys in final state of fabrication.

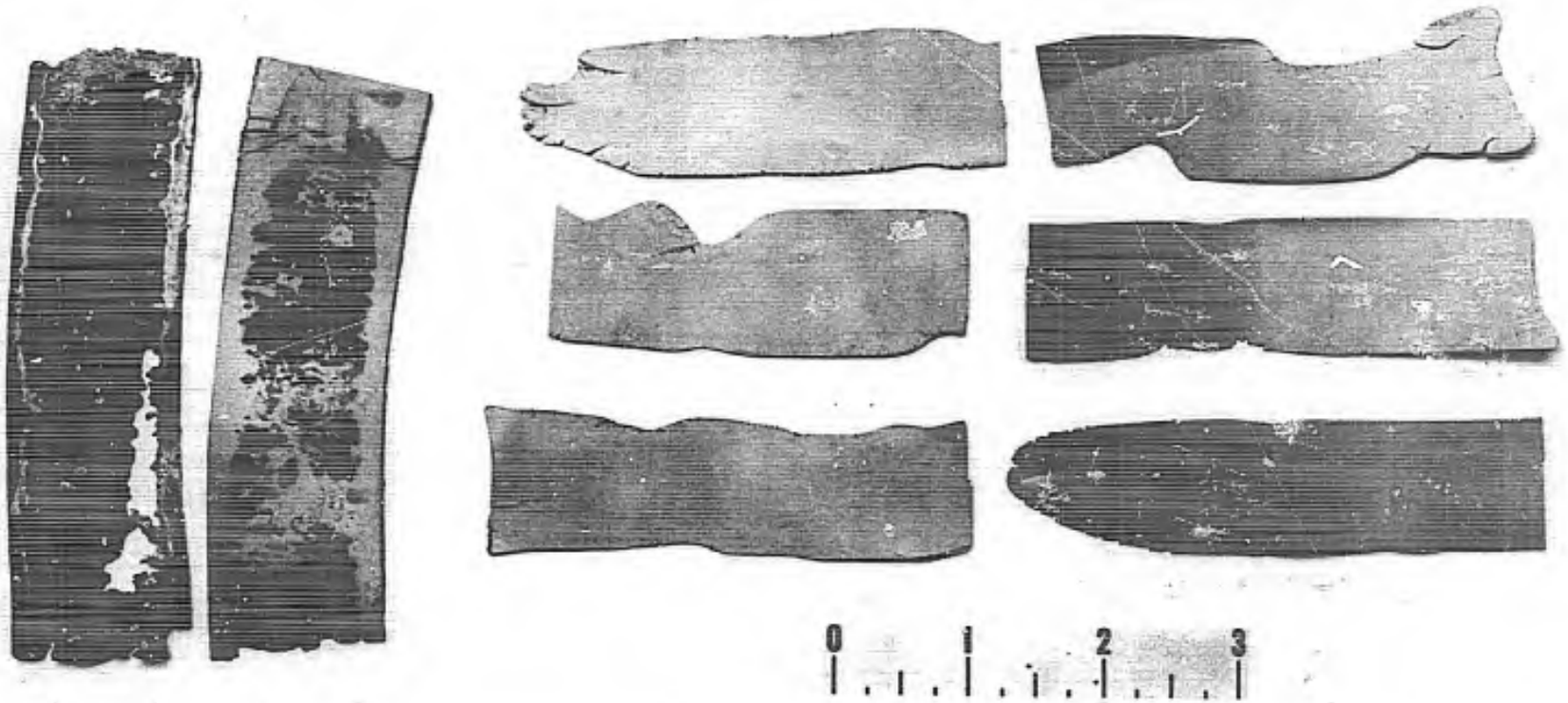

Alloy 9

failed sheet

Alloy 10

0.020", annealed 2400°F

Figure 53. Oxidation resistant alloys in final state of fabrication.

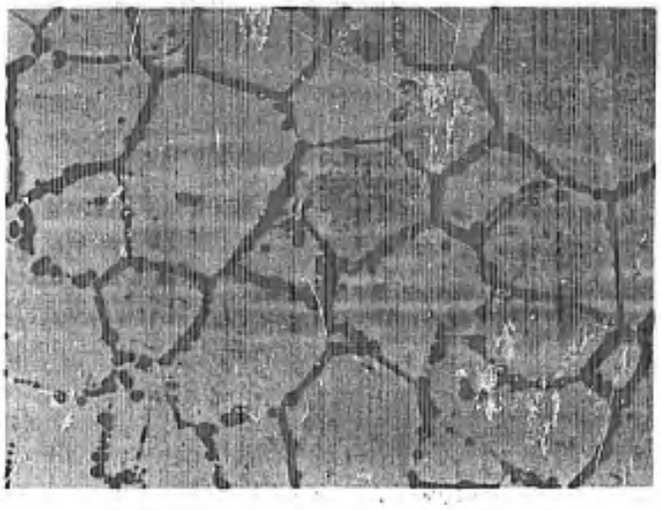

A. Alloy 1, annealed 2200°F

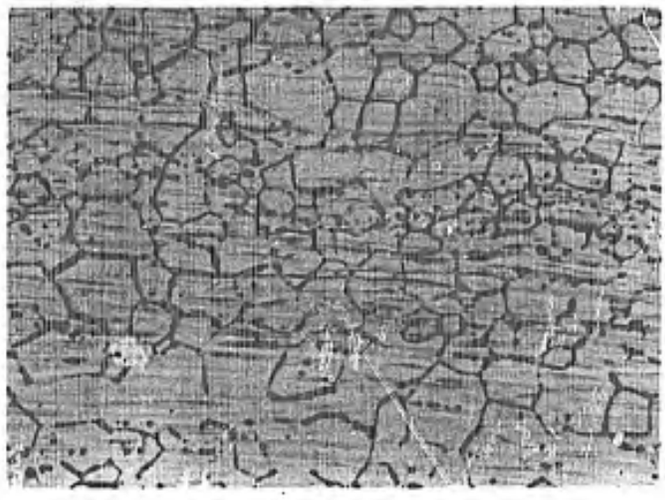

B. Alloy 2, as-fabricated

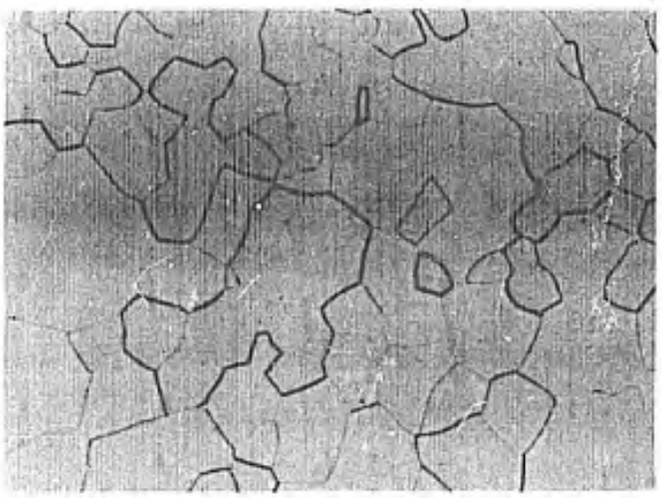

C. Alloy 3, annealed 2200°F

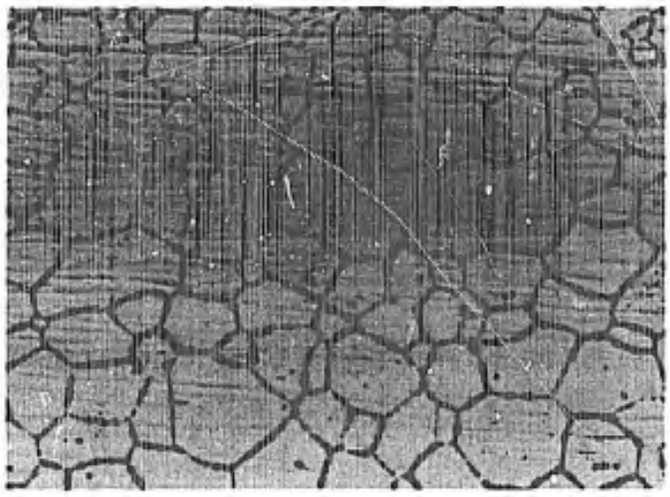

D. Alloy 4, as-fabricated

Figure 54. Microstructures of fabricated oxidation resistant alloys. Magnification: 150X.

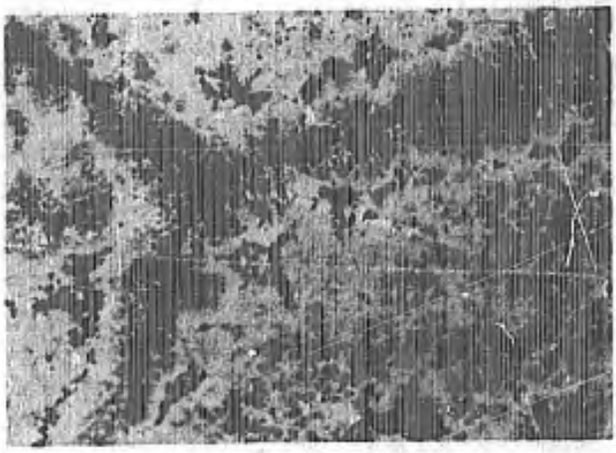

A. Alloy 6, (hafnium base), annealed 2400°F

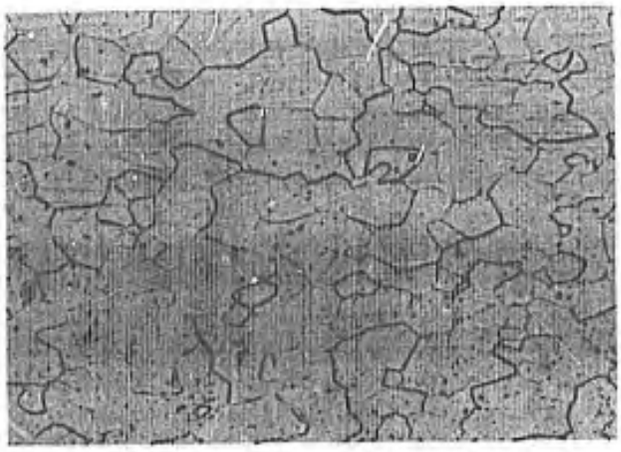

Alloy 7, annealed 2400°F

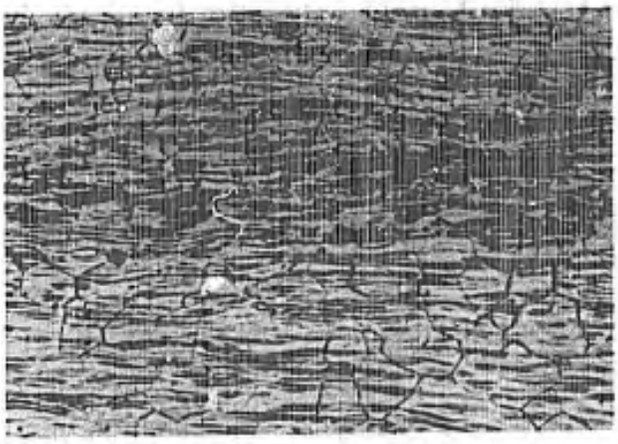

C. Alloy 8, as-fabricated

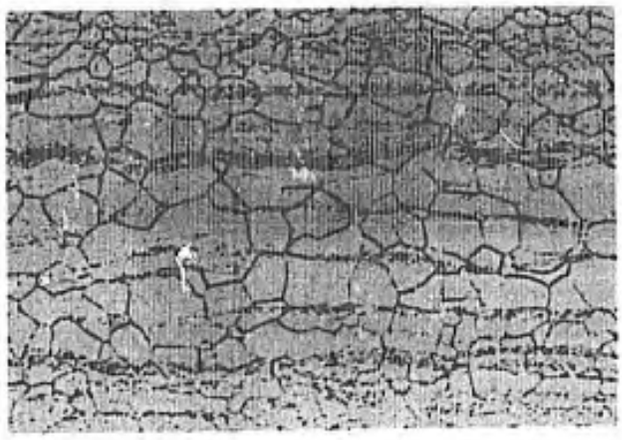

D. Alloy 10, annealed 2400°F

Figure 55. Microstructure of fabricated oxidation resistant alloys. Magnification: 150X.

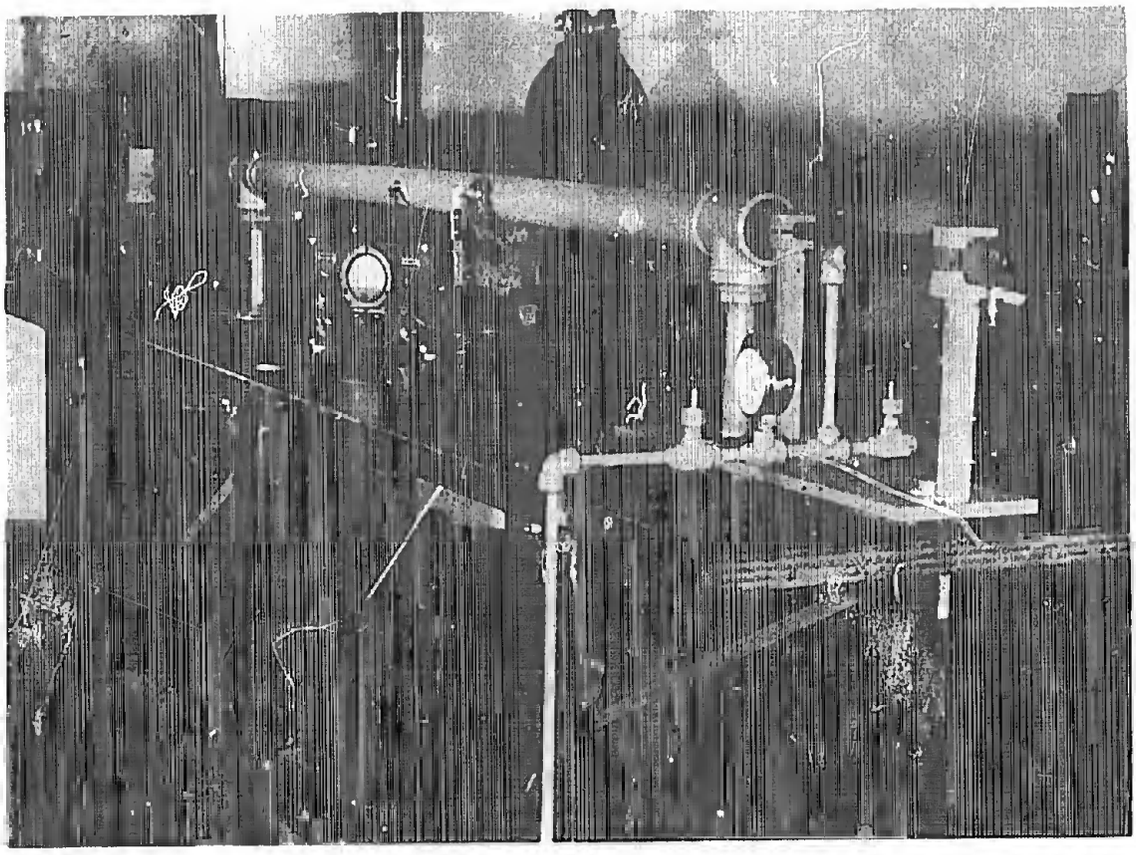

Figure 56. Ballistic impact test apparatus.

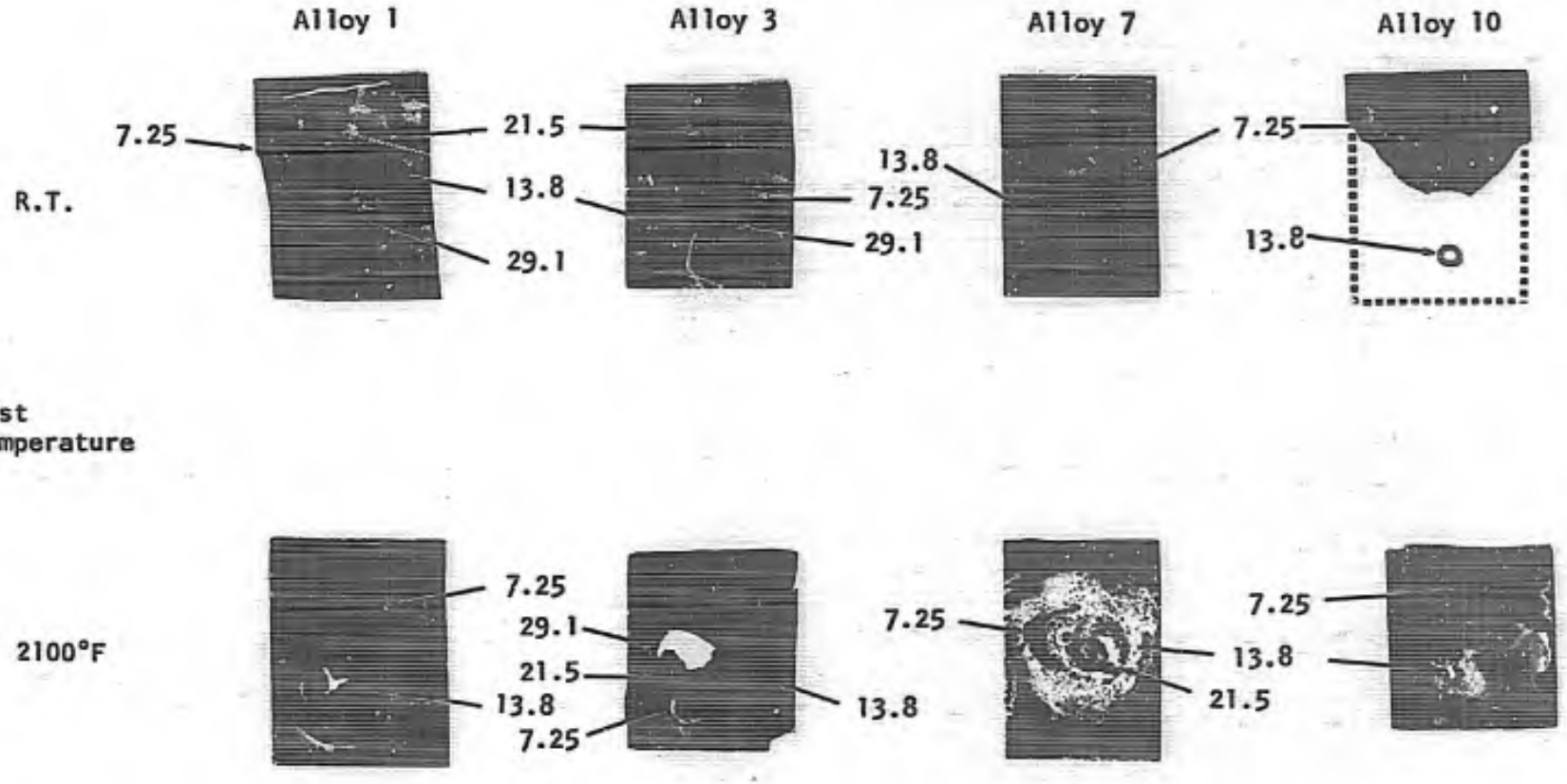

Figure 57. Ballistic impact test specimens showing impact side of sample. Impact energy (ft-lbs) indicated. Magnification: 1X before reproduction.

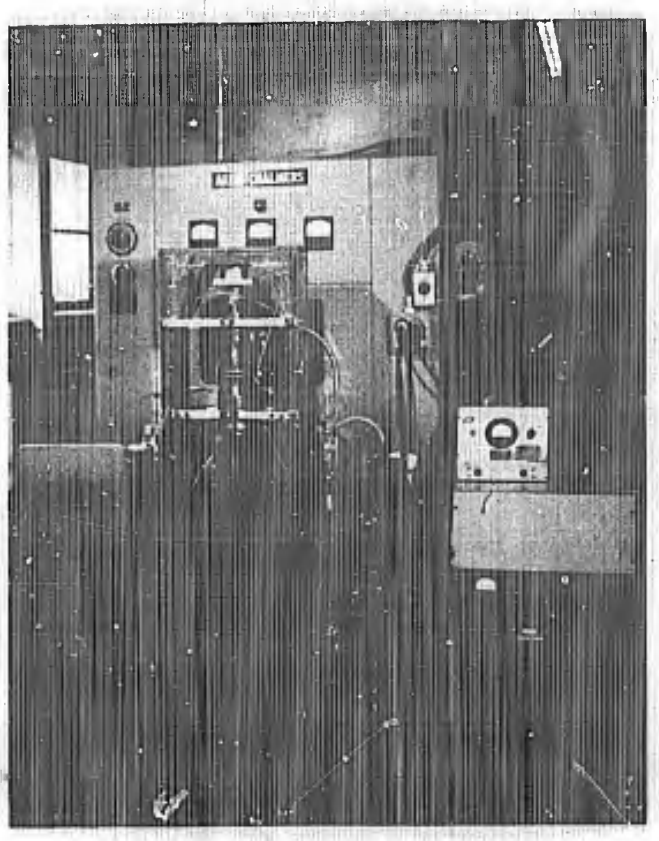

A. View of unit showing quartz chamber, vacuum system, 25KW power unit, and air jack (located beneath chamber)

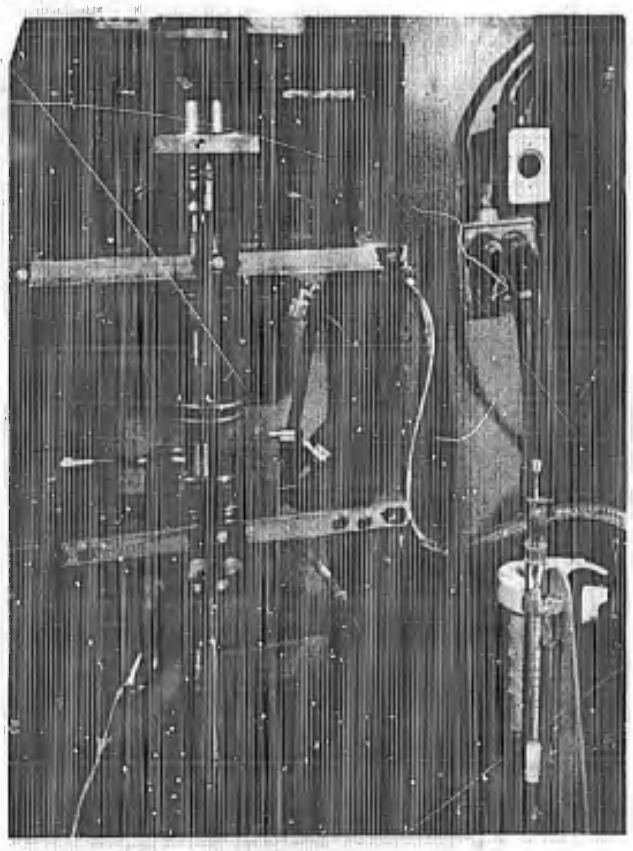

B. Close-up view of diffusion bonding chamber

Figure 58. Experimental induction heated diffusion bonding apparatus.

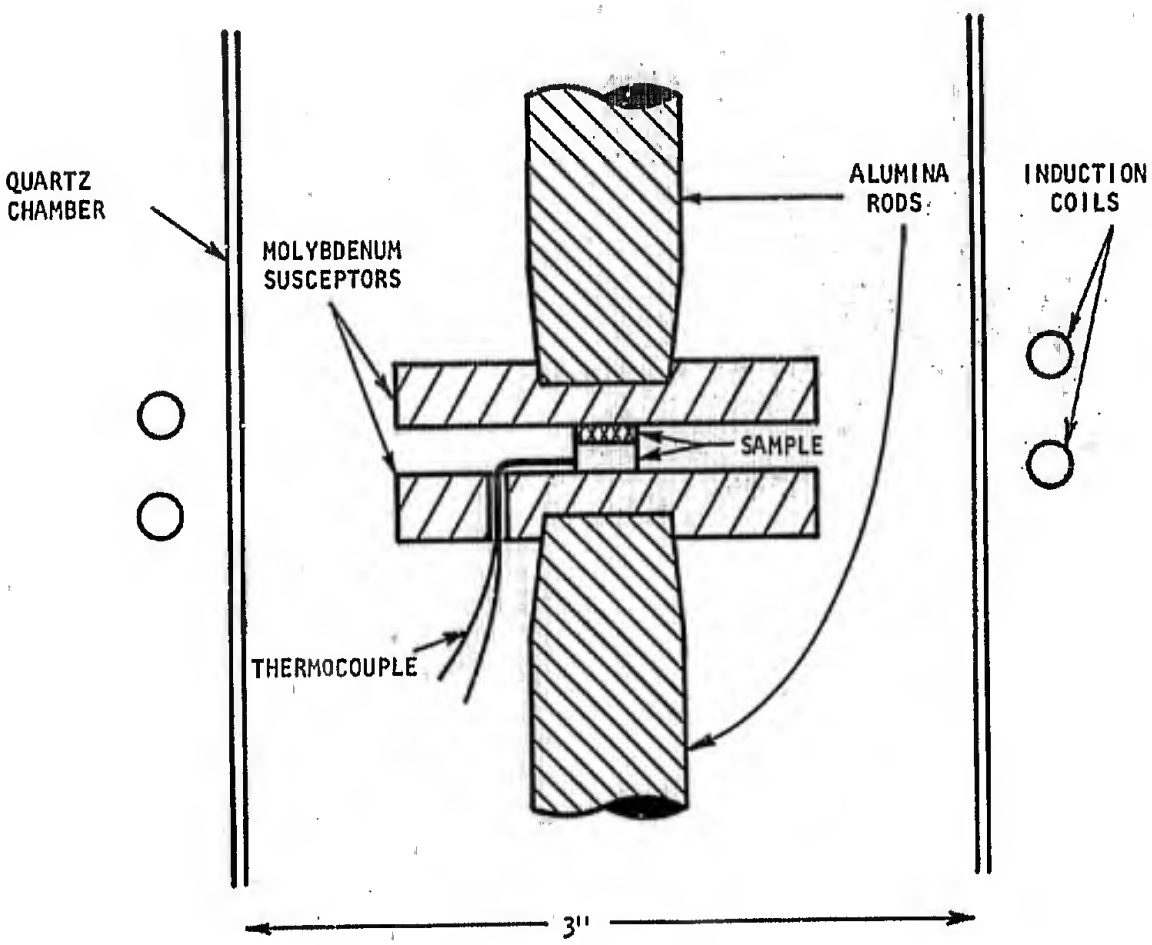

Figure 59. Diagram showing specimen positioning in diffusion bonding chamber.

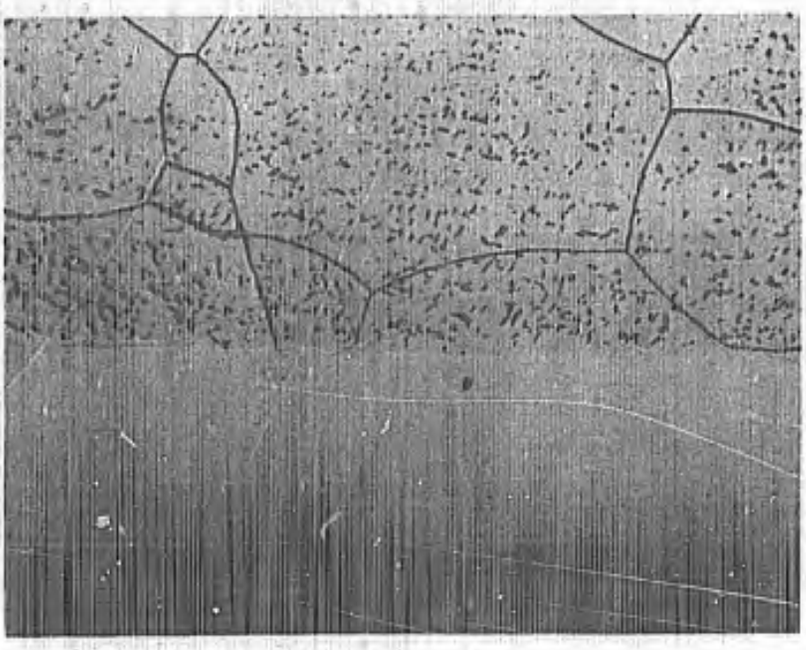

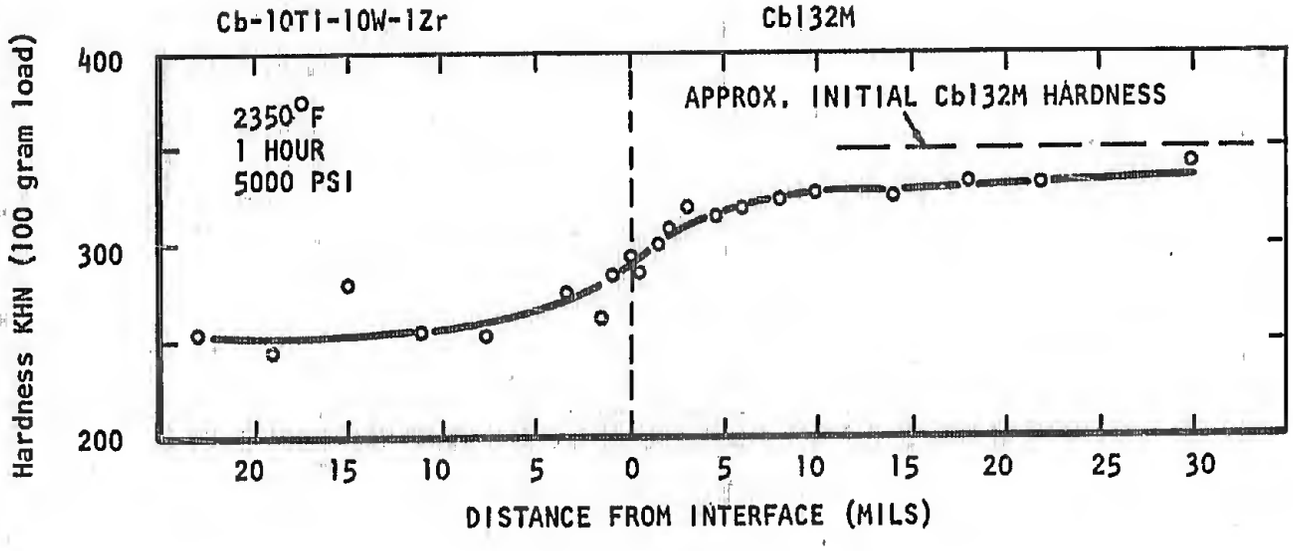

Figure 60. Photomicrograph and microhardness traverse of Bond No. 5. Cb-10Ti-10W-1Zr diffusion bonded to annealed Cb 132M. Bonded at 2350°F for 1 hour. Magnification: 500X.

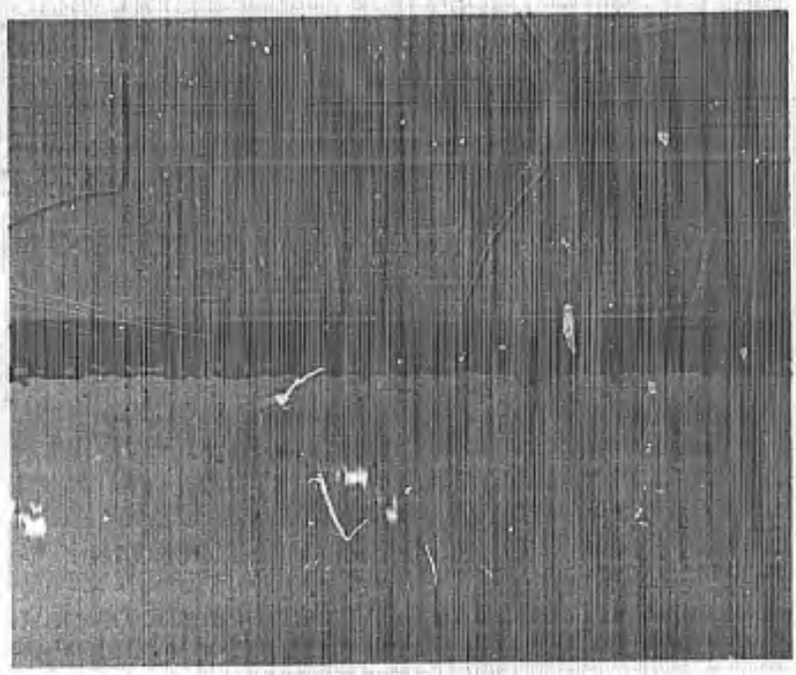

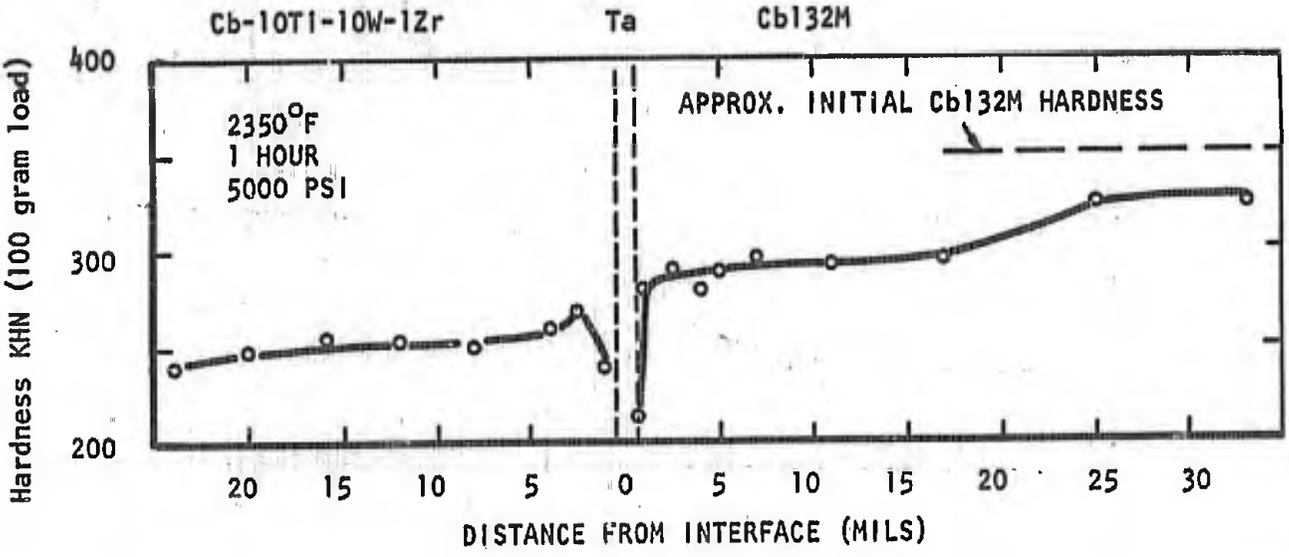

Figure 61. Photomicrograph and microhardness traverse of Bond No. 6. Cb-10Ti-10W-1Zr diffusion bonded to annealed Cb 132M using a Ta foil interlayer. Bonded at 2350°F for 1 hour. Magnification: 500X.

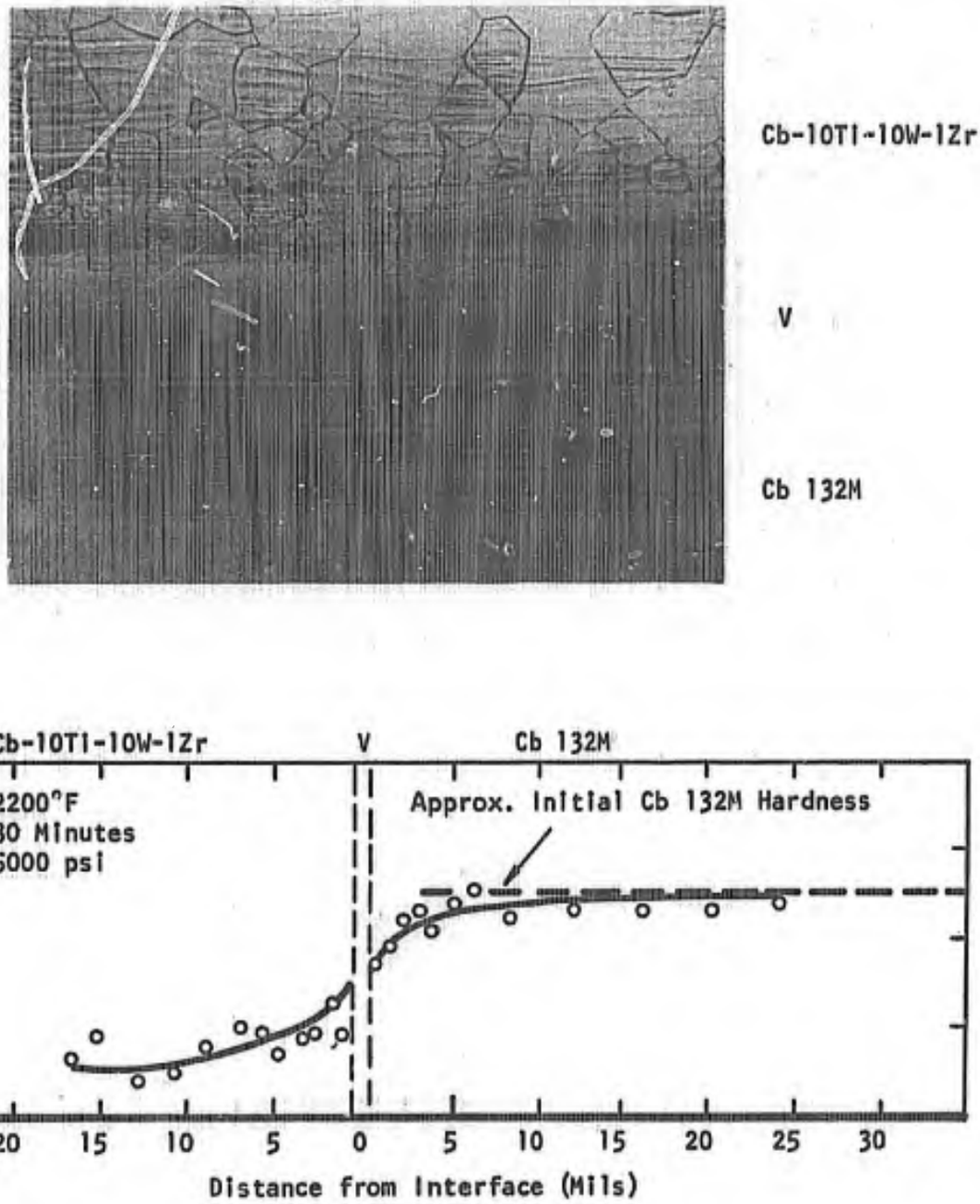

Figure 62. Photomicrograph and microhardness traverse of Bond No. 14. Cb-10Ti-10W-1Zr diffusion bonded to annealed Cb 132M using a V foil interlayer. Bonded at 2200°F for 30 minutes at 5000 psi. Magnification: 500X.

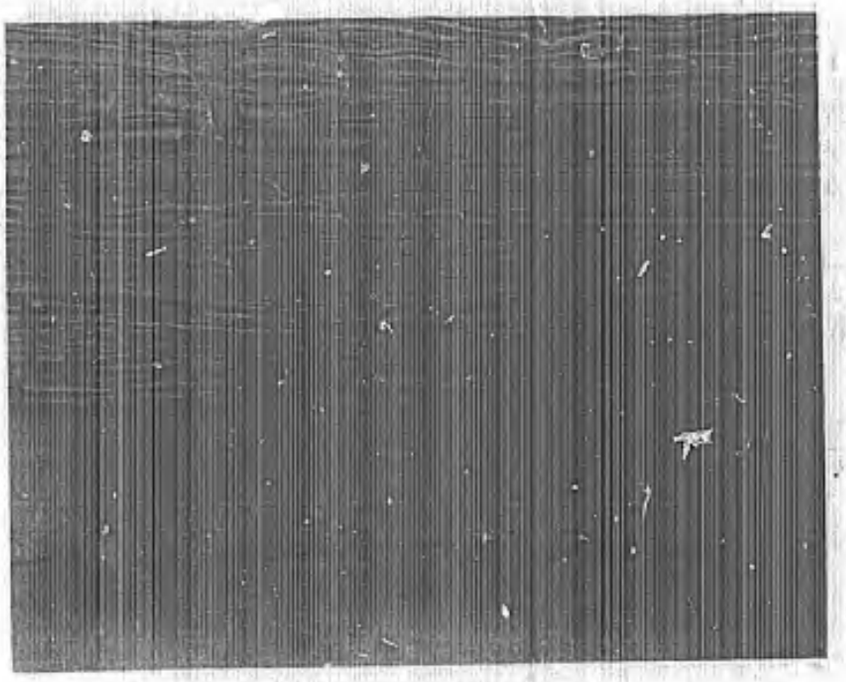

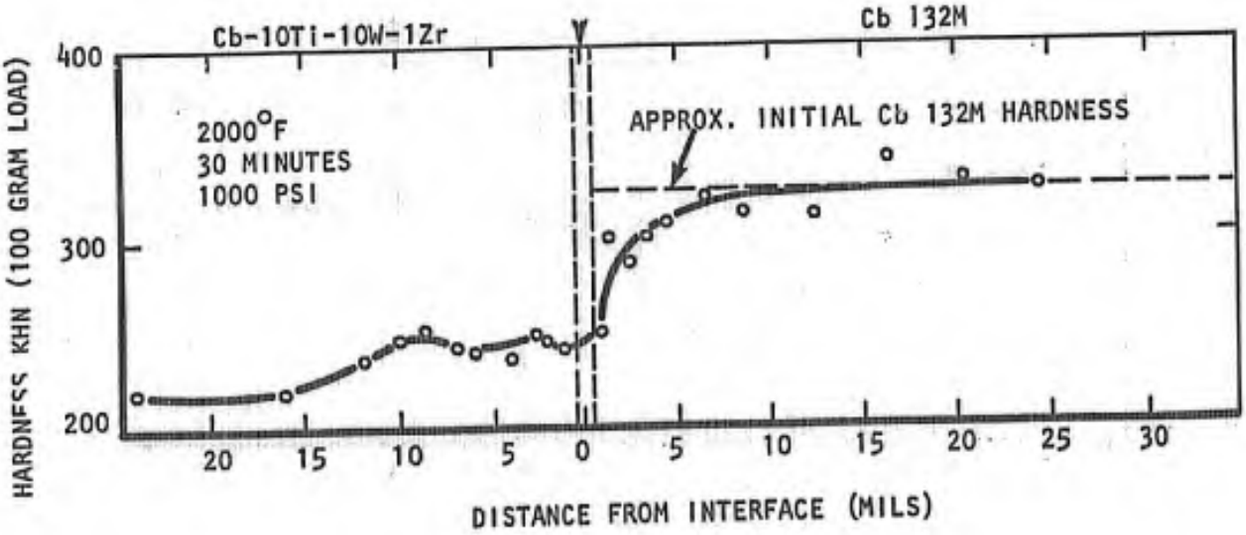

Figure 63. Photomicrograph and microhardness traverse of Bond No. 17. Cb-10Ti-10W-1Zr diffusion bonded to annealed Cb 132M. Bonded at 2000°F for 30 minutes. Magnification: 500X.

SECTION III

PHASE II - COMPATIBILITY STUDY

This section of the report describes investigations dealing with the question of how a columbium alloy combination can be expected to perform in service. In order to evaluate the compatibility of the components and thus the feasibility of the concept from a metallurgical point of view, certain tests should be performed on diffusion bonded coupons. The initial consideration is the ability to obtain a satisfactory bond between the core and cladding alloys selected in Phase I. The bonding procedure should also be compatible with blade processing and thermal-mechanical treatments. Areas of interest in this section of the program required the following tests on bonded samples: long time exposure to evaluate microstructural stability; oxidation exposure; ballistic impact; and limited mechanical property including tensile and creep. The results of these tests and their relation to the question of feasibility of columbium alloy combination blades are discussed in the following sections.

A. Microstructural Stability

The two columbium alloy components in the system being studied were each chosen for unique properties, high temperature strength for the core alloy and oxidation resistance for the cladding. Since it is required that these components be in intimate contact at high temperatures, diffusional processes can rapidly alter these dissimilar compositions. It is imperative that such effects do not completely eliminate the favorable properties for which these alloys were chosen. The cladding alloy is primarily a solid solution. In this case it is necessary to prevent the diffusion of alloying elements such as titanium and aluminum into the core as this would tend to decrease oxidation resistance. The diffusion problem for the core is primarily restricted to the migration of carbon from a strengthening columbium-zirconium carbide dispersion to the cladding alloy. Elements such as titanium and hafnium, present in the cladding alloy can intensify this problem due to the interstitial sink effect[10]. It was hoped that an additional barrier to outward carbon diffusion would be provided by the vanadium foil used in bonding. Hansen notes that the solubility of carbon in vanadium is probably less than 1 wt. % at temperatures up to 2200°F[18]. Although small this could prove significant. By using the bond techniques developed in Phase I to produce small test coupons, these metallurgical effects were studied by vacuum exposure at 2200°F. Effects due to oxidation and stress could thus be eliminated from the preliminary analysis. Extensive carbon depletion or the formation of massive intermetallic phases which would disqualify a clad-core combination could be detected.

1. Materials and Procedures

The selection of alloy combinations for this and the other sections of Phase II have been described in this report. Sufficient amounts of the core alloy, Cb 132M, and one of the sheet cladding alloys chosen, Alloy 10, remained from Phase I studies for use in this part of the study. The chemical analyses are shown, Tables I and VIII respectively. (Table XI contains additional chemistry data for the sheet form of Alloy 10.) Except where noted, all Cb 132M used in Phase II was from heat M-493 which contained the lower zirconium level (1.1% Zr).

A later modification of the second cladding alloy chosen (Alloy 7) was substituted in all Phase II studies[14]. The composition of this alloy (referred to as "7 modified") was provided by the supplier, Westinghouse Astronuclear Laboratory: Cb-15Ti-10W-10Ta-2Hf-2.2Al. The processing schedule for this material is shown in Table XIV. Two separate shipments of 0.020" sheet were received, the first being cut from initial processing trials.

Specimens for elevated temperature vacuum exposure were prepared by diffusion bonding 1/2" x 1/2" x 0.140" forged and annealed (3600°F/1 hour) Cb 132M to 1/2" x 1/2" squares of 0.020" oxidation resistant alloy sheet. Ten coupons were produced, half using Alloy 10 and half with Alloy 7 modified. The bonding procedures established in Phase I of this program were utilized, including a vanadium foil interlayer and stainless steel adapter plates. The parameters were 2000°F, 5000 psi, and 30 minutes at temperature, with pressure being applied throughout the entire cycle. The cleaning and etching procedures established for Phase I were also used.

2. Test Results

The bonded samples were treated at 2200°F for varying times up to 64 hours in a vacuum furnace. In order to evaluate the effects of thermal exposure on the microstructure of these alloys, optical microscopy, microhardness measurements, and microprobe techniques were employed.

Photomicrographs and plots of microhardness traverses are shown for Cb 132M bonded to Alloy 7 modified, Figures 64 through 68, and bonded to Alloy 10, Figures 69 through 73. Generally good bonding was obtained for both combinations of oxidation resistant alloy and Cb 132M. The bond line between the vanadium foil and Cb 132M became indistinguishable as exposure time increased. This was also true of the bond between the vanadium and Alloy 7 modified. However, the Alloy 10-vanadium interface, although apparently well bonded, retained its identity for exposure times up to 64 hours. This may be due to the formation of a surface film prior to or during bonding, as shown in Figure 69, which retards recrystallization across the interface. No such persistent layer was formed by Alloy 7 modified.

An increasingly heavy grain boundary precipitation was observed in both cladding alloys with longer exposure times. This was accompanied by considerable intragranular precipitation adjacent to the bond line in Alloy 10. It is likely that these precipitates are carbides, probably titanium in the case of Alloy 7 modified and hafnium in Alloy 10. The carbides grow in size and appear to a greater depth in the cladding alloy as carbon diffuses from the Cb 132M. In the case of Alloy 10 it is possible that some of the visible particles are oxides although this was not definitely confirmed. Subsequently performed microprobe studies indicated that a considerable number of oxide particles existed in Alloy 10 in the as-bonded condition. These particles can also be seen in the as-fabricated sheet material, Figure 55.

Microhardness readings were also taken corresponding to the microstructures shown and are plotted. The curves generally indicate a hardness increase in the cladding alloy adjacent to the bond line and a corresponding decrease in the Cb 132M. With extended exposures these effects became more pronounced. It is expected that most of these effects are accounted for by the diffusion of carbon from the Cb 132M into the cladding alloy. The vanadium foil through which the carbon must pass has a low solubility for carbon.

TABLE XIV

PROCESSING SUMMARY FOR ALLOY 7 MODIFIED (Cb-15Ti-10W-10Ta-2Hf-2.2Al)

1. 1st melt electrode prepared by nonconsumable electrode, d.c. arc melting.
2. 1st melt electrode consumable electrode vacuum a.c. arc melted into 2 inch diameter mold.
3. Ingot lathe conditioned and sectioned into 1 inch thick x 2 inch dia. forging billets.
4. Forging billets annealed 1 hr. at 3092°F and 1 x 10^{-5} torr.
5. Billets canned in evacuated mild steel containers.
6. Forged at 2192°F, single blow of the Dynapak, to 0.4 inch thickness.
7. Decanned, surface ground to 0.36 inch thickness.
8. Annealed 1 hr. at 2192°F and 1 x 10^{-5} torr.
9. Rolled at 1000°F to 0.18 inch thickness (50% reduction).
10. Annealed 1 hr. at 2192°F and 1 x 10^{-5} torr.
11. Rolled at 1000°F to 0.04 inch thickness.
12. Annealed 1 hr. at 2192°F and 1 x 10^{-5} torr.
13. Rolled to 0.020 inch at 700°F, final 3 passes at room temperature.
14. Annealed 1 hr. at 2192°F and 1 x 10^{-5} torr.

However, as exposure times are increased alloying of the vanadium with titanium, hafnium, rhenium and other elements from the cladding layer can occur, thereby charging the diffusion kinetics of the foil layer. Slight hardness decreases in the Cb 132M well back from the bond line were also noted, dropping from a "pre-exposure" Knoop hardness value of about 325 to approximately 275 after 64 hours at 2200°F. It is not certain whether this decrease is solely attributable to carbon diffusion into the cladding, since overaging effects could also be operative.

Microprobe studies were performed on all bonded and exposed samples depicted in Figures 64 through 73 in an effort to qualitatively determine interdiffusional effects, particularly for carbon. A Phillips Model AMR/3 operated at 20 KV was employed. Ratemetered X-ray line profile analysis was used to record the variation of carbon and certain other elements with exposure time. Unfortunately, changes in carbon content could not be detected across the entire cross-section of the specimens. It was possible to identify the precipitate particles in Alloy 10 and the interfacial layer between Alloy 10 and the vanadium foil as being rich in hafnium. These particles are especially evident after 64 hours exposure at 2200°F, Figure 73. The majority can probably be assumed to be carbides rather than oxide since these treatments were performed in a vacuum chamber. The microprobe data indicate that diffusion of major alloying elements from one component into the vanadium foil layer and vice versa is substantial. However, with the exception of grain boundaries where diffusion is expected to be much faster, concentration of substitutional elements in either the core or the cladding alloy is not significantly altered to a distance of greater than 3 to 4 mils from the respective interface with vanadium after 64 hours at 2200°F. Since the microhardness varies to a greater depth it is assumed that the observed hardness decrease in the Cb 132M and increase in the cladding alloy is due exclusively to carbon transfer. The somewhat smaller hardness drop in the Cb 132M associated with Alloy 7 modified, together with the absence of a hard interfacial layer at the bond line (compare Figures 68 and 73) favors the selection of Alloy 7 modified over Alloy 10 as a cladding alloy.

B. Oxidation Testing

The supposition underlying the concept of a columbium alloy combination is that the outer cladding layer will act as a barrier for a reasonable period preventing oxygen penetration to the rapidly consumed core. In order to test the ability of the cladding to so function, bonded coupons were prepared, coated for high temperature oxidation protection, intentionally damaged as if by particle impact, and exposed in air at 2200°F.

1. Materials and Procedures

Test coupons for oxidation testing were prepared by diffusion bonding in the manner and using the materials described in the previous section on microstructural stability. After bonding, the samples were provided with a high temperature protective coating. The TRW developed Cr Ti-Si coating which is applied in a two stage vacuum pack was used[2]. The coating procedure was as follows: sandblast, chemically clean, and degrease the surface; apply Cr-Ti layer by exposing at 2300°F for 8 hours in a vacuum pack (10^{-2}mm Hg) consisting of 60% Cr and 40% Ti to which KF was added as an activator; apply Si layer and 2100°F for 4 hours under a similar vacuum

pack containing 100% Si and KF activator. After coating, each specimen was intentionally damaged on the cladding alloy surface. A small conical grinding stone mounted in a drill press was used for this purpose. The intent of this procedure was to expose the underlying oxidation resistant alloy. This was easily accomplished although it was not possible to precisely control the amount of metal removed. The samples were then exposed at 2200°F to a normal atmosphere for times from 1 to 64 hours.

2. Test Results

Photographs of the damaged and oxidized test samples are shown Figure 74, for exposure times of 1,4,20 and 64 hours. The areas of damage are indicated. Even after 64 hours at 2200°F visible surface damage is confined to the circular damaged spot. Oxidation of the cladding alloy radially from this area has not occurred to an extent which would cause the coating to spall. A portion of the Alloy 7 modified cladding delaminated during bonding. This can be clearly seen in the 1 hour and 4 hour samples. It is felt that this condition, though undetected initially, existed in the as-rolled sheet and was merely aggravated by the bonding. This appears to be an isolated problem present only in the small initial shipment of the alloy. The second and larger shipment was free of this defect.

Each sample was cut to obtain a cross-section of the oxidized region. Low power photomicrographs of these samples are shown, Figures 75 through 78. The areas shown are as close as possible to the center of the damaged portion of the coating. Indentations from Knoop microhardness measurements are visible. A defect, parallel to the bond line is present in Alloy 7 modified, Figure 75A. This is of the type which caused delamination of certain specimens upon removal from the bonding apparatus. It is felt that the defective material did not significantly affect the results of this study.

Although precipitation generally increased in the cladding alloy and in the Cb 132M as exposure times were increased, the difficulty in obtaining a uniformly etched condition in these composite specimens reduces the effectiveness of metallography. Consequently, Knoop microhardness traverses were performed on all samples, perpendicular to the bonded interface and at approximately the mid-point of the damaged circle. These hardness data are shown, Figures 79 to 85. The curves reflect several changes occurring in the specimen upon exposure, including carbon and substitutional element diffusion from one component to the other as well as oxygen penetration from the exposed surface. However, by recalling the microhardness traverses obtained for the study of microstructural stability, Figures 64 to 73, and discounting this effect a reasonable approximation to the degree of oxygen contamination can be obtained. A considerable hardness increase, probably associated with oxygen contamination, is evident at the exposed edge of the cladding alloy (left side of the graphs). As exposure times were increased the hardness near the center of the cladding layer also increased, slightly. In the case of Alloy 10 the hardness adjacent to the bonded interface also increased and the thickness of the cladding layer decreased significantly as the metal was converted to oxide. A slight hardness increase in the core alloy is also noted. This effect is superimposed upon the hardness decrease caused by carbon depletion.

An electron microprobe analysis using the point counting technique was also attempted in order to establish the oxygen concentration profile in these samples. Unfortunately, the relatively low level of oxygen throughout most of the specimen and the small gradients expected made a quantitative interpretation of the data impossible. However, general trends were observed in some samples which tended to corroborate the microhardness data. Thus, it is assumed that for the levels of contamination encountered here, microhardness data seem to be a more sensitive measurement.

Based on these test results, Alloy 7 modified is preferred as an oxidation resistant barrier alloy. Although both alloys tested appeared to permit some oxygen to penetrate to the core during extended exposure to an oxidizing environment, Alloy 7 modified has several advantages. Foremost, is the much smaller depth of metal loss due to conversion to oxide. The test results indicate that exposures longer than 64 hours will probably result in catastrophic core oxidation if the protective layer is Alloy 10. However, Alloy 7 modified will presumably maintain its metallic identity without spalling for much longer exposures. Furthermore, Alloy 10 has the disadvantage of forming a hard and potentially brittle layer adjacent to the bond which could result in separation upon impact. This condition appears to worsen with exposure to oxidizing atmospheres.

C. Ballistic Impact Testing

It is assumed that the primary need for an oxidation resistant cladding alloy is to act as an oxygen barrier for the high strength core in the event that the outer high temperature coating is damaged. Thus far damage has been artificially inflicted by grinding. In practice, the source of coating failure is most likely to be impact by some ingested particle. For this reason it is important that the cladding have good impact resistance and also that embrittling layers not be formed during bonding and exposure.

1. Materials and Procedures

Ballistic impact test coupons were prepared by diffusion bonding and coating in the manner described in the previous two sections of this report. The materials utilized; Cb 132M, Alloy 10, and Alloy 7 modified have also been discussed and characterized. Since ballistic impact tests had not previously been run on the modified version of Alloy 7, this alloy was also tested in the unbonded condition. Testing was performed as described previously in Section II of this report using a helium powered air pistol to fire weighted steel BB's. Testing in this case was performed at room temperature and 2000°F.

2. Test Results

Photographs of Alloy 7 modified 0.020" sheet coupons, impact tested at room temperature and 2000°F are shown, Figure 86. The impact energies corresponding to each depression are indicated. Test data are summarized in Table XV. Comparing these results with Figure 57 and Table XII, which present the previous ballistic impact data, it appears that the modified version of Alloy 7 is slightly less subject to brittle behavior upon impact than either Alloy 10 or 7. It compares favorably with Alloys 1 and 3, the more impact resistant compositions of those previously tested. It is

TABLE XV

BALLISTIC IMPACT DATA FOR ALLOY 7 MODIFIED AND COLUMBIUM ALLOY COMBINATIONS

Specimen	Test Temp. (°F)	Pellet Velocity cm/sec. ($\times 10^4$)	Pellet Velocity ft/sec.	Impact Energy ergs ($\times 10^8$)	Impact Energy ft/lbs.	Remarks
Alloy 7 mod.	R.T.	1.29	425	0.987	7.25	
"	"	1.78	585	1.875	13.8	slight crack on reverse side
"	"	2.23	730	2.92	21.5	"
"	"	2.59	850	3.96	29.1	"
"	2000	1.29	425	0.987	7.25	
"	"	1.78	585	1.875	13.8	
"	"	2.23	730	2.92	21.5	some cracking
Cb 132M- 7 mod.	R.T.	1.29	425	0.987	7.25	crack in cladding
"	2000	1.29	425	0.987	7.25	
"	"	1.78	585	1.875	13.8	
"	"	2.23	730	2.92	21.5	
"	"	2.59	850	3.96	29.1	
Cb 132M-10	R.T.	1.29	425	0.987	7.25	crack
"	"	1.78	585	1.875	13.8	separated on bond line
"	2000	1.29	425	0.987	7.25	
"	"	1.78	585	1.875	13.8	
"	"	2.23	730	2.92	21.5	

also of interest to compare these results with those recently published by the alloy developer[14]. In the referenced study brittle behavior was noted at room temperature at comparatively low impact energies. The authors speculated that this effect was probably related to the aluminum content of the alloy (approximately 3.4% in this case). The relatively ductile room temperature impact behavior observed on the material tested in this study (2.2% Al) indicates that aluminum is critical in determining the low temperature impact behavior.

The ballistic impact tests performed on bonded and coated coupons are summarized in Table XV, and Figure 87. (The high temperature specimens were sandblasted prior to being photographed.) High temperature behavior is probably acceptable for both combinations tested. These data compare favorably with similar impact data reported here for unbonded sheet. However, brittle behavior was observed at room temperature for both alloys. The presence of the brittle Cb 132M substrate apparently serves to intensify the crack sensitivity of the cladding alloy. In the case of Alloy 10, cracking extended completely through the Cb 132M. Separation on the bond line occurred when impacted a second time. All Cb 132M used for these tests was treated for highest creep strength (i.e. 3600°F/1 hour). Tensile and creep data reported here indicate that this is an embrittling condition, especially at temperatures up to 1200°F. It should probably be considered encouraging that brittle behavior was not encountered when tested at 2000°F. One might expect that other core alloy heat treatments providing better ductility, although lower creep strength, would provide a substrate more tolerant of ballistic impact.

It is not possible to draw quantitative conclusions from these ballistic impact tests. However, it has been shown that at operating temperatures both Alloys 7 modified and 10 will remain intact and bonded to the core when subjected to impact severe enough to damage the protective CrTi-Si coating and substantially deform the specimen. At room temperature neither can withstand impact damage when bonded to the core. Since it is probably the annealed core material which causes the extremely brittle behavior at low temperature, it is possible that any columbium alloy combination treated for high creep strength will exhibit poor room temperature ballistic impact resistance.

D. Mechanical Property Testing

In order to fully evaluate the feasibility of the concept of columbium alloy combinations for turbine blades, it is necessary to consider the effects of an external cladding on the strength properties of the core alloy. Tensile and creep strength can be significantly altered by the effects studied and discussed in the preceding sections. It is likely that strength loss will occur if appreciable carbon is depleted via the interstitial sink effect. Embrittlement can occur through oxygen contamination and the formation of intermetallics at the bond line. Also, the unique properties of the cladding alloy will affect core alloy as in any composite material. Creep testing at 2200°F and intermediate temperature 1200°F tensile tests were performed on clad and coated specimens in order to simulate the situation in an airfoil manufactured as a columbium alloy combination.

1. Materials and Procedures

Coupons were prepared for mechanical testing by diffusion bonding Alloy 7 modified (this alloy having been chosen as superior to Alloy 10 for a cladding material) to both large faces of forged Cb 132M plates (approximately 0.090" x 5/8" x 1 3/4"). Two thermal-mechanically treated conditions were selected for the Cb 132M; forged at 2400°F and annealed 1 hour at 3600°F; and partially forged at 2400°F, recrystallized at 2950°F for 2 hours, and forged 20% at 1600°F. The Alloy 7 modified sheet material was used in the as-received condition (see Table XIV). Additional characterization details for these materials were previously discussed.

The diffusion bonding technique utilized to prepare the tensile specimen blanks were slightly modified from that used for prior Phase II work. Parameters of 2000°F, 5000 psi, and 30 minutes were not changed. However, the larger size of these specimens necessitated the use of a larger bonding unit, Figure 88. The work space in this chamber is a cylinder 5" in diameter x 4" high. It is resistance heated by molybdenum windings giving a maximum temperature of 3000°F. Vacuums of up to 10^{-5} torr can be maintained at operating temperatures.

The arrangement of the various components placed in the bonder is shown, Figure 89. The elements actually comprising the bonded coupon were pre-assembled after surface cleaning and spot welded along two sides for ease of handling. As previously discussed, it was necessary to employ a small stainless steel plate to accommodate nonuniform loading. Generally an adapter is not required since the bonded material itself yields sufficiently to accomplish this. However, at the low temperatures and pressures utilized here in order to minimize diffusional effects, plastic flow of the columbium alloys was insufficient to offset slightly eccentric loading. Therefore, changes in thickness of the samples during bonding were not expected and were found to be insignificant. A bonded coupon and stainless steel adapter plate are shown, Figure 90. Visual examination of each coupon indicated that the cladding alloy was uniformly bonded over both surfaces. Also shown in Figure 90 is the oxide coating applied to the stainless steel in order to prevent bonding between it and the columbium alloy.

Tensile type specimens were machined from the bonded coupons. The specimen configuration was a slightly modified version of that used for Phase I testing, Shown in Figure 23. For this case the specimen was designed so that the thickness of the Cb 132M core was the same as that shown in Figure 23. The inclusion of two layers of the cladding alloy added approximately 0.035" to the thickness. However, they are not considered to significantly add to the overall strength. The specimens were then coated for oxidation protection using the TRW Cr Ti-Si coating. With the procedure used, the specimen edges were not clad but were protected by the oxidation resistant coating.

Considering the bonding and coating processes each specimen was exposed to the following vacuum thermal cycle after the nominal thermal-mechanical treatment of the core alloy was completed: 2000°F for 1 hour, 2300°F for 8 hours, and 2100°F for 4 hours. While not specifically investigated, this thermal cycle has an effect similar to several hours of aging at 2200°F a condition evaluated for several annealing treatments in Phase I.

Prior to tensile or creep testing half of the specimens were exposed for 64 hours in air at 2200°F. This treatment was intended to roughly simulate a service environment for combination columbium alloy blades. Following this exposure the samples were examined for evidence of coating failure. The coating was found to have effectively prevented oxidation of the cladding alloy and the core alloy as well along the unclad edges of the specimen.

2. Tensile Tests

Tensile tests were conducted on an Instron machine utilizing a crosshead speed of 0.020 inches/minute. The specimens were tested at 1200°F in air. Test results are listed, Table XVI, along with comparable data for the unbonded core alloy obtained in Phase I of this program. In calculating the strength levels shown, any effect of the cladding alloy was considered negligible. (Recent test data tends to substantiate this assumption[14].) The data reported in Table XVI indicate that the effect on tensile properties caused by bonding and coating is fairly small. Yield strengths for the recrystallized and cold worked (1600°F) material are comparable to that for Cb 132M alone, although ductility is reduced. Furthermore, the pre-test exposure in air has apparently had little effect on strength and, although the elongation was reduced, ductile behavior was not prevented. In the case of annealed Cb 132M the bonding and exposure treatments appear to successively degrade strength. However, this conclusion is not clear-cut since it was necessary to use two different heats of Cb 132M which previously (Table V) were shown to have a range of tensile properties.

Photographs of the broken tensile specimens and of two representative fracture surfaces are shown, Figures 91 and 92, respectively. The brittle behavior of the annealed specimens is obvious. The more ductile fractures present in the cold worked samples are accompanied by numerous secondary cracks. However, the transgranular shear-type fracture of the Cb 132M core is evident in the photograph of the fracture surface, Figure 92. It should also be noted that the cladding layer fractured with a smaller elongation than did the core. This effect should probably be attributed to the formation of relatively brittle layers at the bond line, since other investigations have indicated tensile elongations greater than 100% at 2200°F for the cladding alloy[14]. The bond line separation caused by necking of the core alloy is clearly shown (arrow) in Figure 92. Behavior away from the fracture and in the annealed specimens indicates that this separation occurred after the onset of substantial plastic deformation.

3. Creep Tests

Creep testing was performed at 2200°F using a Satec creep-rupture machine. The results of this testing are listed, Table XVII, along with comparative data for the core alloy (Cb 132M) obtained in Phase I of this program. Data shown for the unbonded core alloy are from tests performed in

TABLE XVI

1200°F TENSILE PROPERTIES OF COATED COLUMBIUM ALLOY COMBINATIONS* AND Cb 132M

Specimen	U.T.S.+ (KSI)	0.2% Y.S.+ (KSI)	Elong. (%)
Cb 132M: forged 2400°F + 3600°F/1 hr, (Heat M-497)[V]	100.5	65.5	7.9[b]
(Heat M-493)[V]	83.0	57.8	11.8[b]
Combination - Core (forged 2400°F + 3600°F/1 hr.) - Clad - Coated. (Heat M-497)[a]	83.2	82.7	2.8[b]
Combination - Core (forged 2400°F + 3600°F/1 hr.) - Clad - Coated - 2200°F for 64 hours in air. (Heat M-493)[a]	47.7	-	2.8[b]
Cb 132M: 2950°F/2 hrs. + forged 1600°F (Heat M-493)[V]	116.3	98.3	16.1
Combination - Core (2950°F/2 hrs. + forged 1600°F) - Clad - Coated. (Heat M-493)[a]	99.3	95.2	8.5
Combination - Core (2950°F/2 hrs. + forged 1600°F) - Clad - Coated - 2200°F for 64 hours in air. (Heat M-493)[a]	102.9	88.4	4.5

* Combinations consist of Cb 132M core (0.090" thick) with Alloy 7 modified sheet (0.020" thick) bonded to large faces of plate specimen.

+ Strength calculations are based on core alloy only. The contribution to strength and cross-section of the cladding has been disregarded.

[a] Tested in air; cross head speed of 0.020 in./min.

[b] Brittle fracture.

[V] Tested in air; cross head speed of 0.020 in./min.

TABLE XVII

2200°F, 30,000 PSI+ CREEP RUPTURE PROPERTIES OF COATED COLUMBIUM ALLOY COMBINATIONS* AND Cb 132M

Specimen	Min. Creep Rate (%/Hr.)	Approx. Time to Third Stage Creep (Hrs.)	Rupture Life (Hrs.)	Total Elong. (%)
Cb 132M: forged 2400°F + 3600°F/1 hr. (Heat M-493)[V]	.0337	>135.8	>135.8	14.0
(Heat M-497)[V]	.043	53	62.6	6.5
Combination - Core (forged 2400°F + 3600°F/1 hr.) - Clad- Coated. (Heat M-497)[I]	.20	12	12.3	N.A.
Combination - Core (forged 2400°F + 3600°F/1 hr.) - Clad - Coated - 2200°F for 64 hours in air. (Heat M-493)[I]	.103	16	25.9	2.9
Cb 132M: 2950°F/2 hrs. + forged 1600°F. (Heat M-493)[V]	.67	6	7.6	9.6
Combination - Core (2950°F/2 hrs. + forged 1600°F) - Clad - Coated. (Heat M-493)[a]	Test fixture failed after 8 hours.			
Combination - Core (2950°F/2 hrs. + forged 1600°F) - Clad - Coated - 2200°F for 64 hours in air. (Heat M-493)[a]	.98	7	14.5	38.5

+ Strength calculations are based on core alloy only. The contribution to strength and cross-section due to the cladding has been disregarded.

* Combinations consist of Cb 132M core (0.90" thick) with Alloy ? modified sheet (0.020" thick) bonded to large faces of plate specimen.

[a] Tested in air.

[I] Tested in argon atmosphere.

[V] Tested in vacuum of 10^{-5} torr.

a vacuum of 10^{-5} torr; those for the combinations forged at 1600°F are from tests conducted in air; while those reported for the annealed (3600°F/1 hour) material are from inert gas (argon) environment tests. It is desirable to test the clad and coated combinations in air in order to more closely simulate an operating environment for a turbine blade. However, this test condition resulted in severe attack to the specimen grips and the loss of one test. Testing in an argon atmosphere was then chosen as a preferable alternate to vacuum testing since it permitted the coated combination to be tested intact. All testing was performed under a 30,000 psi loading. As with the tensile tests performed on clad combinations, the strength contribution due to the cladding alloy was neglected.

The data reported in Table XVII indicate that the clad and coated combinations have significantly poorer creep rupture strength than bare Cb 132M in roughly the same condition. In the case of forged and annealed material (3600°F for 1 hour) the rupture life and ductility as measured by total elongation were greatly decreased by the cladding and coating operations. However, the minimum creep rate, while increased, remained low when compared to other alloys and conditions, Table VII. The 64 hour air exposure at 2200°F prior to creep testing apparently had little effect on creep strength when the initial variations in the two heats of Cb 132M are considered. Prior to bonding, creep strength of recrystallized (2950°F/2 hours) and cold worked (20% at 1600°F) Cb 132M was relatively low compared with other heat treated conditions. The single test result available for clad and coated Cb 132M in the cold worked condition also showed low creep strength, Table XVII. Elongation and minimum creep rate were quite high, being similar to unclad Cb 132M in the high temperature (2200°F and 2400°F) forged conditions, Table VII.

Photographs of the broken tensile specimens are shown, Figure 93. The fracture behavior of the 3600°F annealed creep specimens was similar to that of the 1200°F tensile test samples in that very brittle fractures of an intercrystalline nature were observed. The exact appearance of the fracture surface at the instant of yielding has probably been altered by oxidation during cool-down from the test temperature. A few small pieces of these specimens tended to break away from the fracture surfaces during handling. This resulted in lower measured elongations than were actually observed during creep. The recrystallized and cold worked sample exhibited ductile behavior. The numerous secondary cracks evident in the tensile test specimens, Figure 91, were not observed for the creep sample. Separation of the bond between cladding and core was not observed in any of the 2200°F creep test specimens.

4. Metallographic Examination

The broken tensile specimens were examined metallographically in the region adjacent to the fracture surface. Typical examples are shown in the unetched condition, Figure 94, and after etching, Figure 95. Separation of the cladding from the core is evident near the fracture surface. However, this did not continue to a great distance away from the fracture and is thought to be associated primarily with differences in the flow characteristics of the two components. Transverse secondary cracking is also evident in the unetched specimens, Figure 94. These cracks are also seen in Figure 91 for the recrystallized and cold worked samples. The brittle, intergranular nature of the fracture in the annealed (3600°F/1 hr.) material is contrasted with a relatively ductile failure in the recrystallized and cold worked samples, Figures 95A and B. There was little optically discernible difference at magnifications to 500X

between the microstructures of the "as bonded and coated" samples and those which received a subsequent exposure at 2200°F. (The etchant used contained HF which attacks the Cr-Ti-Si oxidation resistant coating. Thus the coating can only be seen in the unetched micros, Figure 94.)

Unetched and etched photomicrographs were also prepared from the tested creep-rupture specimens. Typical regions are shown, Figures 96 and 97. As with 1200°F tensile specimens, differences were not detected between the "as bonded and coated" samples and those which had also received a 2200°F exposure. Transverse secondary cracks of an intergranular nature are shown in the 3600°F annealed sample, Figure 96A. This is in keeping with the brittle, intergranular fractures noted at all temperatures for this condition. Secondary cracking was also noted in the more ductile recrystallized and cold worked specimen, Figure 96B. It appears that the crack shown occurred at nearly the same time as final rupture since oxide attack of the core alloy is minimal. Numerous cracks in the coating, some of which resulted in partial oxidation of the underlying cladding, indicate that coating ductility may also be a problem.

Considerable coarsening of the carbide precipitate in the annealed Cb 132M core occurred during creep testing, Figure 97A. (This specimen had a creep life of 12.3 hours.) Comparison of this specimen which was not exposed at 2200°F prior to testing with the 1200°F tensile specimen which did receive a 64 hour 2200°F exposure, Figure 95A, indicates that the coarsening is primarily caused by the combination of temperature and stress rather than temperature alone.

E. Phase II Conclusions

In Phase I various columbium alloys were screened for usefulness either as the load bearing core or the protective cladding of a combination blade. The core alloy Cb 132M and two cladding alloys Cb-15Ti-10Ta-10W-2Hf-3Al and Cb-5W-30Hf-5Ti-3Re were selected for further study of their compatibility. Using diffusion bonding techniques developed here, combination specimens were prepared and evaluated in order to appraise the feasibility of the concept. Conclusions of these studies, which comprised Phase II of the program are as follows:

1. Stability of Microstructure

a. During bonding and subsequent exposure at 2200°F for times up to 64 hours, carbon diffused from the Cb 132M core through the vanadium foil to the cladding alloy. Evidence for this effect consisted of microhardness traverses and the development of particles (identified by microprobe analysis to be carbides) in the cladding alloy adjacent to the bond. Certain alloying constituents of the cladding materials, particularly titanium and hafnium acted as interstitial sinks for carbon.

b. A slight hardness drop occurred throughout the thickness of the Cb 132M core upon exposure. This is thought to be a result of both carbon depletion and overaging.

c. The substitutional alloying elements in both columbium components diffused slowly across the bonded interface. However, even with exposures of up to 64 hours the composition of both the cladding and the core was substantially unaltered at distances in excess of 5 mils away from the interface.

d. The vanadium foil diffused into both the core and cladding during exposure. Certain elements, particularly Ti and Re (and to a lesser extent Hf) alloyed with the vanadium foil.

e. Of the two cladding alloys tested, Alloy 7 modified (Cb-15Ti-10Ta-10W-2Hf-3Al) is preferred because of its lesser effect as an interstitial sink for the carbon in the core alloy.

2. Oxidation Testing

a. A relatively oxidation resistant columbium alloy cladding is capable of preventing catastrophic oxidation of a high strength columbium alloy for times in excess of 64 hours when exposed to air. This system will prevent rapid failure of a central load bearing core should the outer oxidation preventing coating be locally damaged in service.

b. Microhardness and metallographic studies indicate that there was some oxygen penetration through the cladding to the core. However this was localized to regions adjacent to the coating damage and did not result in complete internal oxidation.

c. Based especially on a smaller amount of metal loss upon exposure due to conversion to oxide, Alloy 7 modified (Cb-15Ti-10A-10W-2Hf-3Al) is preferred as a possible cladding alloy for high strength columbium alloys.

3. Ballistic Impact Testing

a. At room temperatures bonded and coated samples exhibited poor resistance to ballistic impact damage. Cracking of the cladding alloy and particularly the substrate Cb 132M occurred at the lowest impact energy tested. This is probably due largely to the brittle condition of the Cb 132M. Bond line separation occurred in the Cb 132M-Alloy 10 sample which formed a hard phase at the bond interface.

b. Ballistic impact resistance was satisfactory at 2000°F although there was some brinelling of the cladding alloy due to its low strength.

4. Mechanical Property Testing

a. Compared to bare Cb 132M tested in vacuum, the 1200°F tensile properties of bonded and coated Cb 132M-Alloy 7 modified combinations were slightly degraded.

b. The 2200°F creep properties of bonded and coated Cb 132M were significantly lowered from those of bare Cb 132M.

c. Allowing for heat-to-heat variations there was little effect of a pre-test exposure at 2200°F on either mechanical properties or microstructure.

d. Significant separation during testing of the cladding from the core occurred only near the fracture surface of the more ductile samples. It was probably due to the differing flow characteristics of each component.

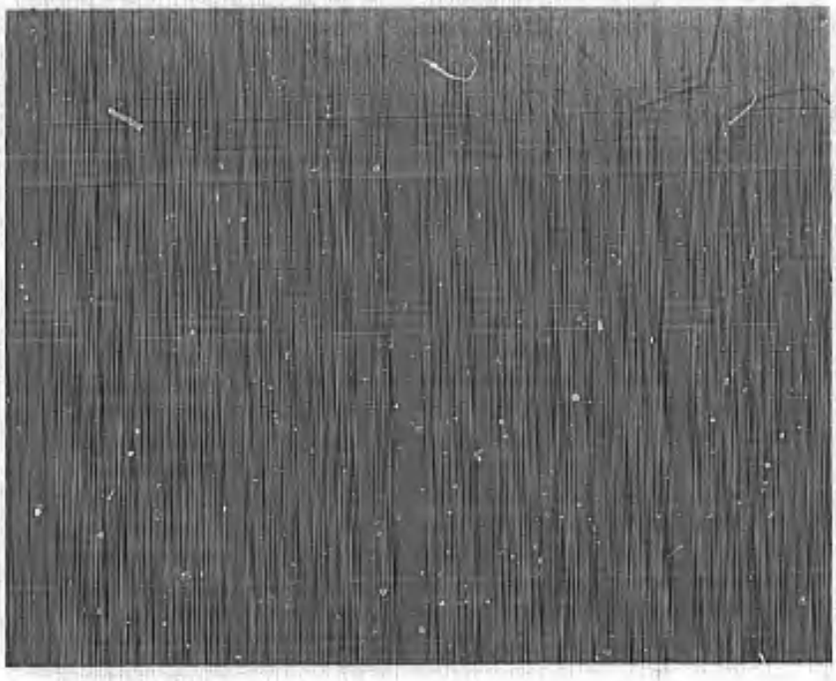

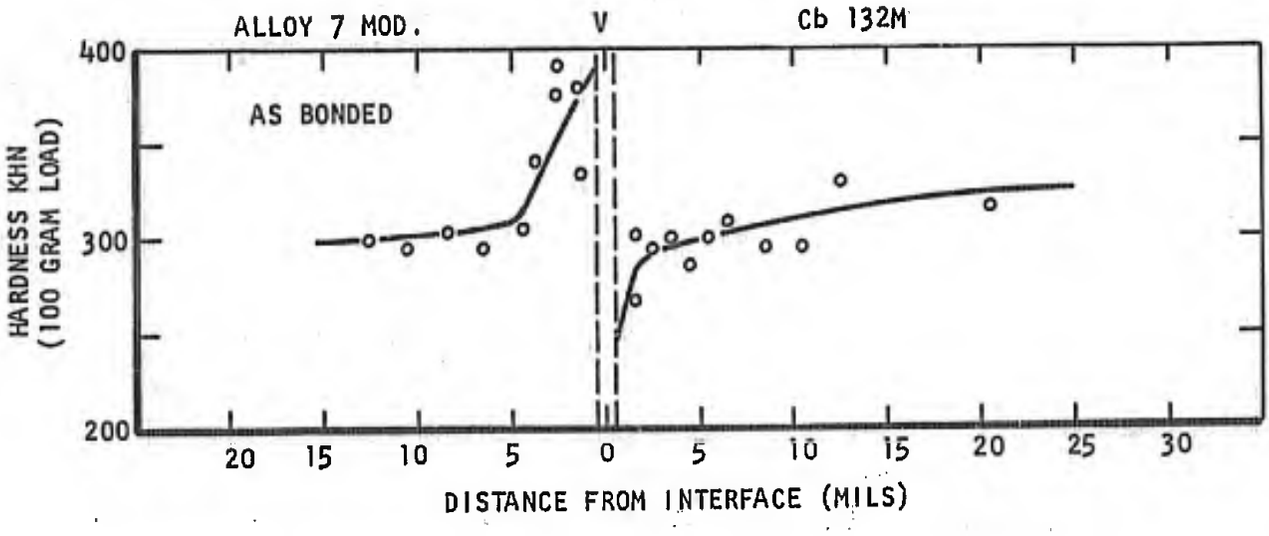

Figure 64. Photomicrograph and microhardness traverse of Cb 132M diffusion bonded to Alloy 7 Modified shown as-bonded at 2000°F for 30 minutes. Magnification: 500X.

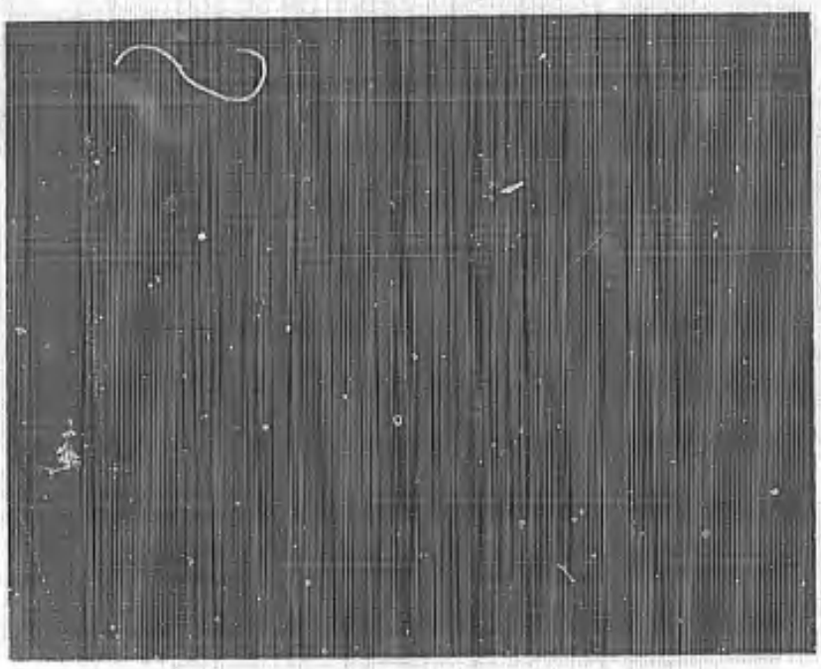

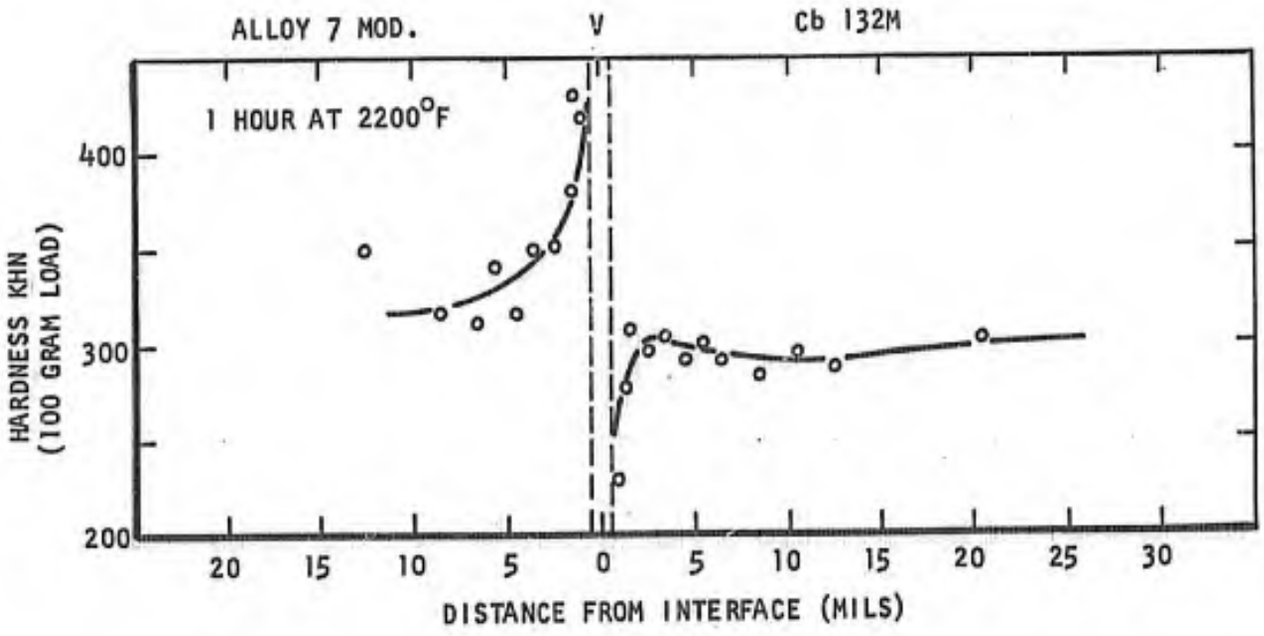

Figure 65. Photomicrograph and microhardness traverse of Cb 132M diffusion bonded to Alloy 7 Modified. Exposed 1 hour at 2200°F after bonding. Magnification: 500X.

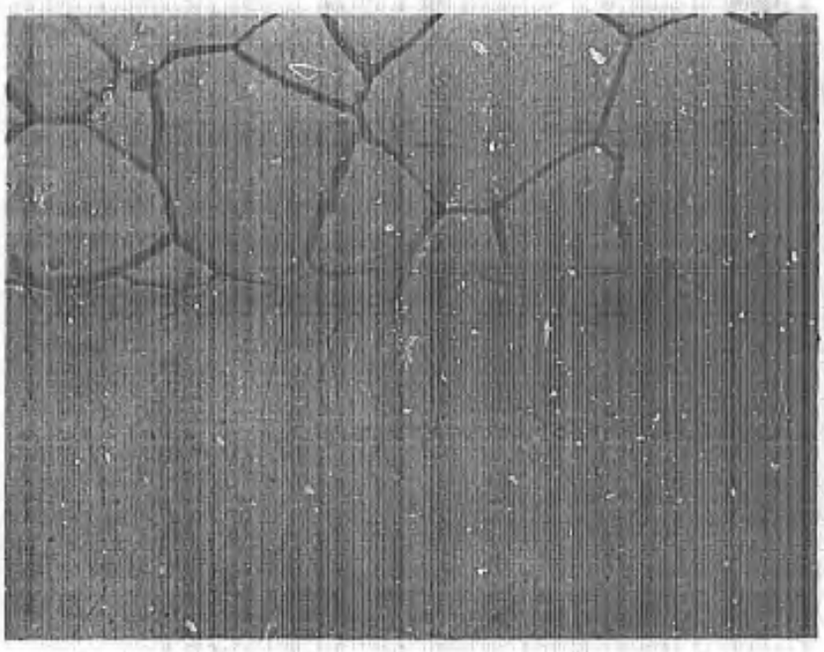

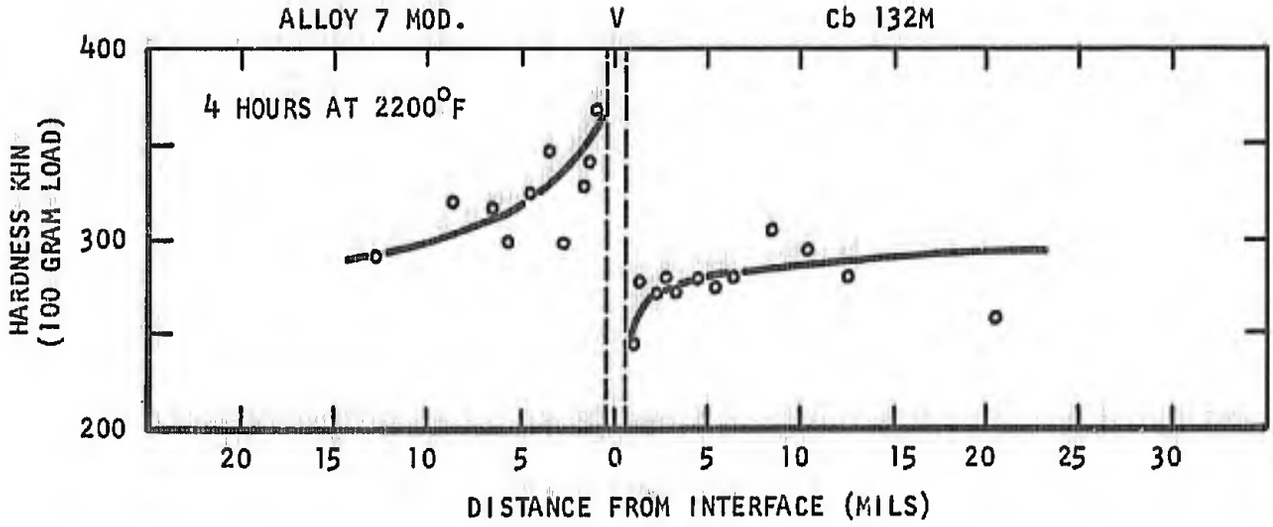

Figure 66. Photomicrograph and microhardness traverse of Cb 132M diffusion bonded to Alloy 7 Modified. Exposed 4 hours at 2200°F after bonding. Magnification: 500X.

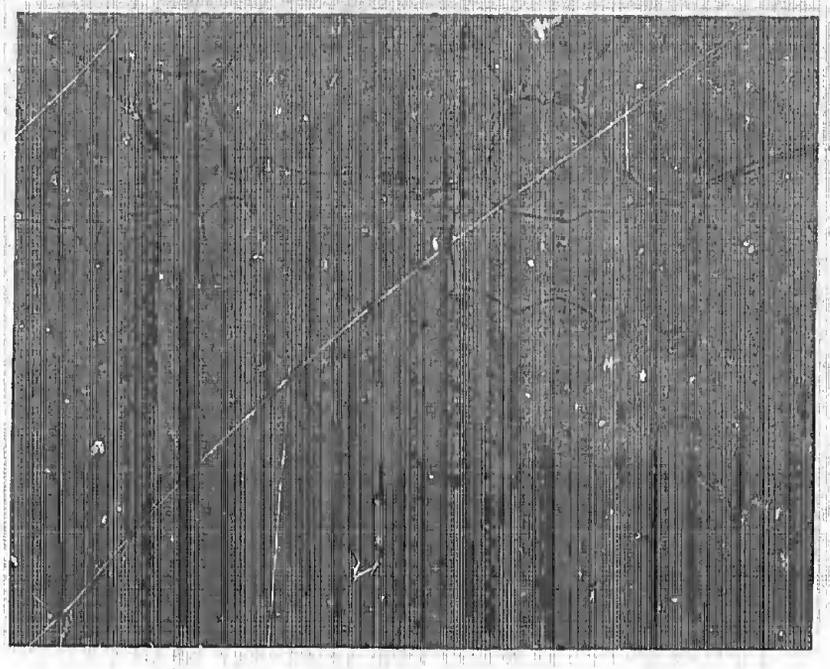

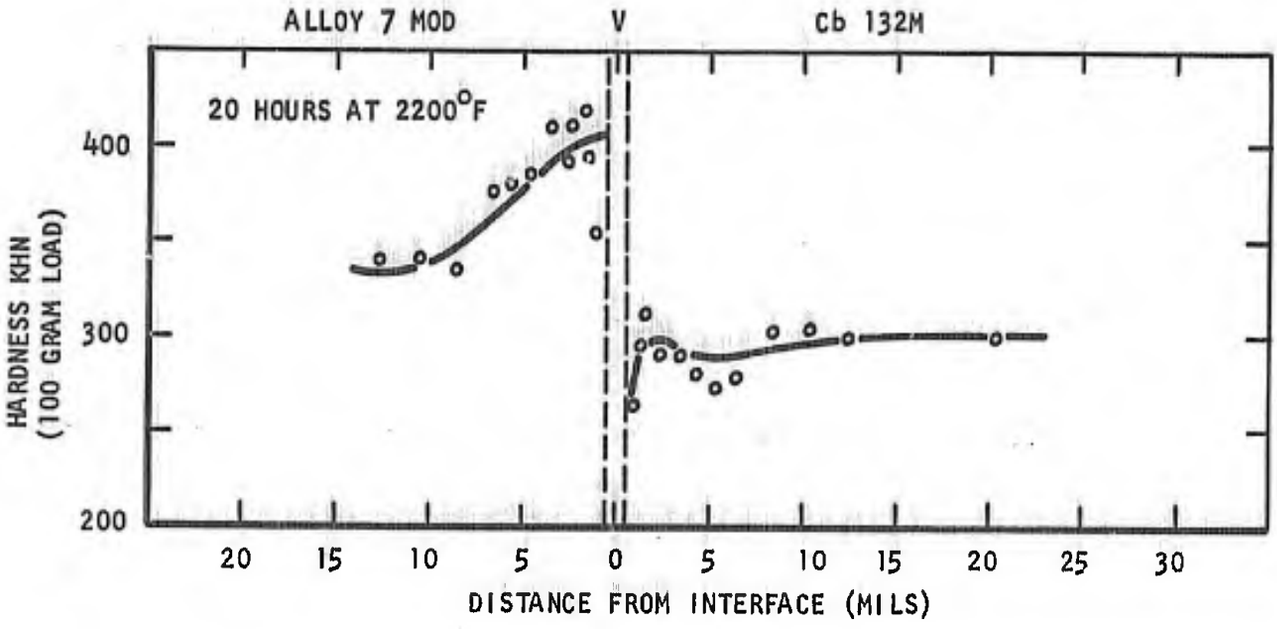

Figure 67. Photomicrograph and microhardness traverse of Cb 132M diffusion bonded to Alloy 7 Modified. Exposed 20 hours at 2200°F after bonding. Magnification: 500X.

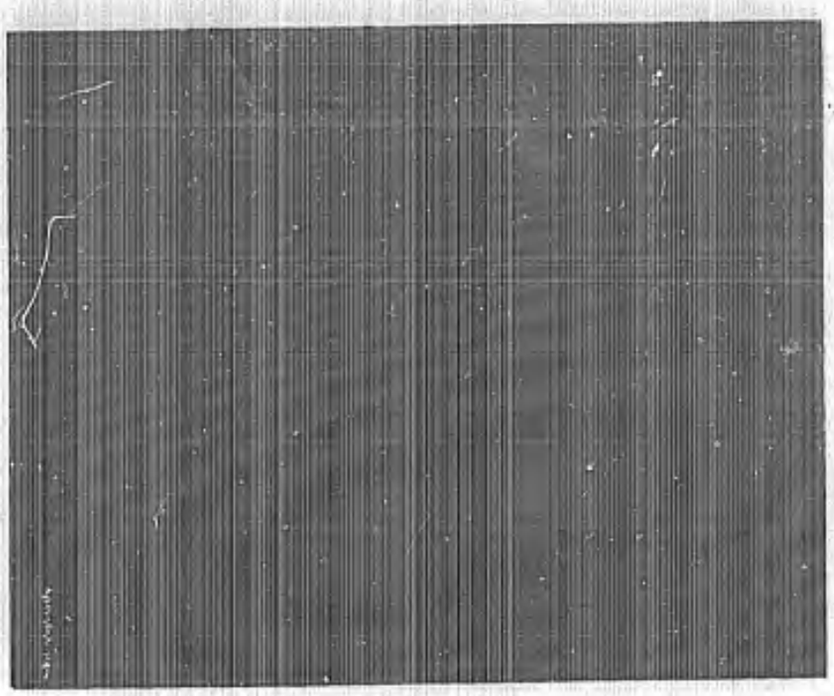

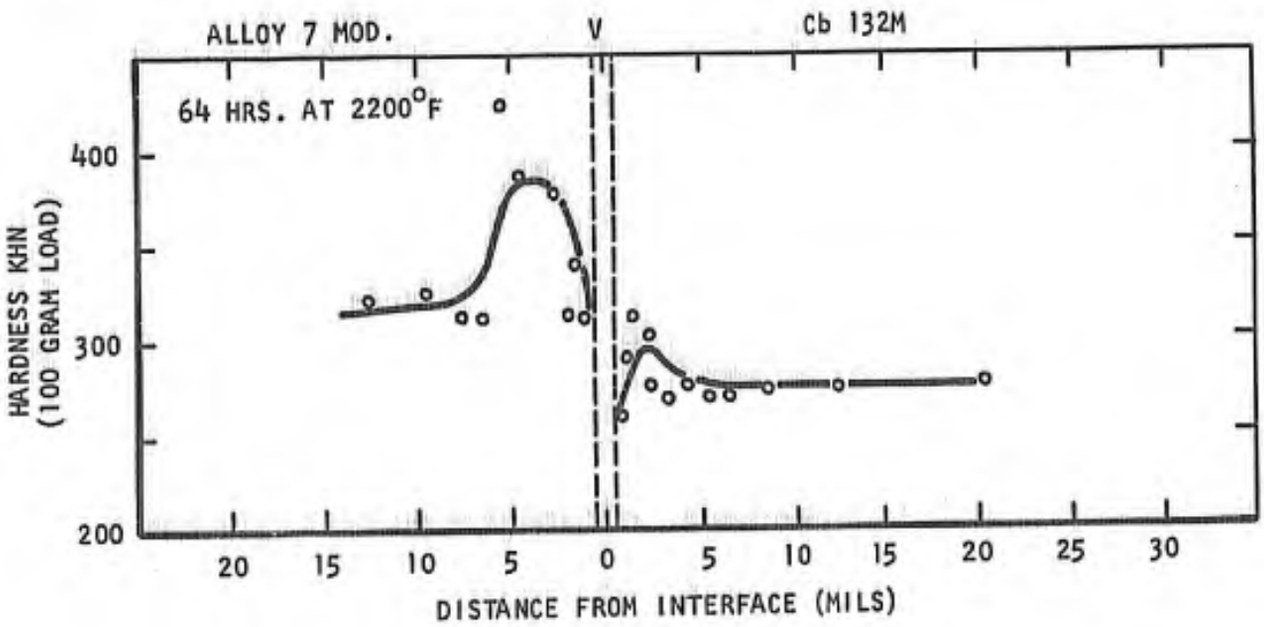

Figure 68. Photomicrograph and microhardness traverse of Cb 132M diffusion bonded to Alloy 7 Modified. Exposed 64 hours at 2200°F after bonding. Magnification: 500X.

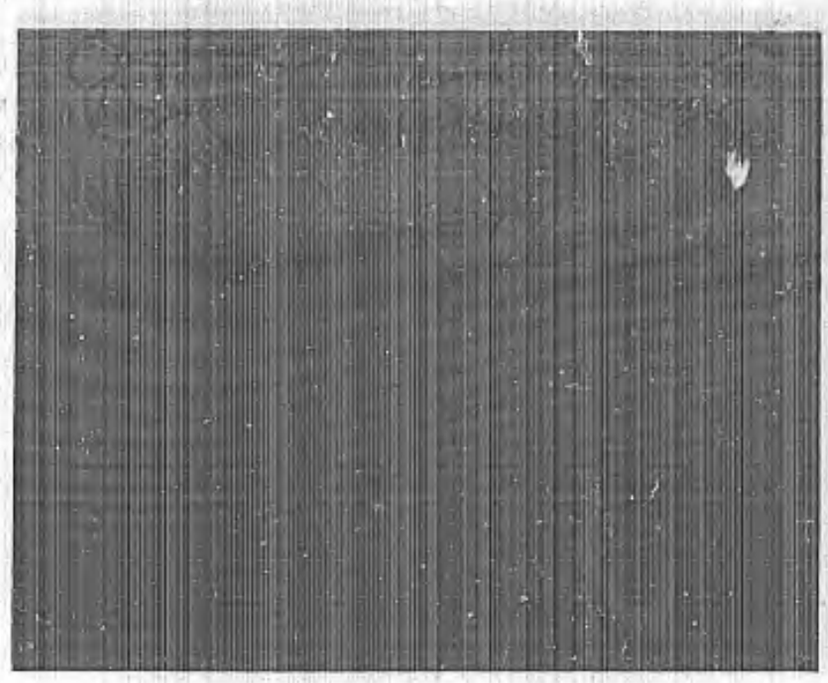

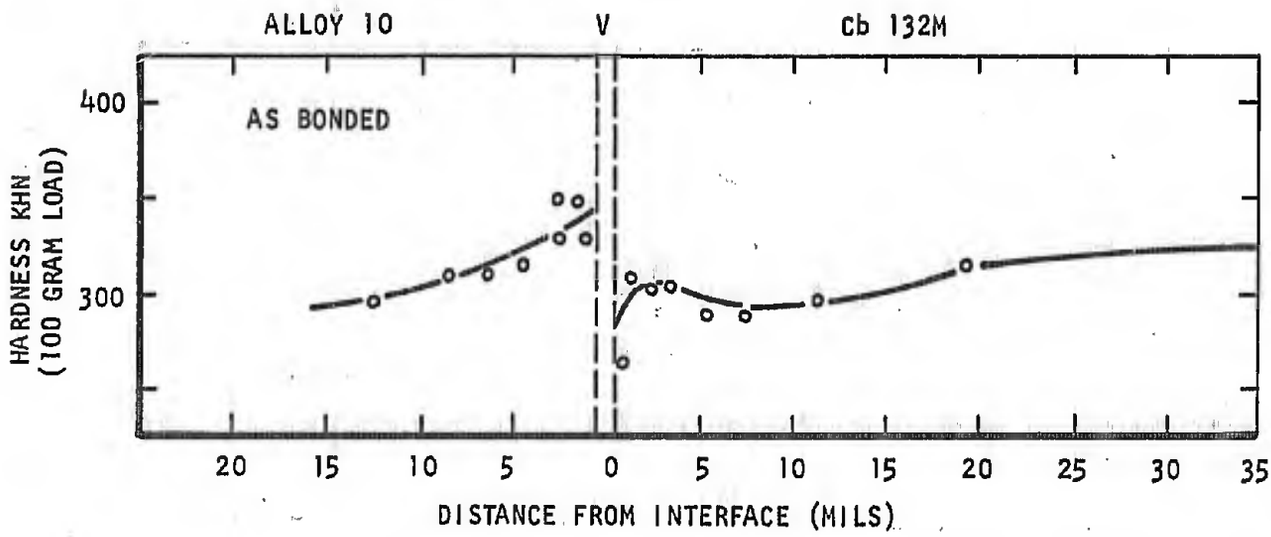

Figure 69. Photomicrograph and microhardness traverse of Cb 132M diffusion bonded to Alloy 10. Shown as-bonded at 2000°F for 30 minutes. Magnification: 500X.

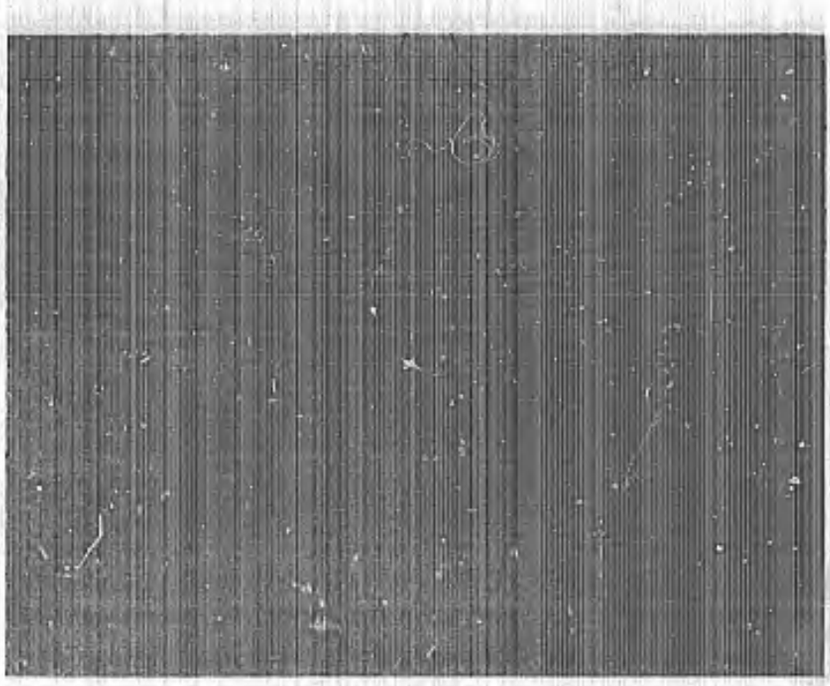

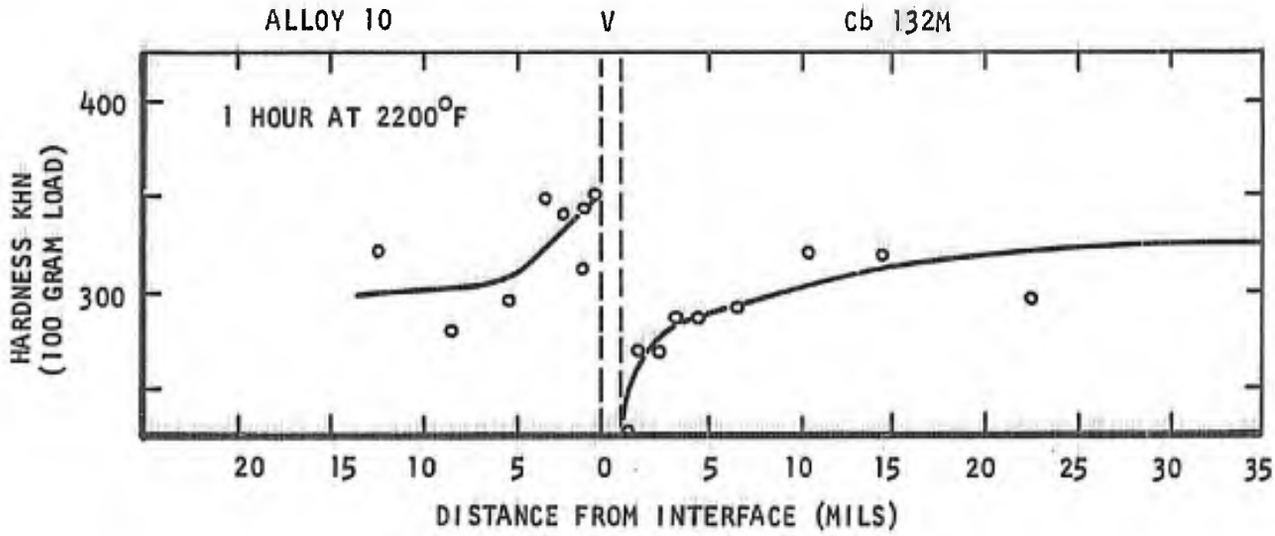

Figure 70. Photomicrograph and microhardness traverse of Cb 132M diffusion bonded to Alloy 10. Exposed 1 hour at 2200°F after bonding. Magnification: 500X.

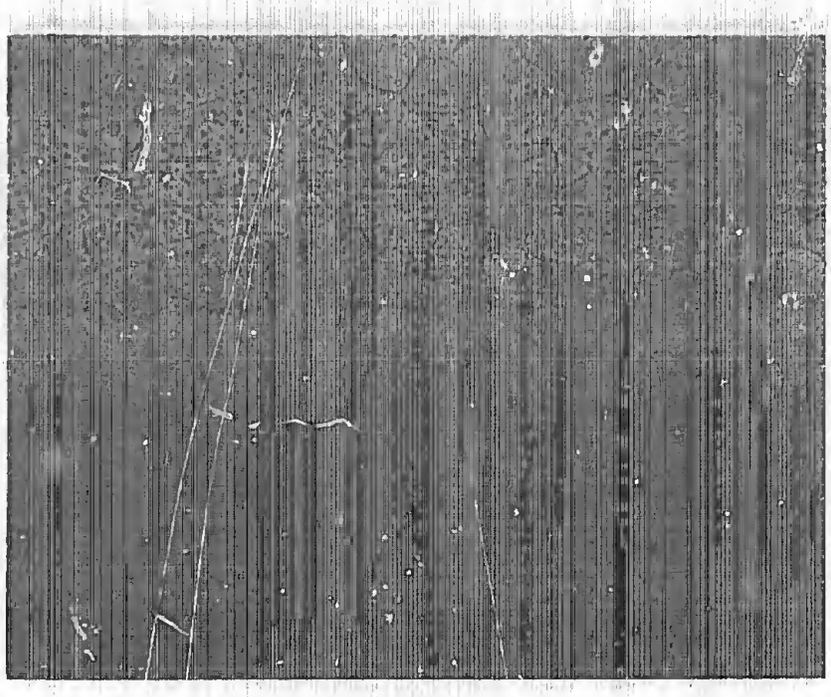

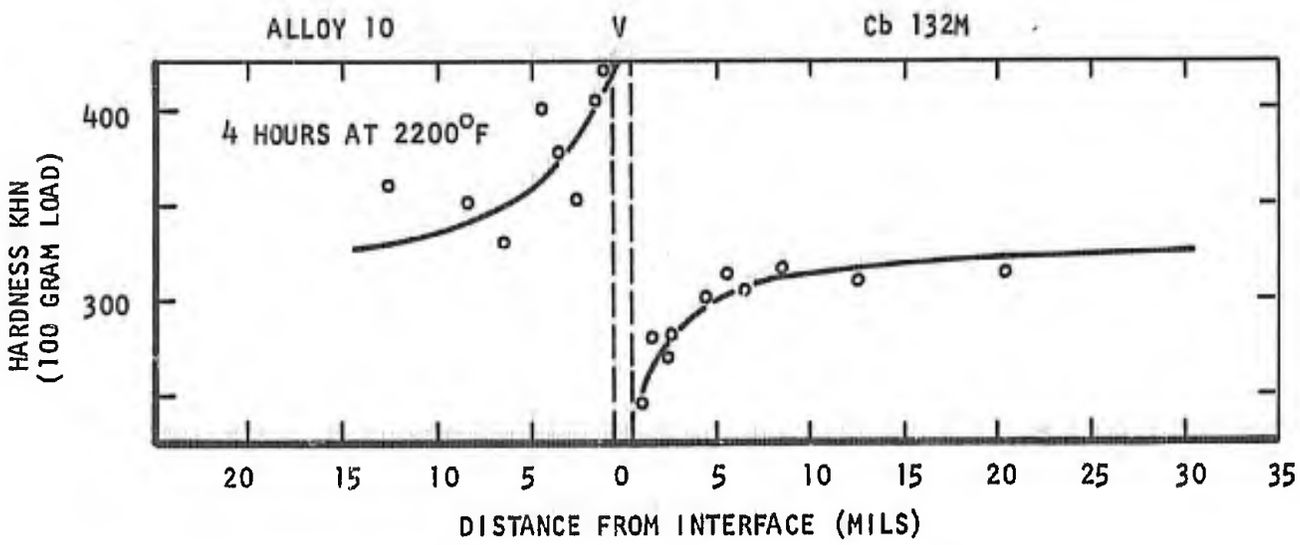

Figure 71. Photomicrograph and microhardness traverse of Cb 132M diffusion bonded to Alloy 10. Exposed 4 hours at 2200°F after bonding. Magnification: 500X.

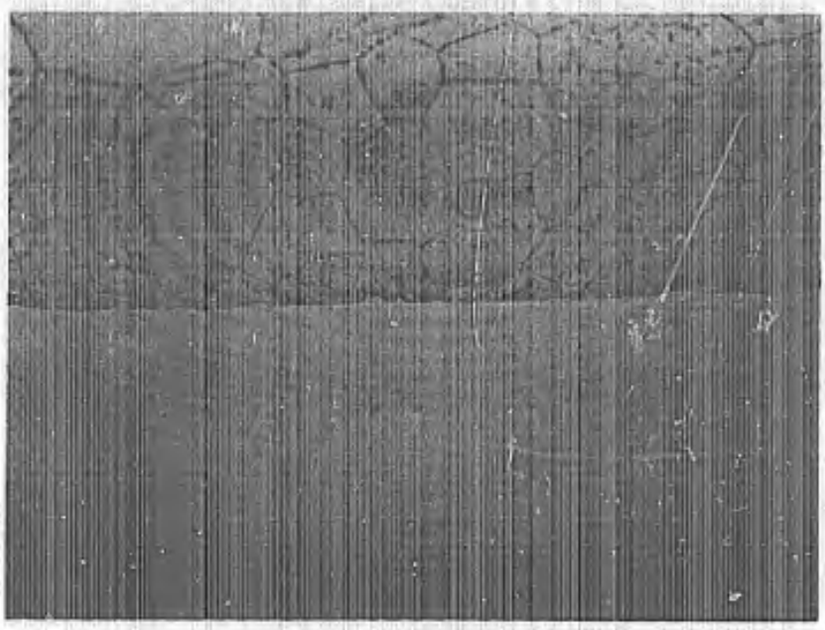

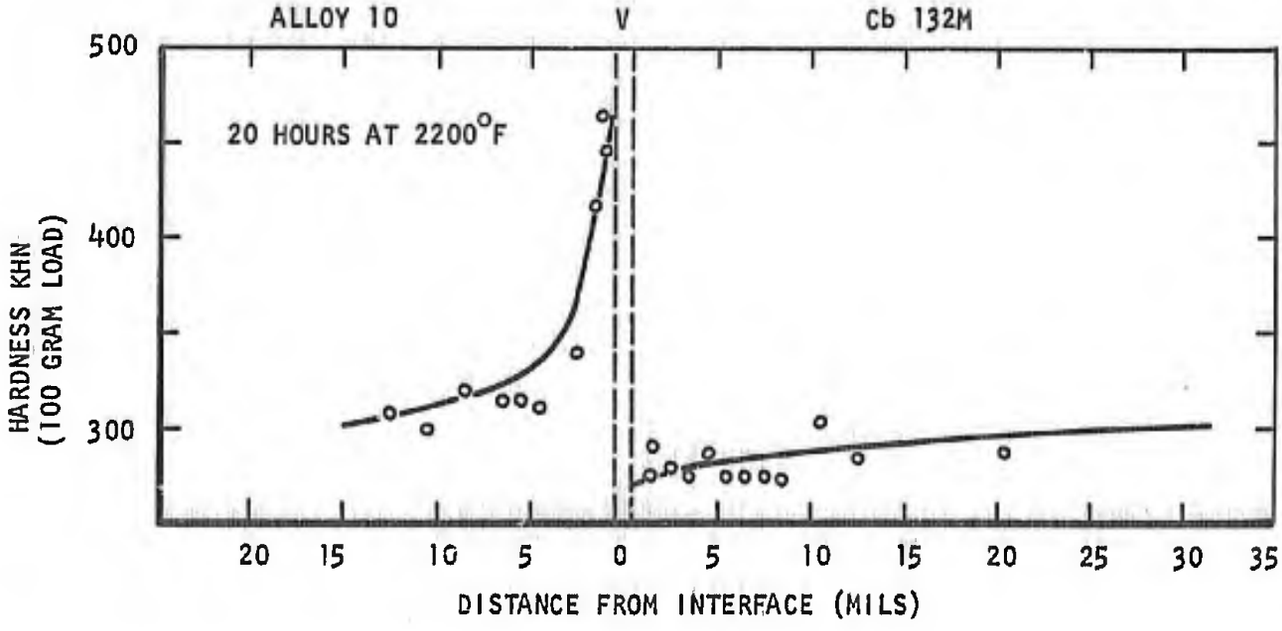

Figure 72. Photomicrograph and microhardness traverse of Cb 132M diffusion bonded to Alloy 10. Exposed 20 hours at 2200°F after bonding. Magnification: 500X.

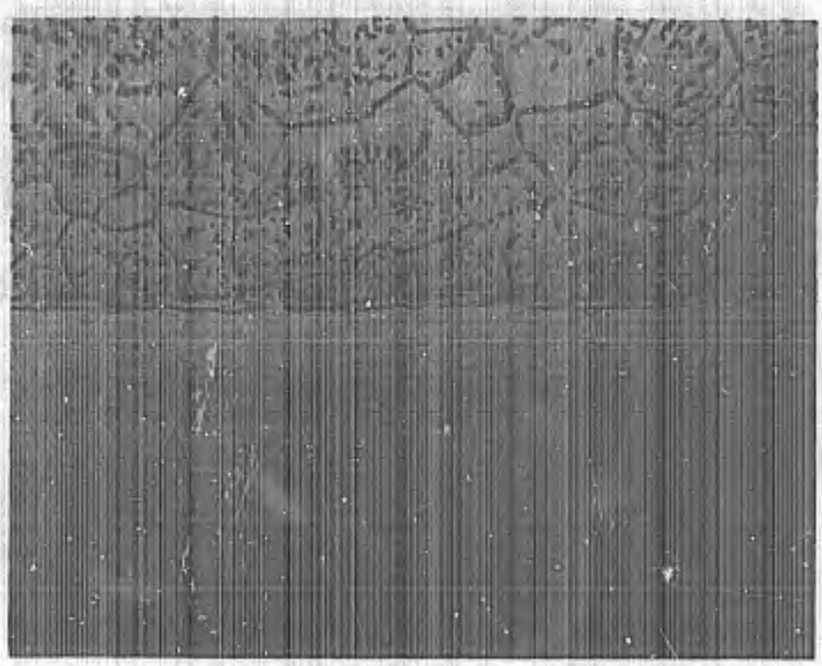

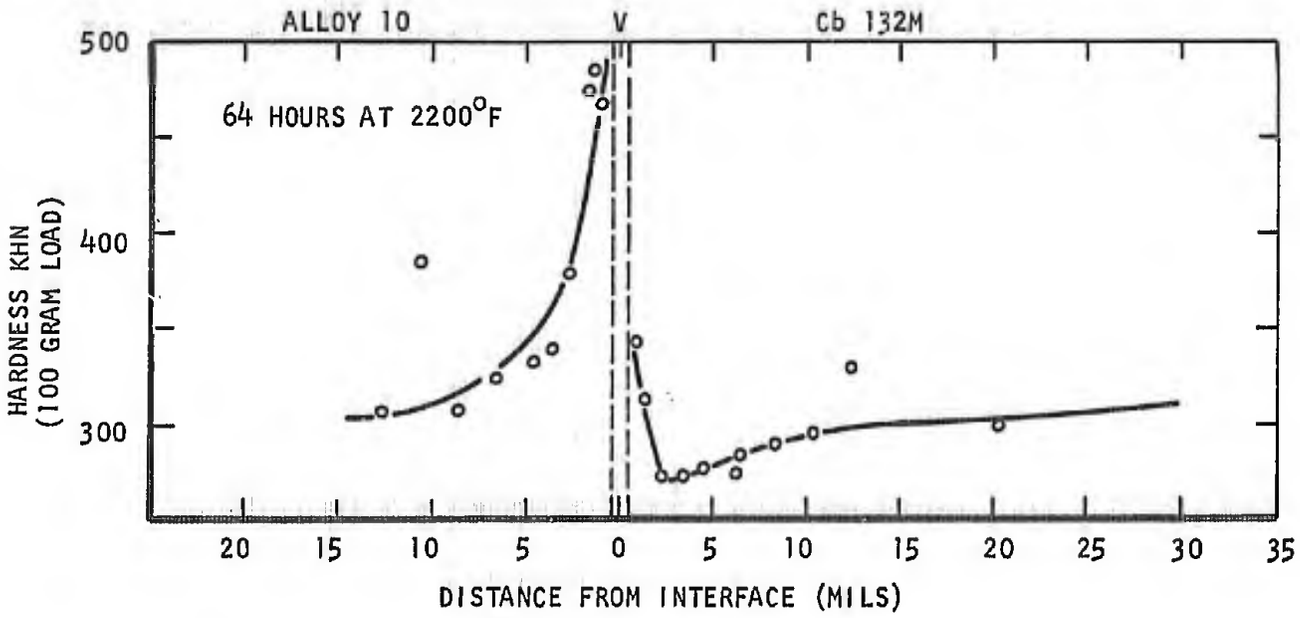

Figure 73. Photomicrograph and microhardness traverse of Cb 132M diffusion bonded to Alloy 10. Exposed 64 hours at 2200°F after bonding. Magnification: 500X.

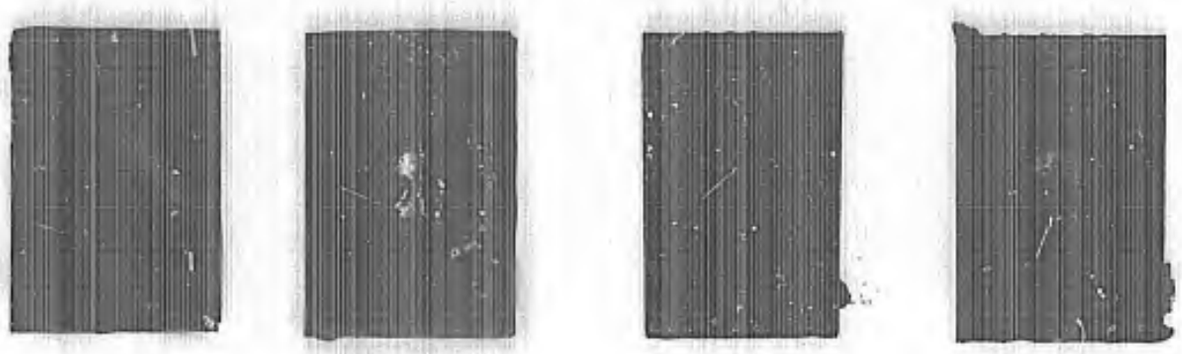

Alloy 7
Modified

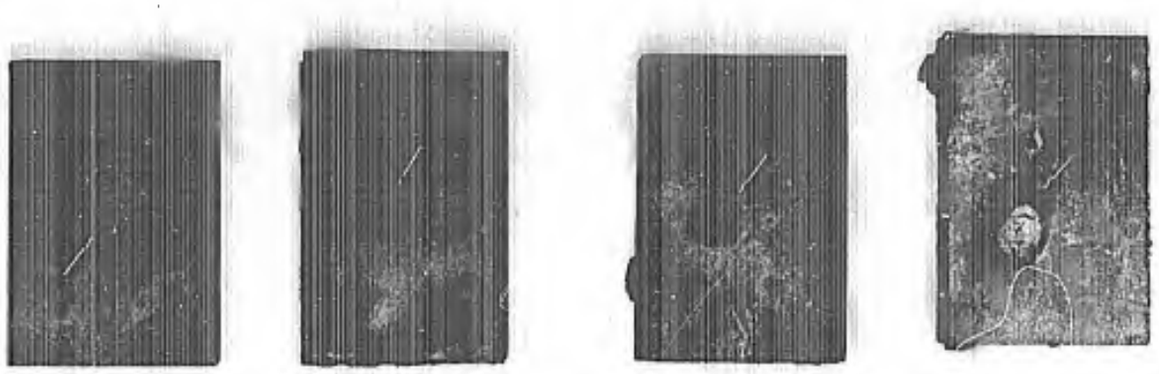

Alloy 10

1 hour | 4 hours | 20 hours | 64 hours

Figure 74. Photographs showing oxidation test samples. Cb 132M bonded to cladding alloy indicated, Cr-Ti-Si coating, damaged, and exposed at 2200°F in air for times indicated. (Arrow shows damaged region.)

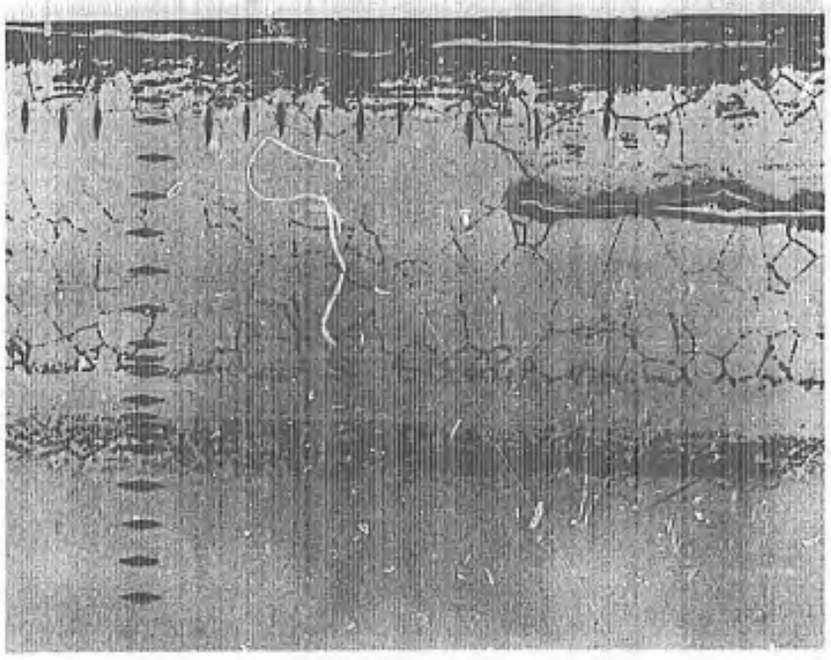

A. 1 hour

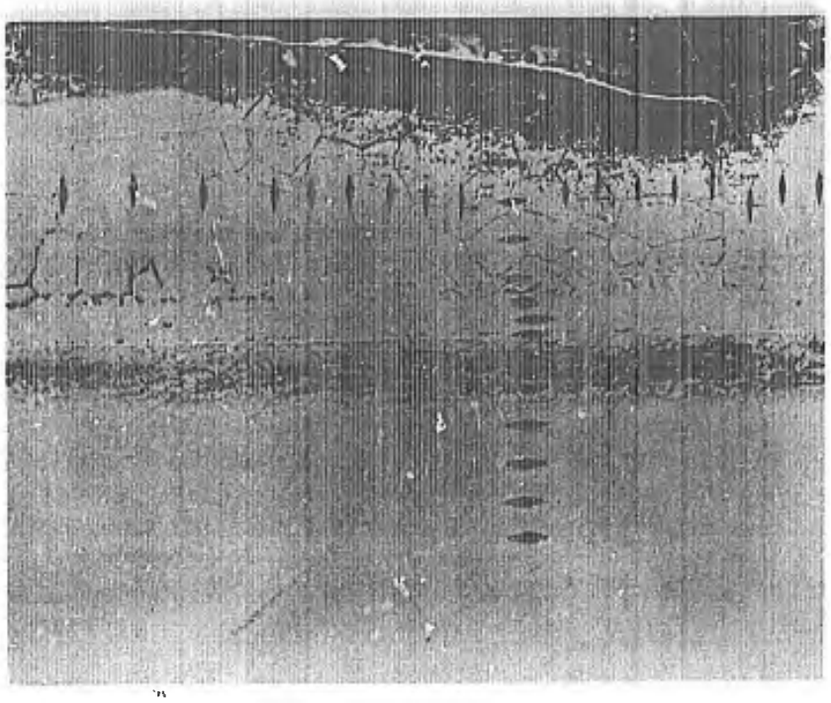

B. 4 hours

Figure 75. Photomicrographs of bonded oxidation test samples. Alloy 7 Modified diffusion bonded to Cb 132M. Exposed for times shown at 2200°F after coating and intentional damage. Magnification: 100X.

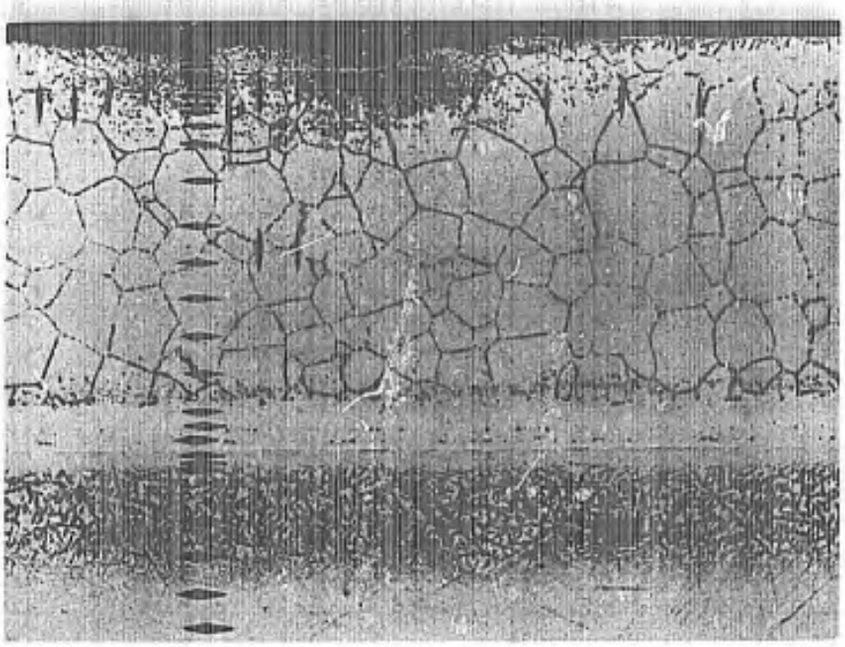

A. 20 hours

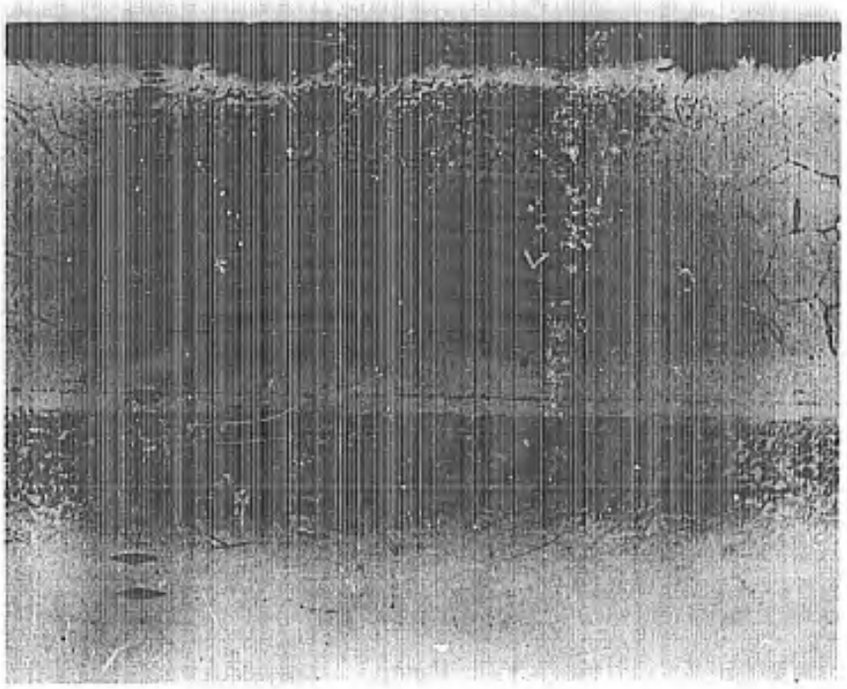

B. 64 hours

Figure 76. Photomicrographs of bonded oxidation test samples. Alloy 7 Modified diffusion bonded to Cb 132M. Exposed for times shown at 2200°F after coating and intentional damage. Magnification: 100X.

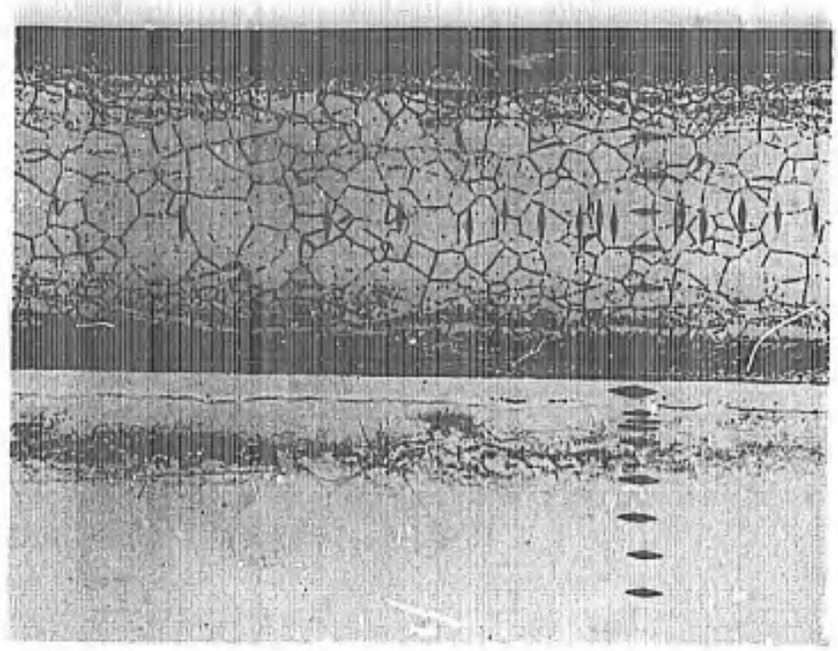

A. 1 hour

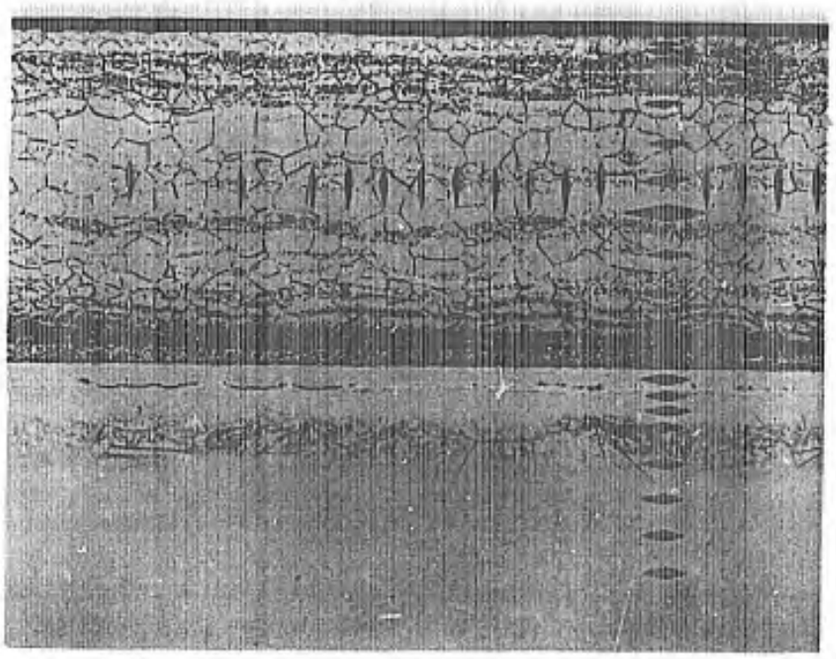

B. 4 hours

Figure 77. Photomicrographs of bonded oxidation test samples. Alloy 10 diffusion bonded to Cb 132M. Exposed for times shown at 2200°F after coating and intentional damage. Magnification: 100X.

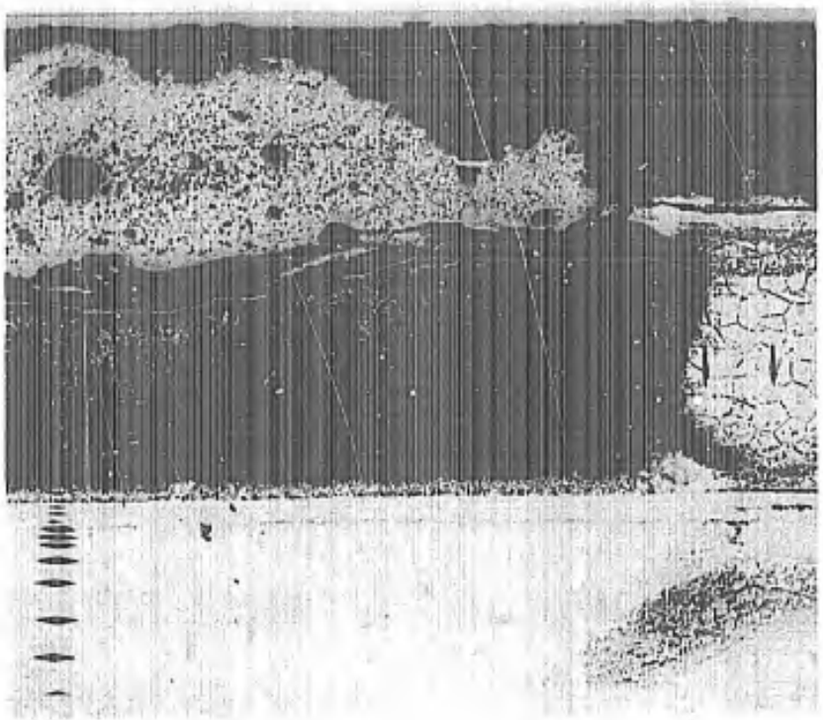

C. 20 hours

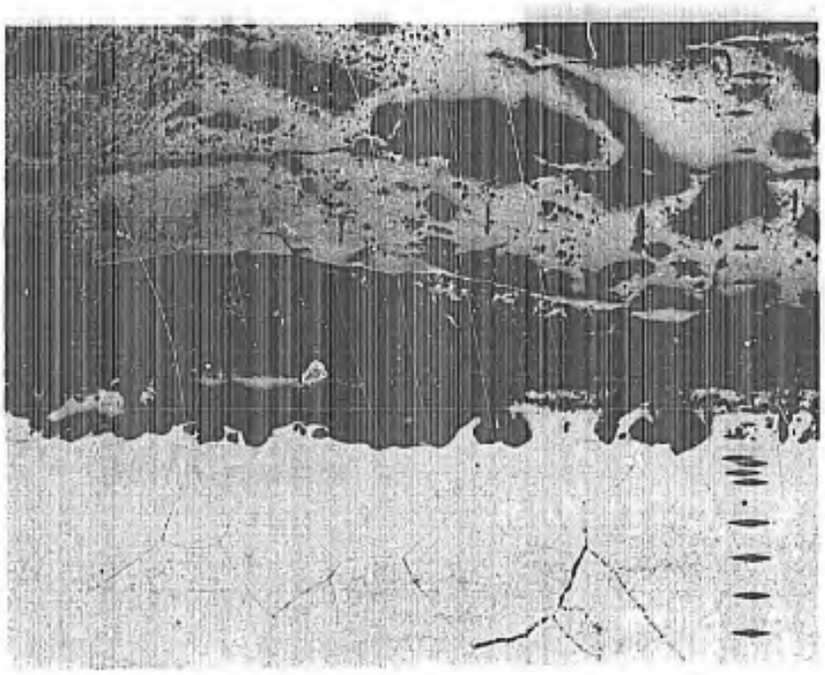

D. 64 hours

Figure 78. Photomicrographs of bonded oxidation test samples. Alloy 10 diffusion bonded to Cb 132M. Exposed for times shown at 2200°F after coating and intentional damage. Magnification: 100X.

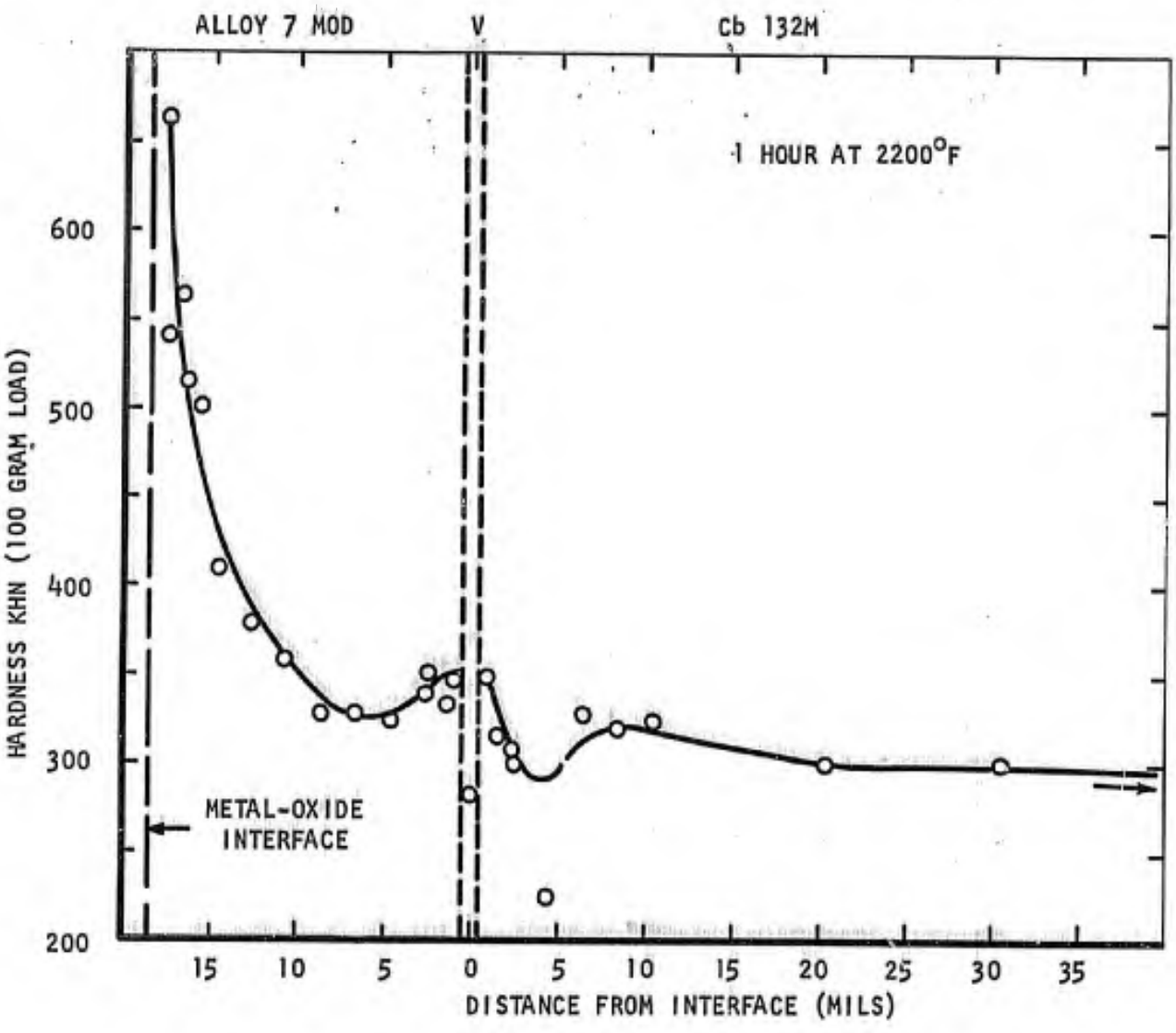

Figure 79. Microhardness traverse for bonded oxidation test sample. Alloy 7 Modified diffusion bonded to Cb 132M. Coated, damaged, and exposed 1 hour at 2200°F.

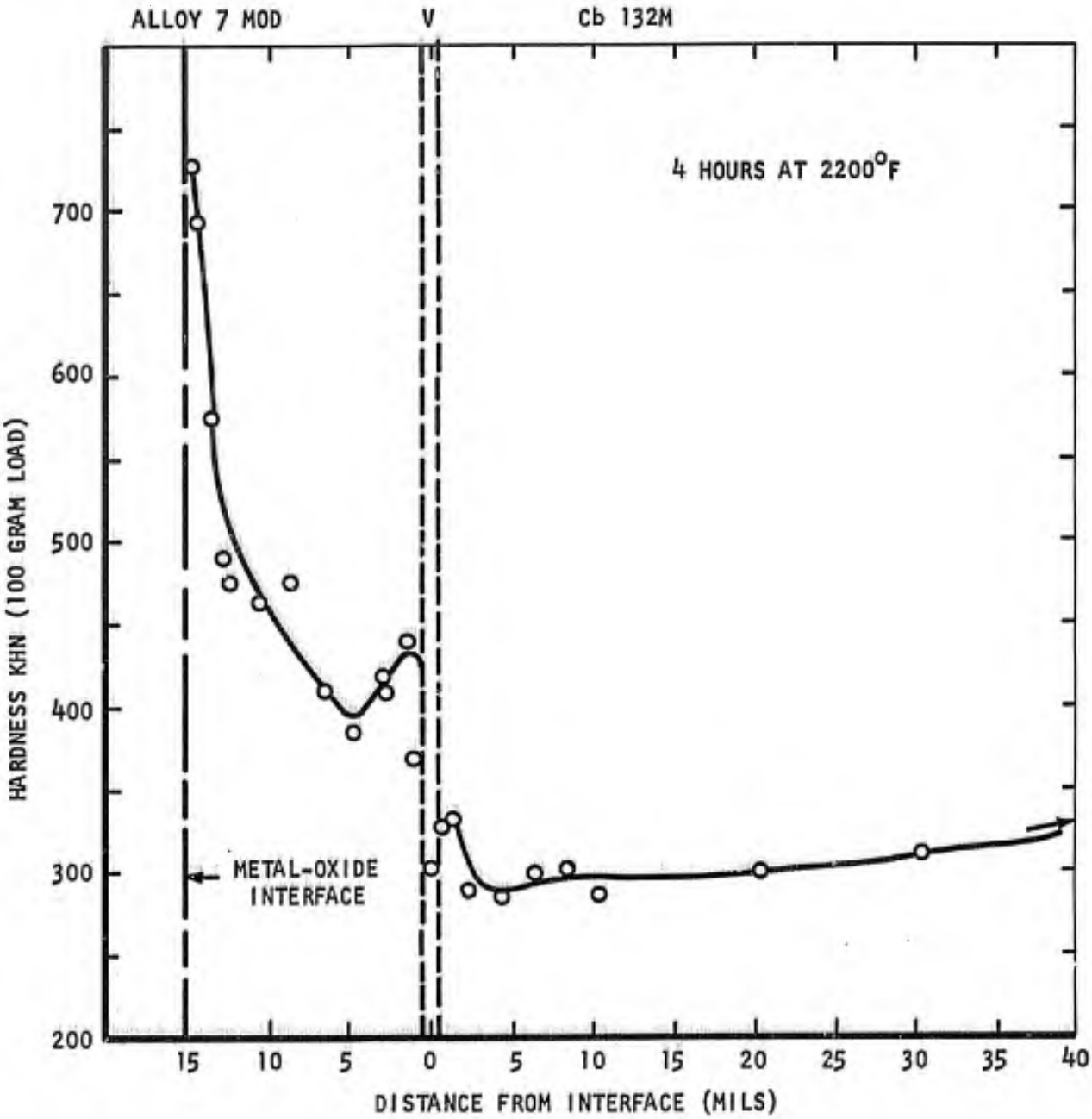

Figure 80. Microhardness traverse for bonded oxidation test sample. Alloy 7 Modified diffusion bonded to Cb 132M. Coated, damaged, and exposed 4 hours at 2200°F.

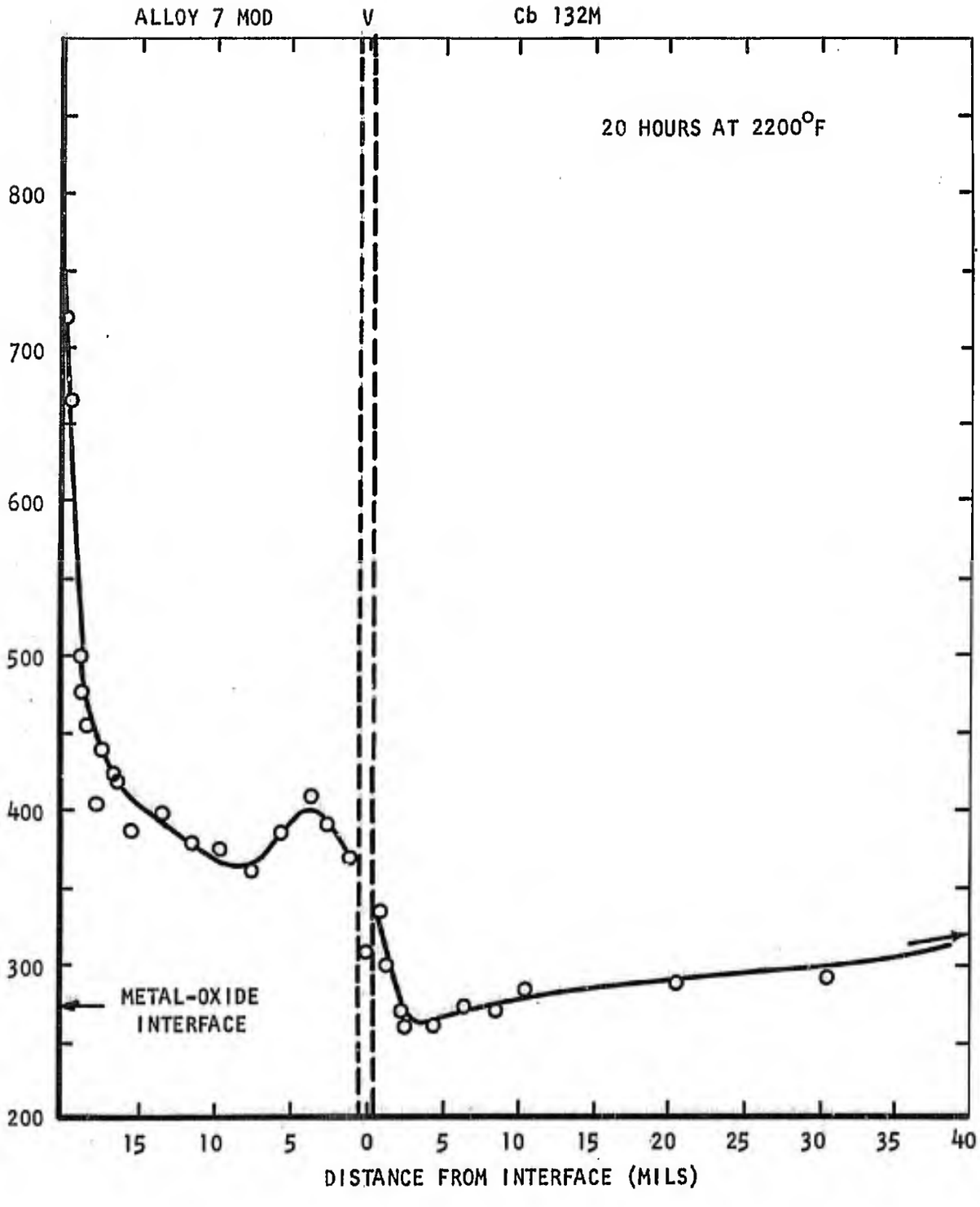

Figure 81. Microhardness traverse for bonded oxidation test sample. Alloy 7 Modified diffusion bonded to Cb 132M. Coated, damaged, and exposed 20 hours at 2200°F.

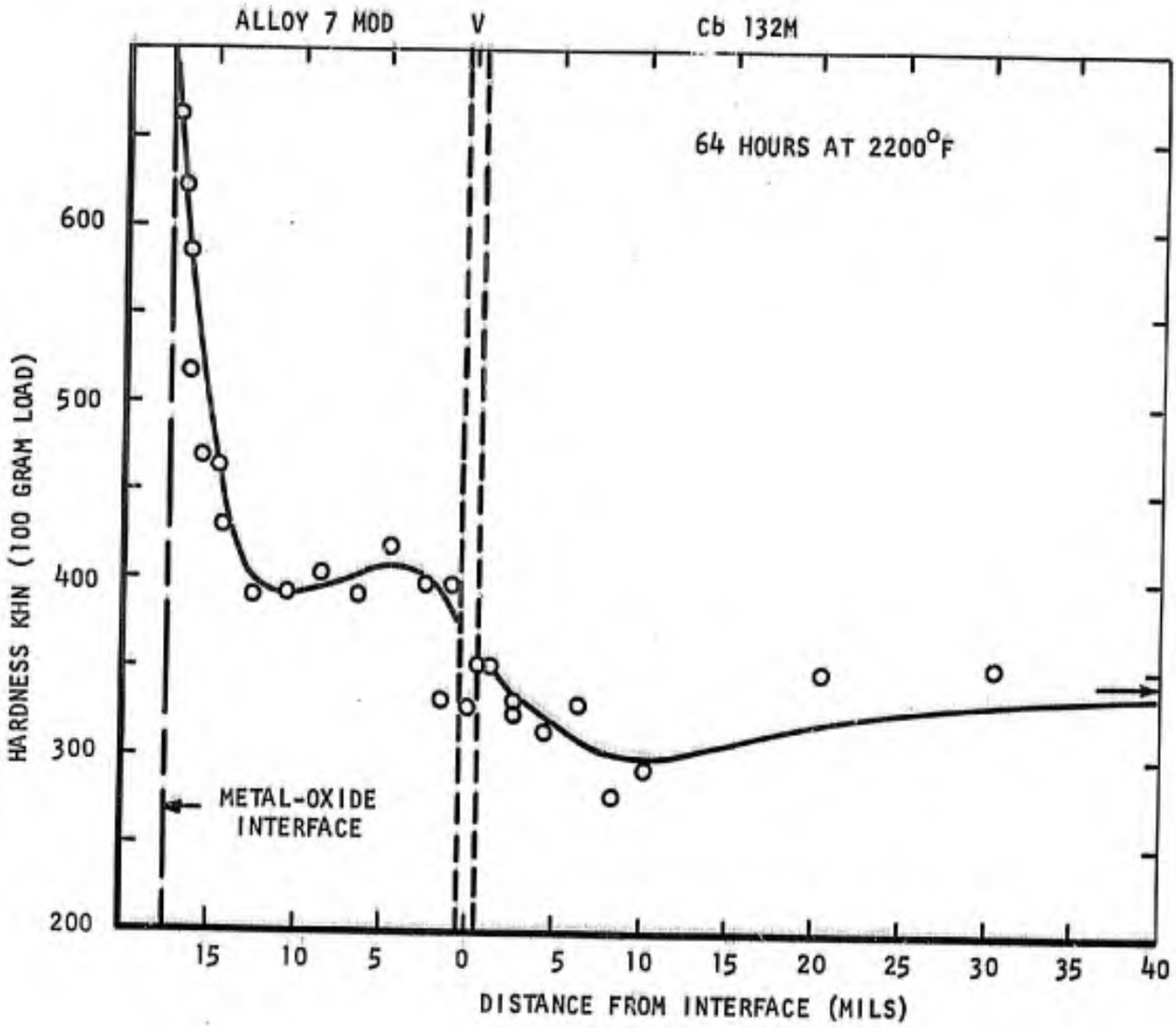

Figure 82. Microhardness traverse for bonded oxidation test sample. Alloy 7 Modified diffusion bonded to Cb 132M. Coated, damaged, and exposed 64 hours at 2200°F.

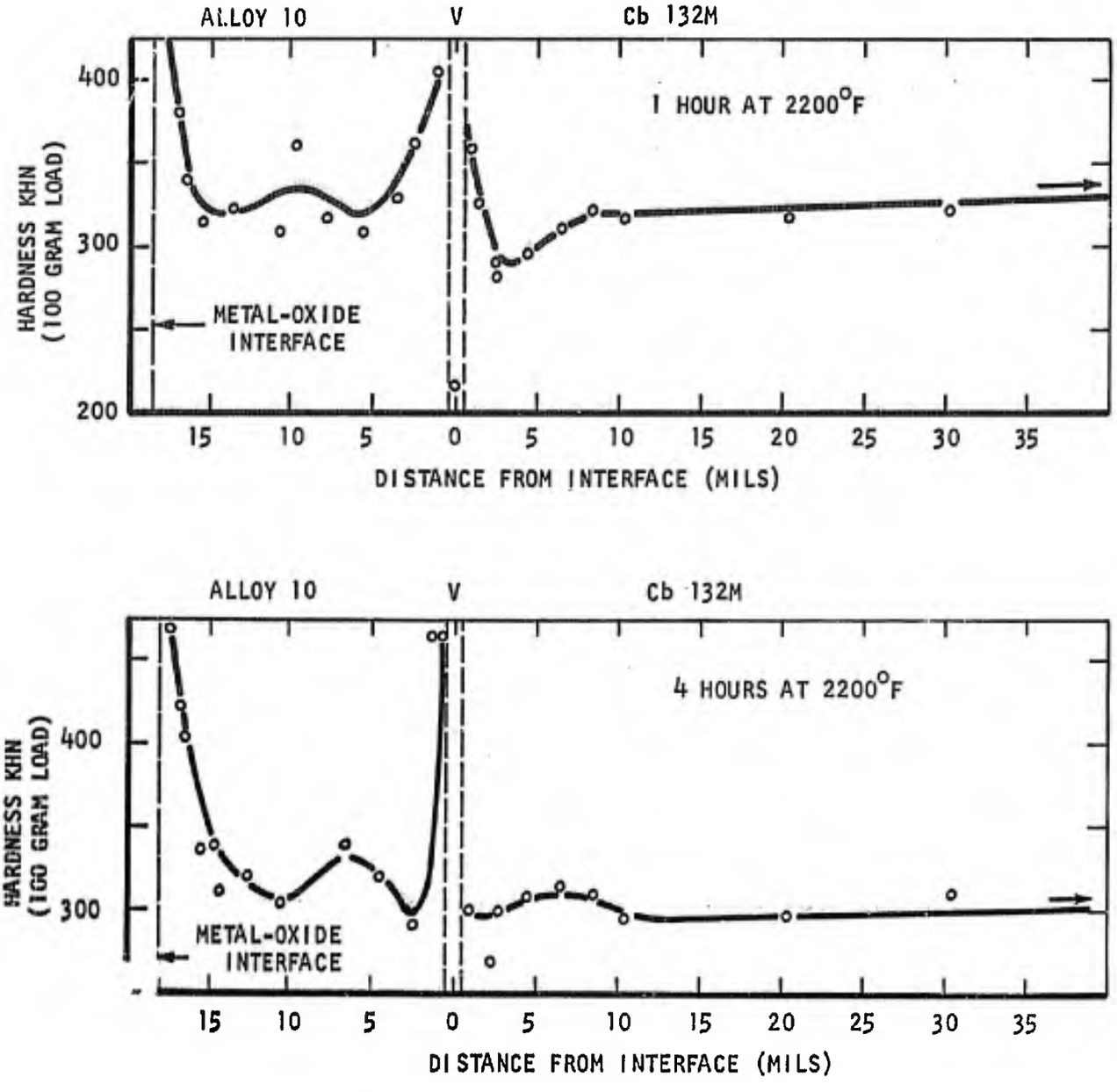

Figure 83. Microhardness traverses for bonded oxidation test samples. Alloy 10 diffusion bonded to Cb 132M. Coated, damaged, and exposed for 1 and 4 hours respectively at 2200°F.

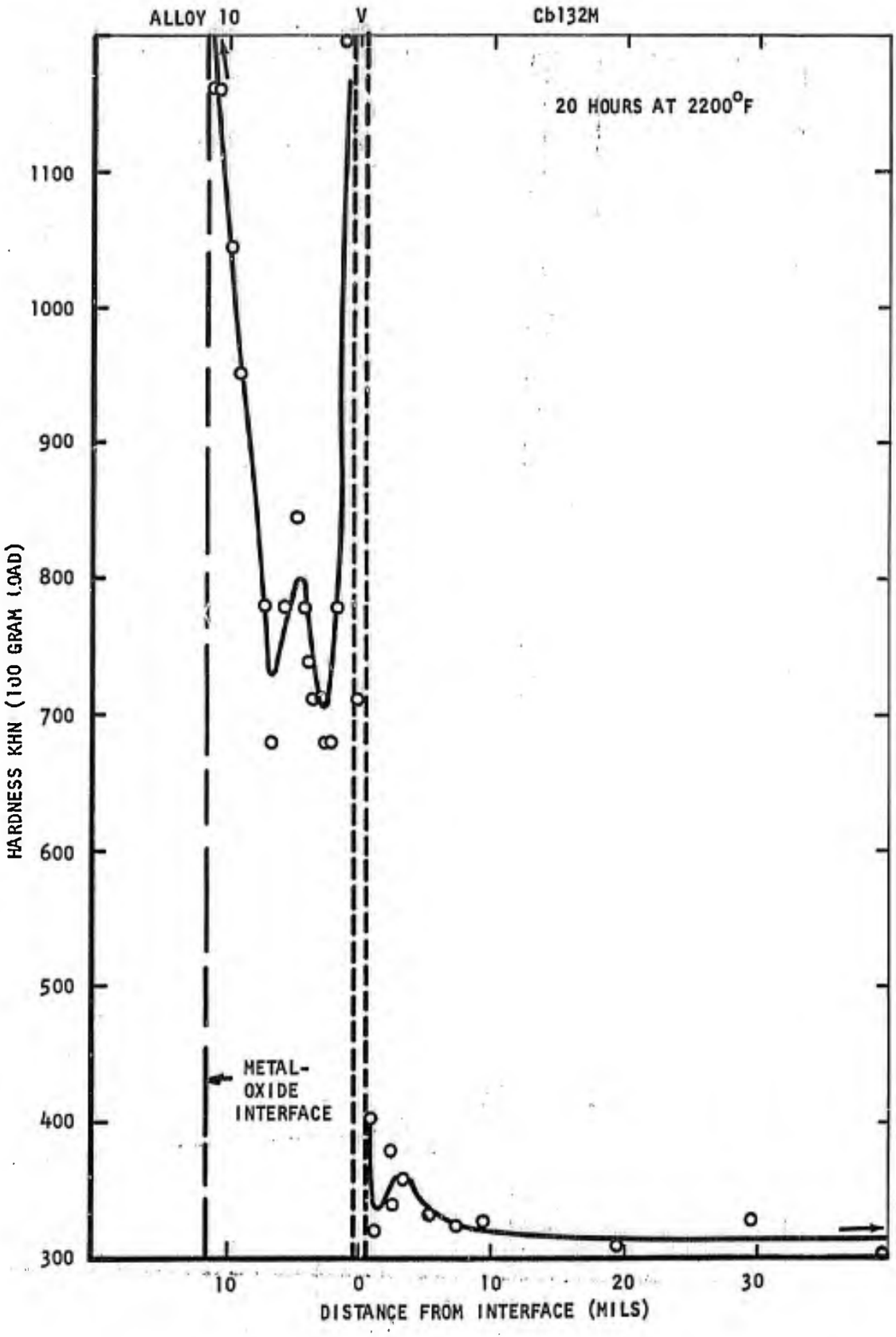

Figure 84. Microhardness traverse for bonded oxidation test sample. Alloy 10 diffusion bonded to Cb 132M. Coated, damaged, and exposed for 20 hours at 2200°F.

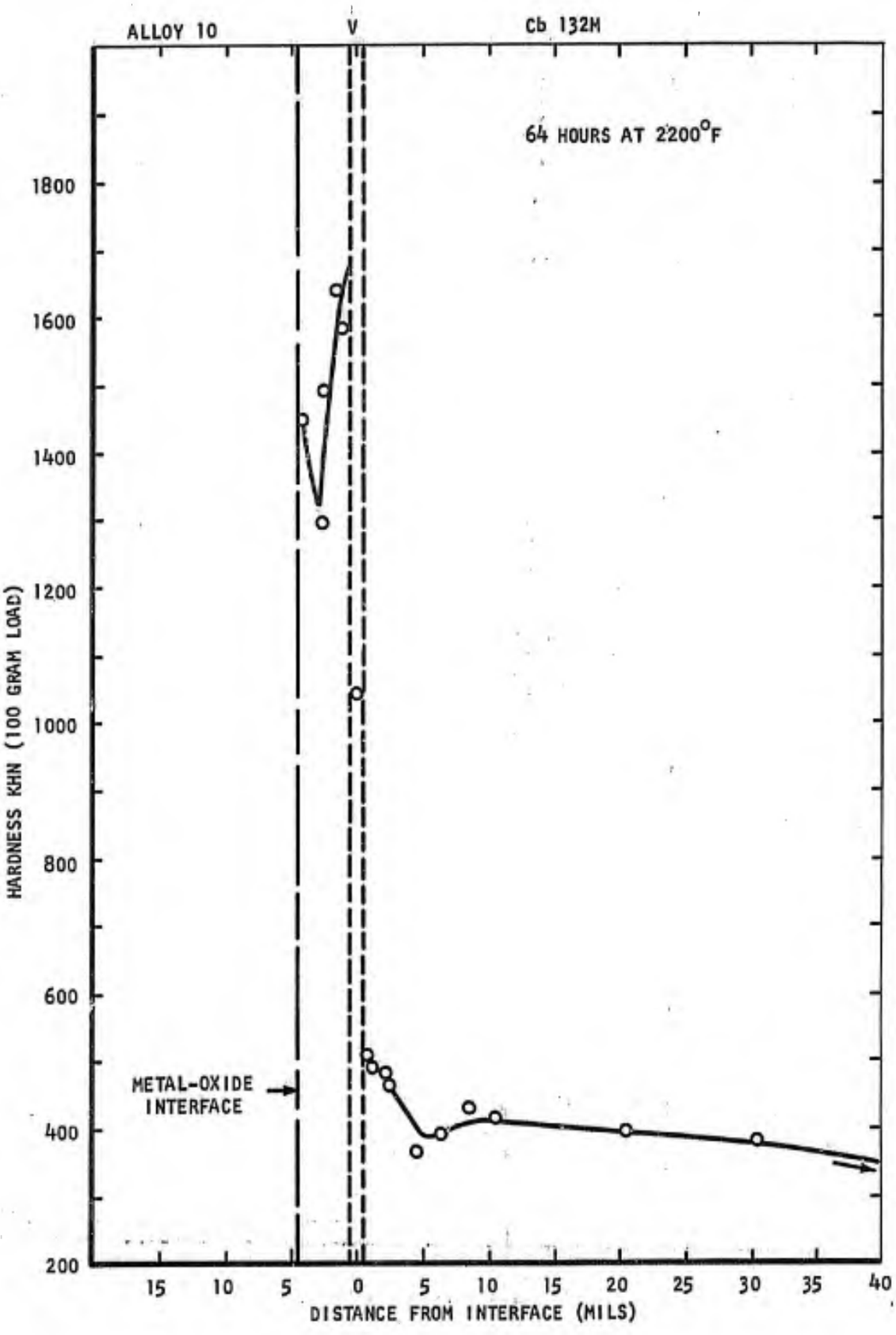

Figure 85. Microhardness traverse for bonded oxidation test sample. Alloy 10 diffusion bonded to Cb 132M. Coated, damaged, and exposed for 64 hours at 2200°F.

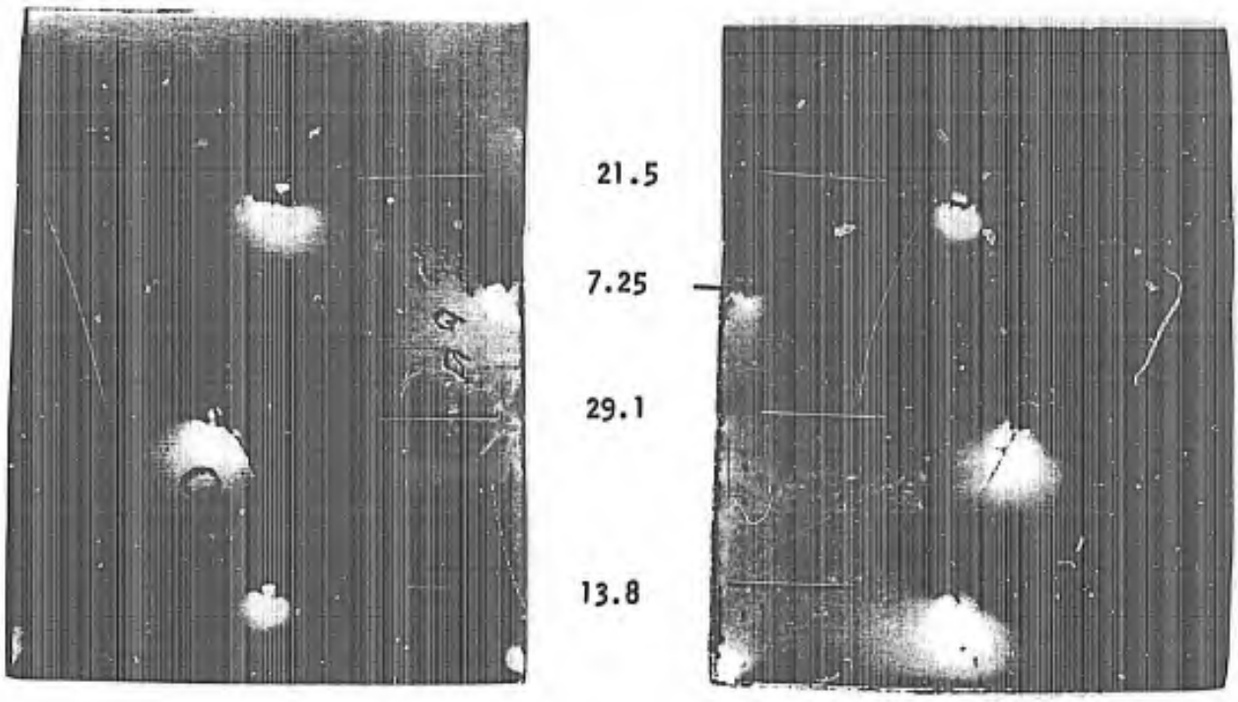

Impact side

Reverse side

A. Room temperature

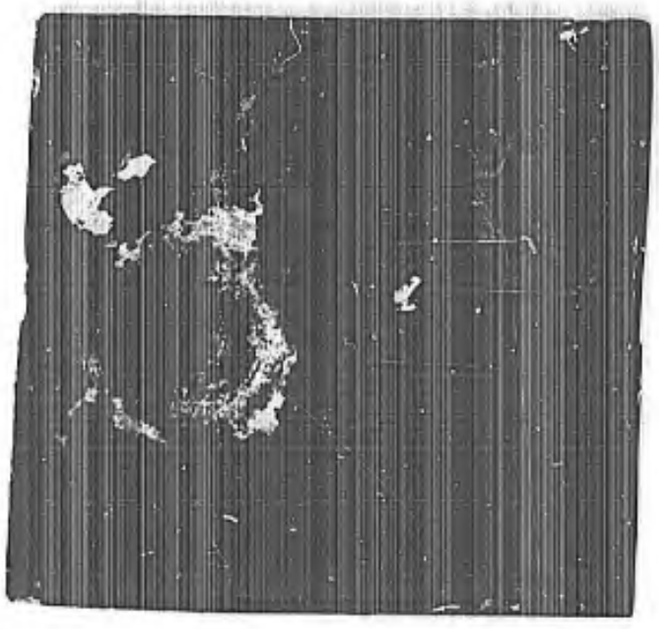

B. 2000°F

Figure 86. Ballistic impact test specimens for Alloy 7 Modified. Impact energy (ft-lbs) and test temperature indicated.

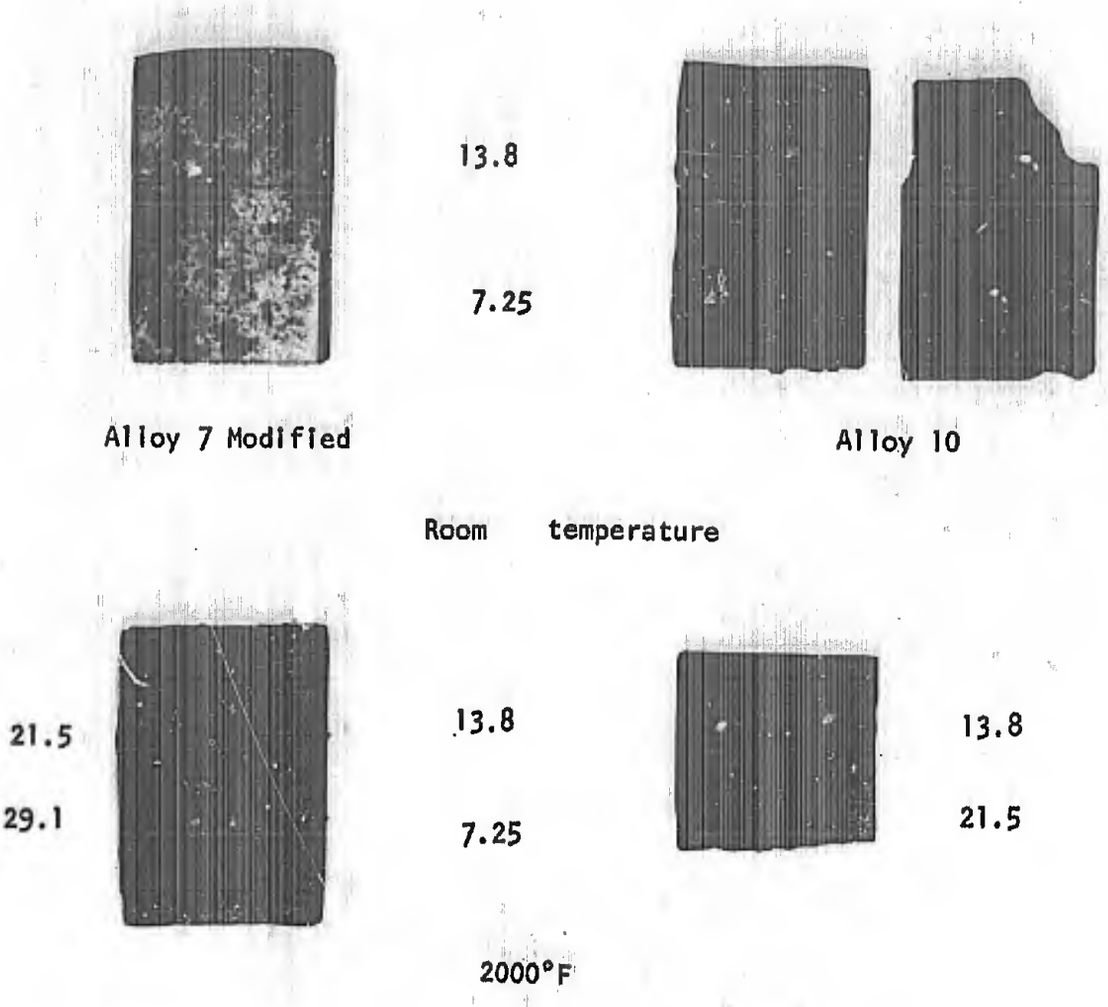

Figure 87. Ballistic impact test specimens for diffusion bonded and coated columbium alloy combinations. Cladding alloy shown, substrate: Cb 132M. Impact energy (ft-lbs) and test temperature indicated.

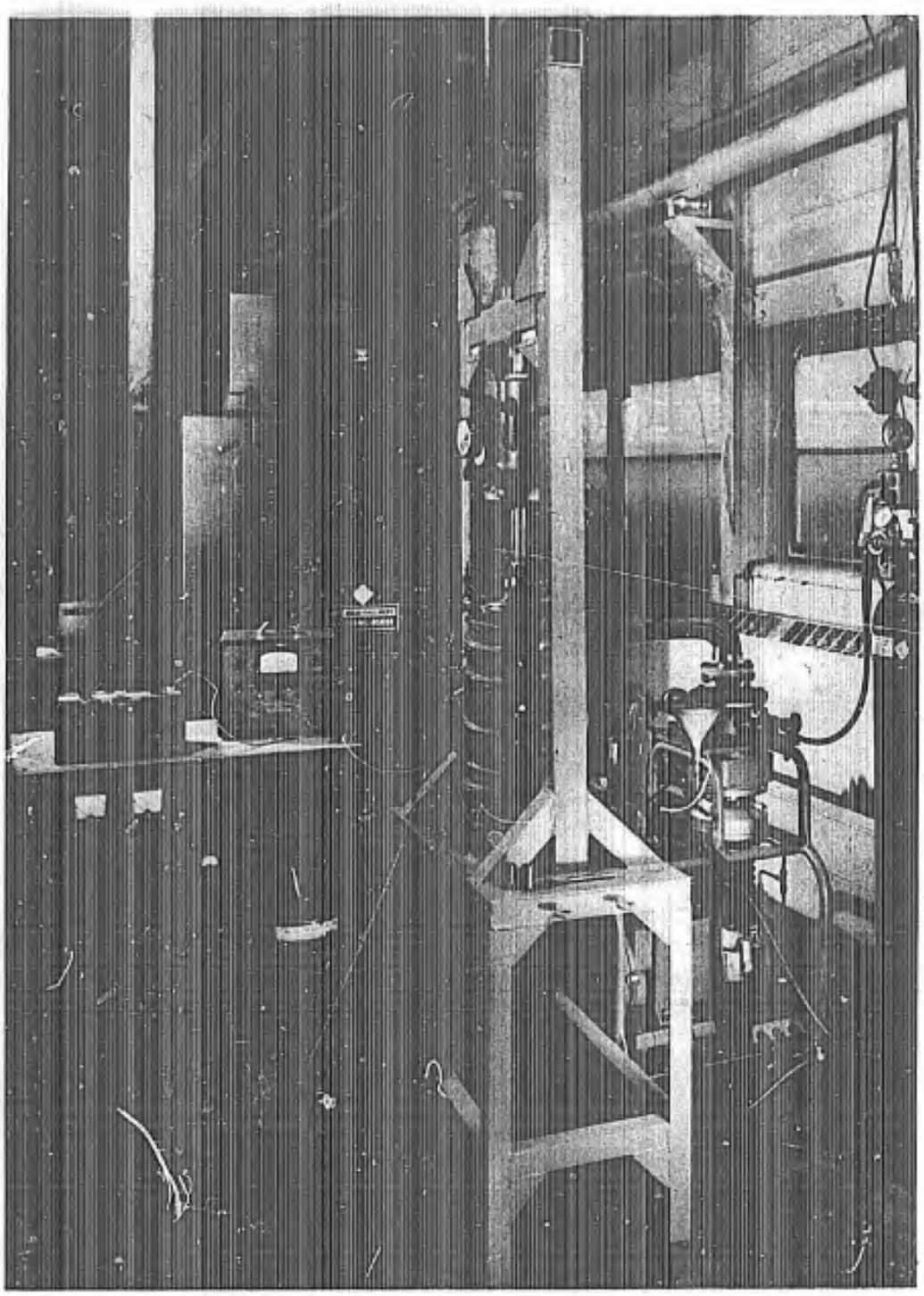

Figure 88. Resistance heated experimental diffusion bonding apparatus.

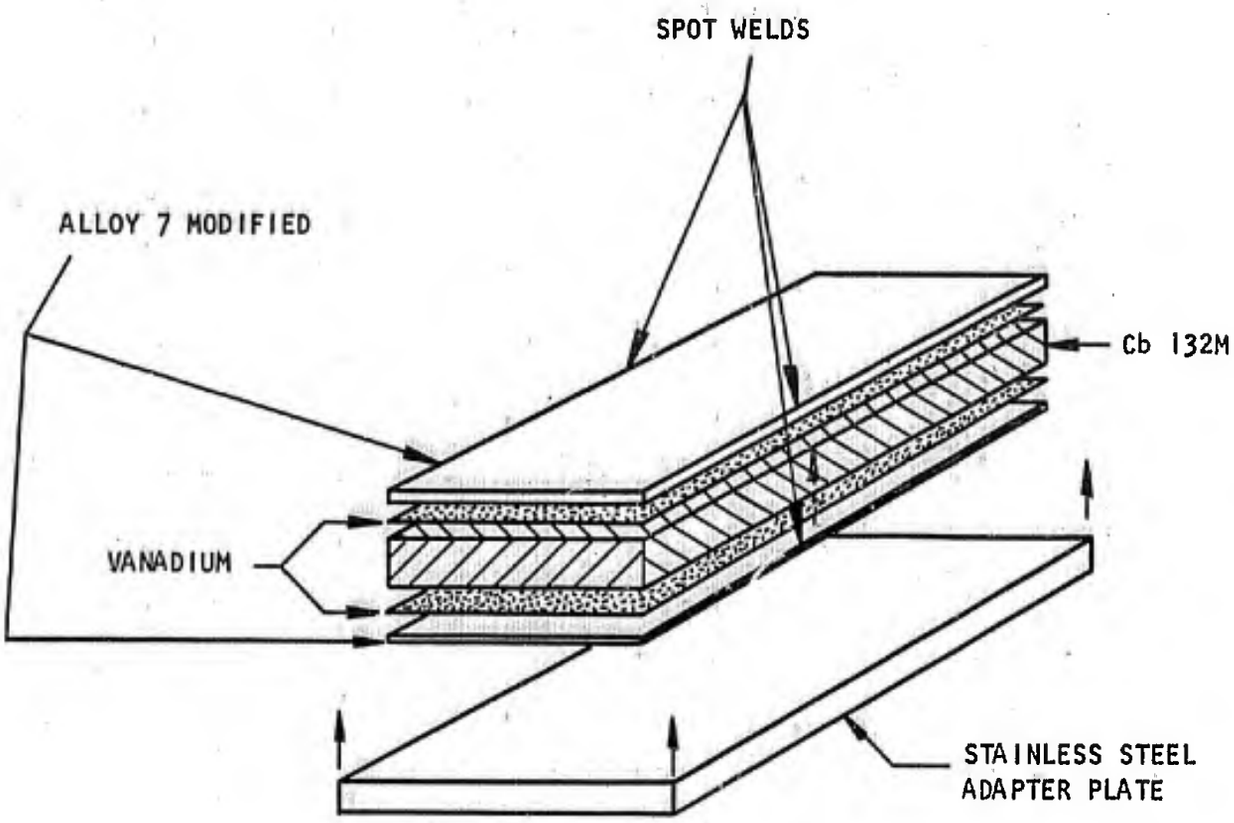

Figure 89. Schematic representation of pre-bonding specimen configuration.

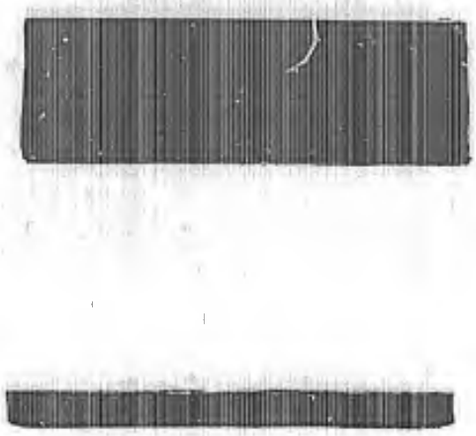

A. Bonded tensile specimen blank

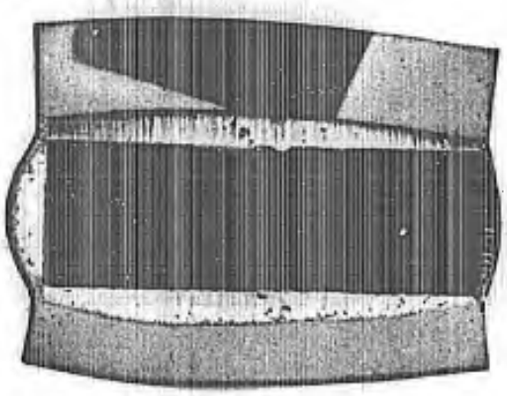

B. Stainless steel adapter plate with oxide coating

Figure 90. Diffusion bonded columbium alloy tensile specimen blank (A), and stainless steel plate used for alignment (B). Magnification: approximately 1.5X.

As-coated

Coated +
exposed 64 hrs
at 2200°F

A. Cb 132M: forged 2400°F +
annealed 3600°F/1 hr

As-coated

Coated +
exposed 64 hours
at 2200°F

B. Cb 132M: recrystallized 2950°F/2 hrs
cold worked 20% at 1600°F

Figure 91. Fractured columbium alloy combination tensile specimens tested at 1200°F. Condition of Cb 132M core indicated.

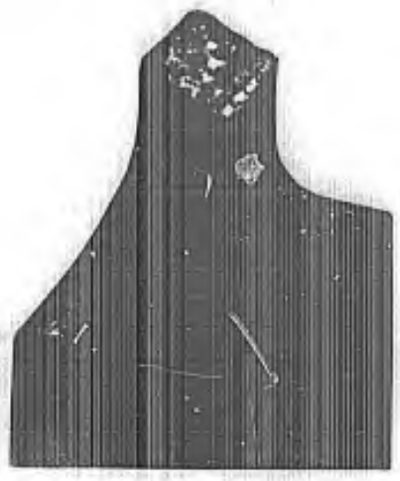

A. Brittle fracture, annealed Cb 132M.

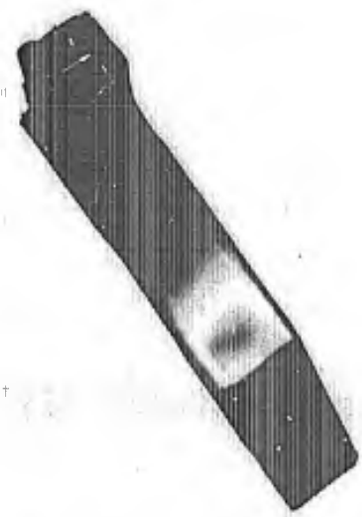

B. Ductile fracture, cold worked Cb 132M. Note separation of core and cladding.

Figure 92. Fractured surfaces of 1200°F tensile tested columbium alloy combinations produced by diffusion bonding.

As-coated

Coated & exposed
64 hrs. at 2200°F

A. Cb 132M: forged 2400°F +
annealed 3600°F/1 hr.

Coated & exposed
64 hrs. at 2200°F

B. Cb 132M: recrystallized 2950°F/2 hrs. +
cold worked 20% at 1600°F

Figure 93. Fractured columbium alloy combination creep rupture specimens tested at 2200°F. Condition of Cb 132M core indicated.

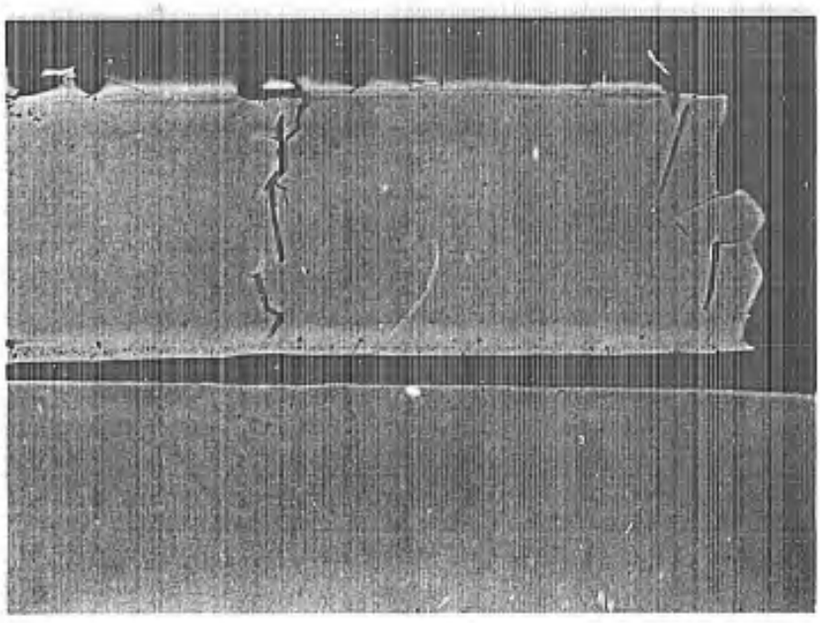

A. Cb132M: Forged 2400°F + 3600°F/1 hr.

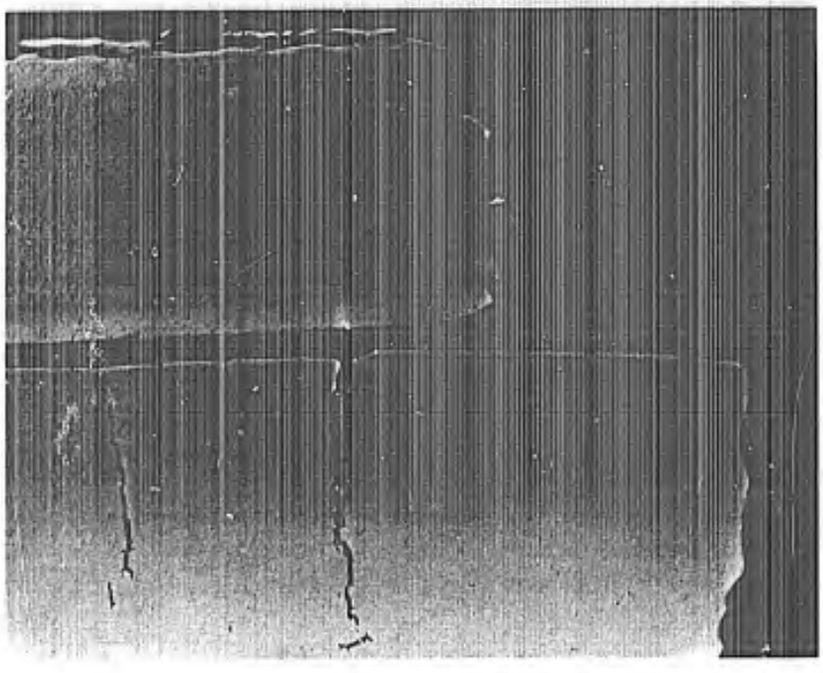

B. Cb132M: Recrystallized 2950°F/ 2 hrs.
Forged 1600°F (20%).

Figure 94. Unetched photomicrographs of columbium alloy combinations showing fracture area of 1200°F tensile specimens. Condition of Cb132M core as indicated. Magnification 100X.

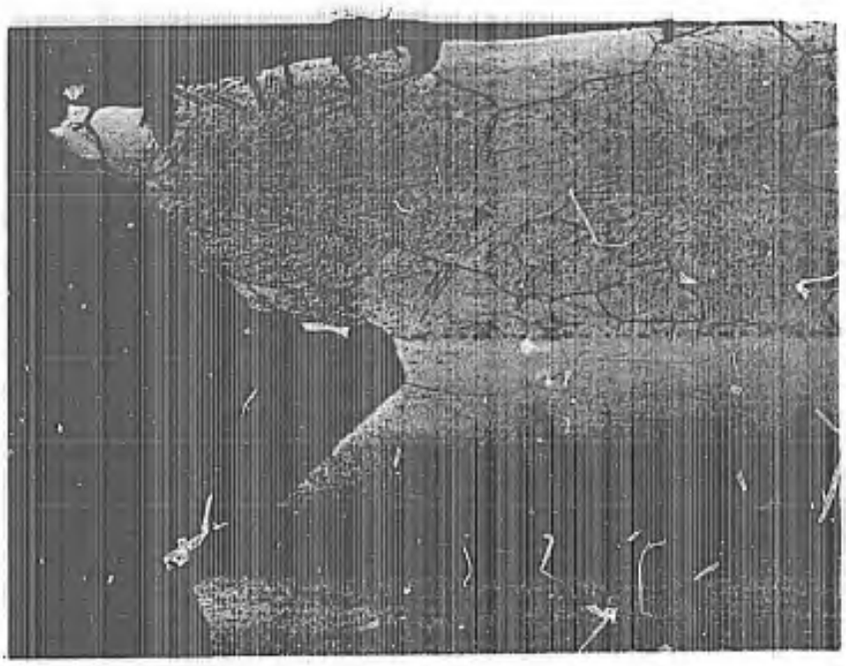

Alloy 7 mod.

Cb132M

A. Cb132M: Forged 2400°F + 3600°F/1hr.
Exposed 64 hrs. at 2200°F after
bonding and coating.

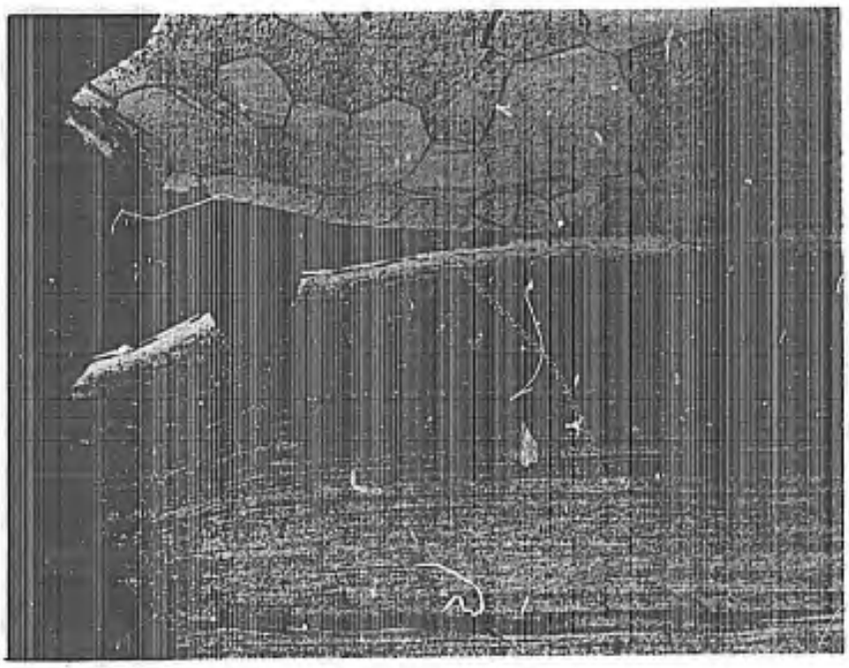

Alloy 7 mod.

Cb132M

B. Cb132M: Recrystallized 2950°F/2 hrs.
Forged 1600°F (20%)
Exposed 64 hrs. at 2200°F after
bonding and coating.

Figure 95. Photomicrographs of columbium alloy combinations showing fracture area and microstructure of 1200°F tensile specimens. Condition of Cb132M core as indicated. Magnification 100X.

525 c

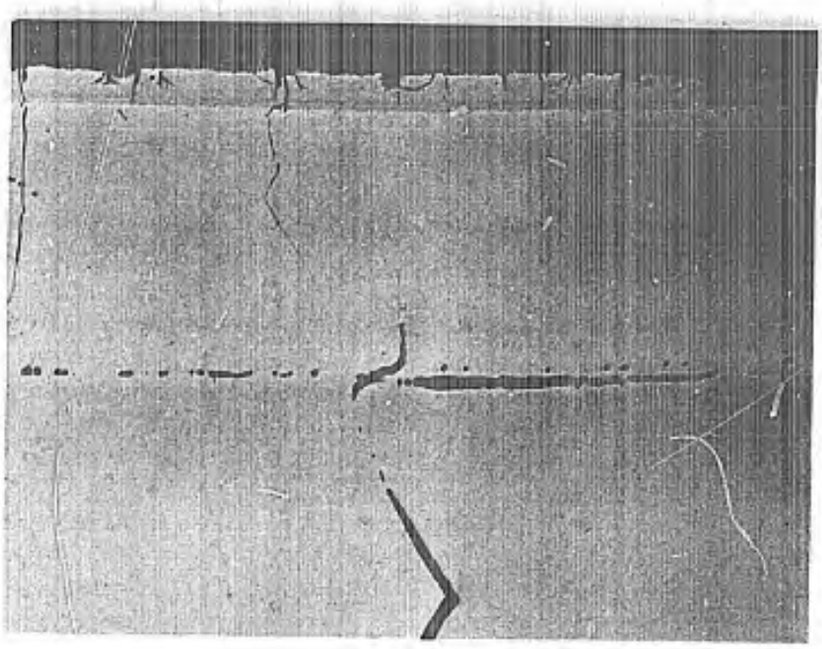

A. Cb132M: Forged 2400°F + 3600°F/1 hr.
Exposed 64 hrs. at 2200°F after bonding and coating.

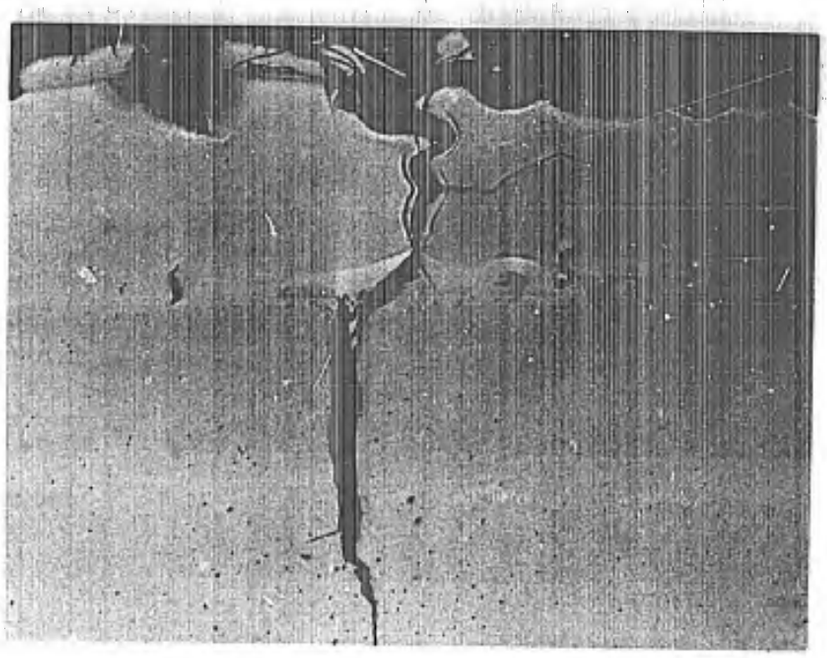

B. Cb132M: Recrystallized 2950°F/2 hrs,
Forged 1600°F (20%)
Exposed 64 hrs. at 2200°F; after bonding and coating

Figure 96. Unetched photomicrographs of columbium alloy combinations showing area near fracture in 2200°F; 30,000 psi creep specimens. Condition of Cb132M core as indicated. Magnification: 100X.

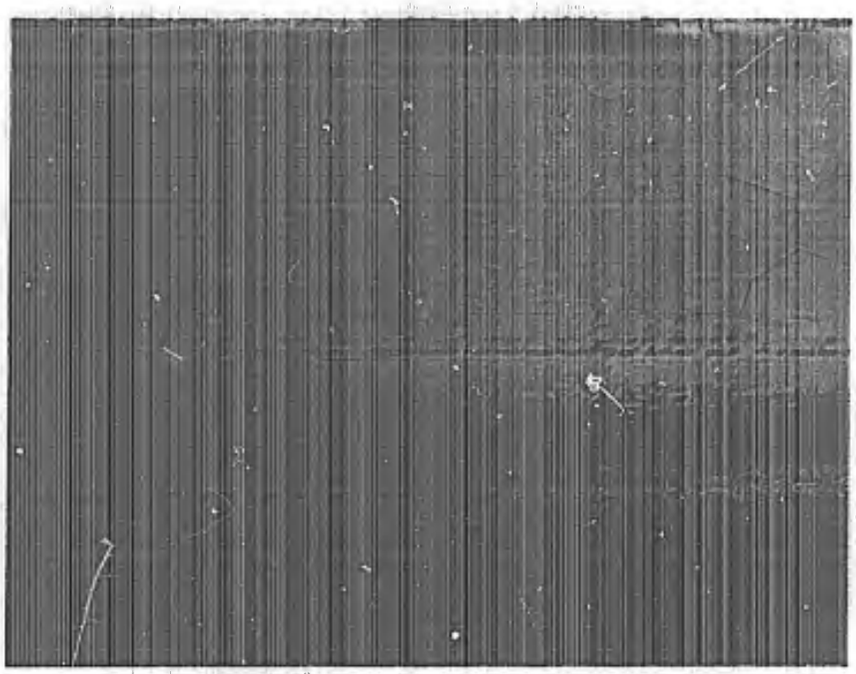

Alloy 7 mod.

Cb132M

A. Cb132M: Forged 2400°F + 3600°F/1 hr.

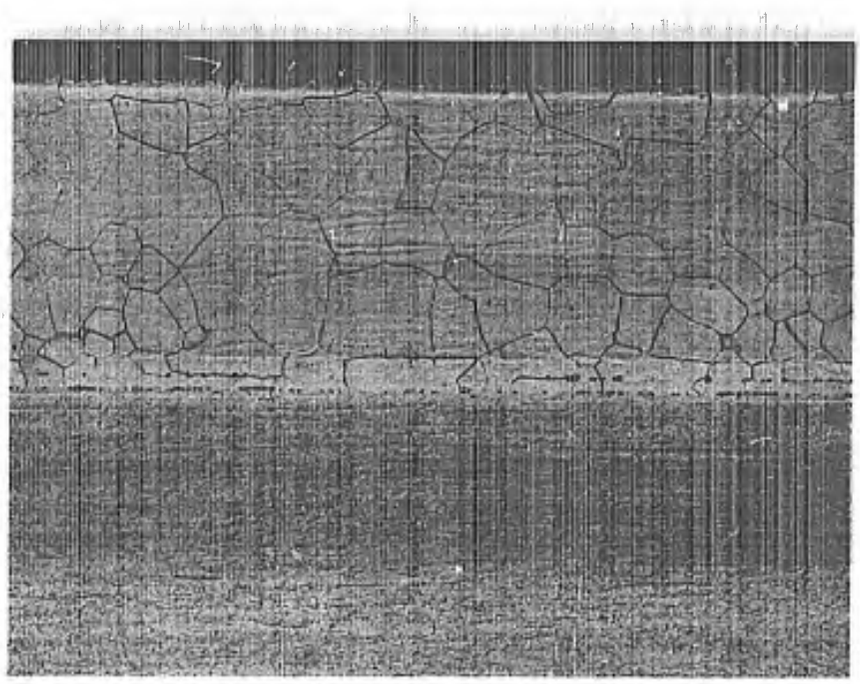

Alloy 7 mod.

Cb132M

B. Cb132M: Recrystallized 2950°F/2 hrs.
Forged 1600°F (20%).

Figure 97. Photomicrographs of columbium alloy combinations showing microstructure after 2200°F; 30,000 psi creep testing. Condition of Cb132M core as indicated. Magnification: 100X.

SECTION IV

CONCLUSIONS AND RECOMMENDATIONS

Specific conclusions to the various tasks and phases of this program have previously been given. These are restated in view of the overall program goals.

1. Fabricable oxidation resistant columbium base alloys developed and tested in this and concurrent programs have been demonstrated to be capable of serving as a cladding layer, protecting a high strength columbium alloy from rapid oxidation. In the event of local damage to an oxidation resistant service coating, the cladding alloy is slowly oxidized, providing at least 64 hours of protection at 2200°F. Undoubtedly with further work, these compositions can be further upgraded and new systems developed which can provide even greater oxidation protection.

2. The diffusion bonding technique for joining the cladding layer to the core was successfully developed and employed for this experimental program. This procedure was acceptable from a metallurgical standpoint in that it did not in itself cause significant microstructural changes in the alloy components. It is felt that this technique can be developed to the point of turbine blade manufacture. Furthermore, other methods exist which show promise for applying a complex alloy cladding to a forged part. However, in the use of any such technique, excessive heat should not be applied to avoid diffusional effects and microstructural changes.

3. The long term stability of bonded clad-core combinations appears to be an area of concern. Carbon diffusion from a carbide strengthened Cb 132M core to the cladding layer is rapid at temperatures of 2200°F and above. The changing carbon concentration and carbide precipitate morphology in the Cb 132M core alloy results in seriously lowered 2200°F creep strength for bonded samples compared to bare Cb 132M. The substitutional alloying elements diffuse much more slowly, resulting in little overall compositional change. Several potential remedies are available to provide microstructural stability and reduce carbon diffusion. These include: The development of cladding alloys which do not contain significant amounts of elements capable of acting as sinks for carbon (e.g. Ti and Hf); possible use of an intermediate foil layer other than vanadium between the cladding and the core which would serve to greatly retard carbon diffusion across it; and the development and use of core alloys strengthened either by a more stable carbide phase than is Cb 132M or by some other means such as a nitride dispersion.

4. The core alloys evaluated in this program either fell short of the desired creep properties in the conditions tested or were unable to combine high temperature creep strength and intermediate temperature tensile properties. Certain recrystallization, cold working, and aging treatments showed promise of achieving this balance but were generally lacking in creep strength. A high strength columbium base alloy and processing sequence is required which will provide strength and non-brittle behavior in all temperature ranges. In order to be of use as a clad and coated forged turbine blade, the thermal-mechanical processing sequence utilized to develop these properties must be compatible with forging, cladding, and coating procedures.

REFERENCES

1. F.N. Lake and C.R. Smeal, "Process Development for Precision Forging Columbium Base Alloys", Final Technical Report, AFML-TR-67-94, Contract AF 33(615)-1391, April, 1967.

2. J.F. Nejedlik and J.D. Gadd, "Coatings for Long Term-Intermediate Temperature Protection of Columbium Alloys", Technical Report AFML-TR-68-170, Contract AF 33(615)-5121, October, 1968.

3. H.A. Hauser and J.F. Holloway, Jr., "Evolution and Improvement of Coatings for Columbium Alloy Gas Turbine Engine Components", Technical Report AFML-TR-66-186, Part II, Contract AF 33(615)-2117, May, 1968.

4. R.T. Begley, J.L. Godshall, and D. Harrod, "Development of Columbium Base Alloys", AFML-TR-65-385, January, 1966.

5. W.H. Chang, "Influence of Heat Treatment on Microstructure and Properties of Columbium-Base and Chromium-Base Alloys", ASD-TDR-62-211, Part IV, March, 1966.

6. R.T. Begley, J.A. Cornie, and R.C. Goodspeed, "Development of Columbium Base Alloys", AFML-TR-67-116, November, 1967.

7. Communications with R.E. Droegkamp and N.R. Gardner, Kawecki-Berylco Industries.

8. R.T. Begley and J.A. Cornie, "Investigation of the Effects of Thermal Mechanical Variables on the Creep Properties of High Strength Columbium Alloys", Quarterly Progress Report No. 5, Contract AF 33615-67-C-1443, October 15, 1968.

9. W.D. Klopp, "Oxidation Behavior and Protective Coatings for Columbium and Columbium-Base Alloys", DMIC Report 123, January 10, 1960.

10. W.D. Brentnall and A.G. Metcalfe, "Interstitial Sink Effects in Columbium Alloys", Technical Report AFML-TR-68-82, April, 1968.

11. A.R. Steson and A.G. Metcalfe, "Ductile Coatings for Columbium Alloys", Progress Reports 1 through 5 on Contract AF 33(615)-1598, November, 1964 to February, 1966.

12. F.E. Bacon and P.M. Moanfeldt, "Reaction with the Common Gases", Chapter 9 in Columbium and Tantalum, F.T. Sisco and E. Epremian eds., J. Wiley and Sons, N.Y., 1963, pp 347-443.

13. R.J. Van Thyne, "Development of Oxidation-Resistant Hafnium Alloys", IITRI, Final Technical Report, Contract NOw 65-0301-f, July 29, 1966.

14. J.A. Cornie and R.C. Goodspeed, "Development of a Ductile Oxidation Resistant Columbium Alloy", Final Technical Report, AFML-TR-69-64, Contract F33615-67-C-1689, July, 1969.

15. R.A. Rapp and G.N. Goldberg, "The Oxidation of Cb-Zr and Cb-Zr-Re Alloys in Oxygen at 1000°C", Trans. AIME, Vol. 236, Nov. 1966, p. 1619.

16. D. Gelselman, T.K. Roche, and D.L. Graham, "Development of Oxidation Resistant, High Strength, Columbium-Base Alloys", Interim Engineering Progress Reports 1 through 7, Contract AF 33(615)-3856, September 1966 to March 1968.

17. S.J. Paprocki, E.S. Hodge, and P.J. Gripshover, "Solid-Phase Bonding of Columbium", in Columbium Metallurgy, D.L. Douglass and F.W. Kunz, eds., Interscience, New York, 1961, pp 13-30.

18. M. Hansen and K. Anderko, Constitution of Binary Alloys, 2nd Ed., McGraw-Hill, New York, 1958, pp 388-390.

Unclassified
Security Classification

DOCUMENT CONTROL DATA - R & D

(Security classification of title, body of abstract and indexing annotation must be entered when the overall report is classified)

1. ORIGINATING ACTIVITY *(Corporate author)*
TRW Inc.
Materials Technology Laboratory
Cleveland, Ohio 44117

2a. REPORT SECURITY CLASSIFICATION
Unclassified
2b. GROUP

3. REPORT TITLE
Development of Columbium Alloy Combinations for Gas Turbine Blade Applications

4. DESCRIPTIVE NOTES *(Type of report and inclusive dates)*
Final Report 1 June 1967 - 31 May 1970

5. AUTHOR(S) *(First name, middle initial, last name)*
Scheirer, Scott T.

6. REPORT DATE	7a. TOTAL NO. OF PAGES	7b. NO. OF REFS
October 1970	166	18

8a. CONTRACT OR GRANT NO.	9a. ORIGINATOR'S REPORT NUMBER(S)
F33615-67-C-1688	ER 7197-7
b. PROJECT NO. 7351	
c. Task No. 73510 1	9b. OTHER REPORT NO(S) *(Any other numbers that may be assigned this report)* AFML-TR-70-187
d.	

10. DISTRIBUTION STATEMENT This document is subject to special export control and each transmittal to foreign governments or foreign nations may be made only with prior approval of the Metals and Ceramics Division (MAMP), Air Force Materials Laboratory, Wright-Patterson AFB, Ohio 45433.

11. SUPPLEMENTARY NOTES	12. SPONSORING MILITARY ACTIVITY
	Air Force Materials Laboratory Wright-Patterson AFB, Ohio 45433

13. ABSTRACT A program designed to evaluate the feasibility of clad-core combination columbium alloy turbine blades has been completed. The concept was one in which a relatively oxidation resistant cladding alloy was used to prevent catastrophic oxidation of a high strength but easily oxidized core alloy. As envisioned, the entire system consisted of an oxidation resistant coating, the cladding alloy acting as an oxygen barrier, and the load bearing core. The program was divided into a screening of potential core and cladding alloys (with a diffusion bonding study) and an evaluation of the compatibility of the two components.

The high strength columbium alloys Cb132M, VAM-79, and SU-31 were evaluated as core alloys using 1200°F tensile and 2200°F creep-rupture testing. Several processing conditions and post-forging annealing treatments were studied. The highest tensile and creep strengths were obtained in Cb132M when in as-forged and forged plus 3600°F annealed conditions respectively. The best balance of tensile and creep properties was obtained in SU-31 when in a recrystallized and cold worked condition.

Nine columbium base alloys and one hafnium alloy were evaluated for possible use as a cladding alloy based on oxidation and ballistic impact resistance and fabricability to sheet. Generally, sheet fabricability and impact resistance were incompatible with oxidation resistance. Two alloys (Cb-15Ti-10Ta-10W-2Hf-3Al and Cb-5W-30Hf-5Ti-3Re) were selected for further study. A diffusion bonding technique was developed to join the core and cladding alloys. Bonding parameters were designed to minimize carbon diffusion from the high strength core alloy to the cladding.

A variety of studies were performed to evaluate the compatibility of the cladding

DD FORM 1 NOV 65 1473

Unclassified
Security Classification

14. KEY WORDS	LINK A		LINK B		LINK C	
	ROLE	WT	ROLE	WT	ROLE	WT
Columbium Alloys Turbine Blades Cladding Extrusion Forging Thermal Mechanical Processing Diffusion Bonding Oxidation Resistance						

ABSTRACT (Continued)

alloys with a Cb132M core. During bonding and exposure at 2200°F carbon diffused from the core alloy to the cladding. This was accompanied by a loss of core hardness adjacent to the bond line and the formation of hafnium and/or titanium carbides in the cladding alloy. Tests of locally damaged bond samples, coated with a CrTi-Si service coating showed that 0.020" of the cladding alloys (especially Cb-15Ti-10Ta-10W-2Hf-3Al) were capable of preventing catastrophic core alloy oxidation at 2200°F for times in excess of 64 hours. The bonded combinations exhibited good ballistic impact resistance at 2000°F although brittle behavior was encountered at room temperature. Compared with the unbonded condition, the 1200°F tensile properties of bonded Cb132M were slightly lowered whereas the 2200°F creep strength was significantly decreased. A 64 hour 2200°F exposure after bonding and coating had little effect on the mechanical properties tested.

The cladding concept for producing columbium alloy turbine blades is feasible in that diffusion bonding is an acceptable technique metallurgically and as a manufacturing technique. Also, a cladding can offer oxidation protection to the core alloy in the event of coating damage. However, the creep strength and microstructural stability of high temperature exposed clad Cb132M are marginal. It is felt that this aspect can be improved through the use of a core alloy having a superior balance of creep and tensile properties.